



UNIVERSITY OF  
BIRMINGHAM

**SCHOOL OF CHEMISTRY**

**MSc by Research**

**Project Report**

*Electrochemical Synthesis of Saturated Nitrogen-Containing Heterocycles*

*JOSEPH PATRICK MILTON*



**February 2021**

**PROJECT SUPERVISOR: *Prof. John S. Fossey***

UNIVERSITY OF  
BIRMINGHAM

**University of Birmingham Research Archive**

**e-theses repository**

This unpublished thesis/dissertation is copyright of the author and/or third parties. The intellectual property rights of the author or third parties in respect of this work are as defined by The Copyright Designs and Patents Act 1988 or as modified by any successor legislation.

Any use made of information contained in this thesis/dissertation must be in accordance with that legislation and must be properly acknowledged. Further distribution or reproduction in any format is prohibited without the permission of the copyright holder.

## Acknowledgements

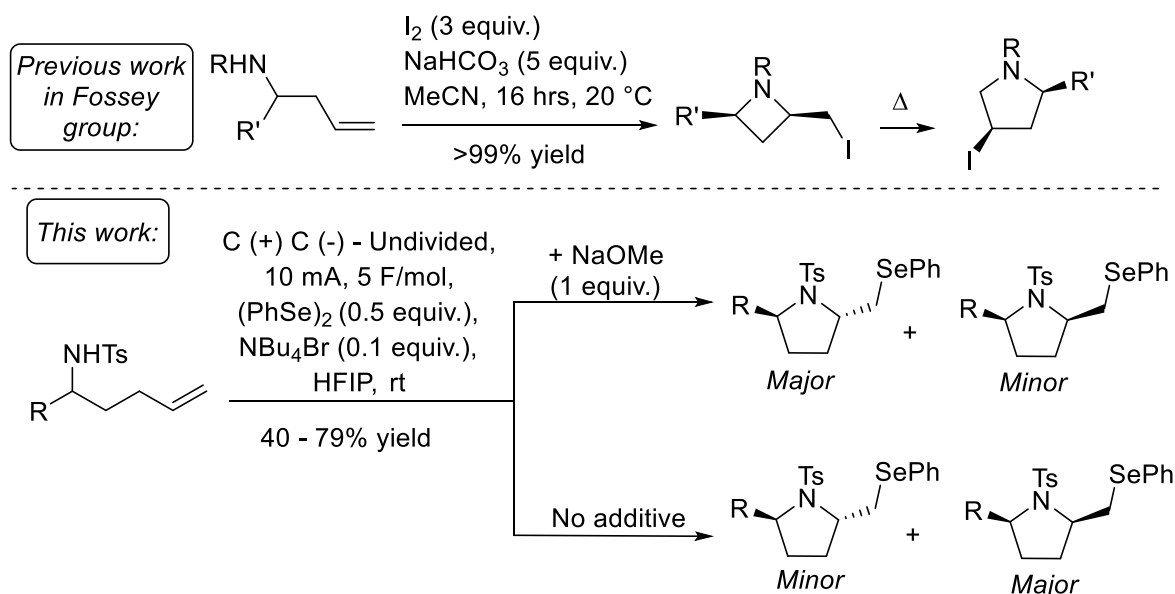
Firstly, I would like to thank Prof. John S. Fossey for giving me the opportunity to commence research within his group and for facilitating the development of so many important skills, which will provide an advantageous background for my future adventure in academia over the coming years. His help, advice and support over the past year have been imperative to my success.

Secondly, I would like to thank all the staff that are part of the analytical facility, in particular Dr. Louise Male who solved both crystal structures described in this thesis which was imperative to identifying key products within my project. I would also like to thank Dr. Cécile Le Duff for her assistance with NMR spectroscopy, Dr. Christopher Williams for running all mass spectra and Dr. Allen Bowden for assistance with gas chromatography.

Thirdly, I would like to thank all the current members of the Fossey group which have all greatly supported me during my research and made my time in the group a fun one to look back on fondly. In particular, I would like to mention Fernanda Meloni and Dr. Huy van Nguyen which both offered countless suggestions that greatly assisted me and influenced the direction of my project.

Finally, I would like to thank my friends and family for their support during my time at the University of Birmingham throughout my undergraduate and postgraduate degrees. I would also like to thank all members of the Wayfarers hiking society that have provided countless hours of entertainment during our travels all over the country while at the university and certainly made my time here infinitely more enjoyable.

## Abstract



**Scheme 1:** Past work from the Fossey group (upper) and the work described herein (lower)

The use of electrochemistry in synthesis is a relatively unexplored area of organic chemistry that is currently experiencing a resurgence of interest, with many expansive review articles<sup>1, 2</sup> and guides<sup>3-5</sup> published in recent years. The launch of the ElectraSyn 2.0 has further accelerated this interest, which is a convenient piece of equipment for organic electrochemistry for newcomers and experts alike. The formation of saturated nitrogen-containing heterocycles *via* electrochemical routes has received little attention and only the groups of Moeller<sup>6-8</sup> and Yoshida<sup>9, 10</sup> have reported the synthesis of pyrrolidine rings in the 21<sup>st</sup> century so far.

Following the interests of our group in developing new methods for the synthesis of nitrogen-containing heterocycles, herein is reported the diastereoselective synthesis of pyrrolidine-derivatives using an electrochemical process which offers a greener alternative to the previously published iodocyclisation method for the formation of azetidines and pyrrolidines.<sup>11, 12</sup> The formation of  $\alpha$ -aryl 2-((phenylselanyl)methyl)-1-tosylpyrrolidines was achieved in a straightforward one-pot manner, with the starting material subjected to the desired electrochemical conditions as inputted into an ElectraSyn 2.0. Diastereoselectivity is controlled *via* the addition or omission of a base, resulting in an approximate 4:1 *trans*:*cis* diastereomeric ratio with a base and 1:4 *trans*:*cis* ratio without. Isolation of the major product was achieved *via* column chromatography and/or preparative thin layer chromatography with a silica stationary phase, which afforded 40 – 79% yield for the major diastereoisomer. In total, 14 pyrrolidine-derivatives, of which, 12 are novel compounds, were synthesised with this methodology in scales ranging from 0.1 to 1.0 mmol. Preliminary attempts to use the same methodology for the formation of azetidines resulted in no cyclisation.

## Abbreviations

ASAP	Atmospheric Solids Analysis Probe
BASF	Badische Anilin und Soda Fabrik (Chemicals company)
Bn	Benzyl
Boc	<i>tert</i> -Butoxycarbonyl
Calc'd	Calculated
COSY	Correlated Spectroscopy
DBU	1,8-Diazabicyclo(5.4.0)undec-7-ene
DCM	Dichloromethane
DFT	Density Functional Theory
DIAD	Diisopropyl azodicarboxylate
DIPEA	<i>N,N</i> -Diisopropylethylamine
DMF	<i>N,N</i> -Dimethylformamide
DMSO	Dimethyl sulfoxide
ECF	Electrochemical fluorination
ES	Electrospray
Et	Ethyl
F/mol	Faradays per mole
GC	Gas chromatography
HFIP	1,1,1,3,3,3-Hexafluoroisopropanol
HMBC	Heteronuclear Multiple Bond Correlation spectroscopy
HMPA	Hexamethylphosphoramide
HPLC	High-Performance Liquid Chromatography
HRMS	High Resolution Mass Spectrometry
HSQC	Heteronuclear Single Quantum Coherence spectroscopy
Hz	Hertz
<i>i</i> Pr	<i>iso</i> -Propyl
IR	Infrared
JMOD	J-modulated spin-echo spectroscopy
Kcal	Kilocalorie
mA	Milliampere
<i>m</i> CPBA	<i>meta</i> -Chloroperoxybenzoic acid
Me	Methyl
MeCN	Acetonitrile
Mol%	Mole percent

MOM	Methoxymethyl
M.P.	Melting point
MS	Mass Spectrometry
<sup>n</sup> Bu	<i>n</i> -Butyl
NMR	Nuclear Magnetic Resonance
NOESY	Nuclear Overhauser Effect spectroscopy
Nu	Nucleophile
OAc	Acetate
Oxone	Potassium peroxymonosulfate (KHSO <sub>5</sub> )
Ph	Phenyl
ppm	Parts per million
R <sub>f</sub>	Retention factor
rt	Room temperature
RVC	Reticulated Vitreous Carbon
SHE	Standard Hydrogen Electrode
TBDPS	<i>tert</i> -Butyldiphenylsilyl
<sup>t</sup> Bu	<i>tert</i> -Butyl
TFA	Trifluoroacetic acid
THF	Tetrahydrofuran
TLC	Thin layer chromatography
TMS	Trimethylsilyl
Ts	Tosyl, <i>para</i> -Toluenesulfonamide
UV	Ultraviolet

## Table of Contents

Acknowledgements .....	2
Abstract.....	3
Abbreviations.....	4
1. Introduction .....	8
1.1. General Introduction.....	8
1.1.1. Fundamentals of Electrochemistry .....	9
1.1.2. Electrochemical Configurations .....	11
1.1.3. An Introduction to the ElectraSyn 2.0.....	13
1.1.4. Electrodes.....	15
1.1.5. Electrolytes.....	16
1.1.6. Solvent Choice.....	16
1.2. Electrochemistry in Organic Synthesis.....	17
1.2.1. Examples from Industry .....	17
1.2.2. Electrochemical Synthesis of Pyrrolidines .....	20
1.2.3. Electrochemical Synthesis of Azetidines.....	26
1.3. Project Aims .....	28
2. Discussion and Results .....	32
2.1. Synthesis of Pyrrolidines .....	32
2.1.1. Electrochemical Synthesis of 2-((Phenylselenanyl)methyl) Heterocycles .....	32
2.1.2. Synthesis of Pyrrolidine Precursors .....	34
2.1.3. Expansion of Methodology .....	36
2.1.4. Identification of Products .....	37
2.1.5. Reaction Optimisation .....	44
2.1.6. Substrate Scope Results.....	48
2.1.7. Mechanism.....	50
2.1.8. Removal of Tosyl Protecting Group .....	52
2.2. Attempted Synthesis of Azetidines.....	55
2.3. Conclusion and Future Work .....	57

3. Publication of a Review Article .....	60
4. Experimental .....	62
4.1. General Procedures .....	62
4.2. Characterisation Data of Compounds.....	64
4.3. X-Ray Crystallographic Information (All data provided by Dr Louise Male, UoB) .....	83
4.3.1. X-Ray Crystallography General Information .....	83
4.3.2. X-Ray Crystallographic Information for <i>trans</i> -Pyrrolidine JPM_237A .....	84
4.3.3. X-Ray Crystallographic Information for <i>cis</i> -Pyrrolidine JPM_355B.....	91
5. References .....	103
6. Appendices.....	107
6.1. Appendix 1 – Hammett Plots .....	107
6.2. Appendix 2 – Green Copy of Review Article .....	108
6.3. Appendix 3 - Representative NMR spectra for <i>N</i> -tosyl imines .....	144
6.4. Appendix 4 - Representative NMR spectra for 2-substituted 4-methyl- <i>N</i> -(pent-4-en-1-yl)benzenesulfonamides .....	147
6.5. Appendix 5 – Representative NMR spectra of <i>trans</i> -pyrrolidines .....	150
6.6. Appendix 6 – Representative NMR spectra for <i>cis</i> -pyrrolidines .....	158
6.7. Appendix 7 – Representative gas chromatography data.....	168

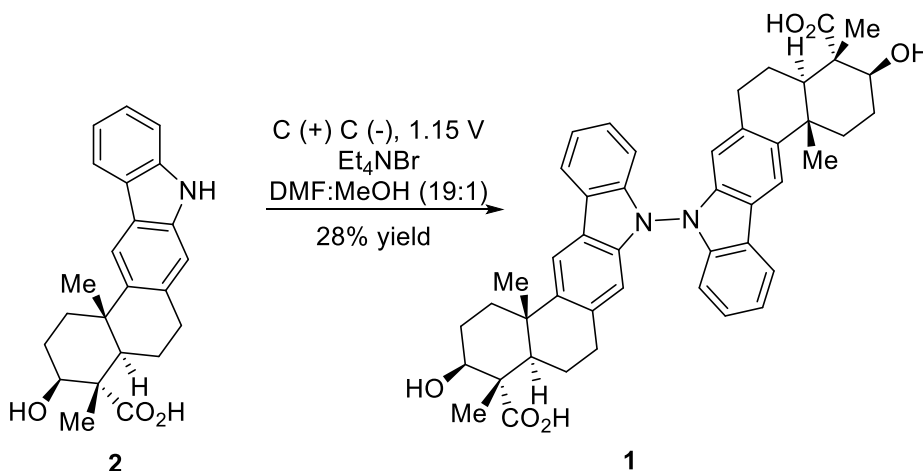


# 1. Introduction

## 1.1. General Introduction

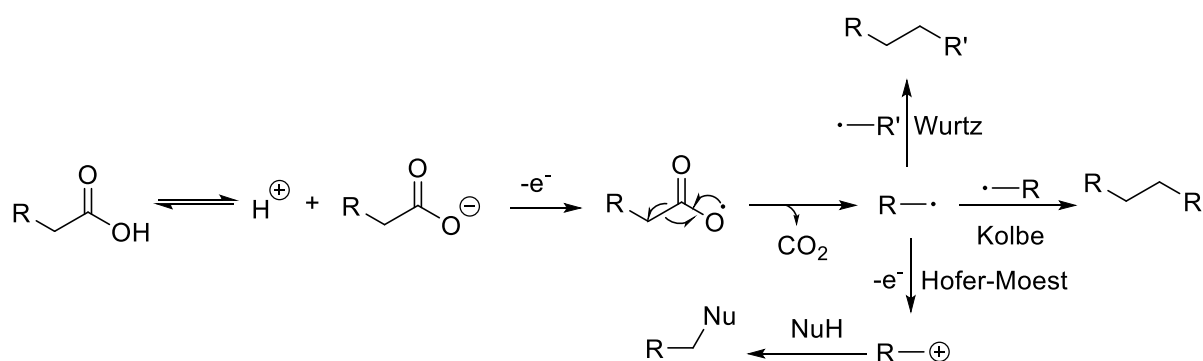
Electrochemistry is a field rarely associated with organic chemistry, but it can be an efficient alternative method to using harsh or toxic chemicals, whilst providing seamless transformations, which would be incredibly difficult to perform with typical chemical reagents. Some refer to organic electrochemistry as reagent-free<sup>13</sup> to demonstrate the efficiency of these reactions where, in general, the only species being added to the system are electrons, which are significantly greener and cheaper in comparison to chemical reagents, in turn reducing the amount of chemical waste. Furthermore, most electrochemical reactions are run at room temperature, which adds to electrochemistry's green credentials with the key electrochemical parameters, potential and current, being adjustable at any time, which drives the reaction.

The foundation of electrochemistry is the anodic oxidative and cathodic reductive processes that occur at the surface of the electrodes within a cell. The formation of reactive intermediates such as cations, anions and radicals within an electrochemical cell form the basis of reactivity and allow a reaction to take place. Running a reaction under constant potential conditions allows careful control of the electrochemical environment, by using a standard electrode that accurately measures the potential at the working electrode, such that only the desired functional group(s) would be subjected to the reaction, allowing electrochemical synthesis to be chemoselective.<sup>3</sup> Rosen *et al.* demonstrates this perfectly with their total synthesis of dixiamycin B (**1**), where their final step utilised an *N,N*-dimerisation of xiamycin A (**2**) which was unsuccessful with all 14 chemical oxidants that were attempted. The reaction only proceeded under constant potential electrochemical conditions, carefully maintained below 1.6 V, which enabled the desired reaction outcome, Scheme 2.<sup>14</sup>



**Scheme 2:** Electrochemical *N,N*-dimerisation of xiamycin A to afford dixiamycin B

Electrochemistry is debatably one of the oldest synthetic chemical techniques,<sup>1</sup> with Michael Faraday pioneering electrochemical methodology in 1834; Faraday reported the decarboxylative dimerisation of acetate salts in the presence of an electrochemical current to afford alkanes such as ethane.<sup>15, 16</sup> From this observation, Hermann Kolbe probed this reactivity further and reported that alkyl carboxylic acids could be coupled in a similar manner to form symmetric alkanes with concomitant loss of carbon dioxide,<sup>17</sup> now known as the Kolbe reaction.<sup>18</sup> Subsequently, Wurtz demonstrated that asymmetric coupling is possible by reacting two different carboxylic acids, however is seldom used due to poor selectivity with three products formed.<sup>19</sup> The Hofer-Moest reaction explores the foundation of this reactivity further, by altering the conditions so the radical intermediate can be further oxidised to a carbocation, allowing a range of nucleophiles to react facilitating the formation of alcohols, ethers and amines, Scheme 3.<sup>20</sup>



**Scheme 3:** Reactions that form the foundation of organic electrochemistry: the Kolbe, Wurtz and Hofer-Moest reactions

### 1.1.1. Fundamentals of Electrochemistry

The basis of organic electrochemistry is the act of one electron oxidation and reduction processes that occur when a substrate adsorbs to the electrode surface; substrates are oxidised at the anode and reduced at the cathode, respectively. A balanced overall reaction must occur to maintain a steady flow of electrons, in other words, the same number of electrons must be used for both oxidation and reduction. Every reaction has a working electrode, the electrode where the desired reaction takes place, and a counter electrode, where an opposing reaction takes place. The reaction at the counter electrode is typically one that generates a side product that is easily removed during work-up or purification, or bubbles out of solution, such as hydrogen gas.<sup>4</sup>

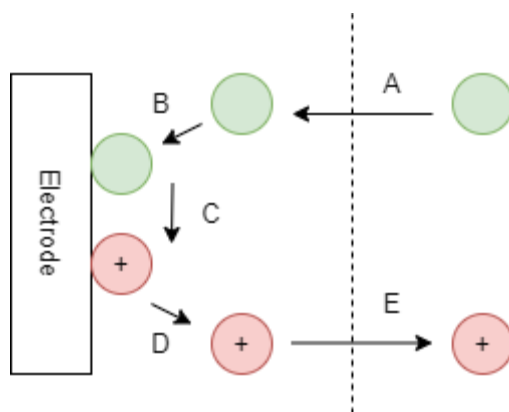


**Figure 1:** A schematic depiction of mass transport: A) Transfer of “X” from the bulk solution to the electrode surface region B) Adsorption of “X” to the electrode surface C) Electron transfer (anodic oxidation) D) Desorption of “X<sup>+</sup>” from the electrode surface E) Diffusion of “X<sup>+</sup>” back to the bulk solution

Mass transport is the movement of a desired substrate from the bulk solution to an area near the surface of an electrode, Figure 1.<sup>21</sup> As reactions take place at the electrode surface it is vital that substrates interact with the electrodes; no heterogeneous electrode-substrate interaction would result in no reaction. Because of this reasoning, mass transport is crucial to electrochemical reactions and can be the rate determining step if the substrate is not coming into contact with the electrode. Mass transport is controlled in three ways: a) Convection – mechanical means of moving the substrate, typically using a magnetic stirrer bar, b) Migration – electrostatic attraction of the substrate to the electrodes and c) Diffusion – movement of the substrate from an area of high concentration to low concentration.<sup>21</sup>

### 1.1.2. Electrochemical Configurations

Several electrochemical set-ups are available for electrochemical reactions; the incorrect choice of cell can result in no reaction or decreased yields, and thus using the correct configuration is critical to maximising a reaction's potential. Three standard cells are described herein:

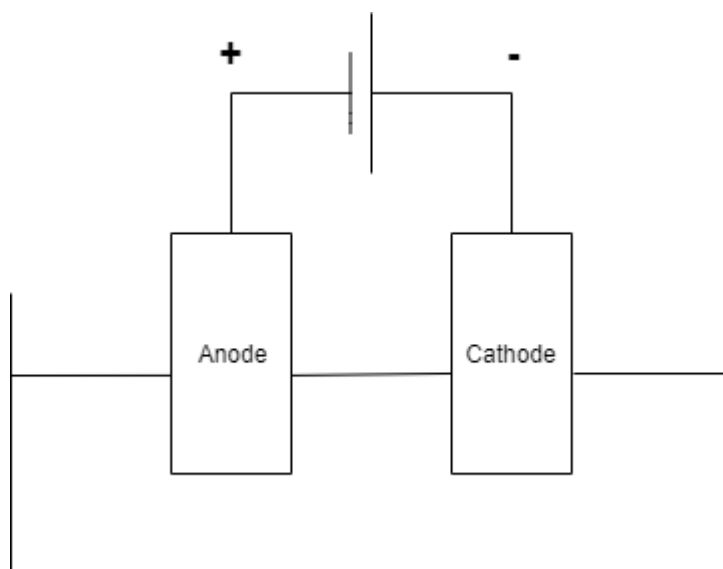


**Figure 2:** A representative diagram of a typical undivided cell

The most convenient electrochemical set-up is the undivided cell, also known as an electrolytic cell, Figure 2.<sup>1,22</sup> To prepare an undivided electrochemical cell, all that is required is a pair of two electrodes and a power supply; a notable portion of these set-ups in the literature are performed in a standard three-necked round-bottomed flask.<sup>10,11</sup> Both oxidation and reduction are performed in the same cell and the reactions are typically performed at a constant current.<sup>23</sup> Whilst highly convenient to set up, not all substrates are suitable for this set-up; for example, if the desired reaction is a cathodic reduction but the product is susceptible to anodic oxidation, then the substrate will just be repeatedly oxidised and reduced,<sup>4</sup> therefore a different set-up should be selected. A large portion of electrochemical reactions are compatible with this set-up though and is typically the first set-up that should be attempted.

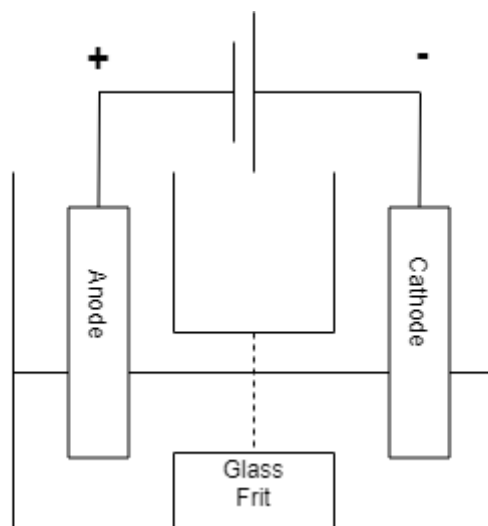


**Figure 3:** A representative diagram of an H-Cell, a typical divided cell

A divided cell, otherwise known as a galvanic cell, is more difficult to set-up in comparison to an undivided cell and specialist glassware is required such as an H-cell, Figure 3. A separator is required, typically a material such as a glass frit or an ion-selective membrane, which isolates the oxidative and reductive compartments and only allows electrons to pass through either section to complete the electrochemical circuit.<sup>24</sup>

Reactions that use a divided cell are often performed at a constant potential, opposed to constant current, which is commonly used with undivided cells. To maintain a constant potential, a reference electrode is required and should be placed in the same compartment as the working electrode.<sup>3</sup> Examples of reference electrodes include the standard hydrogen electrode (SHE), the calomel electrode or a silver/silver chloride electrode.<sup>4</sup> Some electrochemical reactions that require the use of divided cells are those that use transition metals, such as palladium cross couplings,<sup>13</sup> and electrochemical reactions that generate pseudohalogen cations, such as " $\text{Br}^{+}$ ".<sup>14</sup> These intermediates are incredibly prone to reduction which would generate their more stable forms, therefore, they must be separated from the counter electrode.

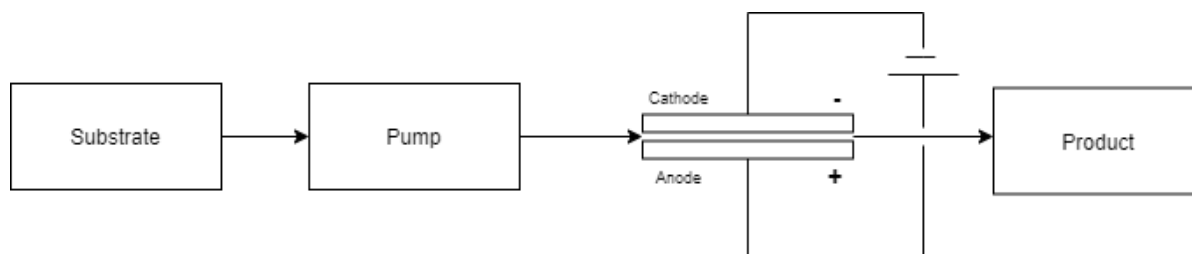


**Figure 4:** A schematic diagram of an undivided flow cell

Flow cells are highly specialised pieces of equipment that increase the efficiency of electrochemical transformations by significantly reducing the distance between the solution and electrode material

hence effectively nullifying the need of mass transport effects.<sup>24</sup> The substrate is pumped into the flow cell where the anode and cathode are placed at an incredibly short distance apart, the substrate is subjected to the electrochemical process as per normal and the solution is then ejected into a flask or vial, Figure 4.

A great example of the benefits of using a flow system was described from Laudadio *et al.*, which coupled thiols and amines in a flow cell with an electrode gap of 250  $\mu\text{m}$  in only 5 minutes in 81% yield. When conducting the same reaction in a standard undivided electrochemical cell in a batch system with a 7 mm electrode gap, a ten-fold amount of electrolyte was required and the reaction took 24 hours accompanied with a reduction in yield to 55%.<sup>25</sup> Another advantage of a flow cell is that some electrochemical reactions can be run electrolyte-free which reduces the cost of the reaction, increases the atom efficiency and potentially eliminates the need to perform a work-up upon completion of the reaction.<sup>26</sup>

### 1.1.3. An Introduction to the ElectraSyn 2.0

The electrochemical reactions performed in this thesis were conducted exclusively with an ElectraSyn 2.0, a pioneering piece of equipment built for electrochemistry by IKA, in collaboration with Prof. Phil S. Baran, from the Scripps Research Institute.<sup>27</sup> The ideal equipment for organic electrochemistry according to Baran and others in the electrochemistry community would adhere to seven key principles: 1) standardisation 2) modularity 3) possess analytical capability 4) be versatile 5) be user-friendly 6) be future-proof and 7) cost efficient.<sup>28</sup> The ElectraSyn 2.0 embodies all of these features and aims to bring organic electrochemistry into the mainstream and is pictured in Figure 5. Many organic chemists would shy away from electrochemistry due to the assumed complexity of setting up an electrochemical reaction which utilises many pieces of specialist equipment uncommon in a standard organic chemistry lab such as a potentiostat, a divided cell or electrodes.<sup>2, 29</sup> The ElectraSyn can facilitate all of these features without taking up a whole fume hood, and is made with the novice electrochemist in mind, with the inclusion of simplistic features such as the assist mode, which analyses a reaction mixture and suggests a recommended current and/or potential for the reaction.



**Figure 5:** The ElectraSyn 2.0

The ElectraSyn 2.0 does not come without its disadvantages though. The default package comes with the ElectraSyn, a stirrer bar, graphite electrodes and a 10 mL undivided cell.<sup>30</sup> Whilst this is perfectly fine for an introduction to electrochemical reactions, optimisations and scale-ups would be hindered. Several accessories are available for the ElectraSyn which allow six<sup>31</sup> or 24 reactions<sup>32</sup> to run in parallel, although the associated cost for either accessory is higher than the ElectraSyn itself, which is unfavourable. Another small issue is that the default package contains only a vial, which limits the scope of reactivity with the ElectraSyn and only allows electrochemical reactions that use an undivided cell to work. However, IKA has recently released a “Pro-divide” accessory, which allows electrochemical reactions with the ElectraSyn to work in a divided fashion.<sup>33</sup> Flow systems are not officially supported to run with the ElectraSyn either but the Hilton and Lam groups have enabled flow electrochemistry with the ElectraSyn *via* a 3D-printed add-on that requires no disassembly of the system.<sup>34</sup> Despite these inconveniences, the ElectraSyn is a convenient piece of equipment for virtually all aspects of organic electrochemistry. Also, reactions can easily be scaled up with the use of a 20 mL vial,<sup>35</sup> which prevents the user having to worry about potential issues that may arise when switching to a different batch reactor.

### 1.1.4. Electrodes

Electrodes are conductors that are sheets of metal (or carbon) that donate or receive electrons in a reaction and are sites at which oxidation and reduction take place. Choosing the correct electrode combination is crucial to a reaction's outcome and selecting the incorrect electrode pairing can severely hinder a reaction, even completely preventing it in some situations.<sup>36</sup> Reference electrodes, as mentioned in Section 1.1.2., are used for constant potential reactions; with the ElectraSyn, a reference electrode is provided as a silver/silver chloride set-up.<sup>37</sup>

One of the most important factors to consider when choosing electrodes for an electrochemical reaction is the overpotential of an electrode, which can notably influence the performance of a cell.<sup>38</sup> Overpotential is defined by Bard and Faulkner as "the potential difference between a half-reaction's thermodynamically determined potential and the potential at which the redox event is experimentally observed".<sup>39</sup> Essentially, every electrode will have a different potential for a reaction than what is predicted with thermodynamic theory. This can be exploited to nullify or encourage side reactions, in particular the oxidation of water forming oxygen and the reduction of protons to afford hydrogen gas, which are two common electrochemical reactions. A table of common electrode materials and their respective overpotential are shown in Table 1.

If the intended reaction is an anodic oxidation, typically cathodic reduction of a proton is coupled with it and hence the chosen cathode should have a small overpotential such as platinum or palladium to encourage hydrogen formation. Likewise, if cathodic reduction of a substrate is intended, graphite or lead would be a good choice as the cathode because of their high hydrogen overpotential, nullifying proton reduction and encouraging the desired reduction.<sup>36</sup>

**Table 1:** Overpotential of common electrodes demonstrating the effect of electrode materials on reactions<sup>40</sup>

Electrode Material	Hydrogen Overpotential (V) $2\text{H}^+ + 2\text{e}^- \rightarrow \text{H}_2$	Oxygen Overpotential (V) $\text{H}_2\text{O} \rightarrow \frac{1}{2}\text{O}_2 + 2\text{H}^+ + 2\text{e}^-$
	Cathode	Anode
Carbon (Graphite)	-0.62	+0.95
Gold	-0.09	+1.02
Lead	-0.71	+0.81
Nickel	-0.28	+0.56
Palladium	-0.07	+0.93
Platinum	-0.07	+0.95
Silver	-0.22	+0.91

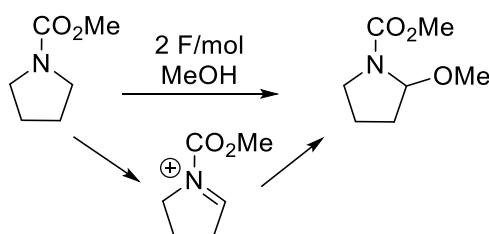


### 1.1.5. Electrolytes

Electrolytes are inorganic salts that increase the conductivity of a solution in an electrochemical reaction and are a necessary additive for almost all reactions because most solvents cannot competently carry an electrical current. The chosen salt should be sufficiently soluble in the desired solvent system whilst staying electrochemically inert, that is to not interact with the electrochemical reaction and to act as spectator ions only.<sup>41</sup> Electrolytes only remain inert when they are used within the electrolyte's potential window; if a reaction operates above or below the potential window of an electrolyte, it is then susceptible to oxidation or reduction respectively.<sup>42</sup> Electrolytes are often employed as tetraalkyl ammonium salts such as tetraethylammonium tosylate, tetrabutylammonium bromide and similar salts. Other salts are utilised but less frequently, such as perchlorates and periodates, and even relatively simple salts such as sodium chloride.<sup>41</sup> Ionic liquids are in a unique position where they can be utilised as both solvent and electrolyte and can be used with high efficiency in some reactions.<sup>43</sup>

### 1.1.6. Solvent Choice

The use of a solvent is no different in electrochemical reactions and must sufficiently dissolve all reagents in a reaction, however this can be a difficult task. As previously stated in Section 1.1.5., the solvent needs to sufficiently dissolve an inorganic electrolyte alongside the organic substrates so the solution may require sonication to encourage full dissolution. It is also important that the potential window of the solvent is considered as well (in an analogous manner to electrolytes in Section 1.1.5.).<sup>21</sup> Solvents such as water, methanol, acetonitrile and DMF are frequently used in the area of organic electrochemistry due to their good affinity for dissolving inorganic salts.<sup>41</sup> Similar to the choice of electrolytes, the solvent should also be electrochemically inert unless it is intended for the solvent to be a reactant. Methanol is frequently used as a source of the methoxide anion in electrochemical reactions<sup>44</sup> and this reactivity has been well-documented for the Shono oxidation of carbamates, Scheme 4.<sup>45</sup>



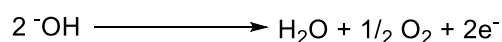
**Scheme 4:** Shono oxidation of methyl pyrrolidine-1-carboxylate, demonstrating the use of methanol as a reactant<sup>46</sup>

## 1.2. Electrochemistry in Organic Synthesis

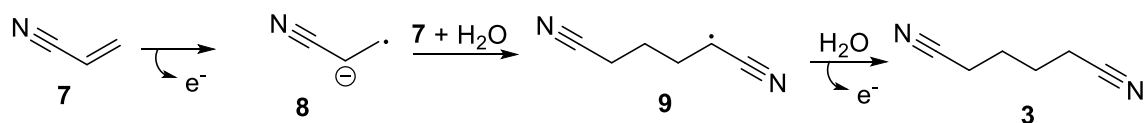
### 1.2.1. Examples from Industry

Electrochemistry is used rarely in industry for the mass production of organic chemicals with an approximate number of 60 compounds synthesised annually with the technology.<sup>47</sup> Some of the most notable are described herein:

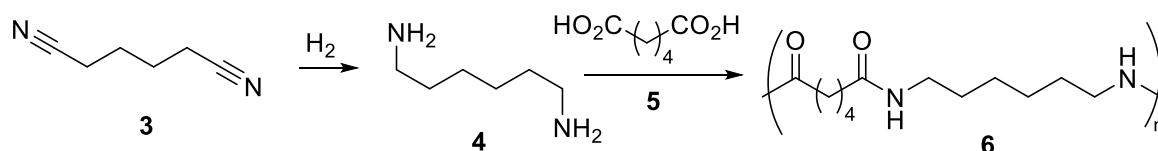
Cadmium Anode



Stainless-steel Cathode:



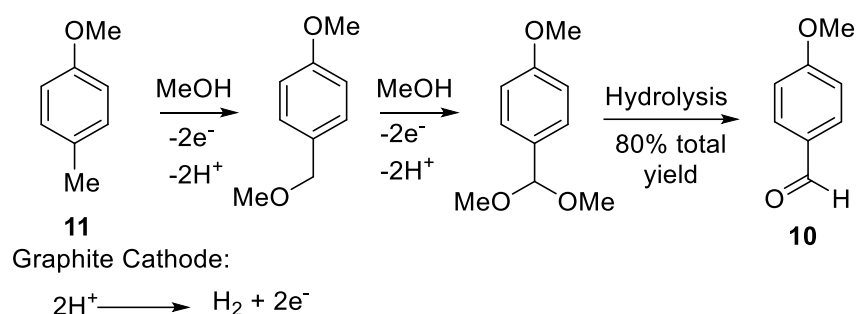
Polymerisation:



**Scheme 5:** Industrial electrochemical synthesis of adiponitrile (3), a key precursor for nylon 66 (6)

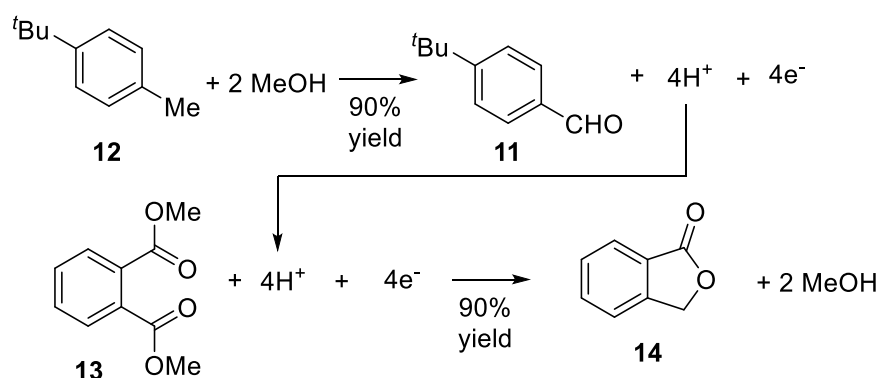
Adiponitrile (3) is an important precursor in industry, where it is readily hydrogenated to hexamethylenediamine (4) and subsequently polymerized with adipic acid (5) forming nylon 66 (6), one of the most common materials in the textile and plastic industries.<sup>48</sup> Acrylonitrile (7) is reduced at the cathode and affords radical anion 8. The intermediate 8 reacts with a second acrylonitrile unit (7) and is subsequently protonated to produce radical 9, which is reduced to an anion and protonated to afford the desired product, Scheme 5.<sup>49, 50</sup> The reaction was originally performed in a divided cell, but modern methods use an undivided cell with a cadmium anode and stainless-steel cathode with a quaternary ammonium salt as electrolyte.<sup>51</sup> The electrolyte strongly binds to the cathode, hindering unwanted electrochemical reactions such as proton reduction, thereby increasing the efficiency of the reaction. Two hundred thousand tonnes of adiponitrile (3) are produced per year *via* this electrochemical process.<sup>52</sup>

Graphite Anode:



**Scheme 6:** Industrial electrochemical synthesis of 4-methoxybenzaldehyde (**10**)

Electrochemical methodology is used for the synthesis of various substituted benzaldehydes with 4-methoxybenzaldehyde (**10**), also known as *para*-anisaldehyde, being the most notable example with BASF producing 3500 tonnes per year of it *via* electrochemical methodology starting from 4-methylanisole (**11**).<sup>51</sup> Methanol is the sole additive to the reaction whilst also doubling as the solvent allowing the process to be highly atom efficient and produces *para*-anisaldehyde in approximate 80% yield, Scheme 6.<sup>51</sup>

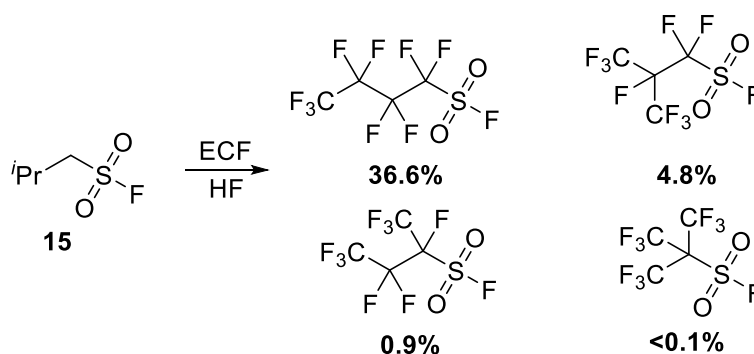


**Scheme 7:** Industrial paired electrochemical synthesis of 4-*tert*-butylbenzaldehyde (**11**) and phthalide (**14**)

In addition to BASF's production of 4-methoxybenzaldehyde (**10**), BASF also produces 4-*tert*-butylbenzaldehyde (**11**) *via* a paired electrolysis set-up, which is noteworthy because it was the first time a paired electrolysis has ever been performed on an industrial scale.<sup>53</sup> 4-*tert*-Butyltoluene (**12**) is oxidised in the same way as seen in Scheme 6, but the protons released are not reduced to hydrogen gas. Instead, they are directly used for a second electrochemical process that converts dimethyl phthalate (**13**) to phthalide (**14**) with the partial regeneration of methanol with both reactions generating 90% yield, Scheme 7.<sup>51</sup>

Molecular fluorine has a strong link to electrochemistry and was first isolated in 1886 by Henri Moissan from an electrochemical protocol.<sup>54</sup> Moissan subjected anhydrous hydrogen fluoride and molten potassium hydrogen difluoride to an electrical current in a specially made platinum electrolyser with platinum-iridium alloy electrodes, which isolated the yellow-green gas.<sup>55</sup> He was later

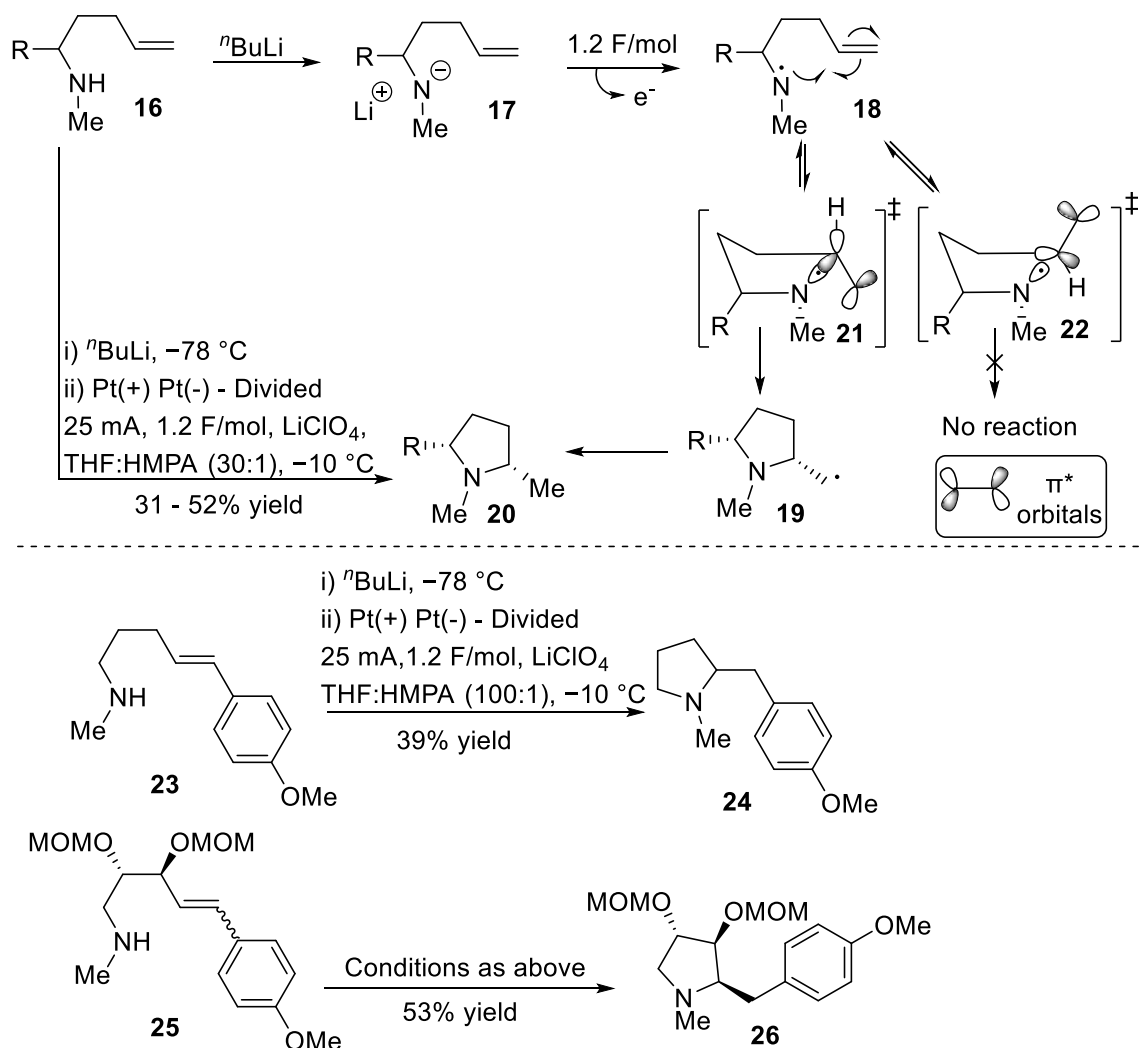
awarded the Nobel Prize in Chemistry in 1906 for the achievement of isolating molecular fluorine.<sup>54</sup> Fluorine is still made in an analogous approach today, using a combination of potassium fluoride and hydrofluoric acid; it is subsequently stored in steel or nickel drums to prevent the highly reactive gas destroying its storage container.<sup>56</sup>



**Scheme 8:** Electrochemical fluorination of *iso*-butylsulfonyl fluoride, percentages are yields for the reaction estimated by <sup>19</sup>F NMR<sup>57</sup>

Natural products that contain fluorine are particularly rare in nature<sup>58</sup> and fluorinated compounds are of interest in research and pharmacology as the effect of fluorine on the biological activity of drugs are typically not understood very well.<sup>59</sup> A common method to generate perfluorinated compounds is *via* the Simon's process, more generally known as electrochemical fluorination (ECF) developed in the early 1940s.<sup>60</sup> A substrate is added to a cell equipped with an iron cathode and a nickel anode followed by hydrofluoric acid.<sup>61</sup> Iron and nickel are relatively resistant to hydrofluoric acid, making them well suited to such applications. It is carefully electrolysed between five and six volts to hinder the production of fluorine gas. The process is still used today and generates a wide variety of compounds including carboxylic acids, sulfonic acids, amines and ethers.<sup>62</sup> Ignat'ev *et al.* demonstrated the electrochemical fluorination of various sulfonyl fluorides, such as *iso*-butylsulfonyl fluoride (**15**), to justify why the majority of ECF processes afford straight-chain fluorinated products even when the starting material utilised a branched alkyl chain, such as that shown Scheme 8.<sup>57</sup>

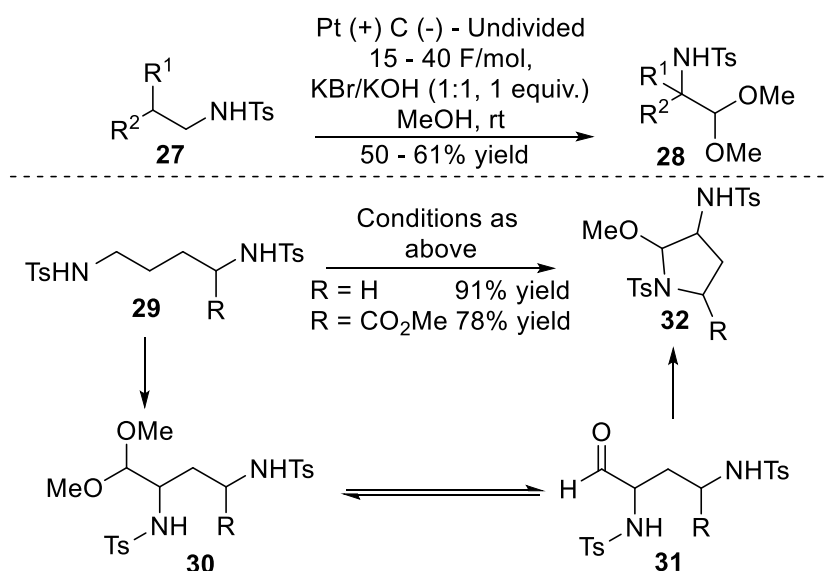
### 1.2.2. Electrochemical Synthesis of Pyrrolidines



**Scheme 9:** Electrochemical synthesis of pyrrolidine rings (**20**) (top). The same method was later used for the total synthesis of (+)-*N*-methylanisomycin (**24**) (bottom)

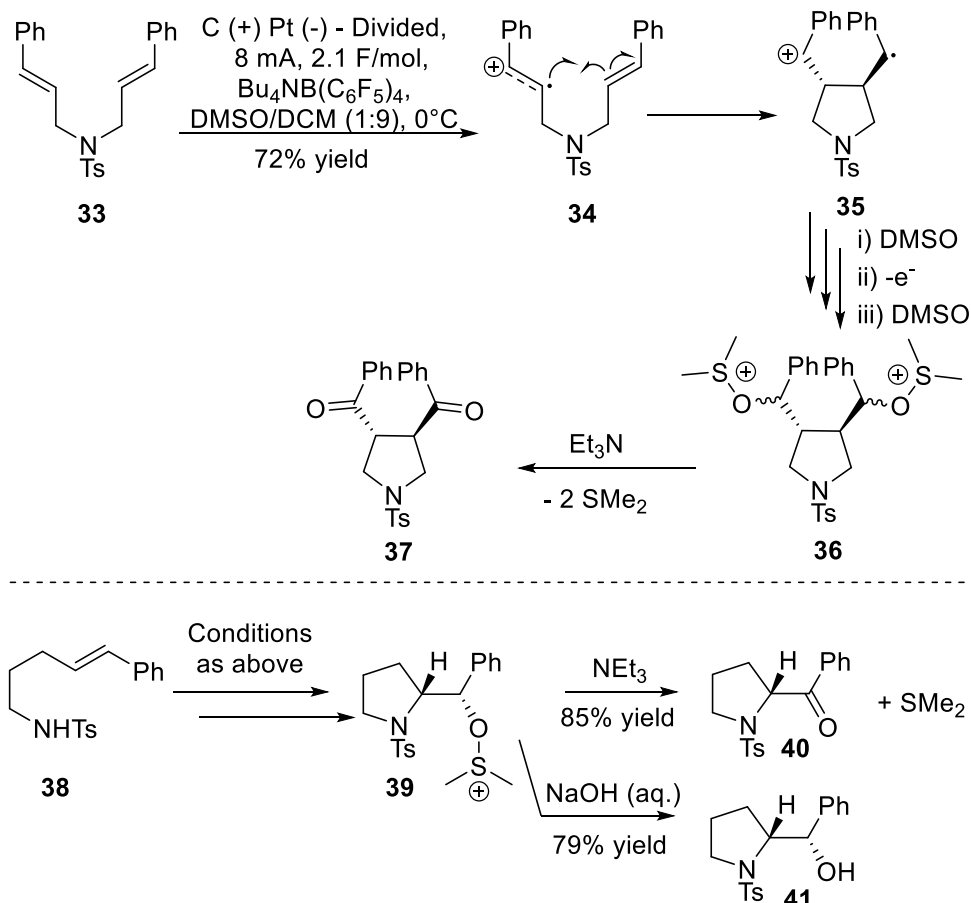
The first electrochemical synthesis of a pyrrolidine was reported by Tokuda *et al.* in 1985, Scheme 9 (top). *n*-Butyllithium is employed to deprotonate the amine starting material (**16**), affording a nitrogen anion (**17**), which is subsequently reduced to a radical (**18**), followed by an intramolecular cyclisation with the alkene (**18**); the methylene radical (**19**) is quenched to afford a *cis*-pyrrolidine (**20**). The reaction was highly stereoselective, where the *trans*-isomer of **20** was undetectable by GC analysis. The stereoselectivity could potentially be rationalised by considering two theoretical transition states (**21**) and (**22**), **21** has constructive overlap of the nitrogen *p*-orbital that contains the radical with the alkene  $\pi^*$  orbitals, which allows the formation of **19**. The transition state **22**, however has the nitrogen *p*-orbital pointing at the side of the  $\pi^*$  orbitals therefore no reaction can occur due to poor orbital overlap. The reaction could have been further optimised however, with reported yields ranging from only poor to moderate with the best substrate only affording 52% yield where R = Ph at  $-10^\circ\text{C}$  but 29% of starting material was recovered.<sup>63</sup> Tokuda *et al.* utilised this method again in their later work when approaching the total synthesis of (+)-*N*-methylanisomycin which is the *N*-methylated

enantiomer of (-)-anisomycin. A test substrate (**23**) was synthesised to investigate the feasibility of the reaction and afforded the desired pyrrolidine (**24**) in 39% yield; surprisingly the actual substrate (**25**) used in the total synthesis achieved a better result with 53% yield for the bis-protected pyrrolidine (**26**), Scheme 9 (bottom).<sup>64</sup>



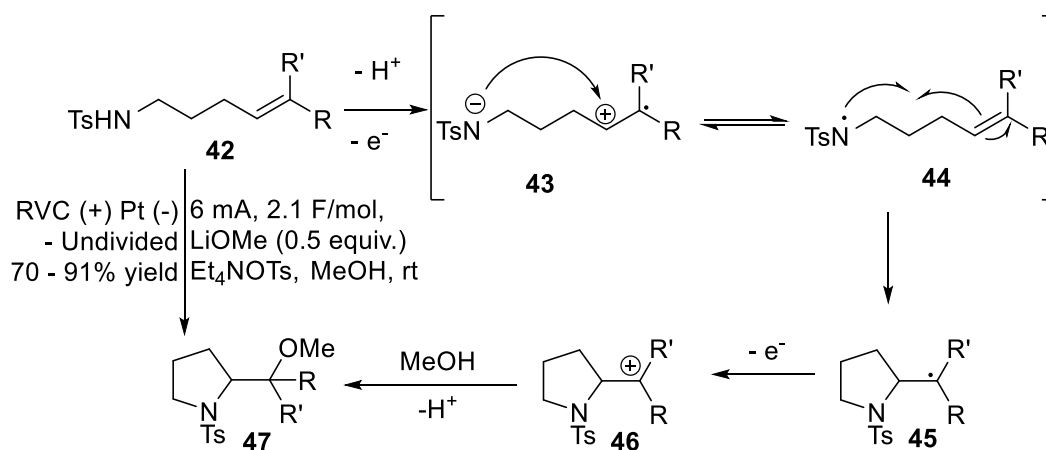
**Scheme 10:** Electrochemical rearrangement reaction sulfonamides (top). Electrochemical rearrangement of bis-sulfonamides was used for the formation of pyrrolidines (bottom)

Shono *et al.* reported an electrochemical rearrangement reaction of sulfonamides in the presence of bromide salts; subjecting a sulfonamide (**27**) to a 1:1 mixture of potassium bromide and potassium hydroxide in methanol shifted the sulfonamide (**27**) by one carbon and generated an acetal group in its place (**28**), Scheme 10 (top). Following this discovery, a bis-sulfonamide substrate (**29**) was tested that performed the same rearrangement reaction at only one site. The acetal (**30**) was subsequently hydrolysed to yield an aldehyde (**31**) which facilitated ring closure using the second amine to form a pyrrolidine ring (**32**) in 91% yield with predominant *trans*-stereochemistry when R = H, Scheme 10 (bottom). This reaction was also able to successively form the six-membered piperidine ring in 79% yield but unfortunately was unable to generate an azetidine ring; instead, the reaction simply stops at the aldehyde/acetal. Shono *et al.* also demonstrated that this methodology is viable to make  $\alpha$ -amino acids as well (**32**, when R = CO<sub>2</sub>Me) which generated the pyrrolidine in a good 78% yield.<sup>65</sup>



**Scheme 11:** Electrochemical ring-closing metathesis-like reaction (top). Similar reactions were possible with substrates containing a single alkene and afforded pyrrolidines **38** and **39** (bottom)

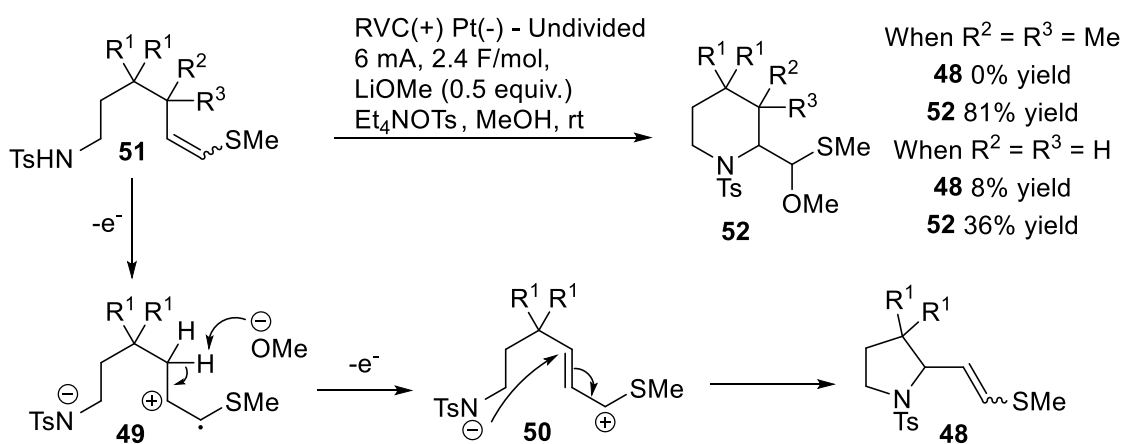
Ashikari *et al.* demonstrated an analogous procedure to ring closing metathesis *via* electrochemical methodology. The reaction initially oxidises one of the double bonds upon *N,N*-dicinnamyl-4-methylbenzenesulfonamide (**33**) facilitating an intramolecular radical ring-closing reaction to occur with the other alkene (**34**). The intermediate carbocation and radical (**35**) are both quenched with DMSO (**36**) and are subsequently oxidised with triethylamine in a Swern-like manner to afford diketones (**37**), Scheme 11 (top). The products have exclusive *trans*-stereoselectivity and this was rationalised using DFT calculations, which determined that the energy was significantly higher when the benzylic substituents were in a *cis*-relationship due to the steric clash of the aromatic rings.<sup>10</sup> The reaction also works for compounds with one alkene, such as **38**, where the alkene is initially partially oxidised, which allows a cyclisation between the nucleophilic nitrogen and the carbocation. DMSO adds in an identical manner producing a sulfoxide (**39**) which similarly can be used for a Swern oxidation affording a ketone (**40**). It was also discovered that with this intermediate, an alternative reaction was possible, where aqueous sodium hydroxide could be used to produce an alcohol (**41**), Scheme 11 (bottom).<sup>10</sup>



**Scheme 12:** Electrochemical intramolecular cyclisation of aminoalkenes affording 2-methoxymethyl pyrrolidines (**45**)

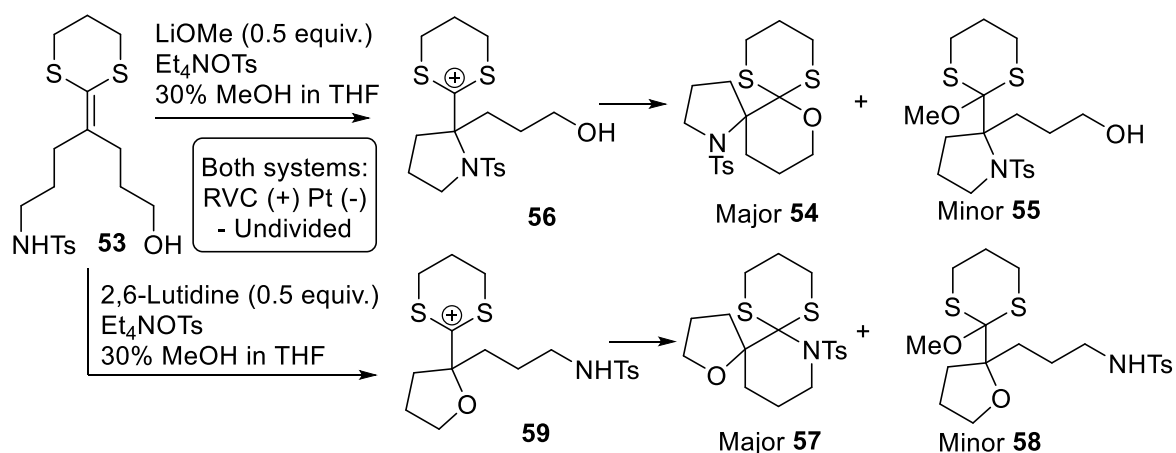
The Moeller group has extensively researched the anodic oxidation of alkenes using nucleophilic moieties such as alcohols<sup>66, 67</sup> and amides<sup>68</sup> to form oxygen-containing heterocycles and have extended their work to synthesise nitrogen-containing heterocycles with sulfonamides, as shown in Scheme 12. The alkenyl sulfonamide (**42**) is initially oxidised to generate two possible intermediates (that exist in rapid equilibrium);<sup>8</sup> intermediate **43** was derived from the oxidation of the alkene and lithium methoxide deprotonating the amine. Alternatively, intermediate **44** is generated by deprotonation of the sulfonamide and the anion is subsequently oxidised to a radical. Either pathway can produce the radical pyrrolidine **45**, which is further oxidised to carbocation **46** then quenched by the solvent (methanol) to afford pyrrolidine **47**, Scheme 12. Initial attempts of the cyclisation resulted in poor to moderate yields using the group's standard conditions for the synthesis of oxygen-containing heterocycles using 2,6-lutidine as base ( $pK_a = 6.7$ ). Upon changing to a stronger base such as LiOMe ( $pK_a = 15$ ) an appreciable increase in the yield of the reaction was observed; 2,6-lutidine was unlikely to be strong enough to deprotonate the sulfonamide. Increasing the polarity of the solution also enhanced the yield, where using 100% methanol instead of a 30% methanol in THF mixture facilitated a 10% increase in yield.<sup>6, 7</sup>





**Scheme 13:** Electrochemical cyclisation of aminoalkenes for the formation of piperidines; an unintentional elimination reaction afforded a 2-vinylpyrrolidine (**48**)

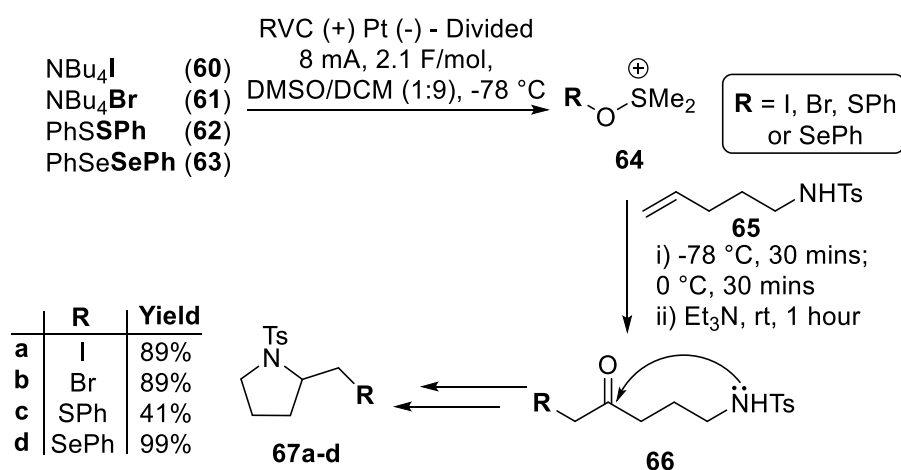
Xu and Moeller attempted to use the same protocol that was described in Scheme 12 for the synthesis of piperidine rings. The formation of a vinylpyrrolidine (**48**) was unintentionally produced as a side product *via* an elimination process (**49** and **50**), Scheme 13. The side reaction that generates the vinylpyrrolidine (**48**) is prevented when replacing either R<sup>2</sup> or R<sup>3</sup> upon **51** with any non-hydrogen substituent. When **51** is substituted with R<sup>1</sup> = H and R<sup>2</sup> = R<sup>3</sup> = Me, the piperidine (**52**) was formed in 81% yield and was the only product; when **51** was substituted with R<sup>1</sup> = Me and R<sup>2</sup> = R<sup>3</sup> = H the piperidine (**52**) was generated in 35% yield with the pyrrolidine (**48**) in 8% yield. Replacing just one allylic substituent on **51** (R<sup>2</sup> or R<sup>3</sup>) is sufficient to prevent the elimination reaction, where the piperidine (**52**), as the sole product, can be synthesised in 44% yield when R<sup>2</sup> (or R<sup>3</sup>) = Me or 62% yield when R<sup>2</sup> (or R<sup>3</sup>) = OTBDPS.<sup>7</sup>



**Scheme 14:** Electrochemical competition reactions between alcohol and sulfonamide tethers to afford tetrahydrofuran or pyrrolidine rings

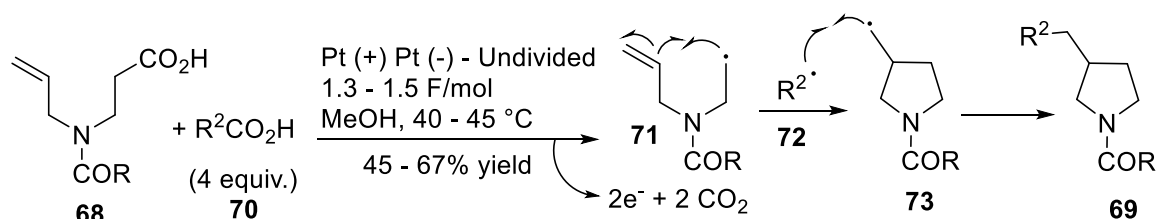
To probe the intermediate and the mechanism of the anodic oxidative cyclisation reaction, previously described from Xu and Moeller (Scheme 12), Xu and Moeller investigated a series of competition reactions with the use of a substrate (**53**) that contained a sulfonamide and an alcohol

propyl tether attached to a ketene dithioacetal, Scheme 14. Firstly, the reactions with the substrate (**53**) demonstrated the importance of base choice, where the pyrrolidines (**54** and **55**), via intermediate **56**, were the major products when using lithium methoxide. When using 2,6-lutidine, which is a notably weaker base than lithium methoxide,<sup>7</sup> only tetrahydrofuran rings (**57** and **58**) from intermediate **59** were formed, indicating that 2,6-lutidine is not basic enough to sufficiently deprotonate sulfonamides. The polarity of the solvent system plays a crucial role too, where the cyclisation with lithium methoxide would only form only pyrrolidine rings **54** and **55** when using 30% MeOH in THF. Increasing the polarity of the system to 60% MeOH in THF or 100% MeOH would produce **57** as a side product. Interestingly, changing the polarity of the system did not have a clear pattern to influence the ratio of **54:55** where 60% MeOH in THF had the highest ratio at 5.3:1 and 30% MeOH in THF had the poorest ratio at 4.1:1; in all situations the major product was derived from an intramolecular cation trap with **54** or **57** as the major. The same observations were reported when the alkenyl substituent was changed from the ketene dithioacetal to a methoxy and thiomethoxy group.<sup>8</sup>



**Scheme 15:** Cation pool formation of DMSO intermediates facilitates intramolecular cyclisation of aminoalkenes to afford pyrrolidines (**65a-d**)

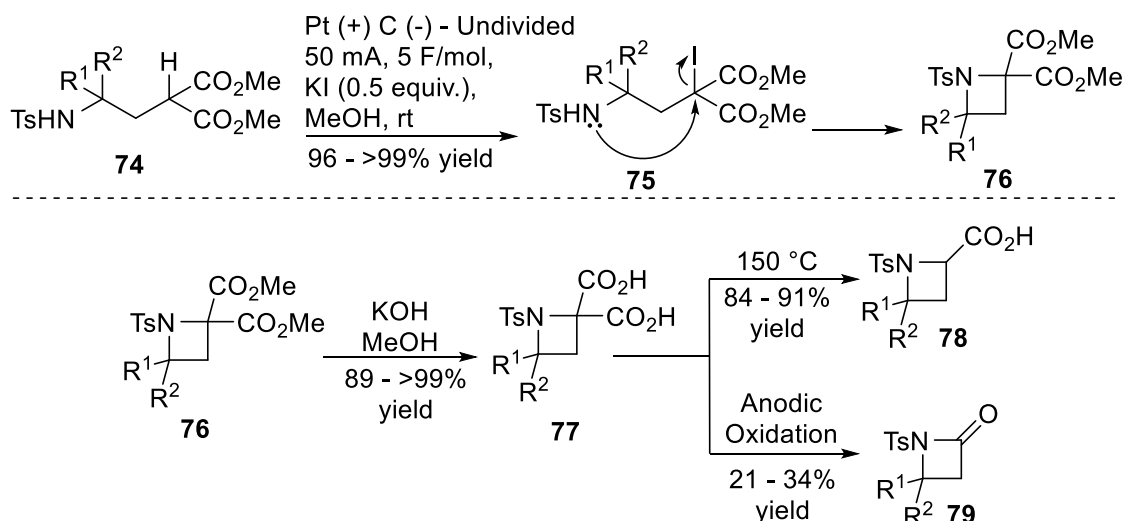
Ashikari *et al.* reported a pyrrolidine cyclisation utilizing the cation pool methodology to generate halogen and phenylchalcogen cations *in-situ*, Scheme 15. Tetrabutylammonium iodide (**60**) or bromide (**61**), diphenyl disulfide (**62**) and diphenyl diselenide (**63**) are subjected to electrolysis in DMSO at -78 °C to form the stabilized cation *in-situ* (**64**). The cation (**64**) adds over an alkene (such as **65**) where the R group adds to the *endo*-position and DMSO adds to the *exo*-position which is subsequently oxidized with triethylamine in a Swern oxidation affording (**66**). The generation of the ketone (**66**) allows the nucleophilic sulfonamide to attack the ketone to generate a five-membered ring (**67a-d**). The reaction completed in 89% yield with both tetrabutylammonium iodide (**60**) and bromide (**61**) and in 99% yield with diphenyl diselenide (**63**); diphenyl disulfide (**62**) observed a large drop in performance with only 41% yield.<sup>9</sup>



**Scheme 16:** Kolbe electrolysis of carboxylic acids to afford pyrrolidine rings

Becking and Schäfer reported the intramolecular cyclisation of  $\beta$ -allylaminoalkanoates (**68**) to afford pyrrolidines (**69**) via the Kolbe electrolysis, Scheme 16. The starting material (**68**) and a co-acid (**70**) are both oxidised to afford radicals **71** and **72** respectively. Radical **71** reacts with the intramolecular alkene to afford radical pyrrolidine **73**, which is subsequently quenched with the co-acid's radical (**72**) to afford the desired product **69**. The reaction was used for the formation of 12 pyrrolidines in 45 – 67% yield<sup>69</sup> and was further explored for the formation of tetrahydrofuran rings<sup>70</sup> as well as the synthesis of prostaglandin precursors.<sup>71</sup>

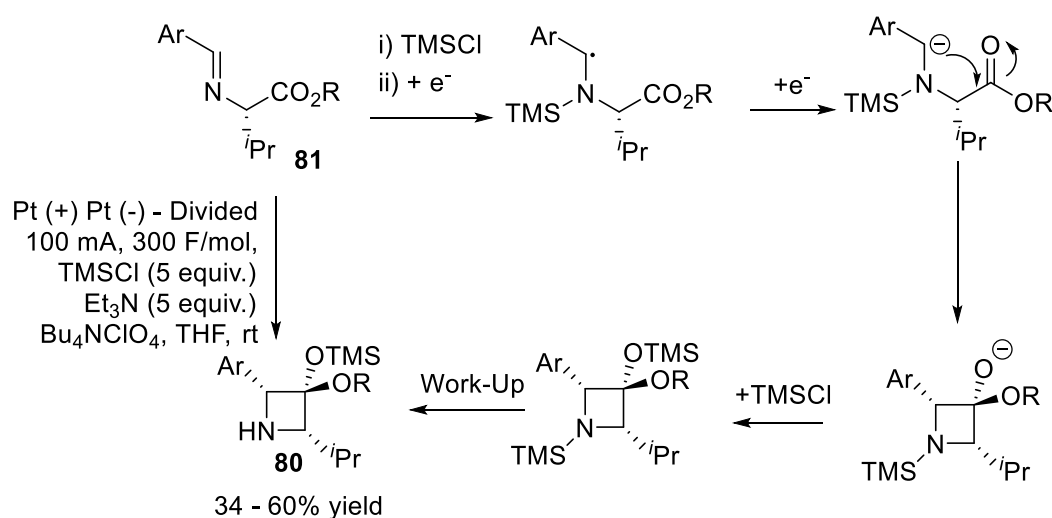
### 1.2.3. Electrochemical Synthesis of Azetidines



**Scheme 17:** Electrochemical formation of 2,2-dicarbonyl-*N*-tosylazetidines (where  $n = 1$ )

Shono *et al.* extended their work on cationic halogen intermediates (as seen in Scheme 10) and developed a cyclisation with  $\gamma$ -malonate sulfonamides (**74**). Electrochemical addition of iodine into the  $\alpha$ -position of the malonate to afford **75** was possible with 0.5 equiv. of potassium iodide which allowed the nucleophilic nitrogen to attack (**75**) and form a ring (**76**), Scheme 17 (top). Yields were impressive for the formation of azetidines, with quantitative yields reported when using gem-dimethyls (**76**,  $R^1 = R^2 = \text{Me}$ ) and without gem-dimethyls (**76**,  $R^1 = R^2 = \text{H}$ ); when **74** was substituted with  $R^1 = \text{Me}$  and  $R^2 = \text{H}$ , a good 96% yield was observed for azetidine formation. The same methodology was applied for the synthesis of pyrrolidine rings which afforded the desired product in 85% yield and for an aziridine, the three-membered congener, was also able to be synthesised,

however in a reduced yield of 46%. The reaction had a strong dependence on the halogen, where changing from potassium iodide to potassium bromide and chloride saw a drastic decrease in the yield when attempting to form the azetidine product (**76**,  $R^1 = R^2 = H$ ) with the iodide producing >99% yield, the bromide 75% yield and the chloride 14% yield. The azetidine product (**76**) is a versatile moiety and can be easily hydrolysed to a dicarboxylic acid (**77**) with potassium hydroxide and methanol. The dicarboxylic acid (**77**) could be further reacted to generate an  $\alpha$ -amino acid (**78**), which was achieved by simply heating **77** at 150 °C for five minutes. Alternatively, **77** could be subjected to anodic oxidation to generate  $\beta$ -lactams (**79**) although in low yields of 21% with  $R^1 = R^2 = H$  or 34% yield when  $R^1 = Me$  and  $R^2 = H$ , Scheme 17 (bottom).<sup>72</sup>

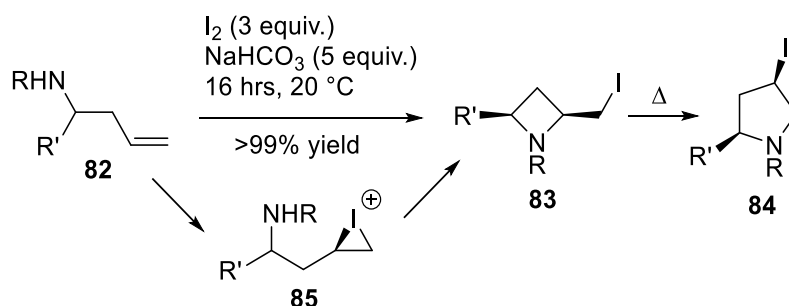


**Scheme 18:** Electrochemical reduction of imines facilitating an intramolecular cyclisation to azetidines

Kise *et al.* demonstrated a series of cyclisations to afford azetidines (**80**) *via* the electroreduction of imines (**81**) derived from naturally occurring amino acids, Scheme 18. Attempting the reaction with no trimethylsilyl chloride and triethylamine resulted in complete reduction of the imine bond (**81**) and no cyclisation; attempting the reaction with trimethylsilyl chloride but no triethylamine does successfully complete the reaction in 50% yield. With both reagents the optimum result of 62% yield was obtained when **81** was substituted with Ar = Ph, R = Me. The reaction is highly stereoselective between the 2- and 4- positions demonstrating 85% ee in the worst case and when using bulky groups (Ar = 2-naphthyl, R = <sup>t</sup>Bu) >99% ee was observed.<sup>73</sup>

### 1.3. Project Aims

The main aim of the project is to synthesise azetidine- and pyrrolidine-derivatives *via* electrochemical methodology and hence produce the target products in a more environmental benign way in comparison to prior works reported from the Fossey group. The iodocyclisation methodology was first published in 2010<sup>11</sup> and further developed in 2013.<sup>12</sup> It is a robust method that affords quantitative yields for a variety of homoallylamine substrates (**82**) with selective formation of *cis*-2,4-azetidines (**83**). *cis*-3,5-Pyrrolidines (**84**) can be made easily from the methyliodoazetidine (**83**) by warming the azetidine to 50 °C, Scheme 19.



**Scheme 19:** Cyclisation of homoallyl amines with the use of iodine

The reaction described in Scheme 19 proceeds with the addition of iodine over the alkene of the homoallylamine (**82**) to form an iodonium intermediate (**85**) which is followed by nucleophilic attack of the nitrogen (which is protected with some form of benzyl substituent) to afford an iodoazetidine (**83**). High stereoselectivity is observed between the substituent in the 2-position and the iodomethylene group; this is justified by observing the two viable transition states, as seen in Figure 6. The iodonium intermediate (**85**) exists in either a pseudo-equatorial (**86**) or pseudo-axial (**87**) form, the latter being more unfavourable in comparison to the former, hence exclusive 2,4-*cis* azetidines (**83**) are formed.<sup>12</sup>

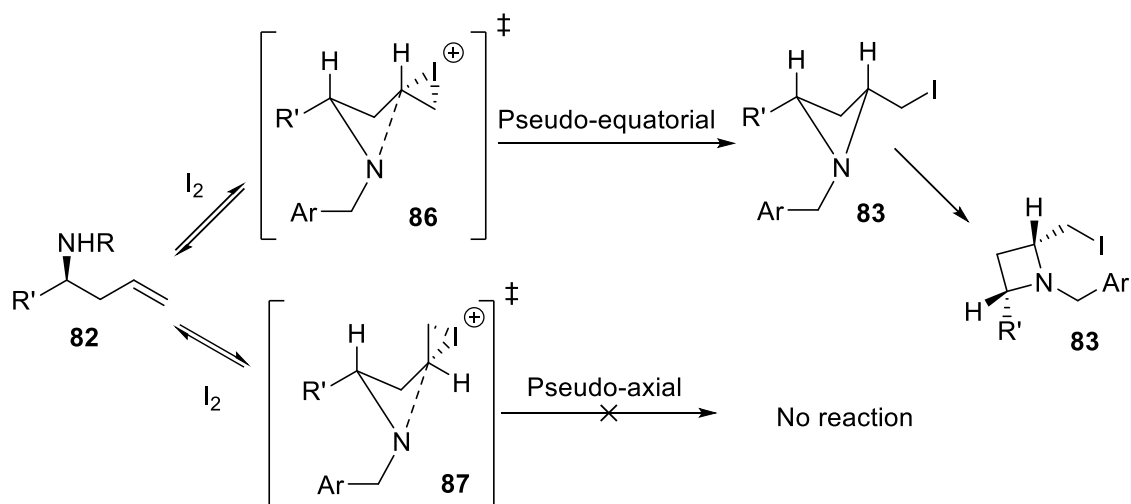


**Figure 6:** Rationalisation of the observed *cis*-stereochemical outcome of the iodocyclisation of homoallyl amines

The iodocyclisation reaction also has a peculiar base and solvent dependence which can radically change the product outcome, Figure 7. Screening the reaction with acetonitrile alongside various bases produces a wide range of product ratios, for example: sodium carbonate forms 61% azetidine (83) and 39% pyrrolidine (84) whereas sodium acetate provided a small increase to azetidine formation with 68.5% azetidine (83) and 31.5% pyrrolidine (84) formation. Some bases provided unwanted side products, such as when using potassium carbonate, which formed 35.5% of the desired azetidine (83) but the other 64.5% was from an oxidation reaction to form an imine (88). Caesium carbonate was the worst base for the cyclisation reaction and was the only one to yield no cyclic moieties, instead it surprisingly only oxidised the homoallylamine and exclusively produced imine products 88 and 89.<sup>74</sup> Sodium bicarbonate was confirmed as the best base for azetidine formation with 100% azetidine (83) selectivity. Keeping the base constant with sodium bicarbonate and utilising different solvents resulted in either azetidine (83) products in partial conversion or a mixture of azetidine (83), pyrrolidine (84) and imine (88) therefore acetonitrile and sodium bicarbonate was the optimum combination for azetidine formation.<sup>12</sup>

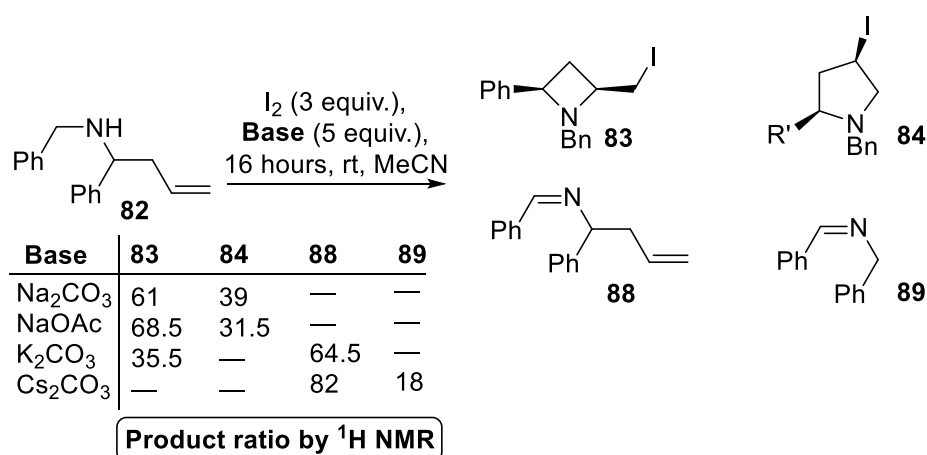
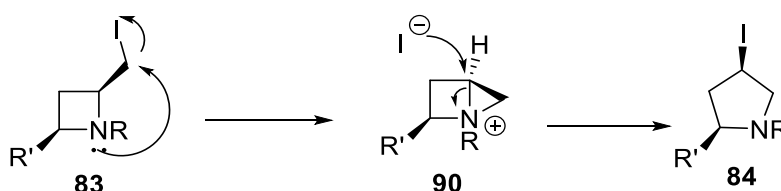


**Figure 7:** Product distribution for the iodocyclisation with various bases

Temperature is an important parameter to maintain constantly below 50 °C with the iodocyclisation method; if the reaction is heated to at least 50 °C, the iodomethylazetidine (**83**) rapidly ring expands to the respective 3,5-pyrrolidine ring (**84**), Scheme 20. Evidence of the bicyclic intermediate (**90**) has been demonstrated by computational studies from Couty *et al.*<sup>44</sup> and analogous reactions have been observed from other groups with the formation of pyrrolidine aziridinium intermediates that ring expanded to the respective piperidines.<sup>45,46</sup> With the azetidine (**81**) as the desired target, the iodine was required to be substituted relatively quickly, and was easily replaced with a large selection of amines.<sup>12</sup>



**Scheme 20:** Ring expansion of iodomethylazetidines *via* thermolysis

The iodocyclisation is a good method to form azetidines (**83**) but there are some issues with the method, such as the stability of the product after the cyclisation, which rapidly ring expands to a pyrrolidine (**84**) at 50 °C which makes removing solvent (typically at 40 °C with a rotary evaporator) a concern. Another issue is the amount of reagents required, three equivalents of iodine and five equivalents of sodium bicarbonate is a significant excess for both of these reagents and there are several risks with using iodine such as its toxicity to aquatic life and the potential of organ damage through repeated exposure.<sup>75</sup> With electrochemical methodology, the aim is to provide a more effective and less environmentally impacting route to synthesising the 4-membered moieties.

Nitrogen-containing heterocycles have been a mainstay in academia and pharmaceuticals and are prevalent throughout their history. Pyrrolidines are present in a large host of naturally-containing molecules, such as nicotine (**91**)<sup>76</sup> and L-proline (**92**).<sup>77</sup> Azetidines are not very common in nature with

only a few examples, such as L-azetidine-2-carboxylic acid (**93**) (L-Aze, a proline analogue),<sup>78</sup> mugineic acid (**94**)<sup>79</sup> and penaresidin A (**95**) and B (**96**), Figure 8.<sup>80</sup> Azetidines are however useful building blocks in synthesis,<sup>81</sup> advantageous monomers in polymerisation<sup>82</sup> and are useful scaffolds in asymmetric catalysis when behaving as ligands or organocatalysts<sup>83</sup> (discussed at further length in Section 3).

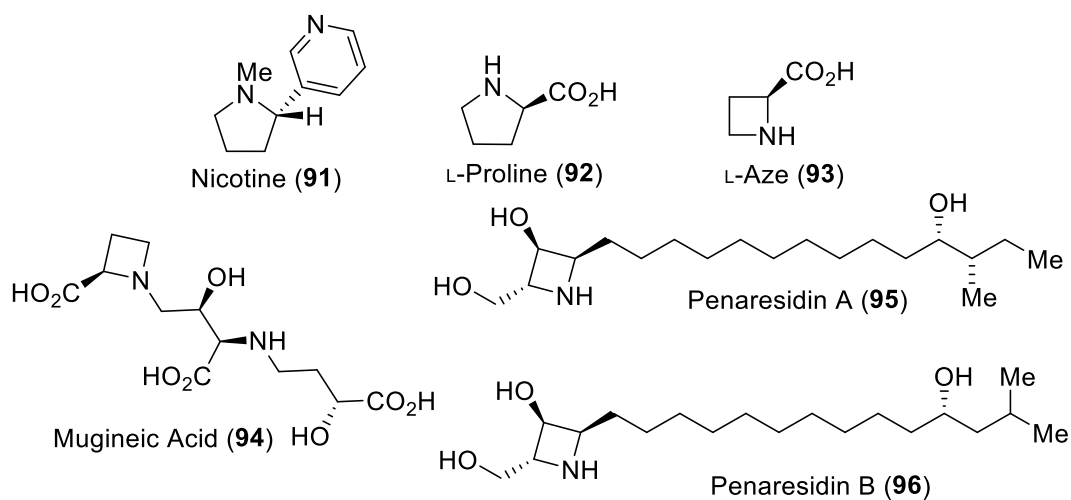


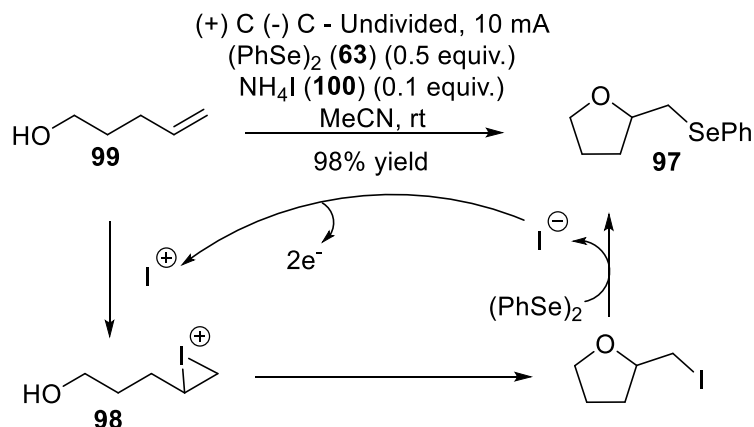
**Figure 8:** A selection of nitrogen-containing heterocycles found in nature



## 2. Discussion and Results

### 2.1. Synthesis of Pyrrolidines

#### 2.1.1. Electrochemical Synthesis of 2-((Phenylselenenyl)methyl) Heterocycles



**Scheme 21:** Proposed mechanism for an electrochemical iodocyclisation, reported by Meng *et al.*

Various electrochemical methods have been presented in the literature to synthesise oxygen-containing heterocycles *via* the use of diphenyl diselenide (**63**) in recent years<sup>84, 85</sup> and in the 1980s.<sup>86-88</sup> Meng *et al.* reported a relatively straightforward procedure for the formation of cyclic ethers (**97**) and lactones, which ranged from 5- to 11-membered rings, with a reaction that was proposed to proceed *via* an iodonium intermediate (**98**), Scheme 21.<sup>84</sup> The authors also stressed the high importance of the electrolyte material, as the reaction would only work with iodide-containing electrolytes with no reaction occurring when using ammonium bromide or chloride. With our methodology already demonstrating the intramolecular cyclisation of homoallylamines with iodine (Section 1.3.), it seemed appropriate to apply the same methodology for nitrogen-containing heterocycles.

To ensure this cyclisation was viable with the ElectraSyn 2.0, the first reaction replicated Meng *et al.*'s method from the literature and conducted the reaction with 4-penten-1-ol (**99**) under constant current with diphenyl diselenide (**63**) and ammonium iodide (**100**) in acetonitrile and worked as prescribed in the literature in 80% yield, Scheme 21. Following this, the same cyclisation was attempted using 4-methyl-*N*-(pent-4-en-1-yl)benzenesulfonamide (**65**), the sulfonamide analogue of 4-penten-1-ol (**99**), which afforded the desired pyrrolidine (**67d**) in an adequate 70% yield; the pyrrolidine was confirmed with its data matching Ashikari *et al.* whom had previously reported the compound.<sup>9</sup> Whilst this reaction was successful, it was noted that the anode was coated in a significant amount of yellow material, which was most likely excess diphenyl diselenide (**63**) coating the electrode. This was believed to be potentially hindering the reactivity by reducing the surface area at

which the reaction could occur on the electrode. Therefore, the reaction was attempted again with the polarity of the electrodes alternating every ten minutes which hindered the build-up upon the electrode surface and facilitated a slight increase to 79% yield.

By using the default conditions by Meng *et al.* for the cyclisation of aminoalkenes to afford pyrrolidines already showing sufficient results, a brief optimisation study was conducted. The aim of the optimisation was to investigate if changing the electrode combination could further improve the reaction to produce quantitative (or near-quantitative) yields, which would be comparable to Meng *et al.*'s results. It is important to note that platinum electrodes were not used as anode material per IKA's advice on their product page because platinum plated on copper electrodes are not as sturdy compared to platinum foil and platinum plated on ceramics.<sup>89</sup> Results were relatively poor when graphite was paired with an electrode of a different material as seen in Table 2, entry 4 - 6. The reticulated vitreous carbon (RVC) electrode performed relatively well when paired with a second RVC electrode producing a 58% yield. RVC and platinum as anode and cathode respectively produced a 64% yield. Ultimately, these yields were not comparable to entry 2's result (79% yield) so the dual graphite combination was maintained for future reactions.

**Table 2:** Electrode optimisation for the electrochemical cyclisation of 4-methyl-*N*-(pent-4-en-1-yl)benzenesulfonamide (**63**)

Electrode Optimisation				
Entry	Anode	Cathode	Alternating Polarity? <sup>a</sup>	Isolated Yield <sup>b</sup>
1	Graphite	Graphite	✗	70%
2	Graphite	Graphite	✓	79%
3	RVC	RVC	✓	58%
4	Graphite	RVC	✗	21%
5	RVC	Graphite	✗	43%
6	Graphite	Platinum	✗	9%
7	RVC	Platinum	✗	64%

<sup>a</sup> The polarity of the electrodes were alternated every ten minutes <sup>b</sup> Isolated yields after purification *via* column chromatography

The electrochemical synthesis of pyrrolidine (**67d**) had been demonstrated once before by Ashikari *et al.*<sup>9</sup> which was discussed in Section 1.2.2., Scheme 15. They reported 99% yield for the reaction to yield **67d**, but their reaction protocol was slightly cumbersome in regard to the temperature requirements, which required a cation pool (at  $-78^{\circ}\text{C}$ ), followed by addition of the alkene at  $0^{\circ}\text{C}$  and a Swern oxidation at room temperature. By comparison, this procedure is significantly more

straightforward with it being a simple one-pot procedure that is run at room temperature for the duration.

### 2.1.2. Synthesis of Pyrrolidine Precursors

4-Methyl-*N*-(pent-4-en-1-yl)benzenesulfonamide (**65**) was synthesised from 5-bromopent-1-ene (**101**) via refluxing *para*-toluenesulfonamide (**102**) and potassium carbonate (**103**) in acetone for 24 hours in 45% yield.<sup>90</sup> To expand the scope of the method, 2-substituted derivatives of 4-methyl-*N*-(pent-4-en-1-yl)benzenesulfonamide (**65**) were synthesised (**104a-h**), as well as a substrate that incorporated an aromatic ring within the alkyl chain (**105**), all compounds are pictured in Figure 9.

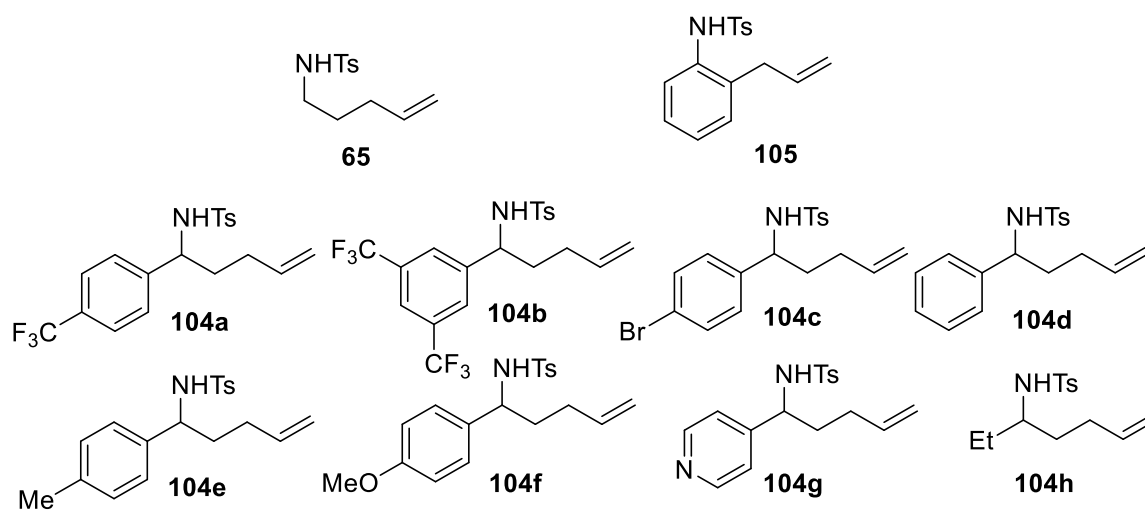
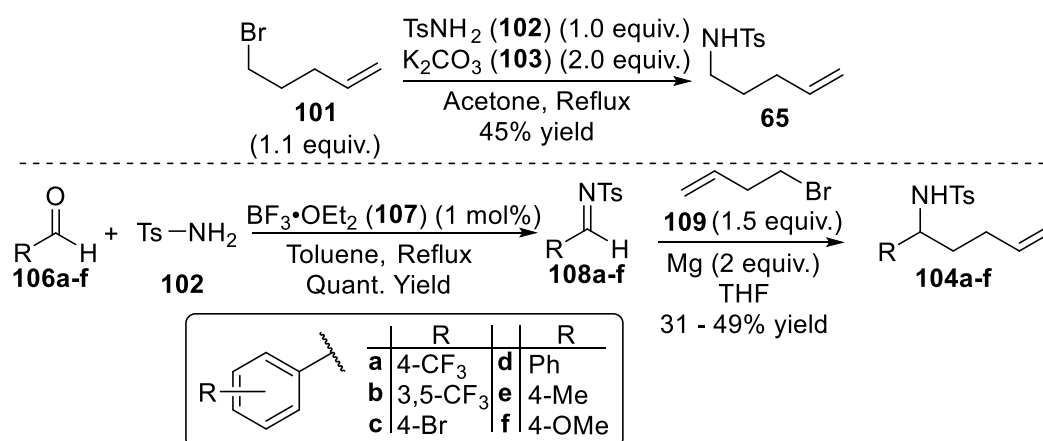


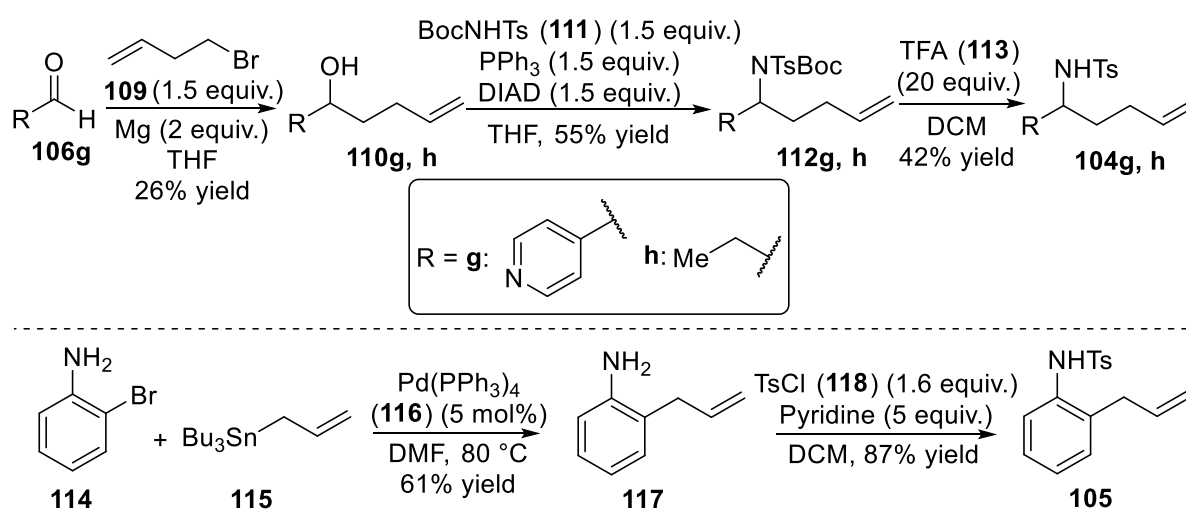
**Figure 9:** All substrates that were synthesised and tested for electrochemical cyclisations in this work

Substrates **104a-f** were synthesised in two steps: the first step required the reflux of benzaldehydes (**106a-f**) and *para*-toluenesulfonamide (**102**) in toluene with a catalytic amount of boron trifluoride etherate (**107**) to generate the desired imine (**108a-f**) which was carried on to the next step without purification.<sup>91</sup> The imine (**108a-f**) was then subjected to a Grignard reaction with 4-bromobutene (**109**) to generate the desired product (**104a-f**) in 34 – 49% yield, Scheme 22.<sup>92</sup> Yields were somewhat poor due to the imine (**108a-f**) typically containing some *para*-toluenesulfonamide (**102**) and/or benzaldehyde (**106a-f**) leftover from the previous step and a notable portion of the product mixture recovered after purification contained the reduced imine. Regardless, the amount of **104a-f** obtained was sufficient to allow multiple attempts of the electrochemical cyclisation.



**Scheme 22:** Reaction schemes for the synthesis of 4-methyl-*N*-(pent-4-en-1-yl)benzenesulfonamide (**65**) (top) and 2-substituted derivatives (**104a-f**) (bottom)

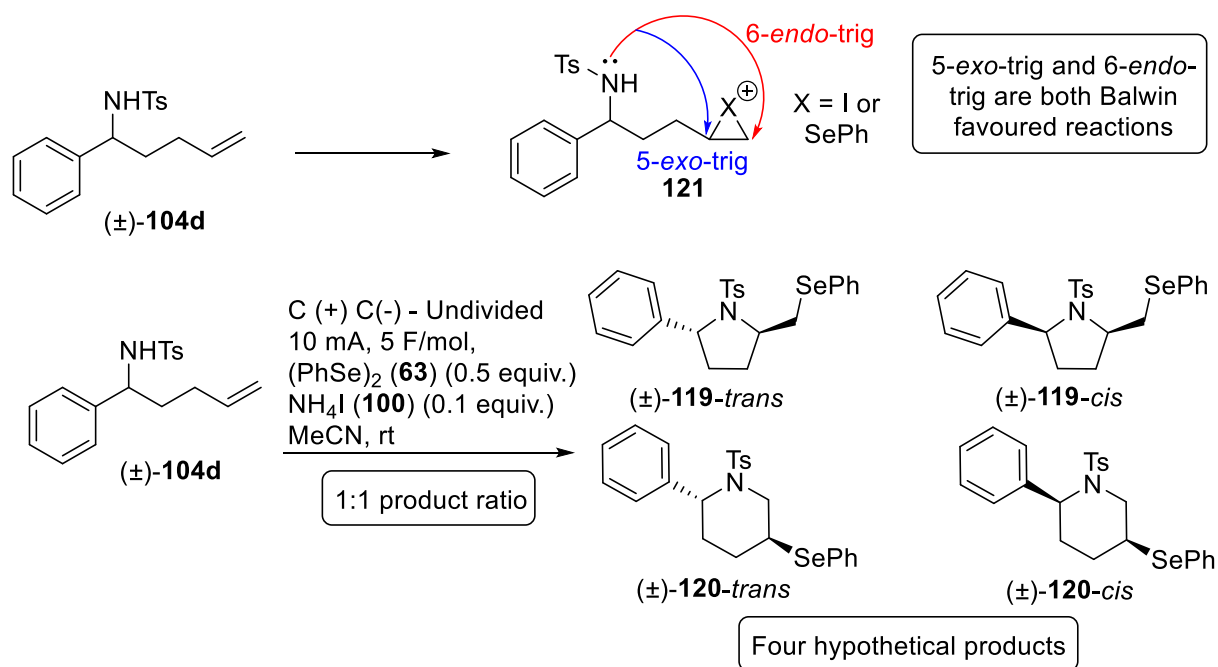
Attempting to synthesise the imine (**108g**) where R = 4-pyridine was not possible, so an alternative synthesis was used: 4-pyridinecarboxaldehyde (**106g**) was subjected to a Grignard reaction of 4-bromobutene (**109**) where the resultant alcohol (**110g**) was substituted *via* a Mitsunobu reaction with *tert*-butyl tosylcarbamate (**111**) to afford **112g**. The Boc group upon **112g** was subsequently removed with an excess of trifluoroacetic acid (**113**) providing **104g**, Scheme 23 (top).<sup>93</sup> The ethyl substituted substrate (**104h**) was synthesised in a similar manner from the commercially available 6-hepten-3-ol (**110h**). Substrate **105** was produced in its own unique procedure: starting from 2-bromoaniline (**114**) and reacting it with allyltributylstannane (**115**) and palladium tetrakis(triphenylphosphine) (**116**) *via* a Stille coupling afforded 2-allylaniline (**117**) in 61% yield.<sup>94</sup> The aniline (**117**) was then subsequently protected with a tosyl group with *para*-toluenesulfonyl chloride (**118**) to afford **105** in 87% yield, Scheme 23 (bottom).<sup>95</sup>



**Scheme 23:** Reaction schemes for the synthesis of 2-substituted derivatives of 4-methyl-*N*-(pent-4-en-1-yl)benzenesulfonamide **104g** and **104h** (top) and for *N*-(2-allylphenyl)-4-methylbenzenesulfonamide (**105**) (bottom)

### 2.1.3. Expansion of Methodology

With the successful synthesis of 2-((phenylselanyl)methyl)-1-tosylpyrrolidine (**67d**) with 4-methyl-*N*-(pent-4-en-1-yl)benzenesulfonamide (**65**) (Section 2.1.1.), the methodology was expanded with the use of sulfonamide **104d** which contained a phenyl group in the 2-position. Attempting the reaction with **104d** produced two products which were separable by TLC and column chromatography, although obtaining pure product was rather challenging because the  $R_f$  values were quite similar. Approximately 30 mg of each product was isolated from the reaction producing a relatively poor 13% yield for each product, 26% total yield, which indicated a 1:1 product ratio. With pure material of both products in hand, it was difficult to decipher what cyclised products were produced in the reaction and the  $^1\text{H}$  NMR spectra of the two products were quite different from each other in the aliphatic region. It was assumed that the two products were either a pair of regioisomers (mixture of **119-trans** and **120-trans** or the *cis* equivalent) or diastereoisomers (mixture of **119** rings or **120** rings), all potential products are pictured in Scheme 24. Considering the reaction potentially went through some three-membered intermediate, such as **121**, it would be theoretically possible for both 5- and 6-membered rings to form with both 5-*exo*-trig and 6-*endo*-trig being Baldwin favoured reactions.<sup>96</sup>



**Scheme 24:** Reaction of **104d**, hypothesised to react *via* intermediate **121**, which was subsequently hypothesised to have formed two of the four illustrated products

The reaction described in Scheme 24 was repeated with **104a**, **104b**, and **104c** which were substituted with a 4-trifluoromethyl, 3,5-bis(trifluoromethyl) and a 4-bromo, group respectively upon the  $\alpha$ -aromatic ring. Similar results were observed in all cases, with the reaction producing a mixture of two products that had a similar  $R_f$  value, alongside closely related NMR spectra of the two products. Importantly, the unknown product that had the higher  $R_f$  value (termed product "A") and the second

unknown product that had the lower  $R_f$  value (termed product “B”) were the same type of cyclised product for all substrates cyclised thus far.

#### 2.1.4. Identification of Products

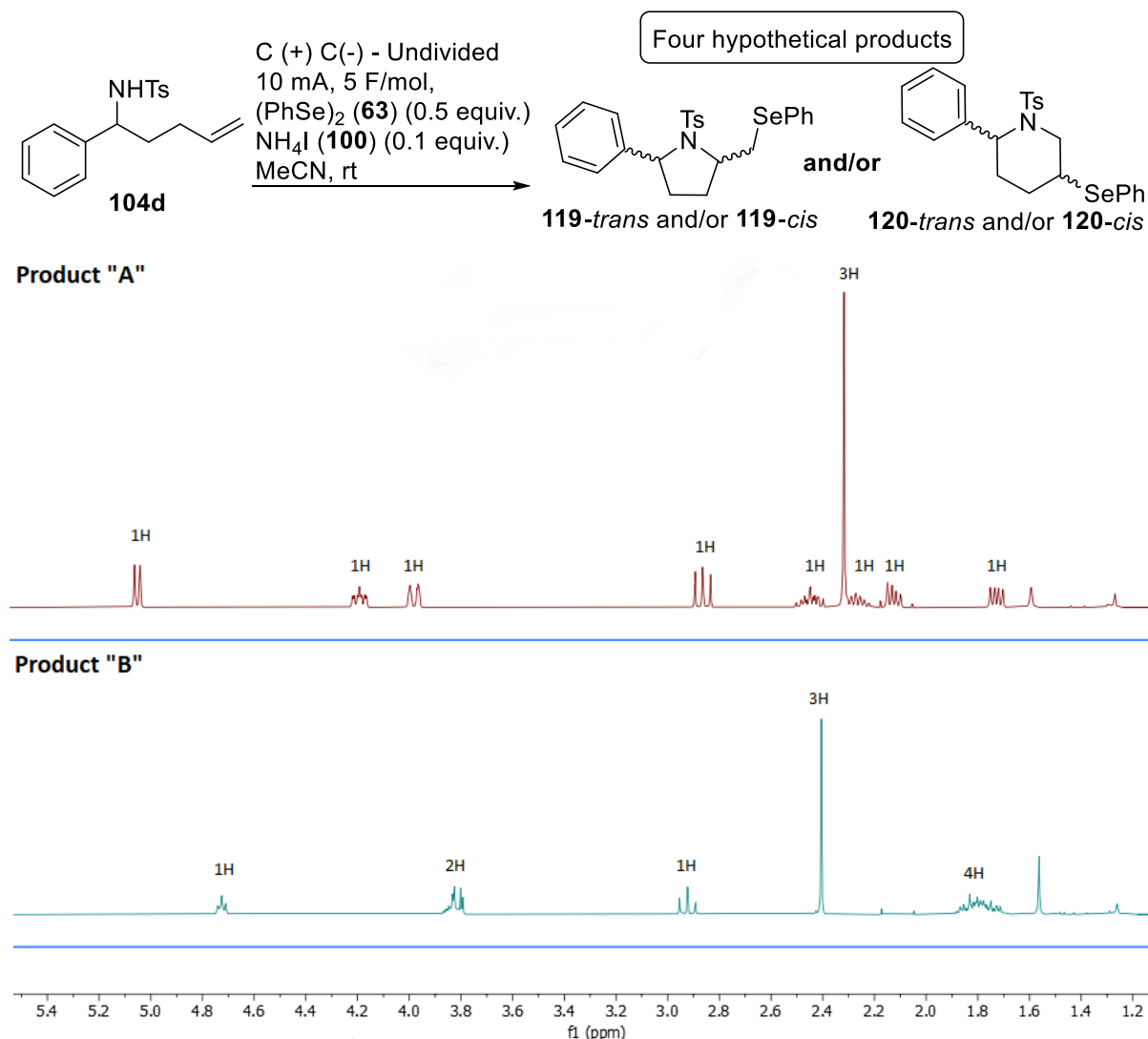


**Figure 10:** NMR spectra for the two unknown products of the electrochemical cyclisation reaction of **104d** in CDCl<sub>3</sub> (400 MHz). Only the aliphatic region is pictured. Unknown product “A” is on top, unknown product “B” is below.

Working out the identities of the two products from the electrochemical cyclisation reaction (Scheme 24, Section 2.1.3.) was a difficult task with four potential products in mind that would all have similar coupling patterns in their respective NMR spectra. Using other standard analytical tools did not greatly assist in this endeavour either, with mass spectrometry giving the same mass for both products and both IR spectra were near identical too, which at least confirmed the two products were highly likely to be isomers. In particular, product “B” was much harder to solve *via* NMR techniques with many peaks appearing at the same frequency on the NMR spectrum, which caused notable peak overlap at approximately 1.8 ppm and 3.8 ppm, Figure 10, which meant that attempting to elucidate the structure, even with 2D NMR techniques, would have been inconvenient. Product “A”’s NMR

spectrum, in contrast, was much easier to interpret, where all the peaks appeared at different frequencies and had minimal peak overlap, Figure 10. To ease the task of identifying both products, it was envisaged that obtaining a crystal structure for at least one of the products would help elucidate the NMR spectra for both rings. If one of the structures were confirmed by X-ray diffraction, we could then interpret the NMR data and accurately assign peaks to carbon and hydrogen atoms. It should then be possible to analogously assign some atoms to its isomer because certain atoms are in a similar position, such as the two  $\alpha$ -carbons adjacent to the nitrogen in the ring. Fortunately, with all reactions attempted so far, product “A” had consistently been a solid, so all compounds were grown for a single crystal *via* vapour diffusion with DCM and hexane.

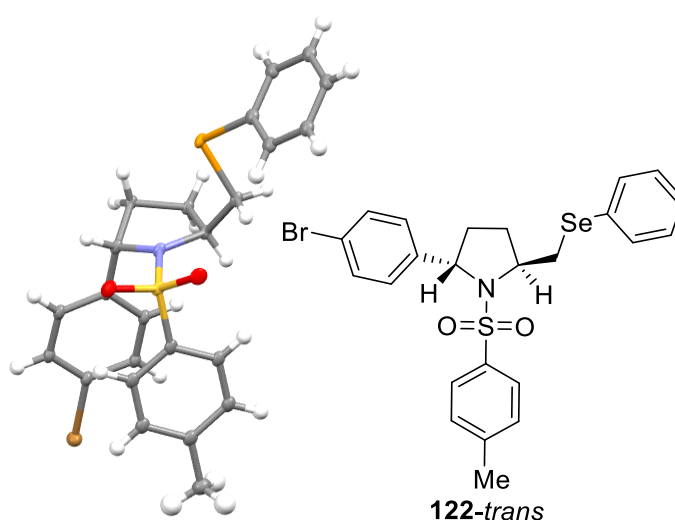


**Figure 11:** X-Ray crystal structure of *trans*-pyrrolidine **122-trans**. Ellipsoids drawn at 50% probability level

The reaction of **104c** under the electrochemical conditions, described in Section 2.1.3., afforded product “A” as pyrrolidine **122-trans**, which was confirmed *via* single crystal X-ray diffraction, performed by Dr. Louise Male, Figure 11. The pyrrolidine was also confirmed to exist as a fifty-fifty mixture of (*S,S*) and (*R,R*)-diastereomers, which was expected with the reaction using a racemic starting material. Some interesting features of the ring (**122-trans**) were observed from the crystal structure. First of all, it appeared that intramolecular  $\pi$ -stacking was occurring between the phenyl ring of the tosyl protecting group and the 2-substituent with a centroid-centroid distance of 3.674(5) Å and a plane-centroid distance of 3.310(8) Å in the solid state (Figure 12), which would provide increased stability to the structure by approximately 1.48 Kcal/mol.<sup>97</sup> In fact, **122-trans** in the solid state was observed to pack with one intramolecular and one intermolecular  $\pi$ -stacking interaction, which would enhance stability to the compound, Figure 13. Another interesting feature was that the C-S-N bond angle around the tosyl protecting group was bent (108.8°) and the nitrogen was relatively planar in the ring, which is indicative of  $sp^2$  hybridisation. This  $sp^2$  character has been explained due to the strong  $d\pi$ - $p\pi$  bonding caused by nitrogen donating its lone pair of electrons into one of sulfur’s

empty 3d orbitals, Figure 14. Cotton and Stokely observed this interaction with dibenzenesulfonamide<sup>98</sup> and similar results have been reported from Klug with *N*-phenylmethanesulfonamide<sup>99</sup> and Jordan *et al.* with tetramethylsulfamide.<sup>100</sup> Laughlin and Yellin have also been able to demonstrate this effect *via* NMR studies of sulfonamides under neutral and acidic conditions.<sup>101, 102</sup>

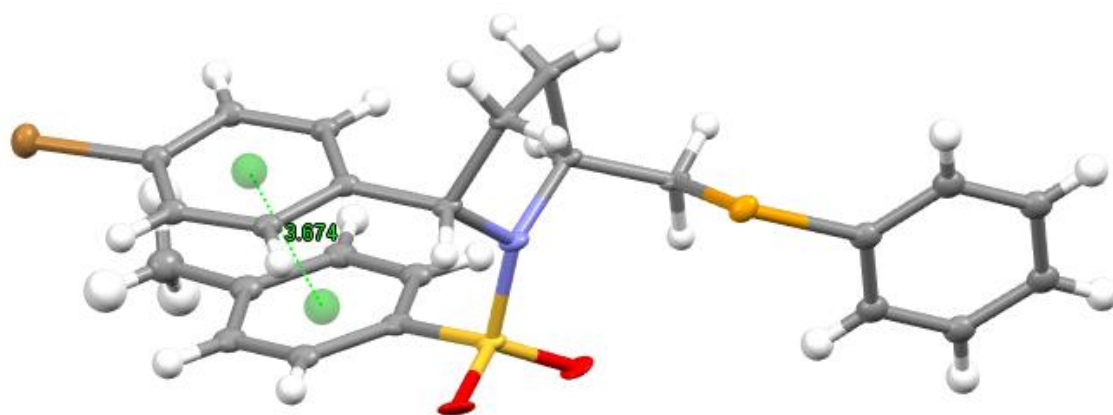


**Figure 12:** Intramolecular  $\pi$ -stacking of aromatic rings upon **122-trans** in the solid state. A centroid-centroid distance of 3.674(5) Å was calculated (highlighted in green)



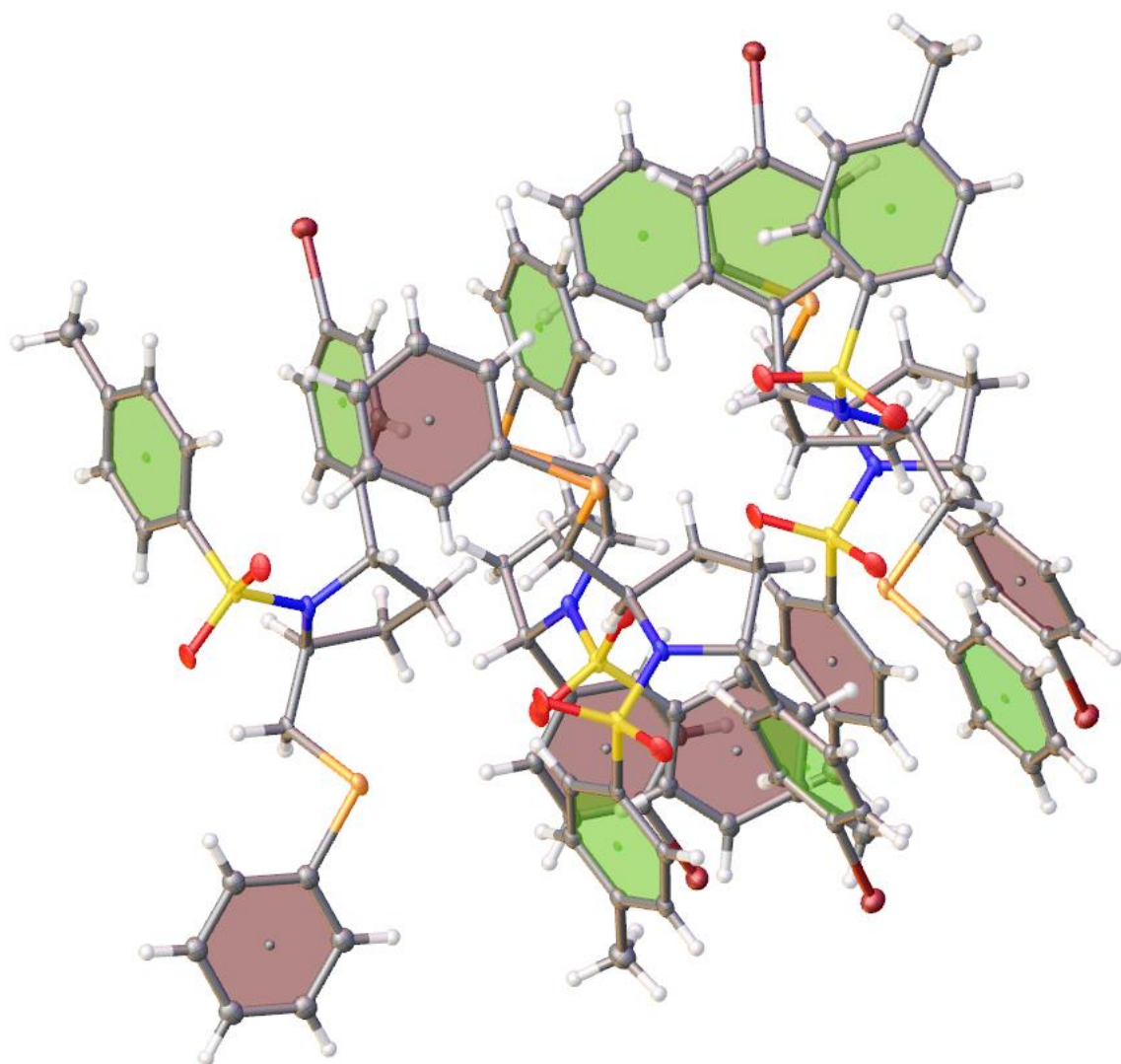


**Figure 13:** Packing of **122-trans**, which forms stacks of three rings allowing one intramolecular and one intermolecular  $\pi$ -stack facilitating interactions between two molecules of **122-trans**. Stacked rings are highlighted in green.

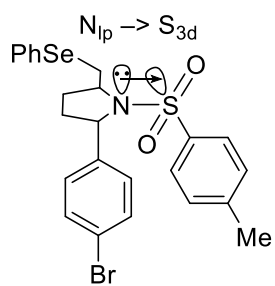


**Figure 14:** Lone pair of nitrogen donating into one of the sulfur's empty 3d orbitals providing some  $sp^2$  character for the N-S bond

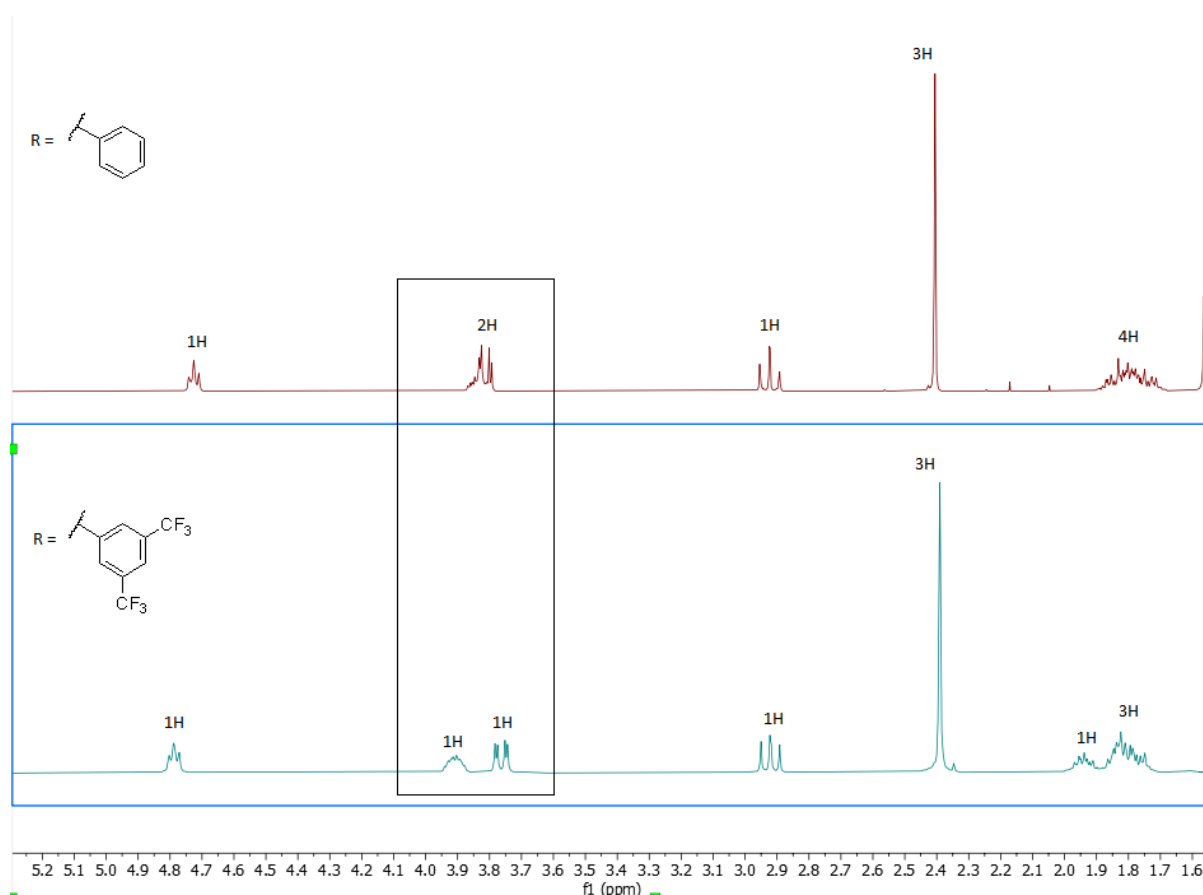


**Figure 15:** NMR spectra of unknown product "B" when  $\text{R} = \text{Ph}$  (top) and  $\text{R} = 3,5\text{-bis(trifluoromethyl)phenyl}$  (bottom) in  $\text{CDCl}_3$  (400 MHz). Only the aliphatic region is pictured.

Working out the identity of product "B" of the electrochemical cyclisation reaction was now the focus which still had some issues regarding the resolution of the multiplets. Recording a  $^1\text{H}$  NMR spectrum at 500 MHz still did not provide sufficient resolution of the multiplets and changing the solvent to benzene- $d_6$  (which in some scenarios provides better peak separation and/or resolution)<sup>103</sup> did not help either to remedy the issue when analysing product "B" of the cyclisation with the phenyl substituted substrate (**104d**). Fortunately, the  $^1\text{H}$  NMR spectrum of product "B" of the electrochemical cyclisation reaction with the 3,5-bis(trifluoromethyl) substrate (**104b**) had improved resolution of two key multiplets around 3.8 ppm, which is highlighted in Figure 15. With the multiplet at 3.8 ppm now separated into a clear multiplet and a doublet of doublets, assignment with 2D NMR techniques, such as COSY, HSQC and NOESY, was now possible which allowed the full structure to be elucidated.

Firstly, analysing the  $^{13}\text{C}$  JMOD NMR spectrum alongside a HSQC NMR spectrum allowed rapid assignment of carbons to protons. The protons that were at 4.8 ppm and 3.9 ppm on the  $^1\text{H}$  NMR spectra, had a HSQC correlation to carbons that only contained a single hydrogen as inferred from the JMOD spectrum. The  $^1\text{H}$  NMR signals at 3.8 ppm and 2.9 ppm were diastereotopic protons that are attached to the same carbon; these protons had exclusive  $^1\text{H}$ - $^1\text{H}$  coupling (from COSY NMR

spectrum) to the proton at 3.9 ppm which allowed the following assignments, shown in Figure 16, for the three hypothetical products.

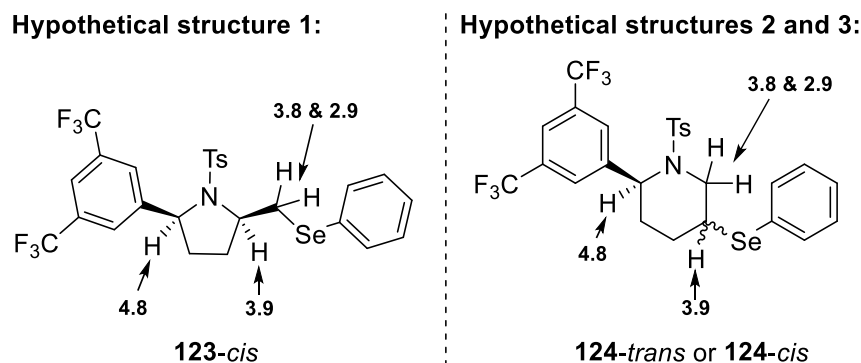


**Figure 16:** Proton assignments of all three hypothetical structures of product “B”; numbers indicate the ppm of the respective proton(s) in CDCl<sub>3</sub> (400 MHz)

From the proton assignments shown in Figure 16 and discussed in the previous paragraph, HMBC became an invaluable tool to determine the ring size. The diastereotopic protons (corresponding to signals in the <sup>1</sup>H NMR spectrum at 3.8 and 2.9 ppm) observed a HMBC coupling to a quaternary aromatic carbon, which was the phenylic carbon bonded to selenium. The proton assigned at 3.9 ppm did not observe any HMBC coupling to carbons in an aromatic carbon environment. Also, the proton signal at 4.8 ppm observed HMBC coupling with all aliphatic carbons within the ring, except the carbon attached to the previously mentioned diastereotopic protons, Figure 17. With this key information, both points lined up with product “B” being the *cis*-pyrrolidine ring (**123-*cis***) and running a NOESY NMR spectrum improved the validity of this theory with a NOESY correlation between the proton signals at 4.8 and 3.9 ppm, as seen in Figure 17. A crystal structure was obtained of **123-*cis*** which confirmed the NMR assignments, and the final structure was indeed a *cis*-pyrrolidine ring, Figure 18. With the structures of the two rings now fully confirmed with the use of single crystal X-ray diffraction and NMR, it was certain that the electrochemical cyclisation reaction was affording a mixture of two diastereomers, a *cis*- and a *trans*-pyrrolidine ring.

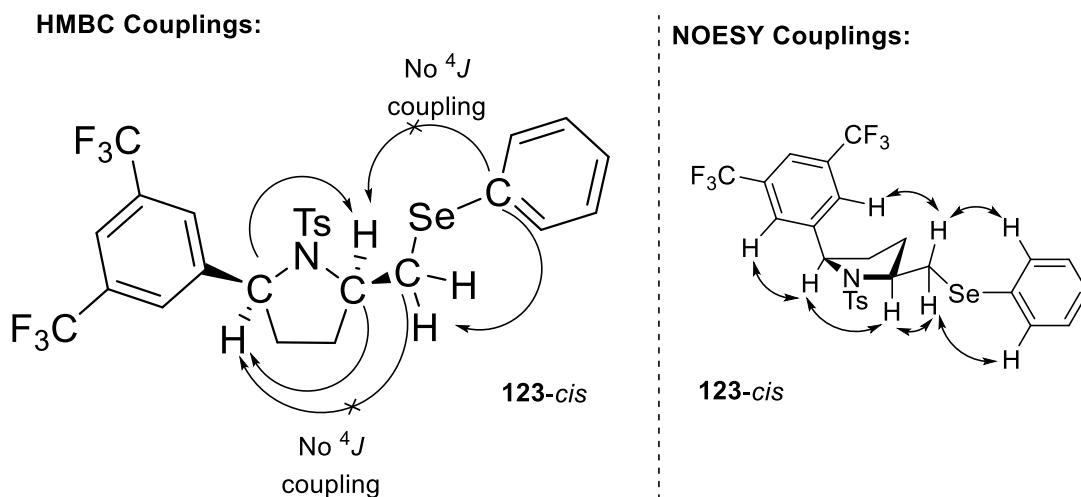


**Figure 17:** Key HMBC (left) and NOESY (right) couplings of **123-cis** that were used to determine the structure of product "B".

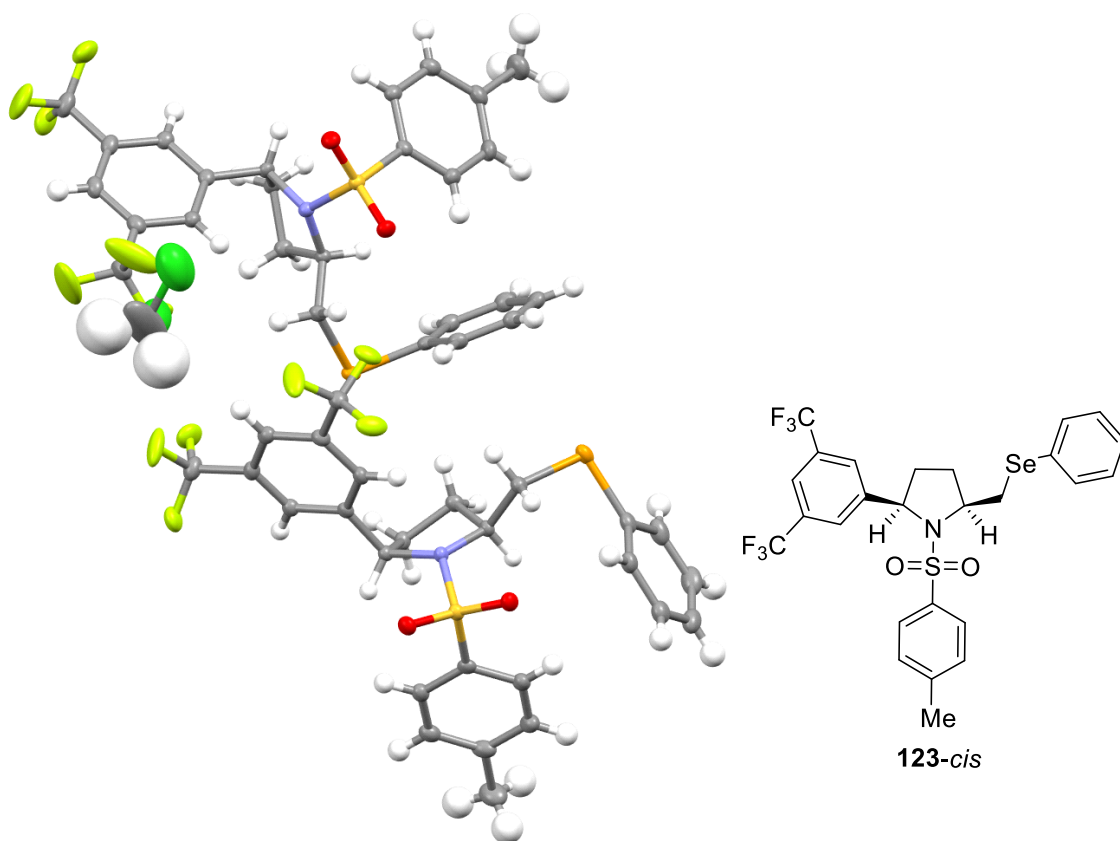
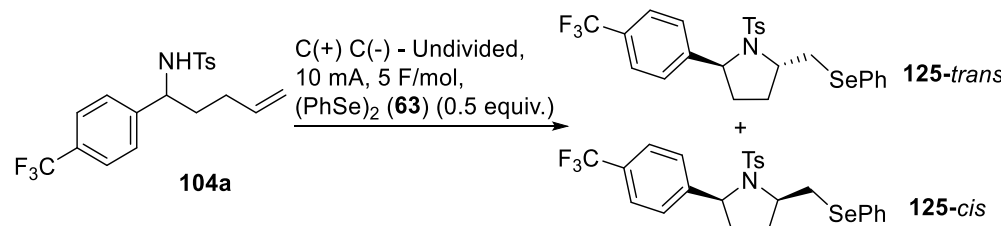


**Figure 18:** X-Ray crystal structure of *cis*-pyrrolidine **123-cis**. Two crystallographically independent molecules of **123-cis** are present per one molecule of DCM. Ellipsoids drawn at 50% probability level

### 2.1.5. Reaction Optimisation

Initial results for the electrochemical cyclisation reaction with the 2-substituted derivatives (**104a-d**) were relatively poor and it was believed a 1:1 mixture of *cis*- and *trans*-diastereoisomers was being formed. To achieve a level of selectivity for either product and to potentially gain some insight to the reaction, an optimisation study was conducted with the use of **104a** and its corresponding products (**125-trans** and **125-cis**). The reactions were all performed on a 0.1 mmol scale, where the only notable change to the conditions used previously (as described in Section 2.1.1. and Section 2.1.3.), was that the concentration of the reaction was at 0.04 M instead of 0.1 M and the amount of electrolyte was increased to 20 mol% (from 10 mol%) to ensure a sufficient current with the more dilute conditions.

**Table 3:** Reaction optimisation of the electrochemical cyclisation of **104a**. Results in bold are entries that generated the best results for *trans*- or *cis*-pyrrolidine formation



Entry	Electrolyte	Solvent	Conv. (%) <sup>a</sup>	<i>trans</i> (%) <sup>b</sup>	<i>cis</i> (%) <sup>b</sup>
1	NH <sub>4</sub> I	MeCN	>99	52	48
2	NaI	MeCN	>99	52	48
3	KI	MeCN	>99	53	47
4	NBu <sub>4</sub> I	MeCN	99	55	45
5	NBu <sub>4</sub> Br	MeCN	>99	56	44
6	NBu <sub>4</sub> Cl	MeCN	>99	48	52
7	NEt <sub>4</sub> OTs	MeCN	>99	48	52
8	NH <sub>4</sub> I	MeOH	>99	46	54
9	NH <sub>4</sub> I	EtOH	93	62	38
10	NH <sub>4</sub> I	DMF	84	65	35
11	NH <sub>4</sub> I	HFIP	>99	65	35
12	NBu <sub>4</sub> I	HFIP	>99	61	39
<b>13</b>	<b>NBu<sub>4</sub>Br</b>	<b>HFIP</b>	<b>&gt;99</b>	<b>21</b>	<b>79</b>
<b>14</b>	<b>NH<sub>4</sub>I</b>	<b>HFIP:H<sub>2</sub>O (9:1)</b>	<b>99</b>	<b>81</b>	<b>19</b>
15	NBu <sub>4</sub> Br	HFIP:H <sub>2</sub> O (9:1)	>99	79	21

<sup>a</sup> Conversion was determined *via* GC analysis with a calibration curve of the starting material <sup>b</sup> % of *trans*- and *cis*-products were determined *via* GC analysis with a calibration curve of both products.

The first phase of the optimisation investigated the use of the electrolyte with entry 1 (Table 3) utilising the standard conditions of ammonium iodide (**100**) and acetonitrile which confirmed the theory that the electrochemical cyclisation reaction under Meng *et al.*'s conditions<sup>84</sup> had little diastereoselectivity. Similar results were observed when using sodium and potassium iodide (Table 3, entry 2 and 3). The *trans*-product (**125-trans**) appeared to be gradually more favoured when using a larger cation especially with tetrabutylammonium iodide (**60**) and bromide (**61**), which demonstrated the best *trans*-selectivity so far (Table 3, entry 4 and 5). Interestingly, tetrabutylammonium chloride

favoured the formation of **125-cis** (Table 3, entry 6), unlike the iodide and bromide counterparts. The most intriguing reaction of the optimisation used tetraethylammonium *para*-toluenesulfonate as an electrolyte (Table 3, entry 7) which in theory should likely not work if the mechanism proposed by Meng *et al.* is true.<sup>84</sup> Yet, the reaction proceeded smoothly and identical results were achieved to when using tetrabutylammonium chloride meaning that either their proposed mechanism is incorrect or not applicable to sulfonamides (discussed at further length in Section 2.2.7.).

Nevertheless, the next phase of the optimisation investigated the use of solvents, testing common solvents in the area of organic electrochemistry whilst keeping ammonium iodide (**100**) constant as electrolyte. Methanol (Table 3, entry 8) demonstrated slight selectivity to the formation of **125-cis** with full conversion whereas ethanol and DMF (Table 3, entry 9 and 10) both had good selectivity for **125-trans**, but full conversion was not possible. 1,1,1,3,3,3-hexafluoroisopropanol (HFIP) was an interesting choice for a solvent (Table 3, entry 11) but it has been demonstrated to be a versatile solvent for many reactions, notably in the area of organic electrochemistry.<sup>104</sup> Despite the solubility of all components in the reaction appearing to be rather poor for the duration of the reaction, the reaction ran with complete conversion of the starting material and had good selectivity for **125-trans**. With HFIP demonstrating good selectivity for the formation of **125-trans**, HFIP was then tested with NBu<sub>4</sub>I (**60**) and NBu<sub>4</sub>Br (**61**), where the bromide salt (**61**) displayed the most surprising result, which afforded good selectivity for **125-cis** in an approximate 1:4 ratio (Table 3, entry 13). Duñach *et al.* reported in their electrochemical cyclisation optimisation when using a 9:1 mixture of ethanol and water opposed to just ethanol, they observed radically different selectivity with their cyclisation.<sup>105</sup> Attempting a similar solvent combination with 9:1 H<sub>2</sub>O:HFIP with NH<sub>4</sub>I (**100**) and NBu<sub>4</sub>Br (**61**) both displayed an approximate 4:1 ratio favouring **125-trans** (Table 3, entry 14 and 15).

**Table 4:** Investigating the use of additives for the electrochemical cyclisation reaction of **104a**. Results in bold are entries that generated the best results for *trans*- or *cis*-pyrrolidine formation

Entry	Electrolyte	Solvent	Additive <sup>a</sup>	Conv. (%) <sup>b</sup>	<i>trans</i> (%) <sup>c</sup>	<i>cis</i> (%) <sup>c</sup>
<b>1</b>	<b>NBu<sub>4</sub>Br</b>	<b>HFIP</b>	-	<b>&gt;99</b>	<b>21</b>	<b>79</b>
2	NBu <sub>4</sub> Br	HFIP	NaHCO <sub>3</sub>	>99	22	78
<b>3</b>	<b>NBu<sub>4</sub>Br</b>	<b>HFIP</b>	<b>NaOMe</b>	<b>&gt;99</b>	<b>85</b>	<b>15</b>
4	NBu <sub>4</sub> Br	HFIP	NaO <sup>t</sup> Bu	>99	85	15
5	NBu <sub>4</sub> Br	HFIP	DIPEA	>99	79	21
6	NBu <sub>4</sub> Br	HFIP	DBU	97	80	20
7	NBu <sub>4</sub> Br	HFIP:H <sub>2</sub> O (9:1)	-	99	81	19
8	NH <sub>4</sub> I	HFIP:H <sub>2</sub> O (9:1)	NaHCO <sub>3</sub>	>99	84	16

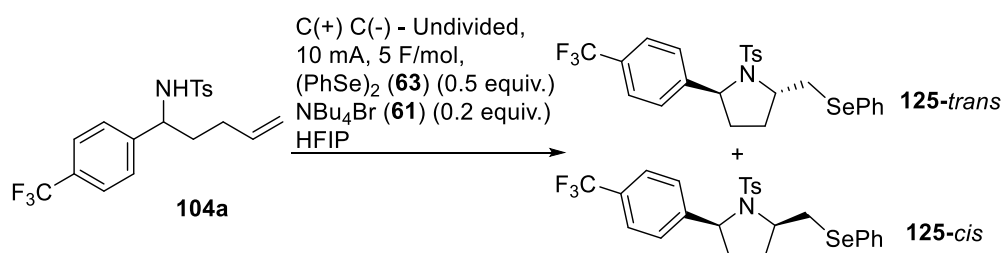
9	NH <sub>4</sub> I	HFIP:H <sub>2</sub> O (9:1)	NaOMe	99	83	17
10	NH <sub>4</sub> I	HFIP:H <sub>2</sub> O (9:1)	NaO <sup>t</sup> Bu	>99	84	16
11	NH <sub>4</sub> I	HFIP:H <sub>2</sub> O (9:1)	DIPEA	99	81	19
12	NH <sub>4</sub> I	HFIP:H <sub>2</sub> O (9:1)	DBU	99	80	20

<sup>a</sup> 1 equivalent of additive <sup>b</sup> Conversion was determined *via* GC analysis with a calibration curve of the starting material <sup>c</sup>

% of *trans*- and *cis*-products were determined *via* GC analysis with a calibration curve of both products. DIPEA = *N,N*-diisopropylethylamine DBU = diazabicyclo[5.4.0]undec-7-ene

From the results shown in Table 3, entry 13 and 14 displayed the best selectivity for the *cis*- and *trans*-pyrrolidine, respectively. Both of these conditions were then screened with five different bases, three inorganic bases (sodium bicarbonate, methoxide and *tert*-butoxide) and two organic bases (DIPEA and DBU) and the results are shown in Table 4. With the exception of Table 4, entry 2 which used tetrabutylammonium bromide (**61**), HFIP and sodium bicarbonate, all reactions conditions that used a base favoured the formation of **125-trans** with at least 58% diastereomeric excess. Table 4, entry 3 and 4 (NBu<sub>4</sub>Br, HFIP, NaOMe/NaO<sup>t</sup>Bu) both displayed the best selectivity for **125-trans** with the methoxide base marginally outperforming the *tert*-butoxide base.

**Table 5:** Reaction optimisation of the electrochemical cyclisation of **104a** investigating the optimum electrode pairing



Entry	Addition of 1 equiv. of NaOMe	Anode	Cathode	Alternating Polarity? <sup>a</sup>	Conversion <sup>b</sup>	<i>trans</i> (%) <sup>c</sup>	<i>cis</i> (%) <sup>c</sup>
1	✓	Graphite	Graphite	✓	>99	85	15
2	✓	RVC	RVC	✓	98	82	18
3	✓	RVC	Pt	✗	98	84	16
4	✗	Graphite	Graphite	✓	>99	21	79
5	✗	RVC	RVC	✓	>99	15	85
6	✗	RVC	Pt	✗	>99	5	95

<sup>a</sup> The polarity of the electrodes was alternated every ten minutes <sup>b</sup> Conversion was determined *via* GC analysis with a calibration curve of the starting material <sup>c</sup> % of *trans*- and *cis*-products were determined *via* GC analysis with a calibration curve of both products

A final round of optimisation was conducted by altering the electrode combination and the results are displayed in Table 5. Informed from the optimisation conducted before, shown in Table 2 (Section 2.1.1.), only two additional combinations were investigated, RVC/RVC and RVC/Pt. Attempting to improve the selectivity for **125-trans** with NBu<sub>4</sub>Br (**61**), HFIP and NaOMe did not afford any improved results over the graphite/graphite combination, Table 5, entries 1 - 3. Improving the selectivity for the *cis*-isomer (**125-cis**) was slightly improved when exchanging two graphite electrodes (Table 5, entry 4) for two RVC electrodes (Table 5, entry 5) and a surprising 95:5 ratio was observed when using RVC as

anode and Pt as cathode (Table 5, entry 6). Unfortunately, this result was unrepeatable when attempting the reaction again and in fact, it often observed worst diastereomeric ratios than the graphite/graphite combination. This was most likely due to the quality of the platinum electrode deteriorating quite rapidly after a few uses, which adversely effected the surface area of the electrode and hence largely reduced its performance in the reaction. Therefore, all reactions were run with a graphite/graphite combination to ensure safe and repeatable results.

Ultimately, all reactions were run with 0.5 equivalents of diphenyl diselenide (**63**), 0.1 equivalents of tetrabutylammonium bromide (**61**) in HFIP (0.1 M) with a graphite anode and cathode with the reaction running under constant current electrolysis at 10 mA which would facilitate an approximate 4:1 *cis:trans* ratio of pyrrolidines. The addition of one equivalent of sodium methoxide would cause a flip in diastereoselectivity yielding an approximate 4:1 *trans:cis* ratio of pyrrolidines.



### 2.1.6. Substrate Scope Results

With all substrates synthesised (as described in Section 2.1.2.) and the optimum reaction conditions for both the *cis*- and *trans*-pyrrolidines in hand (Section 2.1.5.), each precursor was subjected to the electrochemical cyclisations reaction under both conditions. The list of results is displayed in Table 6.

**Table 6:** Electrochemical synthesis of pyrrolidines under basic and base-free conditions. All reactions were performed on a 0.3 mmol scale unless otherwise stated.

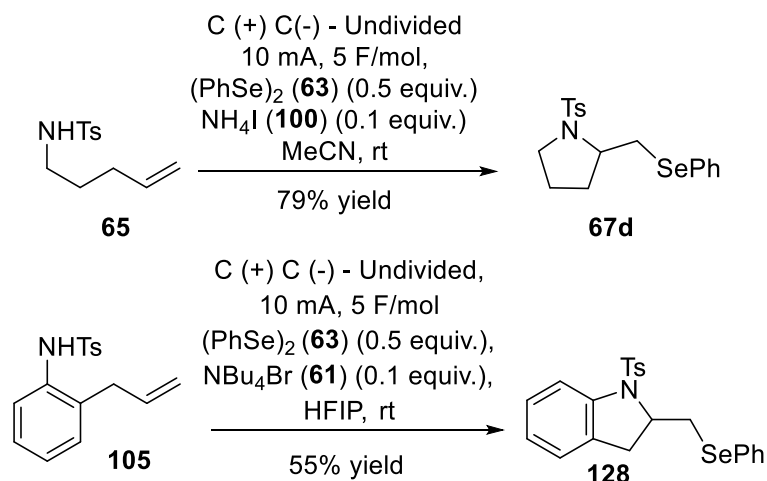
Entry	Sub.	R	NaOMe <sup>a</sup>	Conv. (%) <sup>b</sup>	<i>cis:trans</i> <sup>c</sup>	Isolated Yield of Major Isomer (%) <sup>d</sup>
1	<b>104a</b>	4-(CF <sub>3</sub> )C <sub>6</sub> H <sub>4</sub>	✓	99.4	1:6	56 ( <b>125-trans</b> ) <sup>e</sup>
2			✗	>99	4:1	40 ( <b>125-cis</b> )
3	<b>104b</b>	3,5-(CF <sub>3</sub> ) <sub>2</sub> C <sub>6</sub> H <sub>3</sub>	✓	94.6	1:7	65 ( <b>123-trans</b> ) <sup>f</sup>
4			✗	95.9	3:1	48 ( <b>123-cis</b> )
5	<b>104c</b>	4-BrC <sub>6</sub> H <sub>4</sub>	✓	89.8	1:7	57 ( <b>122-trans</b> )
6			✗	96.0	12:1	65 ( <b>122-cis</b> ) <sup>h</sup>
7	<b>104d</b>	C <sub>6</sub> H <sub>5</sub>	✓	87.4	1:4	46 ( <b>119-trans</b> ) <sup>e</sup>
8			✗	97.1	4:1	50 ( <b>119-cis</b> ) <sup>h</sup>
9	<b>104e</b>	4-MeC <sub>6</sub> H <sub>4</sub>	✓	94.5	1:4	45 ( <b>127-trans</b> ) <sup>h</sup>
10			✗	96.0	2:1	42 ( <b>127-cis</b> ) <sup>f, h</sup>
11	<b>104f</b>	4-OMeC <sub>6</sub> H <sub>4</sub>	✓	93.2	1:4	55 ( <b>126-trans</b> )
12			✗	95.5	11:1	79 ( <b>126-cis</b> ) <sup>g, h</sup>
13	<b>104g</b>	4-pyridinyl	✓			
14			✗			No reaction

<sup>a</sup> 1 equivalent of sodium methoxide <sup>b</sup> Conversion at 5 F/mol, determined *via* GC analysis with the calibration curve of the respective starting material <sup>c</sup> Ratio determined at 5 F/mol *via* GC analysis by comparison of the relative areas of the two products <sup>d</sup> Isolated yields after purification (column chromatography and/or preparative TLC) <sup>e</sup> 0.1 mmol scale <sup>f</sup> 1.0 mmol scale <sup>g</sup> 0.5 mmol scale <sup>h</sup> 7 F/mol used.

Obtaining the entirety of the desired product from the electrochemical cyclisation reaction was a significant challenge due to the difficulty of separating the diastereomers which expectedly had very similar R<sub>f</sub> values; therefore, it is hard to interpret any trends from the isolated yields, unfortunately.

However, a minimum of 40% yield for all compounds was obtainable. Of note, the substrates substituted with a *para*-bromide and *para*-methoxy group upon the aromatic ring (**104c** and **104f** respectively) provided an impressive *cis:trans* ratio with both compounds producing better than a 10:1 ratio under base-free conditions (Table 6, entry 6 and 12). These improved ratios are reflected in the results where the highest isolated yields were obtained under these conditions, with the most impressive result of 79% yield for the formation of **126-cis**. The reaction was also scalable and could be performed on a variety of scales from 0.1 mmol (Table 6, entry 1 and 7) and on a substantially larger scale at 1.0 mmol (Table 6, entry 3 and 10) with no notable effect on the reaction outcome, the only inconvenience was the increased reaction time required on a larger scale. Interestingly, the 4-pyridinyl substrate (**104g**) did not react at all under either set of conditions and even increasing the current to 20 mA and allowing the reaction to run to 10 F/mol did not result in any product formation. The basicity of the pyridine evidently plays a disadvantageous role in the reaction, presumably quenching some key intermediate that is formed during the reaction. Plotting the diastereoselective ratio against the aromatic substituents in a Hammett plot<sup>106</sup> afforded a reaction parameter of 0.05 and 0.02 for the reaction under basic and base-free conditions, respectively (see Appendix 1). Therefore, there is no correlation between the electronic nature of the aromatic ring and the *cis/trans* ratio.

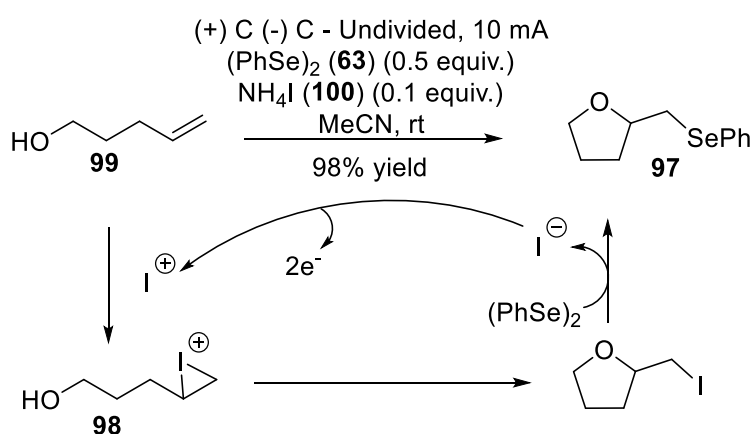
Preliminary work was conducted with the alkyl substituted substrate (**104h**, R = Et) and only resulted with one product spot by TLC and only one peak was observed from the UV trace during column chromatography. Upon NMR analysis, a complex mixture was observed and subjecting the crude mixture to GC analysis revealed that two products were actually present. Purification of the crude mixture was trialled once with an analytical HPLC using a C<sub>18</sub> stationary phase, but minimal separation occurred with 6:4 MeCN:H<sub>2</sub>O. Due to time constraints, further work on the separation was unable to be continued but it was hypothesised that the two diastereomers could be separated with further method development.



**Scheme 25:** Electrochemical synthesis of an achiral pyrrolidine and indoline

As previously described (Section 2.1.1.), pyrrolidine **67d** had been synthesised in 79% yield. Subjecting substrate **105** to the basic conditions synthesised the desired indoline **128** in 55% yield, Scheme 25. The reaction also worked under the base-free conditions although a lower yield of 15% was observed.

### 2.1.7. Mechanism



**Scheme 21:** Proposed mechanism for an electrochemical iodocyclisation, reported by Meng *et al.*

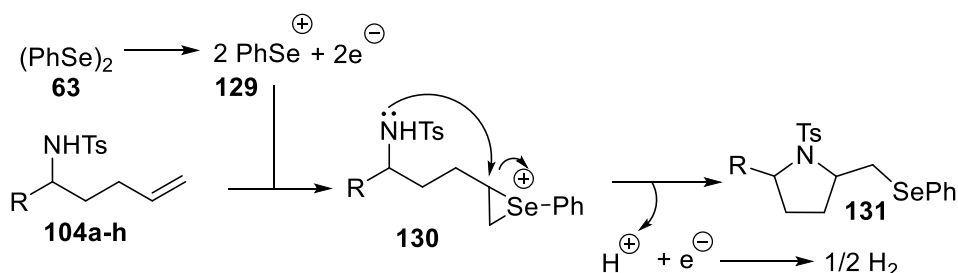
As previously mentioned in Section 2.1.1., the inspiration for this work was from Meng *et al.*'s electrochemical iodocyclisation reported at the end of 2019 outlining the formation of cyclic ethers (**97**), Scheme 21.<sup>84</sup> One area that was interestingly very different to our results was the reliance on the electrolyte material for the reaction. For Meng *et al.*'s reaction optimisation, they state that 98% yield was achieved when using ammonium iodide (**100**) as electrolyte, but no reaction occurred when using ammonium bromide or chloride.<sup>84</sup> This displays a significant contrast to the results achieved in the reaction optimisation discussed in Section 2.1.5., Table 3, which facilitated near-to or complete conversion of the reaction with all electrolytes in acetonitrile, whether the halogen was an iodide, bromide or chloride. Interestingly, the reaction was attempted with a non-halogenated electrolyte

with tetraethylammonium *para*-toluenesulfonate, which also demonstrated no issue with the consumption of the starting material. Naturally, if we theoretically assume the formation of a  $^+OTs$  cation *in-situ*, it could be possible that an epoxide would form, and the reaction would proceed in an analogous manner. Therefore, two additional reactions were performed using lithium tetrafluoroborate and potassium hexafluorophosphate as the electrolyte material, which contain anions that would be unable to add over an alkene even in a cationic state (if one existed) and both reactions performed with no issues. In conclusion, it appears that the mechanism proposed from Meng *et al.* is not applicable for the cyclisation of sulfonamides.

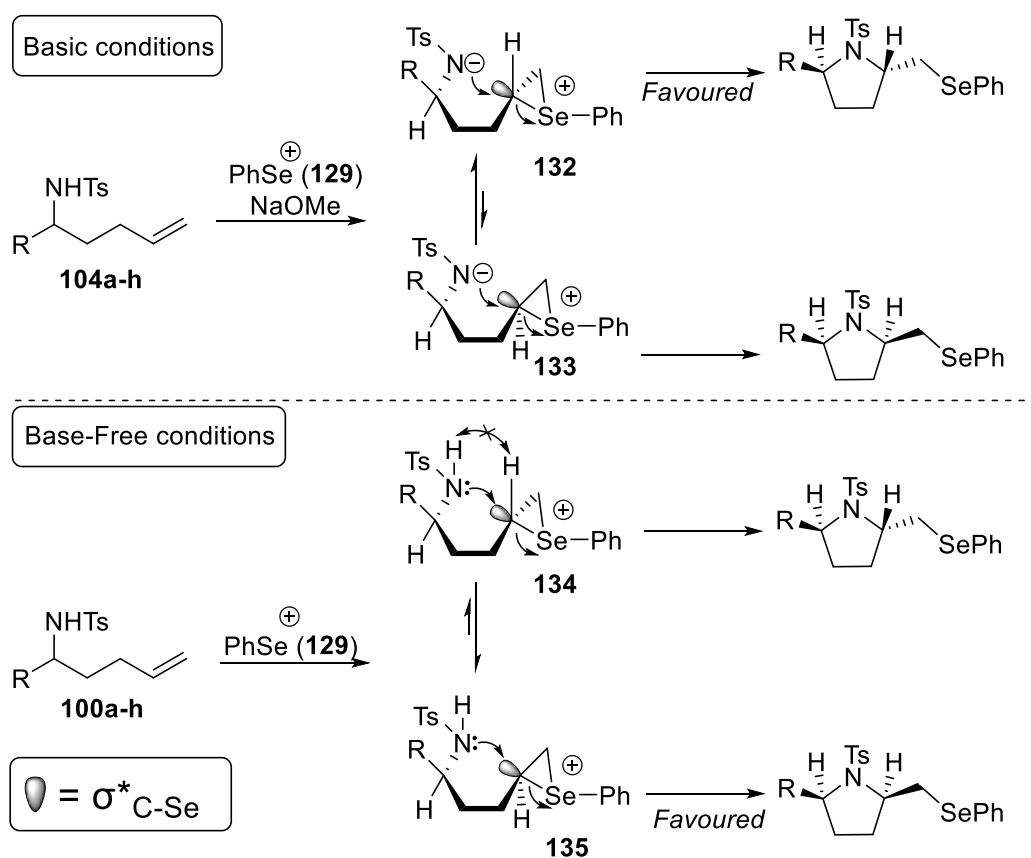
Electrochemical cyclisations of oxygen-containing heterocycles with diphenyl diselenide (**63**) from other groups have been reported, although minor mechanistic details are discussed which makes it hard to infer the mechanism with literature support. Uneyama *et al.* reported the formation of phenylselenanol (PhSeOH) with an acetonitrile-water mixture which would subsequently add over an alkene and facilitate cyclisation and a similar mechanism had been previously described from Torii *et al.*<sup>86, 107</sup> With the majority of reactions performed in HFIP with only trace amounts of residual water from reagents and solvents, it is unlikely that this is occurring. Konstantinović *et al.* demonstrated the cyclisation of carboxylic acids to afford lactones with diphenyl diselenide (**63**), ammonium bromide and methanol but did not offer any mechanistic insight.<sup>87</sup>

Vukićević *et al.* suggested an alternative explanation for electrochemical cyclisations with diphenyl diselenide (**63**) for the formation of cyclic ethers (**97**) and lactones. Their theory was the formation of a phenylselenium cation (**129**) generated *in-situ* during the reaction with the electrolyte, a bromide salt, behaving as a mediator.<sup>88</sup> With the generation of the phenylselenium cation (**129**), it can then add over a double bond which allows the cyclisation to occur with the nucleophilic oxygen attacking the three-membered cationic intermediate. Röse *et al.* operated a similar cyclisation featuring dienes and also suspected the formation of the 3-membered selenium ring although no thorough explanation was detailed.<sup>85</sup> Similar reactivity has been described for non-electrochemical cyclisations that utilise phenylselenanyl chloride or bromide, which emulates the phenylselenium cation (**129**), and has been used for the formation of cyclic lactones,<sup>108</sup> as well as nitrogen-containing heterocycles such as indolines,<sup>108</sup> azetidines<sup>109</sup> and pyrrolidines<sup>110, 111</sup> which makes this theory more plausible. The only issue with this theory is again the reliance on the electrolyte for some electrochemical process, this time for it to behave as a mediator. All electrochemical cyclisations discussed in this section have utilised an electrolyte that contains a halogen for their reaction, yet we have already demonstrated that the reaction can proceed with a large variety of anions ( $I^-$ ,  $Br^-$ ,  $Cl^-$ ,  $TsO^-$ ,  $BF_4^-$  and  $PF_6^-$ ) with no negative effect on the conversion of the starting material. Therefore, it is believed the reaction proceeds *via* the formation of the phenylselenium cation (**129**), but it is uncertain exactly how; Vukićević *et al.*'s theory is potentially true but does not appear to justify why the reaction proceeds

with a tosylate or tetrafluoroborate anion. Ultimately, it is likely that diphenyl diselenide (**63**) undergoes a two-electron oxidation process to form two phenylselenium cations (**129**); this oxidation process is imperative as no reaction was observed in the absence of a current. The cation **129** then adds over the alkene of **104a-h**, which allows the nucleophilic nitrogen to perform an intramolecular ring-closing (**130**) and afford the appropriate pyrrolidine ring (**131**). The hydrogen from the sulfonamide is removed and subsequently reduced in a one-electron process to afford hydrogen gas as illustrated in Scheme 26.



**Scheme 26:** Proposed mechanism for the electrochemical formation of 2-((phenylselenanyl)methyl)-1-tosylpyrrolidines



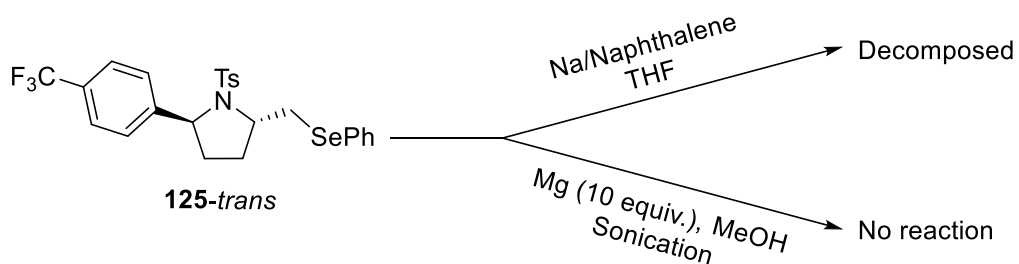
**Scheme 27:** Mechanistic justification for the observed stereoselectivity with the electrochemical cyclisation

The final mechanistic hurdle to discuss is to justify the diastereoselectivity between the two conditions. As a brief reminder, a combination of diphenyl diselenide (**63**), HFIP and

tetrabutylammonium bromide (**61**) predominantly affords a *cis*-pyrrolidine and with the addition of one equivalent of sodium methoxide, the selectivity flips to predominantly form a *trans*-pyrrolidine. From this information, the basicity of the solution is imperative to the diastereoselective outcome of the reaction. With the hydrogen attached to nitrogen being the most acidic proton in the starting material (**104a-h**), deprotonation of the sulfonamide is most likely where the change in reaction outcome originates from. Another factor to consider is that the phenylselenium cation (**129**) can add over the double bond of **104a-h** in two different ways that would result in the proposed three-membered cationic intermediate to exist in one of two different conformations, a pseudo-equatorial (**132**) or a pseudo-axial (**133**) conformation. In a typical system, the three-membered intermediate in a pseudo-equatorial position (**132**) facilitates the reaction to proceed *via* a lower energy reaction pathway in comparison to the pseudo-axial conformer and is therefore preferred. Under the basic conditions, this justifies the *trans*-selectivity with the three-membered intermediate existing in the pseudo-equatorial position (**132**), which consequentially has the proton in the pseudo-axial position and allows the more energetically favourable pathway to proceed, Scheme 27 (top). Under the base-free conditions, the hydrogen attached to the nitrogen must impose some unfavourable interaction(s) within the system, which could be N-H C-H steric interactions, which raises the energy of the pseudo-equatorial transition state for the formation of the *trans*-pyrrolidine and makes it no longer energetically favourable (**134**) in comparison to the other conformation. Therefore, the phenylselenium cation (**129**) preferably adds to the other face, generating the three-membered intermediate upon the pseudo-axial face (**135**), which minimises the aforementioned unfavourable interactions in the transition state and facilitates the preferential formation of a *cis*-pyrrolidine, Scheme 27 (bottom). This explanation may also justify why high diastereomeric ratios were not possible (such as 20:1 d.r. or above) as one can envisage a very small difference in energy between the two configurations in both cases. Regardless, a thorough investigation into the mechanism is necessary to fully comprehend the reaction and would require kinetic studies and/or computational analysis.

### 2.1.8. Removal of Tosyl Protecting Group

With the successful cyclisation of various pyrrolidine rings under electrochemical methodology, the next synthetic challenge would be to attempt the removal of the tosyl protecting group. Two of the most common methods for tosyl deprotection were attempted with **125-trans**. The first method used sodium naphthalenide (generated *in-situ* from elemental sodium and naphthalene), a strong reducing agent, which was added to the pyrrolidine (**125-trans**) at  $-78\text{ }^{\circ}\text{C}$  and stirred for an hour.<sup>112</sup> Complete decomposition of the starting material was observed with only leftover naphthalene being present by  $^1\text{H}$  NMR of the crude mixture in a post work-up state.

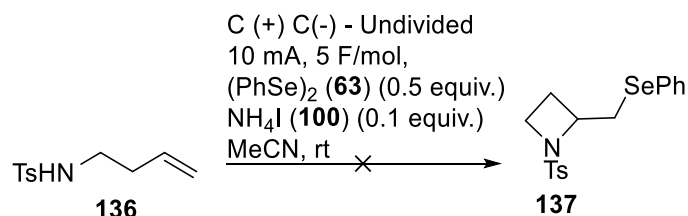


**Scheme 28:** Tosyl deprotection methods attempted on **125-trans**

A second tosyl deprotection method was attempted that described to sonicate the pyrrolidine (**125-trans**) in dry methanol with a large excess of magnesium powder, which is a mild method for the removal of the sulfonamide group.<sup>113</sup> After three hours, no change was observed by TLC and the starting material (**125-trans**) was recovered completely. Unfortunately, it appears that the tosyl group upon the pyrrolidines is irremovable or would require a deprotection method that is approximately in the middle of the two. With the sodium naphthalenide method resulting in decomposition, it is too strong of a reducing agent, but magnesium and methanol sonication produced no reaction which meant it was too mild of a method, Scheme 28. Alternative tosyl deprotection methods are discussed in Section 2.3.

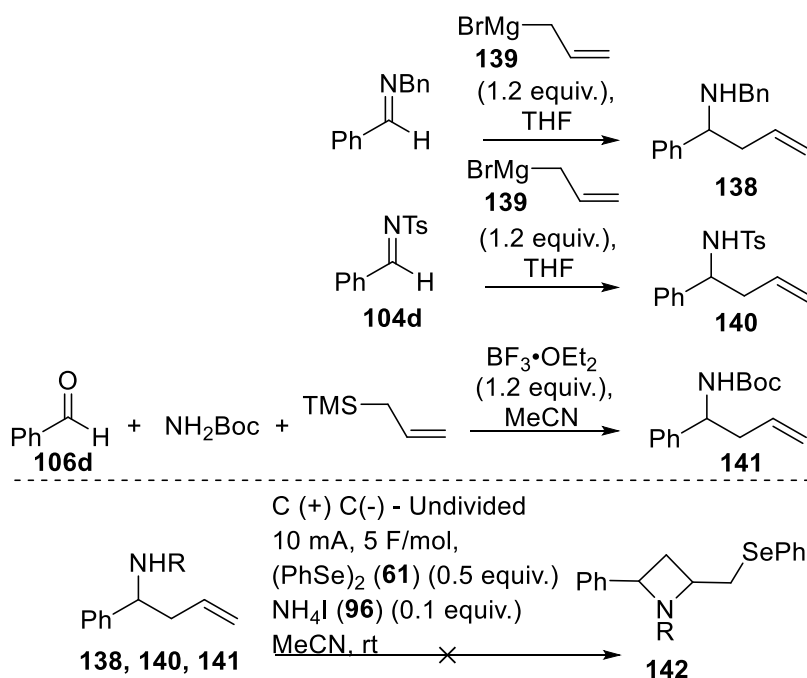
## 2.2. Attempted Synthesis of Azetidines

With the successful synthesis of pyrrolidines as described in Section 2.1., attention was turned to attempt the synthesis of azetidines using the same methodology. However, attempting to cyclise *N*-(but-3-en-1-yl)-4-methylbenzenesulfonamide (**136**) to the desired azetidine product (**137**) resulted in no reaction surprisingly, Scheme 29.



**Scheme 29:** Attempted electrochemical synthesis of 2-((phenylselanyl)methyl)-1-tosylazetidine

With the failure of the reaction described in Scheme 29, reflecting on Feula *et al.*'s work<sup>11, 12</sup> revealed that all of their azetidine products were synthesised with benzyl protecting group upon the starting material, therefore, to closely emulate their work, *N*-benzyl-1-phenylbut-3-en-1-amine (**138**) was synthesised. Alongside the synthesis of **138**, tosyl imine **108d** was also reacted with allylmagnesium bromide (**139**) to provide the tosyl analogue (**140**) of **138** and the Boc-protected version (**141**) was also generated *via* a one-pot procedure reported by Veenstra and Schmid.<sup>114</sup> All schemes are shown in Scheme 30 (top).

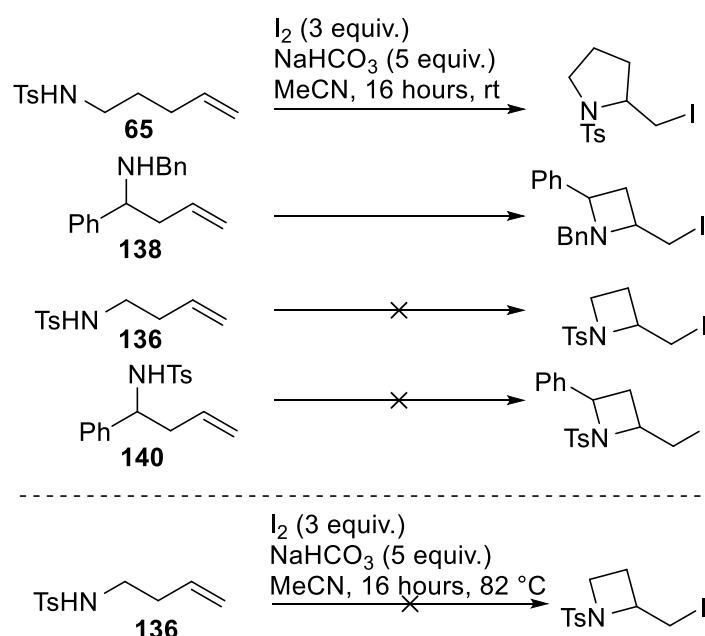


**Scheme 30:** Reaction schemes for the synthesis of azetidine precursors (top) and conditions used for the attempted electrochemical cyclisation of azetidines.



Attempting the electrochemical cyclisation reaction, shown in Scheme 30 (bottom), with the benzyl-protected substrate (**138**) resulted in the solution turning an uncharacteristic black colour and produced a complex reaction mixture of products during purification, from which no desired product (**142**) could be found. Therefore, it is likely that the reaction with the benzyl protecting group (**138**) is not viable under electrochemical conditions and results in either decomposition and/or debenzylation. Predictably, the tosyl-protected substrate (**140**) still resulted in no reaction and the Boc-protected substrate (**141**) observed an analogous result, which at least displayed two protecting groups that were stable under electrochemical conditions.

To demonstrate the viability of the substrates for cyclisation, a simple diagnostic test was attempted to observe the possibility of cyclisation. All substrates were subjected to Feula *et al.*'s iodocyclisation conditions<sup>11, 12</sup> and after 16 hours, acetonitrile was removed *in vacuo* and the crude material remaining was dissolved in CDCl<sub>3</sub> and transferred to an NMR tube, Scheme 31. All starting materials contained a doublet of doublet of triplets at approximately 5.6 ppm, therefore if this key multiplet in the NMR of the crude material was missing, it was likely that complete conversion to the desired product was observed, such as in the case of the pyrrolidine substrate **65**. The benzyl substrate (**138**) similarly observed complete conversion as reported from Feula *et al.*<sup>11, 12</sup> but neither tosyl substrate (**136** and **140**) cyclised under these conditions. Even attempting the iodocyclisation at reflux with **136** resulted in no product formation by TLC. These reactions are summarised in Scheme 31.



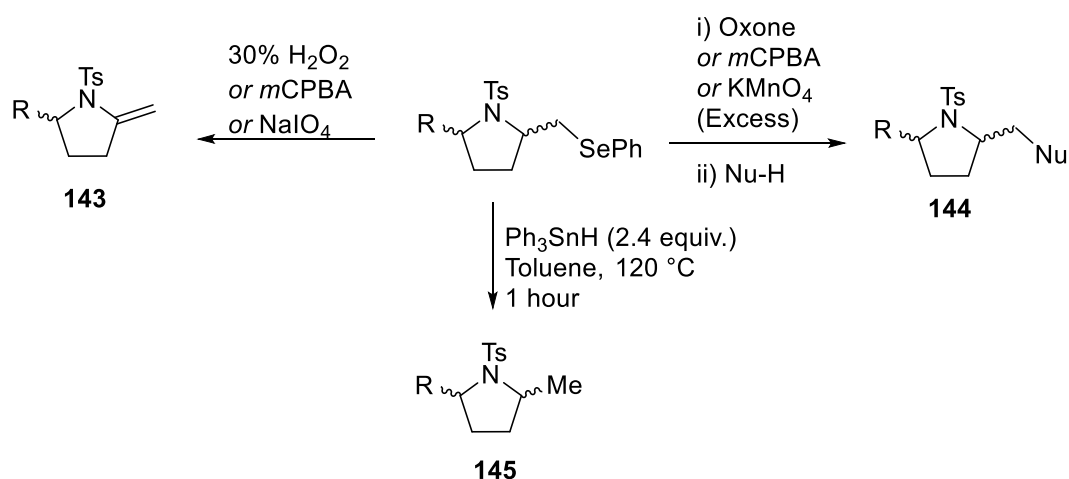
**Scheme 31:** Iodocyclisation of aminoalkenes to observe the viability of cyclisation reactions.

With the unsuccessful synthesis of novel azetidine substrates, from both the iodocyclisation and electrochemical methodologies, complete focus was put on the electrochemical synthesis of

pyrrolidines. Unfortunately, no further time was available to work on the synthesis of azetidines, but it is certainly future work for the group as discussed in section 2.3.

## 2.3. Conclusion and Future Work

A novel electrochemical diastereoselective synthesis of selenium-containing pyrrolidine rings has been described with moderate to good yields and meets the aim of the project to develop an electrochemical cyclisation protocol with enhanced atom economy. The only waste product is a sub-stoichiometric amount of tetrabutylammonium bromide which makes the method efficient from a green perspective. The method was able to deliver a total of 14 cyclised compounds, with 12 out of the 14 being new novel compounds, and two single crystals were obtained, which represent the two diastereomers that are generated in the reaction. The methodology is unable to cyclise homoallylamines to provide azetidines though. With the development of this method, many exciting new directions are possible that could facilitate the formation of a large host of new products being viable.



**Scheme 32:** Further potential reactions on the pyrrolidine products, taking advantage of the reactivity of the phenylselenium group

Firstly, the biggest question to solve is what to do with the products of the reaction? Utilisation of the phenylselenium group is one option and a short review has been previously published that discusses the options available, although it is somewhat limited and often requires relatively harsh conditions.<sup>115</sup> Oxidation of the selenium can facilitate elimination to a double bond which would produce an enamide (**143**); alternatively oxidation of the selenium with large excesses of oxidant can completely oxidise the selenium to a selenone which is a good leaving group and can therefore be readily replaced with nucleophiles (**144**). One other option is the complete removal of the phenylselenium group with organotin reagents such as triphenylstannane or tributylstannane (**145**). Cooper and Ward have previously reported the replacement of the phenylselenium group with an

alcohol and ether *via* oxidation to the corresponding selenone of pyrrolidine **67d** (R = H), which places more validity upon the theorised ideas.<sup>110</sup>

Another potential avenue is to investigate the compound's pharmaceutical properties. With the pyrrolidine rings containing selenium, a notoriously toxic element,<sup>116</sup> this may initially appear to be counter-intuitive, yet selenium has already been used in a small selection of investigatory drugs such as Ebselen (**146**) and a selenophene alternative to AVE6971 (**147**), Figure 19.<sup>117</sup> The starting material can be easily modified by using a different aldehyde, and further functionality could be explored upon the phenylselenium group as previously described which may facilitate a diverse library of compounds for biological testing.

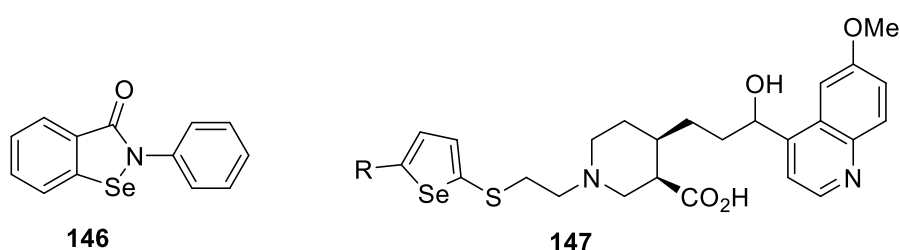
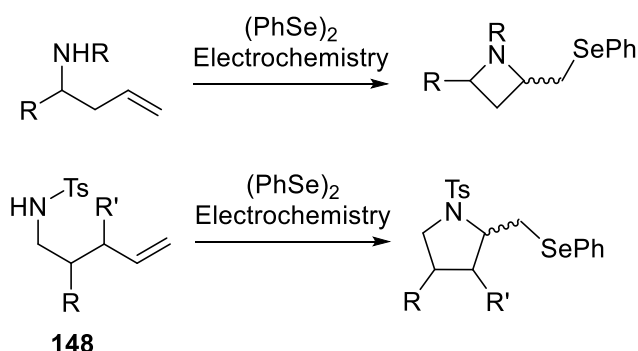


**Figure 19:** Drugs that contain the element selenium: Ebselen (**141**) and an analogue of AVE6971 (**142**)

One other area that would most likely need to be addressed before undertaking any biological testing though, would be to further explore the removal of the tosyl protecting group. As previously described, it had been attempted with **125-trans** *via* the sodium naphthalenide and magnesium/methanol sonication methods, which both provided unsuccessful results. Other methods could potentially be attempted such as refluxing the compound in hydrobromic acid and acetic acid,<sup>118</sup> using samarium iodide<sup>119</sup> or attempting electrochemical deprotection methods. Debatably, the most common electrochemical tosyl deprotection method involves the use of a divided cell with a mercury pool cathode,<sup>120</sup> which by modern standards is rather unsafe and would be unsuitable for the production of pharmaceuticals due to the possibility of introducing mercury poisoning. Some non-mercury electrochemical tosyl deprotection procedures have been developed though, such as Scialdone *et al.*'s system which was able to completely deprotect tetratosylcyclen (containing four tosyl groups) with a dimensionally-stable anode, otherwise known as a mixed metal oxide anode, and graphite cathode in a divided cell.<sup>121</sup> Senboku *et al.* also described a convenient mercury-free electrolysis using naphthalene as an electron-transfer mediator and could operate in an undivided cell with a platinum cathode and a sacrificial magnesium anode.<sup>122</sup> If tosyl deprotection still proves to be difficult after attempting the methods described above, changing the protecting group could be a more convenient method, such as using a Boc protecting group, which is also stable under electrochemical conditions and is much easier to remove, typically with trifluoroacetic or hydrochloric acid.

Preliminary findings with the new methodology were described in the attempt of synthesising azetidines (Section 2.2.) with no promising result so far. With a more thorough optimisation of the reaction conditions, such as what is described in Table 3 (Section 2.1.5), for the diastereoselectivity optimisation, it is with hope the synthesis of azetidines should be viable. If the proposed mechanism is correct then the reaction would be synonymous to that reported by Paulmier and co-workers<sup>109, 111, 123</sup> with the main difference being the nitrogen protecting group. The benzyl group appears to be unstable under electrochemical conditions but is commonly used for the cyclisation of homoallylamines and were utilised from both Feula *et al.*<sup>11, 12</sup> and Paulmier *et al.* Potentially running the reaction under constant potential conditions, alongside cyclic voltammetry results, could prevent the decomposition of the starting material. Another straightforward suggestion would be to use the method for the synthesis of 3,5- and 4,5-substituted pyrrolidines. The synthesis of the starting materials would have to be changed but the synthesis of both compounds with R = Ph, R' = H<sup>124</sup> or R = H, R' = Ph<sup>125</sup> (**148**) has already been published in the literature, Scheme 33.



**Scheme 33:** Application of the electrochemical cyclisation for azetidines as well as 3,5- and 4,5- substituted pyrrolidines

Combining all these ideas together could facilitate an exciting new project that would generate a large library of 4- and 5- membered nitrogen-containing heterocycles. Substitution upon the 2-, 3- and 4- position (upon a pyrrolidine ring) is theoretically possible with many functional groups and finding functionality with the phenylselenium group provides even more options. Therefore, the electrochemical method described could potentially facilitate the synthesis of a large library of compounds, providing access to new pharmaceutical scaffolds.

### 3. Publication of a Review Article

During the period of my postgraduate MSc study, I published my first peer-reviewed publication, “Azetidines and their applications in asymmetric catalysis”,<sup>83</sup> where I am the corresponding and first author and was co-authored with my supervisor (Prof. John S. Fossey). I provided the majority of the writing and sourced the references as well, while Prof. Fossey provided transformative comments and advice throughout, which heavily influenced all aspects of the article, such as figures, schemes and the writing style. The manuscript was a review article and made up my main body of work during the school shutdown due to the COVID-19 pandemic, which prevented me from working in the lab for four months. The pre-peer review (the “green copy”) of the manuscript is available as part of the appendices (Section 6.2., appendix 2) to this thesis and should be considered as part of my thesis outputs. The published version is available at [doi.org/10.1016/j.tet.2020.131767](https://doi.org/10.1016/j.tet.2020.131767) as part of a *Tetrahedron* special edition in memory of Prof. Jonathan M. J. Williams from the University of Bath. The review evaluates and discusses a large array of works that demonstrate the use of azetidine moieties in asymmetric catalysis whether that is as a ligand for metal-mediated catalysis or as an organocatalyst. A large portion of the review compares the use of Wang *et al.*’s azetidine-containing “AzePhenol” ligand (**149**) and Trost *et al.*’s pyrrolidine-derived “ProPhenol” ligand (**150**)<sup>126</sup> which are congeners of one another, Figure 20. A multitude of reactions have been demonstrated from both ligands including Michael additions, Friedel-Crafts, aza-Henry reactions and even more complex tandem reactions.

The other half of the review discusses novel catalyst designs that have also been used for a wide range of reaction such as *N*-methyleneferrocenyl azetidine (**151**) as a ligand for diethylzinc additions to benzaldehydes.<sup>127</sup> Work from our own group was also discussed that utilises a selection of azetidines for the copper-catalysed Henry reaction of aldehydes with the optimum results achieved with **152**,<sup>128</sup> which was synthesised from the previously described iodocyclisation method.<sup>11, 12</sup> An intriguing azetidine-containing BINOL derivative (**153**) had also been used for a magnesium-catalysed ring-opening of aziridines.<sup>129</sup> A final example was **154** being used as an organocatalyst for the stereoselective epoxidation of chalcones with *tert*-butyl hydroperoxide.<sup>130</sup> In conclusion, the review catalogues the use of azetidines in asymmetric catalysis and evaluates their use against the 5-membered analogue in many cases. In the majority of reactions, one congener would largely outperform the other, but no clear pattern could be discerned which should be interpreted in a positive light, where both azetidine and pyrrolidine versions of a catalyst should be trialled with both providing equal opportunity for optimal results.

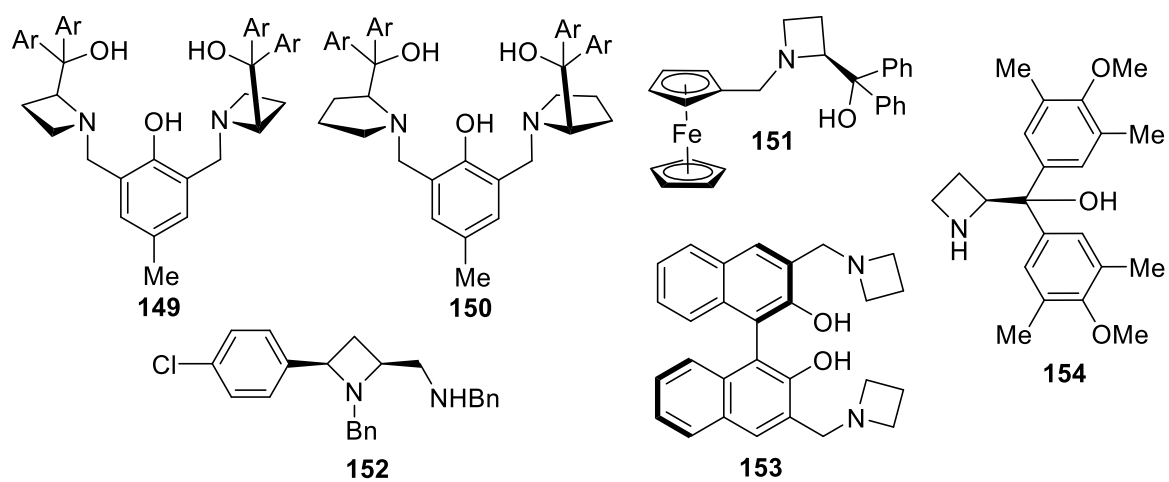


**Figure 20:** A selection of prominent catalysts and ligands that are featured in Azetidines and their application in asymmetric catalysis

## 4. Experimental

Commercially available solvents and reagents were purchased and used from suppliers without further purification. Dry THF was obtained from a solvent purification system. Dry MeOH was dried over 4 Å molecular sieves for a week before use. All  $^1\text{H}$  and  $^{13}\text{C}$  NMR spectra were recorded with either a Bruker AVIII400 or a Bruker AVANCE NEO NMR spectrometer at room temperature at 400 and 100 MHz respectively.  $^{13}\text{C}$  NMR spectra were all recorded as  $^1\text{H}$  decoupled.  $^{19}\text{F}$  and  $^{77}\text{Se}$  spectra were recorded with a Bruker AVANCE NEO at room temperature at 377 MHz and 76 MHz respectively. Chemical shifts ( $\delta$ ) are reported in ppm relative to  $\text{CDCl}_3$  ( $\delta$  7.26) or TMS ( $\delta$  0.00) for  $^1\text{H}$  NMR, relative to  $\text{CDCl}_3$  ( $\delta$  77.16) for  $^{13}\text{C}$  NMR, indirectly referenced to  $\text{CFCl}_3$  ( $\delta$  0.00) for  $^{19}\text{F}$  NMR and indirectly referenced to  $(\text{PhSe})_2$  at ( $\delta$  463.00) for  $^{77}\text{Se}$ . Coupling constants ( $J$ ) are reported in Hertz (Hz). Multiplicities of the signals are abbreviated as singlet (s), doublet (d), triplet (t), quartet (q), pentet (p) and multiplet (m). The abbreviation app denotes apparent multiplets. Column chromatography was carried out using a Combiflash Rf 200i with silica stationary phase columns and column traces were recorded at two wavelengths (254 nm and 280 nm) alongside an ELS system. Reactions were monitored by thin layer chromatography (TLC) on Merck silica gel 60 F254 plates. TLC plates were visualised with UV light and/or vanillin dip and subsequently heated. Mass spectra were recorded with electrospray MS Waters LCT Time of Flight Mass Spectrometer and with EI (GC/MS) Waters GCT Premier Time of Flight Mass Spectrometer. Gas chromatography data was obtained with a Shimadzu GC-2010 with FID using a Phenomenex ZB-5 column (95% dimethylpolysiloxane/5% diphenylpolysiloxane) of dimensions 30m x 0.25 mm (ID) x 0.25  $\mu\text{m}$  (film thickness).

### 4.1. General Procedures

**General procedure A:** Modified procedure described from Stark *et al.*<sup>131</sup> Benzaldehyde (1 equiv.) and *p*-toluenesulfonamide (1 equiv.) are dissolved in toluene (0.33 M) followed by the addition of boron trifluoride etherate (1 mol %) and heated at reflux for 16 hours with a Dean-Stark apparatus. Toluene is removed *in vacuo* and the resultant solid is used as is for the following reaction. Approximately 100 – 200 mg of the sample is taken for purification by column chromatography and used purely for data collection.

**General procedure B:** Modified procedure described from Thai *et al.*<sup>92</sup> Magnesium (2 equiv.) and a few crystals of iodine are added to an oven-dried flask under argon and vigorously stirred for 15 minutes, at which time dry tetrahydrofuran (0.2 M) and 4-bromobutene (1.5 equiv.) is added and stirred for 30 minutes at which point the solution turns grey. Imine or aldehyde (1 equiv.) is added portion/dropwise to the Grignard mixture and stirred for 16 hours. Upon completion of the reaction, the mixture is quenched with saturated aqueous sodium bicarbonate and left to stir for 15 minutes. The solution is transferred to a separating funnel and diluted with ethyl acetate and water. The

aqueous is extracted with ethyl acetate three times and the combined organic layers are washed with brine, dried (MgSO<sub>4</sub>), filtered and concentrated. The crude product is then subjected to column chromatography (0 -> 20% ethyl acetate in hexane gradient) to afford a solid product.

**General procedure C:** Procedure described from Teichert *et al.*<sup>93</sup> Alcohol, triphenylphosphine (1.5 equiv.) and *tert*-butyl tosylcarbamate (1.5 equiv.) are added to a flask and dissolved in tetrahydrofuran (0.2 M). Diisopropyl azodicarboxylate (DIAD) (1.5 equiv.) is then added to the reaction dropwise and the reaction is left to stir for 16 hours. Upon completion of the reaction, solvent is removed *in vacuo* and the crude mixture is subjected to column chromatography (0 -> 10% EtOAc in hexane gradient) to afford a colourless oil.

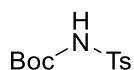
**General procedure D:** Procedure described from Teichert *et al.*<sup>93</sup> Boc-protected sulfonamide is dissolved in dichloromethane and cooled to 0 °C. Trifluoroacetic acid (20 equiv.) is then added dropwise and the reaction is allowed to warm to room temperature and then stirred for four hours. Upon completion of the reaction, saturated aqueous sodium bicarbonate and ethyl acetate is added to the reaction mixture and stirred for 15 minutes. The biphasic mixture is transferred to a separating funnel and the aqueous layer is removed. The organic phase is then washed with saturated aqueous sodium bicarbonate four times and is then washed with brine. The organic phase is dried (MgSO<sub>4</sub>), filtered and the solvent removed *in vacuo* to afford the desired product without further purification.

**General procedure E:** Sulfonamide, diphenyl diselenide (0.5 equiv.), tetrabutylammonium bromide (0.1 equiv.), sodium methoxide (1 equiv.) and HFIP (0.1 M) are added to an ElectraSyn vial that is equipped with a graphite anode and cathode. The mixture is then subjected to constant current electrolysis at 10 mA with the polarity of the electrodes alternating every 10 minutes until the specified amount of F/mol has been reached. Upon completion of the reaction, the mixture is transferred to a round bottomed flask and all components are thoroughly rinsed with MeCN; solvent is subsequently removed *in vacuo*. The crude mixture is then purified *via* column chromatography (0 -> 5% ethyl acetate in hexane gradient), unless otherwise stated, to afford predominant *trans*-pyrrolidine.

**General procedure F:** Sulfonamide, diphenyl diselenide (0.5 equiv.), tetrabutylammonium bromide (0.1 equiv.) and HFIP (0.1 M) are added to an ElectraSyn vial that is equipped with a graphite anode and cathode. The mixture is then subjected to constant current electrolysis at 10 mA with the polarity of the electrodes alternating every 10 minutes until the specified amount of F/mol has been reached. Upon completion of the reaction, the mixture is transferred to a round bottomed flask and all components are thoroughly rinsed with MeCN; solvent is then removed *in vacuo*. The crude mixture is then purified *via* column chromatography (0 -> 5% ethyl acetate in hexane gradient), unless otherwise stated, to afford predominant *cis*-pyrrolidine.

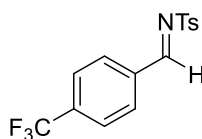


## 4.2. Characterisation Data of Compounds



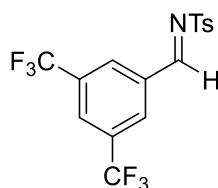
### ***tert*-Butyl tosylcarbamate (111)**

Procedure described by Barrett *et al.*<sup>132</sup> *p*-Toluenesulfonamide (8.56 g, 50 mmol), triethylamine (8.40 mL, 60 mmol, 1.1 equiv.), 4-dimethylaminopyridine (610 mg, 5 mmol, 0.1 equiv.) and CH<sub>2</sub>Cl<sub>2</sub> (62 mL, 0.8 M) were stirred in a flask under a balloon of argon followed by the addition of di-*tert*-butyl dicarbonate in one portion (13.1 g, 60 mmol, 1.1 equiv.) for three hours. CH<sub>2</sub>Cl<sub>2</sub> is removed *in vacuo* and the residue was diluted in EtOAc (120 mL) and was washed subsequently with 100 mL of 1 M HCl, 100 mL of water and 100 mL of brine to produce sufficiently pure *tert*-butyl tosylcarbamate as a white solid in 99% yield (13.5 g). <sup>1</sup>H NMR (400 MHz, CDCl<sub>3</sub>) δ 7.89 (d, *J* 8.4, 2H), 7.33 (d, *J* 8.0, 2H), 2.45 (s, 3H), 1.38 (s, 9H); <sup>13</sup>C NMR (101 MHz, CDCl<sub>3</sub>) δ 149.2, 144.9, 136.1, 129.6, 128.4, 84.2, 28.0, 21.8; MS: (ES<sup>+</sup>) 294.08 [M + Na]<sup>+</sup>; HRMS: Calc'd for C<sub>12</sub>H<sub>17</sub>NO<sub>4</sub>SN<sup>+</sup>: 294.0776; found: 294.0774. Data is consistent with that reported for the title compound by Henry *et al.*<sup>133</sup>



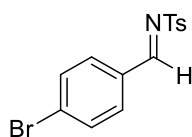
### **(*E*)-4-Methyl-*N*-(4-(trifluoromethyl)benzylidene)benzenesulfonamide (108a)**

Following general procedure A, a mixture of 4-(trifluoro)benzaldehyde (2.70 mL, 3.44 g, 20 mmol), *p*-toluenesulfonamide (3.39 g, 20 mmol) and boron trifluoride etherate (30 μL, 26 mg, 0.02 mmol) were refluxed in toluene (60 mL) for 24 hours. The title compound was afforded as a beige powder and used without further purification. <sup>1</sup>H NMR (400 MHz, CDCl<sub>3</sub>) δ 9.07 (s, 1H), 8.05 (d, *J* 8.1, 2H), 7.90 (d, *J* 8.4, 2H), 7.74 (d, *J* 8.2, 2H), 7.37 (d, *J* 8.0, 2H), 2.45 (s, 3H); <sup>13</sup>C NMR (101 MHz, CDCl<sub>3</sub>) δ 168.5, 145.2, 136.1 (q, <sup>2</sup>*J*<sub>CF</sub> 32.9), 135.5, 134.6, 131.5, 130.1, 128.4, 126.2 (q, <sup>3</sup>*J*<sub>CF</sub> 3.7), 123.4 (q, <sup>1</sup>*J*<sub>CF</sub> 273.0), 21.8; <sup>19</sup>F NMR (377 MHz, CDCl<sub>3</sub>) δ -63.31. IR: 1610, 1569 cm<sup>-1</sup>; MS: (ES<sup>+</sup>) 328.06 [M + H]<sup>+</sup>; HRMS: Calc'd for C<sub>15</sub>H<sub>13</sub>F<sub>3</sub>NO<sub>2</sub>S<sup>+</sup>: 328.0619; found: 328.0614. Data is consistent with that reported for the title compound by Stead.<sup>134</sup>



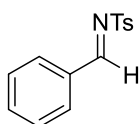
### **(*E*)-*N*-(3,5-Bis(trifluoromethyl)benzylidene)-4-methylbenzenesulfonamide (108b)**

Following general procedure A, a mixture of 3,5-bis(trifluoromethyl)benzaldehyde (3.30 mL, 4.85 g, 20 mmol), *p*-toluenesulfonamide (3.44 g, 20 mmol) and boron trifluoride etherate (30  $\mu$ L, 35 mg, 0.02 mmol) were refluxed in toluene (60 mL) for 24 hours. The title compound was afforded as a beige powder and used without further purification.  $^1\text{H}$  NMR (400 MHz,  $\text{CDCl}_3$ )  $\delta$  9.11 (s, 1H), 8.37 (s, 2H), 8.09 (s, 1H), 7.91 (d, *J* 8.4, 2H), 7.39 (d, *J* 8.0, 2H), 2.46 (s, 3H);  $^{13}\text{C}$  NMR (101 MHz,  $\text{CDCl}_3$ )  $\delta$  166.7, 145.6, 134.4, 134.0, 133.1 (q,  $^2J_{\text{CF}}$  34.2), 130.8 (q,  $^3J_{\text{CF}}$  3.9), 130.2, 128.6, 127.7 (q,  $^3J_{\text{CF}}$  3.7), 122.7 (q,  $^1J_{\text{CF}}$  273.3), 21.9.;  $^{19}\text{F}$  NMR (377 MHz,  $\text{CDCl}_3$ )  $\delta$  -63.09; IR: 1630, 1598, 1456  $\text{cm}^{-1}$ ; MS: ( $\text{ES}^+$ ) 396.05 [ $\text{M} + \text{H}$ ] $^+$ ; HRMS: Calc'd for  $\text{C}_{16}\text{H}_{11}\text{F}_6\text{NO}_2\text{S}^+$ : 396.0493; found: 396.0503. M.P.: 88 – 90  $^\circ\text{C}$ .



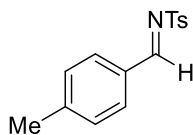
#### **(*E*)-4-Methyl-*N*-(4-(trifluoromethyl)benzylidene)benzenesulfonamide (108c)**

Following general procedure A, a mixture of 4-bromobenzaldehyde (3.70 g, 20 mmol), *p*-toluenesulfonamide (3.43 g, 20 mmol) and boron trifluoride etherate (30  $\mu$ L, 35 mg, 0.02 mmol) were refluxed in toluene (60 mL) for 24 hours. The title compound was afforded as a white powder and used without further purification.  $^1\text{H}$  NMR (400 MHz,  $\text{CDCl}_3$ )  $\delta$  8.98 (s, 1H), 7.88 (d, *J* 8.3, 2H), 7.78 (d, *J* 8.5, 2H), 7.63 (d, *J* 8.5, 2H), 7.35 (d, *J* 8.0, 2H), 2.44 (s, 3H);  $^{13}\text{C}$  NMR (101 MHz,  $\text{CDCl}_3$ )  $\delta$  168.9, 144.9, 135.0, 132.7, 132.5, 131.3, 130.4, 130.0, 128.3, 21.8; IR: 1654, 1603, 1586, 1558  $\text{cm}^{-1}$ ; MS: ( $\text{ES}^+$ ) 339.98 [ $\text{M} + \text{H}$ ] $^+$ ; HRMS: Calc'd for  $\text{C}_{14}\text{H}_{13}\text{BrNO}_2\text{S}^+$ : 337.9850; found: 337.9859. Data is consistent with that reported for the title compound by Stead.<sup>134</sup>



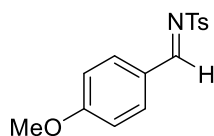
#### **(*E*)-*N*-Benzylidene-4-methylbenzenesulfonamide (108d)**

Following general procedure A, a mixture of benzaldehyde (3.00 mL, 3.13 g, 29.5 mmol), *p*-toluenesulfonamide (5.05 g, 29.5 mmol) and boron trifluoride etherate (40  $\mu$ L, 46 mg, 0.0295 mmol) were refluxed in toluene (60 mL) for 24 hours. The title compound was afforded as a beige powder and used without further purification.  $^1\text{H}$  NMR (400 MHz,  $\text{CDCl}_3$ )  $\delta$  9.03 (s, 1H), 7.95 – 7.87 (m, 4H), 7.65 – 7.58 (m, 1H), 7.49 (t, *J* 7.7, 2H), 7.35 (d, *J* 8.0, 2H), 2.44 (s, 3H);  $^{13}\text{C}$  NMR (101 MHz,  $\text{CDCl}_3$ )  $\delta$  170.3, 144.8, 135.3, 135.1, 132.5, 131.5, 130.0, 129.3, 128.3, 21.8; IR: 1650, 1596, 1574  $\text{cm}^{-1}$ ; MS: ( $\text{ES}^+$ ) 282.06 [ $\text{M} + \text{Na}$ ] $^+$ ; HRMS: Calc'd for  $\text{C}_{14}\text{H}_{13}\text{NO}_2\text{S}^+$ : 282.0565; found: 282.0567. Data is consistent with that reported for the title compound by Reed-Berendt.<sup>135</sup>



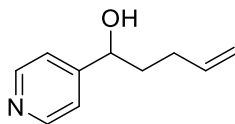
**(E)-4-Methyl-N-(4-methylbenzylidene)benzenesulfonamide (108e)**

Following general procedure A, a mixture of 4-methylbenzaldehyde (2.40 mL, 2.45 g, 20 mmol), *p*-toluenesulfonamide (3.49 g, 20 mmol) and boron trifluoride etherate (30  $\mu$ L, 35 mg, 0.02 mmol) were refluxed in toluene (60 mL) for 24 hours. The title compound was afforded as an orange powder and used without further purification.  $^1\text{H}$  NMR (400 MHz,  $\text{CDCl}_3$ )  $\delta$  8.99 (s, 1H), 7.88 (d, *J* 8.3, 2H), 7.82 (d, *J* 8.2, 2H), 7.34 (d, *J* 8.0, 2H), 7.29 (d, *J* 8.0, 2H), 2.434 (s, 3H), 2.428 (s, 3H);  $^{13}\text{C}$  NMR (101 MHz,  $\text{CDCl}_3$ )  $\delta$  170.1, 146.5, 144.6, 135.5, 131.6, 130.1, 130.0, 129.9, 128.2, 22.2, 21.8; IR: 2917, 1667, 1594, 1562  $\text{cm}^{-1}$ ; MS: ( $\text{ES}^+$ ) 274.09 [ $\text{M} + \text{H}$ ] $^+$ ; HRMS: Calc'd for  $\text{C}_{15}\text{H}_{15}\text{NO}_2\text{S}^+$ : 274.0902; found: 274.0907. Data is consistent with that reported for the title compound by Huang *et al.*<sup>136</sup>



**(E)-N-(4-Methoxybenzylidene)-4-methylbenzenesulfonamide (108f)**

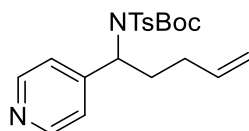
Following general procedure A, a mixture of 4-methoxybenzaldehyde (2.40 mL, 2.69 g, 20 mmol), *p*-toluenesulfonamide (3.43 g, 20 mmol) and boron trifluoride etherate (30  $\mu$ L, 35 mg, 0.02 mmol) were refluxed in toluene (60 mL) for 24 hours. The title compound was afforded as a purple powder and used without further purification.  $^1\text{H}$  NMR (400 MHz,  $\text{CDCl}_3$ )  $\delta$  8.94 (s, 1H), 7.90 – 7.84 (m, 4H), 7.35 – 7.30 (m, 2H), 6.96 (d, *J* 8.9, 2H), 3.88 (s, 3H), 2.43 (s, 3H);  $^{13}\text{C}$  NMR (101 MHz,  $\text{CDCl}_3$ )  $\delta$  169.3, 165.4, 144.4, 133.8, 129.8, 128.0, 126.5, 125.3, 114.8, 55.8, 21.7; IR: 1672, 1593, 1558, 1511  $\text{cm}^{-1}$ ; MS: ( $\text{ES}^+$ ) 290.09 [ $\text{M} + \text{H}$ ] $^+$ ; HRMS: Calc'd for  $\text{C}_{15}\text{H}_{16}\text{NO}_3\text{S}^+$ : 290.0851; found: 290.0856. Data is consistent with that reported for the title compound by Stead.<sup>134</sup>



**1-(Pyridin-4-yl)pent-4-en-1-ol (110g)**

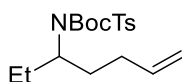
Following general procedure B, a mixture of 4-pyridinecarboxaldehyde (880  $\mu$ L, 1.00 g, 9.34 mmol), 4-bromobutene (1.90 g, 14 mmol) and magnesium turnings (486 mg, 20 mmol) and THF (30 mL) were stirred for 16 hours. Purified by column chromatography (0 -> 70% EtOAc in Hexane gradient) to afford the title compound as a brown oil in 26% yield (390 mg).  $^1\text{H}$  NMR (400 MHz,  $\text{CDCl}_3$ )  $\delta$  8.55 – 8.46 (m,

2H), 7.28 (d, *J* 6.4, 2H), 5.84 (ddt, *J* 16.9, 10.2 & 6.6, 1H), 5.12 – 4.96 (m, 2H), 4.73 (dd, *J* 7.7 & 5.2, 1H), 3.07 (s, 1H), 2.24 – 2.11 (m, 2H), 1.98 – 1.73 (m, 2H);  $^{13}\text{C}$  NMR (101 MHz,  $\text{CDCl}_3$ )  $\delta$  154.0, 149.8, 137.9, 121.0, 115.6, 72.4, 38.0, 29.9; IR: 3190, 3077, 2977, 2917, 2850, 1641, 1604, 1561, 1413  $\text{cm}^{-1}$ ; MS: ( $\text{ES}^+$ ) 164.11 [ $\text{M} + \text{H}$ ] $^+$ ; HRMS: Calc'd for  $\text{C}_{10}\text{H}_{14}\text{NO}^+$ : 164.1075; found: 164.1077;  $R_f$  = 0.21 (70% EtOAc in hexane).



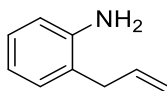
#### ***tert*-Butyl (1-(pyridin-4-yl)pent-4-en-1-yl)(tosyl)carbamate (112g)**

Following general procedure C, a mixture of 1-(pyridin-4-yl)pent-4-en-1-ol (370 mg), triphenylphosphine (894 mg), *tert*-butyl tosylcarbamate (925 mg) and DIAD (670  $\mu\text{L}$ , 688 mg) were stirred in THF (10 mL) for 16 hours. Purified by column chromatography (0  $\rightarrow$  70% EtOAc in Hexane gradient) to afford the title compound as a colourless oil in 55% yield (517 mg).  $^1\text{H}$  NMR (400 MHz,  $\text{CDCl}_3$ )  $\delta$  8.60 – 8.54 (m, 2H), 7.74 (d, *J* 8.4, 2H), 7.33 – 7.27 (m, 4H), 5.89 (ddt, *J* 16.8, 10.2 & 6.5, 1H), 5.61 (d, *J* 7.7, 1H), 5.14 – 5.02 (m, 2H), 2.45 (s, 3H), 2.43 – 2.35 (m, 2H), 2.31 – 2.13 (m, 2H), 1.25 (s, 9H);  $^{13}\text{C}$  NMR (101 MHz,  $\text{CDCl}_3$ )  $\delta$  150.6, 150.0, 149.3, 144.7, 137.1, 136.7, 129.3, 128.7, 122.4, 115.9, 84.9, 59.1, 31.1, 31.0, 27.9, 21.7; IR: 3676, 2988, 2902, 1728, 1642, 1597, 1559, 1495, 1455  $\text{cm}^{-1}$ ; MS: (ASAP $^+$ ) 417.18 [ $\text{M} + \text{H}$ ] $^+$ ; HRMS: Calc'd for  $\text{C}_{22}\text{H}_{29}\text{SN}_2\text{O}_4^+$ : 417.1848; found: 417.1845;  $R_f$  = 0.63 (70% EtOAc in hexane).



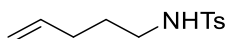
#### ***tert*-Butyl hept-6-en-3-yl(tosyl)carbamate (112h)**

Following general procedure C, a mixture of 6-hepten-3-ol (503 mg, 4.4 mmol), *tert*-butyl tosylcarbamate (1.80 g, 6.6 mmol), DIAD (1.3 mL, 1.34 g, 6.6 mmol), triphenylphosphine (1.73 g, 6.6 mmol) were stirred in THF (20 mL) for 16 hours. The title compound was obtained as a colourless oil, 65% yield (1.05 g).  $^1\text{H}$  NMR (400 MHz,  $\text{CDCl}_3$ )  $\delta$  7.83 (d, *J* 8.4, 2H), 7.29 (d, *J* 8.0, 2H), 5.83 (ddt, *J* 16.8, 10.2 & 6.5, 1H), 5.04 (dq, *J* 17.1 & 1.7, 1H), 4.98 (ddt, *J* 10.2, 2.0 & 1.2, 1H), 4.34 (tt, *J* 8.6 & 6.3, 1H), 2.43 (s, 3H), 2.16 – 1.69 (m, 6H), 1.37 (s, 9H), 0.93 (t, *J* 7.5, 3H);  $^{13}\text{C}$  NMR (101 MHz,  $\text{CDCl}_3$ )  $\delta$  151.1, 144.0, 138.1, 137.8, 129.2, 128.5, 115.1, 84.0, 61.4, 33.0, 31.3, 28.1, 26.6, 21.7, 11.8; IR: 2976, 2935, 2879, 1722, 1641, 1598  $\text{cm}^{-1}$ ; MS: ( $\text{ES}^+$ ) = 390.17 [ $\text{M} + \text{Na}$ ] $^+$ ; HRMS: Calc'd for  $\text{C}_{19}\text{H}_{29}\text{NO}_4\text{SNa}^+$ : 390.1715; found: 390.1723;  $R_f$  = 0.47 (10% EtOAc in hexane).



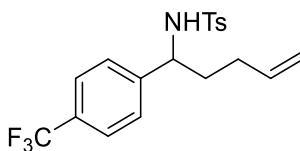
### 2-Allylaniline (117)

Procedure described by Cheng-Sánchez *et al.*<sup>94</sup> 2-bromoaniline (1.00 g, 5.81 mmol) and Pd(PPh<sub>3</sub>)<sub>4</sub> (336 mg, 0.29 mmol, 5 mol%) is added to an oven-dried flask under argon followed by the addition of 15 mL of dry DMF. Allyltributylstannane (2.20 mL, 2.35 g, 7.10 mmol, 1.2 equiv.) is added dropwise and then the reaction mixture is heated at 80 °C for 21 hours. The following day, the reaction mixture is cooled to room temperature and diluted with 20 mL diethyl ether and 20 mL water. The mixture is transferred to a separating funnel and the ether layer is washed with water three times followed by a brine wash. The organic layer is dried (MgSO<sub>4</sub>), filtered and concentrated followed by column chromatography (5% EtOAc in hexane) to afford the title compound as a brown oil, 61% yield (470 mg). <sup>1</sup>H NMR (400 MHz, CDCl<sub>3</sub>) δ 7.12 – 7.01 (m, 2H), 6.76 (t, *J* 7.3, 1H), 6.69 (dd, *J* 7.8, 1.2, 1H), 6.03 – 5.90 (m, 1H), 5.17 – 5.07 (m, 2H), 3.67 (s, 2H), 3.32 (d, *J* 6.2, 2H); <sup>13</sup>C NMR (101 MHz, CDCl<sub>3</sub>) δ 144.9, 136.1, 130.3, 127.7, 124.1, 119.0, 116.2, 115.9, 36.6; IR: 3449, 3371, 3225, 3077, 3024, 3008, 2976, 2911, 1620, 1583, 1494 cm<sup>-1</sup>; MS: (ES<sup>+</sup>) = 134.10 [M + H]<sup>+</sup>; HRMS: Calc'd for C<sub>9</sub>H<sub>12</sub>N<sup>+</sup>: 134.0970; found: 134.0970. Data is consistent with that reported for the title compound by Cheng-Sánchez *et al.*<sup>94</sup>



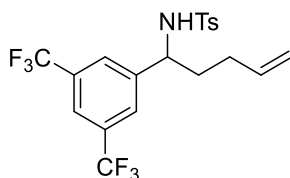
### 4-Methyl-*N*-(pent-4-en-1-yl)benzenesulfonamide (65)

Procedure described by Feltenberger *et al.*<sup>90</sup> 5-Bromo-1-pentene (800 µL, 1.01 g, 6.71 mmol), *p*-toluenesulfonamide (1.04 g, 6.1 mmol) and potassium carbonate (1.69 g, 12.2 mmol) were dissolved in acetone (6 mL) and refluxed for 24 hours. The following day the mixture is filtered through celite (EtOAc) and the solvent is removed *in vacuo*. The crude mixture is subjected to column chromatography (0 → 20% EtOAc in hexane gradient) to afford the title compound as a colourless oil in 45% yield (660 mg). <sup>1</sup>H NMR (400 MHz, CDCl<sub>3</sub>) δ 7.76 – 7.72 (m, 2H), 7.32 – 7.27 (m, 2H), 5.69 (ddtd, *J* 16.9, 10.2, 6.7 & 1.0, 1H), 5.10 – 4.78 (m, 3H), 2.93 (td, *J* 7.0 & 1.4, 2H), 2.42 (s, 3H), 2.08 – 1.96 (m, 2H), 1.55 (p, *J* 7.2, 2H); <sup>13</sup>C NMR (101 MHz, CDCl<sub>3</sub>) δ 143.5, 137.3, 137.0, 129.8, 127.2, 115.6, 42.7, 30.7, 28.8, 21.6; IR 3280, 2929 cm<sup>-1</sup>; MS: (ES<sup>+</sup>) 262.09 [M + Na]<sup>+</sup>; HRMS: Calc'd for: C<sub>12</sub>H<sub>17</sub>NO<sub>2</sub>S<sup>+</sup>: 262.0878; found: 262.0883; R<sub>f</sub> = 0.34 (20% EtOAc in hexane). Data is consistent with that reported for the title compound by Zhang *et al.*<sup>137</sup>



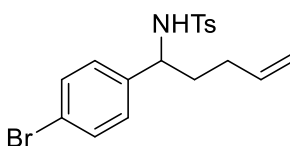
#### 4-Methyl-*N*-(1-(4-(trifluoromethyl)phenyl)pent-4-en-1-yl)benzenesulfonamide (104a)

Following general procedure B, a mixture of 4-methyl-*N*-(4-(trifluoromethyl)benzylidene)benzenesulfonamide (2.01 g, 6.11 mmol), 4-bromobutene (1.28 g, 9.17 mmol) and magnesium turnings (243 mg, 10 mmol) were stirred in dry THF (20 mL) to afford the title compound as a yellow solid in 47% yield (1.10 g).  $^1\text{H}$  NMR (400 MHz,  $\text{CDCl}_3$ )  $\delta$  7.46 (d,  $J$  8.3, 2H), 7.35 (d,  $J$  8.1, 2H), 7.11 (d,  $J$  8.1, 2H), 7.05 (d,  $J$  8.0, 2H), 5.69 (ddt,  $J$  16.9, 10.3 & 6.5, 1H), 5.34 (d,  $J$  7.5, 1H), 5.02 – 4.89 (m, 2H), 4.38 (q,  $J$  7.3, 1H), 2.32 (s, 3H), 2.03 – 1.92 (m, 2H), 1.92 – 1.81 (m, 1H), 1.79 – 1.68 (m, 1H);  $^{13}\text{C}$  NMR (101 MHz,  $\text{CDCl}_3$ )  $\delta$  144.7, 143.4, 137.4, 136.8, 129.6 (q,  $^2J_{\text{CF}}$  32.4), 129.4, 127.2, 127.1, 125.4 (q,  $^3J_{\text{CF}}$  4.0), 123.6 (q,  $^1J_{\text{CF}}$  272.0), 116.1, 57.5, 36.5, 29.9, 21.4;  $^{19}\text{F}$  NMR (377 MHz,  $\text{CDCl}_3$ )  $\delta$  -62.63; IR: 3271, 2928, 1716, 1642, 1620, 1599, 1495, 1428  $\text{cm}^{-1}$ ; MS: ( $\text{ES}^+$ ) 406.11  $[\text{M} + \text{Na}]^+$ ; HRMS: Calc'd for  $\text{C}_{19}\text{H}_{20}\text{F}_3\text{NO}_2\text{S}^+$ : 406.1065; found: 406.1071;  $R_f$  = 0.19 (10% EtOAc in hexane); M.P.: 72-75  $^\circ\text{C}$ .



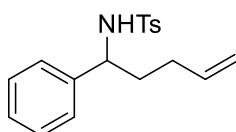
#### *N*-(1-(3,5-Bis(trifluoromethyl)phenyl)pent-4-en-1-yl)-4-methylbenzenesulfonamide (104b)

Following general procedure B, a mixture of *N*-(3,5-bis(trifluoromethyl)benzylidene)-4-methylbenzenesulfonamide (3.17 g, 8 mmol), 4-bromobutene (1.35 g, 10 mmol) and magnesium turnings (292 mg, 12 mmol) were stirred in dry THF (15 mL) to afford the title compound as a white solid in 31% yield (1.13 g).  $^1\text{H}$  NMR (400 MHz,  $\text{CDCl}_3$ )  $\delta$  7.60 (s, 1H), 7.47 (s, 1H), 7.45 (d,  $J$  2.2, 3H), 7.05 (d,  $J$  8.1, 2H), 5.75 (d,  $J$  7.1, 1H), 5.68 (ddt,  $J$  17.1, 10.3 & 7.0, 1H), 5.04 – 4.91 (m, 2H), 4.48 (q,  $J$  7.2, 1H), 2.31 (s, 3H), 2.06 – 1.97 (m, 2H), 1.95 – 1.84 (m, 1H), 1.81 – 1.71 (m, 1H);  $^{13}\text{C}$  NMR (101 MHz,  $\text{CDCl}_3$ )  $\delta$  143.9, 143.5, 137.1, 136.4, 131.8 (q,  $^2J_{\text{CF}}$  = 33.3), 129.6, 127.06, 127.02, 123.1 (q,  $^1J_{\text{CF}}$  = 272.8), 121.4 (app p,  $^3J_{\text{CF}}$  = 3.8), 116.6, 57.1, 36.5, 29.9, 21.4;  $^{19}\text{F}$  NMR (377 MHz,  $\text{CDCl}_3$ )  $\delta$  -63.00; IR: 3282, 3253, 3066, 2959, 2920, 2862, 1645, 1624, 1599, 1496, 1441  $\text{cm}^{-1}$ ; MS: ( $\text{ES}^+$ ) 469.14  $[\text{M} + \text{NH}_4]^+$ ; HRMS: Calc'd for  $\text{C}_{20}\text{H}_{23}\text{F}_6\text{N}_2\text{O}_2\text{S}^+$ : 469.1384; found: 469.1389;  $R_f$  = 0.58 (20% EtOAc in hexane); M.P.: 112 – 115  $^\circ\text{C}$ .



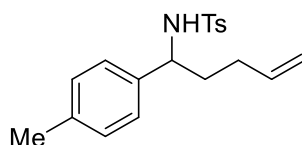
#### *N*-(1-(4-Bromophenyl)pent-4-en-1-yl)-4-methylbenzenesulfonamide (104c)

Following general procedure B, a mixture of 4-methyl-*N*-(4-(bromo)benzylidene) benzenesulfonamide (3.01 g, 8.87 mmol), 4-bromobutene (1.81 g, 13.31 mmol) and magnesium turnings (365 mg, 15 mmol) were stirred in dry THF (30 mL) to afford the title compound as a white solid in 34% yield (1.19 g).  $^1\text{H}$  NMR (400 MHz,  $\text{CDCl}_3$ )  $\delta$  7.48 (d,  $J$  8.3, 2H), 7.26 (d,  $J$  8.5, 3H), 7.12 (d,  $J$  7.8, 2H), 6.87 (d,  $J$  8.4, 2H), 5.68 (ddt,  $J$  16.9, 10.3 & 6.5, 1H), 5.01 – 4.84 (m, 3H), 4.27 (q,  $J$  7.2, 1H), 2.38 (s, 3H), 2.01 – 1.90 (m, 2H), 1.89 – 1.78 (m, 1H), 1.77 – 1.66 (m, 1H);  $^{13}\text{C}$  NMR (101 MHz,  $\text{CDCl}_3$ )  $\delta$  143.5, 139.7, 137.6, 136.9, 131.6, 129.5, 128.5, 127.2, 121.5, 116.0, 57.3, 36.6, 30.0, 21.6; IR: 3246, 3064, 2920, 1642, 1598  $\text{cm}^{-1}$ ; MS: ( $\text{ES}^+$ ) 418.03 [ $\text{M} + \text{Na}$ ] $^+$ ; HRMS: Calc'd for  $\text{C}_{18}\text{H}_{20}\text{BrNO}_2\text{SNa}^+$ : 416.0296; found: 416.0300;  $R_f$  = 0.17 (10% EtOAc in hexane); M.P.: 139 – 141  $^\circ\text{C}$ .



#### 4-Methyl-*N*-(1-phenylpent-4-en-1-yl)benzenesulfonamide (104d)

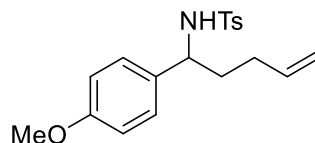
Following general procedure B, a mixture of *N*-benzylidene-4-methylbenzenesulfonamide (1.15 g, 7.71 mmol), 4-bromobutene (1.55 g, 11.5 mmol) and magnesium turnings (365 mg, 15 mmol) were stirred in dry THF (40 mL) to afford the title compound as a white solid in 47% yield (662 mg).  $^1\text{H}$  NMR (400 MHz,  $\text{CDCl}_3$ )  $\delta$  7.52 (d,  $J$  8.3, 2H), 7.19 – 7.13 (m, 3H), 7.11 (d,  $J$  8.0, 2H), 7.03 – 6.96 (m, 2H), 5.70 (ddt,  $J$  17.0, 10.4 & 6.3, 1H), 4.99 – 4.79 (m, 3H), 4.29 (q,  $J$  7.1, 1H), 2.35 (s, 3H), 2.03 – 1.72 (m, 4H);  $^{13}\text{C}$  NMR (101 MHz,  $\text{CDCl}_3$ )  $\delta$  143.1, 140.7, 137.8, 137.3, 129.4, 128.6, 127.6, 127.2, 126.6, 115.7, 58.0, 36.8, 30.1, 21.6; IR: 3249, 3077, 2943, 2917  $\text{cm}^{-1}$ ; MS: ( $\text{ES}^+$ ) 338.1 [ $\text{M} + \text{Na}$ ] $^+$ ; HRMS: Calc'd for  $\text{C}_{18}\text{H}_{21}\text{NO}_2\text{SNa}^+$ : 338.1191; found: 338.1200;  $R_f$  = 0.21 (10% EtOAc in hexane); M.P.: 78 – 80  $^\circ\text{C}$ .



#### 4-Methyl-*N*-(1-(p-tolyl)pent-4-en-1-yl)benzenesulfonamide (104e)

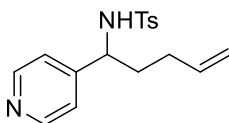
Following general procedure B, a mixture of 4-methyl-*N*-(4-methylbenzylidene) benzenesulfonamide (1.00 g, 3.66 mmol), 4-bromobutene (743 mg, 5.5 mmol) and magnesium turnings (178 mg, 7.32 mmol) were stirred in dry THF (18 mL) to afford the title compound as a yellow solid in 36% yield (432 mg).  $^1\text{H}$  NMR (400 MHz,  $\text{CDCl}_3$ )  $\delta$  7.54 (d,  $J$  8.3, 2H), 7.11 (d,  $J$  7.9, 2H), 6.95 (d,  $J$  7.9, 2H), 6.88 (d,  $J$  8.1, 2H), 5.69 (ddt,  $J$  17.0, 10.5 & 6.3, 1H), 5.17 (d,  $J$  7.2, 1H), 4.99 – 4.85 (m, 2H), 4.24 (q,  $J$  7.3, 1H), 2.36 (s, 3H), 2.26 (s, 3H), 2.00 – 1.82 (m, 3H), 1.81 – 1.70 (m, 1H);  $^{13}\text{C}$  NMR (101 MHz,  $\text{CDCl}_3$ )  $\delta$  143.0, 137.8, 137.7, 137.4, 137.2, 129.3, 129.2, 127.2, 126.6, 115.5, 57.7, 36.7, 30.1, 21.6, 21.1; IR: 3249, 2979, 2919, 1911, 1820, 1642, 1598, 1517, 1497  $\text{cm}^{-1}$ ; MS: ( $\text{ES}^+$ ) 352.14 [ $\text{M} + \text{Na}$ ] $^+$ ;

HRMS: Calc'd for  $C_{19}H_{23}NO_2S^+$ : 352.1347 found: 352.1353;  $R_f$  = 0.41 (20% EtOAc in hexane); M.P.: 102 – 104 °C.



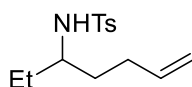
#### ***N*-(1-(4-Methoxyphenyl)pent-4-en-1-yl)-4-methylbenzenesulfonamide (104f)**

Following general procedure B, a mixture of *N*-(4-methoxybenzylidene)-4-methylbenzenesulfonamide (2.01 g, 6.91 mmol), 4-bromobutene (1.40 g, 10.37 mmol) and magnesium turnings (335 mg, 13.8 mmol) were stirred in dry THF (20 mL) to afford the title compound as a white solid in 49% yield (1.17 g).  $^1H$  NMR (400 MHz,  $CDCl_3$ )  $\delta$  7.53 (d,  $J$  8.3, 2H), 7.12 (d,  $J$  7.9, 2H), 6.91 (d,  $J$  8.6, 2H), 6.67 (d,  $J$  8.8, 2H), 5.78 – 5.60 (m, 1H), 5.02 – 4.84 (m, 3H), 4.23 (q,  $J$  7.4, 1H), 3.74 (s, 3H), 2.36 (s, 3H), 2.01 – 1.82 (m, 3H), 1.81 – 1.68 (m, 1H);  $^{13}C$  NMR (101 MHz,  $CDCl_3$ )  $\delta$  159.0, 143.0, 137.9, 137.4, 132.8, 129.4, 127.8, 127.2, 115.6, 113.9, 57.5, 55.4, 36.7, 30.1, 21.6; IR: 3249, 3065, 2914, 2836, 1641, 1614, 1586, 1514  $cm^{-1}$ ; MS: (ES $^+$ ) 368.13 [M + Na] $^+$ ; HRMS: Calc'd for  $C_{19}H_{23}NO_3SNa^+$ : 368.1296; found: 368.1306;  $R_f$  = 0.31 (20% EtOAc in hexane); M.P.: 84 – 86 °C.



#### **4-Methyl-*N*-(1-(pyridin-4-yl)pent-4-en-1-yl)benzenesulfonamide (104g)**

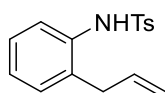
Following general procedure D, a mixture of *tert*-butyl (1-(pyridin-4-yl)pent-4-en-1-yl)(tosyl)carbamate (1.80 g, 4.48 mmol) and trifluoroacetic acid (7.00 mL, 10.4 g, 90 mmol) were stirred in  $CH_2Cl_2$  (28 mL) for four hours. The title compound was afforded as a white powder in 42% yield (568 mg).  $^1H$  NMR (400 MHz,  $CDCl_3$ )  $\delta$  8.39 (dd,  $J$  4.2 & 1.6, 2H), 7.54 (d,  $J$  8.3, 2H), 7.14 (d,  $J$  8.0, 2H), 6.97 (dd,  $J$  4.3 & 1.5, 2H), 5.67 (ddt,  $J$  16.9, 10.2 & 6.5, 1H), 5.37 (d,  $J$  7.6, 1H), 5.03 – 4.86 (m, 2H), 4.32 (q,  $J$  7.3, 1H), 2.36 (s, 3H), 2.06 – 1.89 (m, 2H), 1.86 – 1.70 (m, 2H).  $^{13}C$  NMR (101 MHz,  $CDCl_3$ )  $\delta$  150.0, 150.0, 143.7, 137.4, 136.6, 129.6, 127.1, 121.7, 116.3, 56.7, 36.3, 29.8, 21.6. IR: 3033, 2925, 2859, 2770, 1642, 1601, 1563, 1494, 1436, 1414  $cm^{-1}$ ; MS: (ASAP $^+$ ) 317.13 [M + H] $^+$ ; HRMS: Calc'd for  $C_{17}H_{21}N_2O_2S^+$ : 317.1324; found: 317.1324;  $R_f$  = 0.53 (70% EtOAc in hexane); M.P.: 170 – 173 °C.



#### ***N*-(Hept-6-en-3-yl)-4-methylbenzenesulfonamide (104h)**

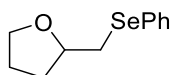


Following general procedure D, a mixture of *tert*-butyl hept-6-en-3-yl(tosyl)carbamate (1.03 g, 2.8 mmol) and trifluoroacetic acid (4.30 mL, 6.40 g, 56 mmol) were stirred in CH<sub>2</sub>Cl<sub>2</sub> (18 mL) for four hours. The title compound was afforded as a colourless oil in 93% yield (695 mg). <sup>1</sup>H NMR (400 MHz, CDCl<sub>3</sub>) δ 7.75 (d, *J* 8.3, 2H), 7.29 (d, *J* 7.9, 2H), 5.67 (ddt, *J* 17.7, 9.6 & 6.6, 1H), 4.97 – 4.85 (m, 2H), 4.23 (d, *J* 9.0, 1H), 3.26 – 3.12 (m, 1H), 2.43 (s, 3H), 2.05 – 1.85 (m, 2H), 1.54 – 1.24 (m, 5H), 0.76 (t, *J* 7.4, 3H); <sup>13</sup>C NMR (101 MHz, CDCl<sub>3</sub>) δ 143.3, 138.5, 137.9, 129.7, 127.2, 115.2, 55.1, 33.9, 29.7, 27.8, 21.7, 9.7; IR: 3280, 2969, 2934, 2878, 1777, 1641, 1599 cm<sup>-1</sup>; MS: (ES<sup>+</sup>) 290.12 [M + Na]<sup>+</sup>; HRMS: Calc'd for C<sub>14</sub>H<sub>21</sub>NO<sub>2</sub>SN<sup>+</sup>: 290.1191; found: 290.1198; R<sub>f</sub> = 0.50 (20% EtOAc in hexane).



### **N-(2-Allylphenyl)-4-methylbenzenesulfonamide (105)**

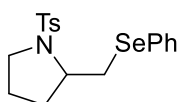
Procedure described by Yamamoto *et al.*<sup>95</sup> 2-allylaniline (441 mg, 3.31 mmol) and *p*-toluenesulfonyl chloride (953 mg, 5 mmol, 1.6 equiv.) is added to flask in CH<sub>2</sub>Cl<sub>2</sub> (11 mL) followed by the dropwise addition of pyridine (1.33 mL, 1.30 g, 16.6 mmol, 5 equiv.) and stirred for four hours. Upon completion of the reaction, the reaction mixture is transferred to a separating funnel and washed with water (x2) and brine and subsequently dried (MgSO<sub>4</sub>), filtered and concentrated. The crude mixture is subjected to column chromatography (5% EtOAc in hexane) to afford the title compound as a beige solid in 87% yield (832 mg). <sup>1</sup>H NMR (400 MHz, CDCl<sub>3</sub>) δ 7.59 (d, *J* 8.3, 2H), 7.41 (dd, *J* 8.0 & 1.3, 1H), 7.25 – 7.18 (m, 3H), 7.14 – 7.04 (m, 2H), 6.50 (s, 1H), 5.78 (ddt, *J* 17.3, 10.1 & 6.0, 1H), 5.12 (dq, *J* 10.1 & 1.5, 1H), 4.94 (dq, *J* 17.2 & 1.7, 1H), 3.00 (dt, *J* 6.0 & 1.8, 2H), 2.39 (s, 3H). <sup>13</sup>C NMR (101 MHz, CDCl<sub>3</sub>) δ 143.8, 136.8, 135.6, 135.0, 131.8, 130.5, 129.6, 127.8, 127.1, 126.3, 124.5, 117.1, 36.2, 21.6; IR: 3282, 3098, 3019, 2922, 1917, 1842, 1644, 1598, 1582, 1490 cm<sup>-1</sup>; MS: (ES<sup>+</sup>) 288.11 [M + H]<sup>+</sup>; HRMS: Calc'd for C<sub>16</sub>H<sub>18</sub>NO<sub>2</sub>S<sup>+</sup>: 288.1058; found: 288.1066. Data is consistent with that reported for the title compound by Yamamoto *et al.*<sup>95</sup>



### **2-((Phenylselanyl)methyl)tetrahydrofuran (97)**

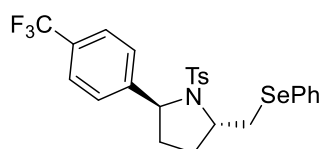
Procedure described from Meng *et al.*<sup>84</sup> Pent-4-en-1-ol (43 mg, 0.5 mmol), diphenyl diselenide (79 mg, 0.25 mmol) and ammonium iodide (9 mg, 0.05 mmol) were added to an ElectraSyn vial and dissolved in MeCN (6 mL) and subjected to 10 mA constant current electrolysis with the polarity altering every 10 minutes until 5 F/mol had been passed. Upon completion of the reaction, the contents of the vial were transferred to a separating funnel and all components of the reaction were washed with EtOAc and water was added to the separating funnel. The aqueous layer was extracted

with EtOAc (x2) and then the organic layers were washed with brine, dried (MgSO<sub>4</sub>), filtered and the solvent was removed *in vacuo*. The crude reaction mixture was subjected to column chromatography (0 -> 20% EtOAc in hexane gradient) to afford the title compound as a brown oil in 80% yield (94 mg). <sup>1</sup>H NMR (400 MHz, CDCl<sub>3</sub>) δ 7.56 – 7.47 (m, 2H), 7.30 – 7.17 (m, 3H), 4.09 (app p, *J* 6.8, 1H), 3.95 – 3.84 (m, 1H), 3.75 (ddd, *J* 8.3, 7.5, 6.2, 1H), 3.12 (dd, *J* 12.2 & 5.8, 1H), 2.98 (dd, *J* 12.2 & 6.9, 1H), 2.05 (dddd, *J* 11.9, 8.3, 6.6 & 5.1, 1H), 1.98 – 1.79 (m, 2H), 1.62 (ddt, *J* 12.1, 8.6 & 7.2, 1H); <sup>13</sup>C NMR (101 MHz, CDCl<sub>3</sub>) δ 132.6, 130.4, 129.1, 126.9, 78.4, 68.4, 33.1, 31.6, 26.0; <sup>77</sup>Se NMR (76 MHz, CDCl<sub>3</sub>) δ 269.81 (d, *J* 23.8); IR: 2973, 2869, 2242, 1579, 1478, 1438 cm<sup>-1</sup>; MS: (ES<sup>+</sup>) 243.03 [M + H]<sup>+</sup>; HRMS: Calc'd for C<sub>11</sub>H<sub>15</sub>O<sup>76</sup>Se<sup>+</sup>: 239.0315; found: 239.0314. Data is consistent with that reported for the title compound by Meng *et al.*<sup>84</sup>



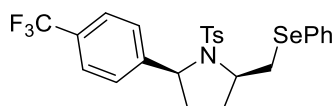
#### 2-((Phenylselanyl)methyl)-1-tosylpyrrolidine (67d)

Procedure described from Meng *et al.*<sup>84</sup> 4-methyl-*N*-(pent-4-en-1-yl)benzenesulfonamide (116 mg, 0.5 mmol), diphenyl diselenide (79 mg, 0.25 mmol) and ammonium iodide (8 mg, 0.05 mmol) were added to an ElectraSyn vial and dissolved in MeCN (6 mL) and subjected to 10 mA constant current electrolysis with the polarity altering every 10 minutes until 5 F/mol had been passed. Upon completion of the reaction, the contents of the vial were transferred to a separating funnel and all components of the reaction were washed with EtOAc and water was added to the separating funnel. The aqueous layer was extracted with EtOAc (x2) and then the organic layers were washed with brine, dried (MgSO<sub>4</sub>), filtered and the solvent was removed *in vacuo*. The crude reaction mixture was subjected to column chromatography (0 -> 20% EtOAc in hexane gradient) to afford the title compound as a brown oil in 79% yield (151 mg). <sup>1</sup>H NMR (400 MHz, CDCl<sub>3</sub>) δ 7.61 – 7.56 (m, 2H), 7.51 (d, *J* 8.3, 2H), 7.35 – 7.27 (m, 3H), 7.22 (d, *J* 8.0, 2H), 3.70 – 3.55 (m, 2H), 3.53 – 3.43 (m, 1H), 3.12 (dt, *J* 9.8 & 7.2, 1H), 2.89 – 2.78 (m, 1H), 2.39 (s, 3H), 1.87 – 1.72 (m, 2H), 1.72 – 1.60 (m, 1H), 1.55 – 1.40 (m, 1H); <sup>13</sup>C NMR (101 MHz, CDCl<sub>3</sub>) δ 143.5, 134.0, 132.5, 129.7, 129.4, 129.3, 127.5, 127.0, 59.9, 50.0, 33.0, 31.1, 23.9, 21.6; <sup>77</sup>Se NMR (76 MHz, CDCl<sub>3</sub>) δ 269.81 (d, *J* 23.8); IR: 3064, 2967, 2921, 2873, 2254, 1736, 1597, 1579, 1497, 1479, 1438 cm<sup>-1</sup>; MS: (ES<sup>+</sup>) 396.05 [M + H]<sup>+</sup>; HRMS: Calc'd for C<sub>18</sub>H<sub>22</sub>NO<sub>2</sub>S<sup>76</sup>Se<sup>+</sup>: 392.0563; found: 392.0563. Data is consistent with that reported for the title compound by Ashikari *et al.*<sup>9</sup>



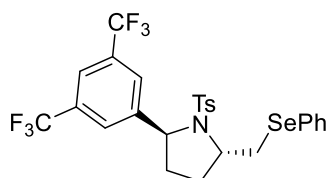
***trans*-2-((Phenylselanyl)methyl)-1-tosyl-5-(4-(trifluoromethyl)phenyl)pyrrolidine (125-*trans*)**

Following general procedure E, a mixture of 4-methyl-*N*-(1-(4-(trifluoromethyl)phenyl)pent-4-en-1-yl)benzenesulfonamide (38 mg, 0.1 mmol), diphenyl diselenide (16 mg, 0.05 mmol), sodium methoxide (6 mg, 0.1 mmol) and tetrabutylammonium bromide (7 mg, 0.02 mmol) were dissolved in HFIP (2.5 mL) and subjected to constant current electrolysis until 5 F/mol had passed. The title compound was afforded as a white solid in 56% yield (30 mg).  $^1\text{H}$  NMR (400 MHz,  $\text{CDCl}_3$ )  $\delta$  7.67 – 7.60 (m, 2H), 7.38 – 7.26 (m, 5H), 7.09 (d,  $J$  8.3, 2H), 6.98 (d,  $J$  8.1, 2H), 6.93 (d,  $J$  8.0, 2H), 5.06 (d,  $J$  8.6, 1H), 4.27 (ddd,  $J$  10.9, 7.2 & 2.6, 1H), 3.95 (ddd,  $J$  12.6, 2.8 & 1.5, 1H), 2.87 (dd,  $J$  12.6 & 11.3, 1H), 2.50 (app tt,  $J$  13.0 & 8.2, 1H), 2.31 (s, 3H), 2.28 – 2.12 (m, 2H), 1.72 (dd,  $J$  12.7 & 6.6, 1H);  $^{13}\text{C}$  NMR (101 MHz,  $\text{CDCl}_3$ )  $\delta$  145.6, 143.1, 138.1, 132.4, 129.5, 129.4 (q,  $^2J_{\text{CF}}$  32.4), 129.2, 127.2, 127.2, 126.9, 126.8 (q,  $^1J_{\text{CF}}$  272.0), 125.1 (q,  $^3J_{\text{CF}}$  3.9), 63.9, 61.7, 32.6, 31.5, 29.0, 21.4 [1 carbon missing];  $^{19}\text{F}$  NMR (376 MHz,  $\text{CDCl}_3$ )  $\delta$  -62.55;  $^{77}\text{Se}$  NMR (76 MHz,  $\text{CDCl}_3$ )  $\delta$  277.39 (d,  $J$  25.0); IR: 3063, 2952, 2927, 1941, 1670, 1619, 1579  $\text{cm}^{-1}$ ; MS: (ASAP $^+$ ) 540.07 [ $\text{M} + \text{H}$ ] $^+$ ; HRMS: Calc'd for  $\text{C}_{25}\text{H}_{25}\text{NO}_2\text{F}_3\text{S}^{76}\text{Se}^+$ : 536.0750; found: 536.0743;  $R_f$  = 0.53 (20% EtOAc in hexane); M.P.: 137- 140  $^\circ\text{C}$ .



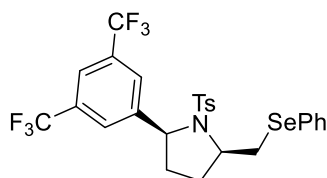
***cis*-2-((Phenylselanyl)methyl)-1-tosyl-5-(4-(trifluoromethyl)phenyl)pyrrolidine (125-*cis*)**

Following general procedure F, a mixture of 4-methyl-*N*-(1-(4-(trifluoromethyl)phenyl)pent-4-en-1-yl)benzenesulfonamide (115 mg, 0.3 mmol), diphenyl diselenide (48 mg, 0.15 mmol) and tetrabutylammonium bromide (10 mg, 0.03 mmol) were dissolved in HFIP (3 mL) and subjected to constant current electrolysis until 5 F/mol had passed. 41 mg of pure material was obtained after column chromatography and a further 23 mg was obtained from recollecting impure fractions and subjected the mixture to preparative TLC (10% EtOAc in hexane). The title compound was afforded as a brown oil in 40% yield (64 mg).  $^1\text{H}$  NMR (400 MHz,  $\text{CDCl}_3$ )  $\delta$  7.64 – 7.60 (m, 2H), 7.58 (d,  $J$  8.2, 2H), 7.50 (d,  $J$  8.5, 2H), 7.47 (d,  $J$  8.2, 2H), 7.40 – 7.29 (m, 3H), 7.21 (d,  $J$  7.9, 2H), 4.73 (t,  $J$  6.4, 1H), 3.91 – 3.82 (m, 1H), 3.79 (dd,  $J$  12.3 & 3.3, 1H), 2.92 (dd,  $J$  12.3 & 11.1, 1H), 2.41 (s, 3H), 1.95 – 1.69 (m, 4H);  $^{13}\text{C}$  NMR (101 MHz,  $\text{CDCl}_3$ )  $\delta$  146.6, 144.0, 134.0, 132.8, 129.9, 129.6 (q,  $^2J_{\text{CF}}$  32.2), 129.4, 129.1, 127.7, 127.3, 126.6, 125.5 (q,  $^3J_{\text{CF}}$  3.9), 123.8 (q,  $^1J_{\text{CF}}$  272.1), 65.2, 61.9, 34.2, 32.8, 30.0, 21.6;  $^{19}\text{F}$  NMR (377 MHz,  $\text{CDCl}_3$ )  $\delta$  -62.42;  $^{77}\text{Se}$  NMR (76 MHz,  $\text{CDCl}_3$ )  $\delta$  275.85 (d,  $J$  24.3); IR: 3064, 2925, 1698, 1619, 1598, 1578, 1542, 1525, 1494, 1479, 1438  $\text{cm}^{-1}$ ; MS: (ES $^+$ ) 540.07 [ $\text{M} + \text{H}$ ] $^+$ ; HRMS: Calc'd for  $\text{C}_{25}\text{H}_{25}\text{NO}_2\text{F}_3\text{S}^{76}\text{Se}^+$ : 536.0750; found: 536.0746;  $R_f$  = 0.44 (20% EtOAc in hexane).



***trans*-2-(3,5-Bis(trifluoromethyl)phenyl)-5-((phenylselanyl)methyl)-1-tosylpyrrolidine (123-*trans*)**

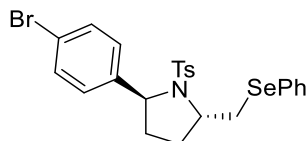
Following general procedure E, a mixture of *N*-(1-(3,5-bis(trifluoromethyl)phenyl)pent-4-en-1-yl)-4-methylbenzenesulfonamide (451 mg, 1 mmol), diphenyl diselenide (156 mg, 0.5 mmol), sodium methoxide (54 mg, 1 mmol) and tetrabutylammonium bromide (32 mg, 0.1 mmol) were dissolved in HFIP (10 mL) and subjected to constant current electrolysis until 5 F/mol had passed. The title compound was afforded as a white solid in 65% yield (392 mg).  $^1\text{H}$  NMR (400 MHz,  $\text{CDCl}_3$ )  $\delta$  7.69 – 7.64 (m, 2H), 7.62 (s, 1H), 7.39 – 7.29 (m, 5H), 7.11 (d,  $J$  8.3, 2H), 6.95 (d,  $J$  8.0, 2H), 5.14 (dd,  $J$  9.0 & 1.3, 1H), 4.39 – 4.26 (m, 1H), 3.99 (app dq,  $J$  12.6 & 1.5, 1H), 2.92 (dd,  $J$  12.6 & 11.3, 1H), 2.63 – 2.49 (m, 1H), 2.28 (s, 3H), 2.25 – 2.11 (m, 2H), 1.75 – 1.67 (m, 1H);  $^{13}\text{C}$  NMR (101 MHz,  $\text{CDCl}_3$ )  $\delta$  144.3, 143.6, 137.6, 132.5, 131.6 (q,  $^2J_{\text{CF}}$  33.3), 129.5, 129.4, 129.3, 127.2, 126.9 (app d,  $^3J_{\text{CF}}$  3.1), 126.7, 123.1 (q,  $^1J_{\text{CF}}$  273.0), 121.3 (app p,  $^3J_{\text{CF}}$  3.6), 63.1, 62.0, 32.7, 31.2, 28.9, 21.3.;  $^{19}\text{F}$  NMR (377 MHz,  $\text{CDCl}_3$ )  $\delta$  -62.88;  $^{77}\text{Se}$  NMR (76 MHz,  $\text{CDCl}_3$ )  $\delta$  278.59 (d,  $J$  23.9); IR: 3070, 2979, 2955, 1810, 1626, 1600, 1580, 1497, 1482  $\text{cm}^{-1}$ ; MS: ( $\text{ES}^+$ ) 608.06 [ $\text{M} + \text{H}$ ] $^+$ ; HRMS: Calc'd for  $\text{C}_{26}\text{H}_{24}\text{NO}_2\text{S}^{76}\text{SeF}_6$ : 604.0624; found: 604.0635;  $R_f$  = 0.62 (20% EtOAc in hexane); M.P.: 90 – 92°C.



***cis*-2-(3,5-Bis(trifluoromethyl)phenyl)-5-((phenylselanyl)methyl)-1-tosylpyrrolidine (123-*cis*)**

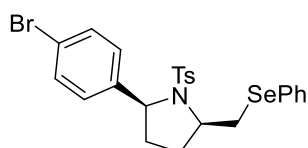
Following general procedure F, a mixture of *N*-(1-(3,5-bis(trifluoromethyl)phenyl)pent-4-en-1-yl)-4-methylbenzenesulfonamide (135 mg, 0.3 mmol), diphenyl diselenide (47 mg, 0.3 mmol) and tetrabutylammonium bromide (10 mg, 0.03 mmol) were dissolved in HFIP (3 mL) and subjected to constant current electrolysis until 5 F/mol had passed. The title compound was afforded as a white solid in 48% yield (87 mg).  $^1\text{H}$  NMR (400 MHz,  $\text{CDCl}_3$ )  $\delta$  7.81 (s, 2H), 7.76 (s, 1H), 7.64 – 7.57 (m, 2H), 7.44 (d,  $J$  8.3, 2H), 7.39 – 7.32 (m, 3H), 7.21 (d,  $J$  7.9, 2H), 4.79 (t,  $J$  6.4, 1H), 3.99 – 3.87 (m, 1H), 3.76 (dd,  $J$  12.4 & 3.3, 1H), 2.92 (dd,  $J$  12.4 & 10.9, 1H), 2.40 (s, 3H), 1.99 – 1.91 (m, 1H), 1.89 – 1.72 (m, 3H);  $^{13}\text{C}$  NMR (101 MHz,  $\text{CDCl}_3$ )  $\delta$  145.3, 144.3, 133.9, 133.0, 131.9 (q,  $^2J_{\text{CF}}$  33.3), 129.9, 129.5, 129.0, 127.8, 127.5, 126.6 (app d,  $^3J_{\text{CF}}$  3.7), 123.4 (q,  $^1J_{\text{CF}}$  273.0), 121.5 (app p,  $^3J_{\text{CF}}$  3.3), 64.8, 62.0, 34.4, 32.8, 29.9, 21.7;  $^{19}\text{F}$  NMR (377 MHz,  $\text{CDCl}_3$ )  $\delta$  -62.74;  $^{77}\text{Se}$  NMR (76 MHz,  $\text{CDCl}_3$ )  $\delta$  275.50 (d,  $J$  23.8); IR: 3067, 2970,

2934, 2873, 1626, 1600, 1578, 1497, 1478, 1459  $\text{cm}^{-1}$ ; MS: ( $\text{ES}^+$ ) 608.06  $[\text{M} + \text{H}]^+$ ; HRMS: Calc'd for  $\text{C}_{26}\text{H}_{24}\text{NO}_2\text{S}^{76}\text{SeF}_6^+$ : 604.0624; found: 604.0638;  $R_f = 0.50$  (20% EtOAc in hexane); M.P.: 107 – 110  $^{\circ}\text{C}$ .



***trans*-2-(4-Bromophenyl)-5-((phenylselanyl)methyl)-1-tosylpyrrolidine (124-*trans*)**

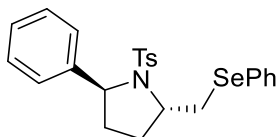
Following general procedure E, a mixture of *N*-(1-(4-bromophenyl)pent-4-en-1-yl)-4-methylbenzenesulfonamide (118 mg, 0.3 mmol), diphenyl diselenide (47 mg, 0.15 mmol), sodium methoxide (16 mg, 0.3 mmol) and tetrabutylammonium bromide (10 mg, 0.03 mmol) were dissolved in HFIP (3 mL) and subjected to constant current electrolysis until 5 F/mol had passed. The title compound was afforded as a beige solid in 57% yield (94 mg).  $^1\text{H}$  NMR (400 MHz,  $\text{CDCl}_3$ )  $\delta$  7.67 – 7.60 (m, 2H), 7.38 – 7.27 (m, 3H), 7.15 (d,  $J$  8.4, 2H), 7.09 (d,  $J$  8.3, 2H), 6.98 (d,  $J$  8.1, 2H), 6.75 (d,  $J$  8.4, 2H), 4.97 (d,  $J$  8.4, 1H), 4.21 (ddd,  $J$  10.7, 6.9 & 2.8, 1H), 3.93 (ddd,  $J$  12.6, 2.9 & 1.6, 1H), 2.84 (dd,  $J$  12.5 & 11.3, 1H), 2.52 – 2.38 (m, 1H), 2.35 (s, 3H), 2.27 – 2.07 (m, 2H), 1.69 (dd,  $J$  12.6 & 6.8, 1H);  $^{13}\text{C}$  NMR (101 MHz,  $\text{CDCl}_3$ )  $\delta$  142.9, 140.6, 138.1, 132.4, 131.2, 129.4, 129.4, 129.1, 128.6, 127.1, 126.9, 121.0, 63.9, 61.3, 32.6, 31.5, 29.0, 21.5;  $^{77}\text{Se}$  NMR (76 MHz,  $\text{CDCl}_3$ )  $\delta$  277.06 (d,  $J$  24.2); IR: 3051, 2975, 2928, 1897, 1736, 1594, 1578, 1486, 1480  $\text{cm}^{-1}$ ; MS: ( $\text{ES}^+$ ) 549.99  $[\text{M} + \text{H}]^+$ ; HRMS: Calc'd for  $\text{C}_{24}\text{H}_{25}\text{BrNO}_2\text{S}^{76}\text{Se}^+$ : 545.9982; found: 545.9978;  $R_f = 0.50$  (20% EtOAc in hexane); M.P.: 123 – 125  $^{\circ}\text{C}$ .



***cis*-2-(4-Bromophenyl)-5-(phenylselanyl)-1-tosylpiperidine (124-*cis*)**

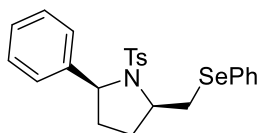
Following general procedure F, a mixture of *N*-(1-(4-bromophenyl)pent-4-en-1-yl)-4-methylbenzenesulfonamide (118 mg, 0.3 mmol), diphenyl diselenide (48 mg, 0.15 mmol) and tetrabutylammonium bromide (10 mg, 0.03 mmol) were dissolved in HFIP (3 mL) and subjected to constant current electrolysis until 7 F/mol had passed. The title compound was afforded as a beige solid in 65% yield (107 mg).  $^1\text{H}$  NMR (400 MHz,  $\text{CDCl}_3$ )  $\delta$  7.62 – 7.58 (m, 2H), 7.46 (d,  $J$  8.3, 2H), 7.43 (d,  $J$  8.5, 2H), 7.36 – 7.29 (m, 3H), 7.26 (d,  $J$  8.6, 2H), 7.20 (d,  $J$  7.9, 2H), 4.63 (t,  $J$  6.2, 1H), 3.86 – 3.69 (m, 2H), 2.88 (dd,  $J$  12.1 & 10.9, 1H), 2.39 (s, 3H), 1.81 – 1.66 (m, 4H);  $^{13}\text{C}$  NMR (101 MHz,  $\text{CDCl}_3$ )  $\delta$  143.8, 141.5, 134.0, 132.7, 131.5, 129.8, 129.4, 129.1, 128.0, 127.7, 127.2, 121.1, 65.0, 61.8, 34.0, 32.9, 29.9, 21.6;  $^{77}\text{Se}$  NMR (76 MHz,  $\text{CDCl}_3$ )  $\delta$  275.81 (d,  $J$  24.3); IR: 3052, 2976, 1732, 1596, 1578, 1488, 1480  $\text{cm}^{-1}$ .

<sup>1</sup>; MS: (ES<sup>+</sup>) 550.00 [M + H]<sup>+</sup>; HRMS: Calc'd for C<sub>24</sub>H<sub>24</sub>BrNO<sub>2</sub>S<sup>76</sup>Se<sup>+</sup>: 545.9982; found: 545.9976; R<sub>f</sub>: 0.44 (20% EtOAc in hexane); M.P.: 112 - 114 °C.



***trans*-2-Phenyl-5-((phenylselanyl)methyl)-1-tosylpyrrolidine (119-*trans*)**

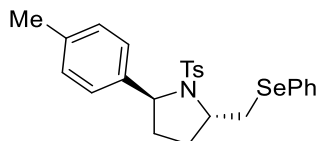
Following general procedure E, a mixture of 4-methyl-*N*-(1-phenylpent-4-en-1-yl)benzenesulfonamide (32 mg, 0.1 mmol), diphenyl diselenide (16 mg, 0.05 mmol), sodium methoxide (6 mg, 0.1 mmol) and tetrabutylammonium bromide (7 mg, 0.02 mmol) were dissolved in HFIP (2.5 mL) and subjected to constant current electrolysis until 5 F/mol had passed. The compound was purified by prep TLC (10% EtOAc in hexane). The title compound was afforded as a white solid in 46% yield (22 mg). <sup>1</sup>H NMR (400 MHz, CDCl<sub>3</sub>) δ 7.67 – 7.63 (m, 2H), 7.39 – 7.27 (m, 3H), 7.16 – 7.09 (m, 1H), 7.08 – 7.01 (m, 4H), 6.93 (d, *J* 8.1, 2H), 6.88 (d, *J* 7.2, 2H), 5.05 (d, *J* 8.4, 1H), 4.19 (ddd, *J* 10.7, 7.4 & 2.6, 1H), 3.98 (ddd, *J* 12.5, 2.7 & 1.6, 1H), 2.86 (dd, *J* 12.5 & 11.3, 1H), 2.51 – 2.37 (m, 1H), 2.31 (s, 3H), 2.30 – 2.20 (m, 1H), 2.12 (dd, *J* 13.0 & 7.0, 1H), 1.72 (dd, *J* 12.4 & 6.9, 1H); <sup>13</sup>C NMR (101 MHz, CDCl<sub>3</sub>) δ 142.5, 141.5, 138.1, 132.5, 129.6, 129.4, 129.0, 128.2, 127.1, 127.1, 127.0, 126.9, 64.8, 61.1, 32.7, 31.8, 29.1, 21.5; <sup>77</sup>Se NMR (76 MHz, CDCl<sub>3</sub>) δ 276.97 (d, *J* 24.6); IR: 3059, 2976, 1712, 1599, 1579, 1495, 1479, 1453 cm<sup>-1</sup>; MS: (ES<sup>+</sup>) 472.09 [M + H]<sup>+</sup>; HRMS: Calc'd for C<sub>24</sub>H<sub>26</sub>NO<sub>2</sub>S<sup>76</sup>Se<sup>+</sup>: 468.0876 found: 468.0883; R<sub>f</sub> = 0.50 (20% EtOAc in hexane); M.P.: 113 – 115 °C.



***cis*-2-Phenyl-5-((phenylselanyl)methyl)-1-tosylpyrrolidine (119-*cis*)**

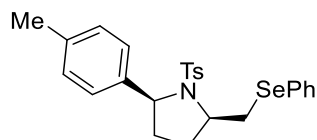
Following general procedure F, a mixture of 4-methyl-*N*-(1-phenylpent-4-en-1-yl)benzenesulfonamide (95 mg, 0.3 mmol), diphenyl diselenide (48 mg, 0.15 mmol) and tetrabutylammonium bromide (10 mg, 0.03 mmol) were dissolved in HFIP (3 mL) and subjected to constant current electrolysis until 7 F/mol had passed. The title compound was afforded as a colourless oil in 50% yield (70 mg). <sup>1</sup>H NMR (400 MHz, CDCl<sub>3</sub>) δ 7.64 – 7.58 (m, 2H), 7.49 (d, *J* 8.3, 2H), 7.41 – 7.28 (m, 7H), 7.28 – 7.23 (m, 1H), 7.21 (d, *J* 7.9, 2H), 4.73 (t, *J* 6.2, 1H), 3.89 – 3.77 (m, 2H), 2.92 (dd, *J* 12.1 & 11.9, 1H), 2.41 (s, 3H), 1.91 – 1.65 (m, 4H); <sup>13</sup>C NMR (101 MHz, CDCl<sub>3</sub>) δ 143.6, 142.4, 134.4, 132.7, 129.8, 129.4, 129.3, 128.5, 127.7, 127.3, 127.2, 126.3, 65.5, 61.9, 34.1, 32.9, 30.1, 21.7; <sup>77</sup>Se NMR (76 MHz, CDCl<sub>3</sub>) δ 275.24 (d, *J* 23.5); IR: 3058, 2934, 1712, 1599, 1579, 1494, 1479, 1438 cm<sup>-1</sup>.

<sup>1</sup>; MS: (ES<sup>+</sup>) 472.09 [M + H]<sup>+</sup>; HRMS: Calc'd for C<sub>24</sub>H<sub>26</sub>NO<sub>2</sub>S<sup>76</sup>Se<sup>+</sup>: 468.0876; found: 468.0887; R<sub>f</sub>: 0.44 (20% EtOAc in hexane).



***trans*-2-((Phenylselanyl)methyl)-5-(*p*-tolyl)-1-tosylpyrrolidine (127-*trans*)**

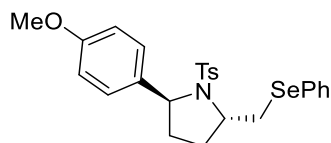
Following general procedure E, a mixture of 4-methyl-*N*-(1-(*p*-tolyl)pent-4-en-1-yl)benzenesulfonamide (99 mg, 0.3 mmol), diphenyl diselenide (47 mg, 0.15 mmol), sodium methoxide (16 mg, 0.3 mmol) and tetrabutylammonium bromide (10 mg, 0.03 mmol) were dissolved in HFIP (3 mL) and subjected to constant current electrolysis until 5 F/mol had passed. The title compound was afforded as a beige solid in 45% yield (66 mg). <sup>1</sup>H NMR (400 MHz, CDCl<sub>3</sub>) δ 7.64 (d, *J* 7.2, 2H), 7.39 – 7.25 (m, 3H), 7.08 (d, *J* 8.2, 2H), 6.94 (d, *J* 8.1, 2H), 6.86 (d, *J* 7.8, 2H), 2.36 – 2.19 (m, 1H), 6.78 (d, *J* 8.1, 2H), 5.00 (d, *J* 8.3, 1H), 4.19 (ddd, *J* 10.8, 7.5 & 2.7, 1H), 3.96 (dt, *J* 12.7 & 2.1, 1H), 2.85 (dd, *J* 12.5 & 11.3, 1H), 2.49 – 2.36 (m, 1H), 2.32 (s, 3H), 2.27 (s, 3H), 1.72 (dd, *J* 12.5 & 6.8, 1H); <sup>13</sup>C NMR (101 MHz, CDCl<sub>3</sub>) δ 142.4, 138.6, 138.2, 136.8, 132.4, 129.6, 129.4, 128.9, 128.8, 127.1, 127.0, 126.9, 64.5, 61.1, 32.8, 31.8, 29.1, 21.5, 21.1; <sup>77</sup>Se NMR (76 MHz, CDCl<sub>3</sub>) δ 276.33 (d, *J* 24.2); IR: 3054, 3030, 2974, 2917, 2860, 1947, 1744, 1597, 1577, 1514, 1496 cm<sup>-1</sup>; MS: (ES<sup>+</sup>) 486.10 [M + H]<sup>+</sup>; HRMS: Calc'd for C<sub>25</sub>H<sub>28</sub>NO<sub>2</sub>S<sup>76</sup>Se<sup>+</sup>: 482.1033; found: 482.1036; R<sub>f</sub> = 0.50 (20% EtOAc in hexane); M.P.: 105 – 107 °C



***cis*-2-((Phenylselanyl)methyl)-5-(*p*-tolyl)-1-tosylpyrrolidine (127-*cis*)**

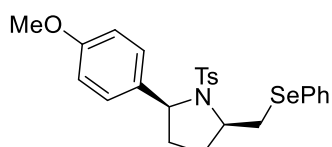
Following general procedure F, a mixture of 4-methyl-*N*-(1-(*p*-tolyl)pent-4-en-1-yl)benzenesulfonamide (330 mg, 1 mmol), diphenyl diselenide (157 mg, 0.5 mmol), and tetrabutylammonium bromide (32 mg, 0.1 mmol) were dissolved in HFIP (10 mL) and subjected to constant current electrolysis until 7 F/mol had passed. The title compound was afforded as a beige solid in 42% yield (202 mg). <sup>1</sup>H NMR (400 MHz, CDCl<sub>3</sub>) δ 7.64 – 7.59 (m, 2H), 7.50 (d, *J* 8.2, 2H), 7.38 – 7.27 (m, 5H), 7.22 (d, *J* 8.0, 2H), 7.15 (d, *J* 7.8, 2H), 4.68 (t, *J* 12.4, 1H), 3.89 – 3.75 (m, 2H), 2.92 (t, *J* 12.4, 1H), 2.41 (s, 3H), 2.34 (s, 3H), 1.89 – 1.69 (m, 4H); <sup>13</sup>C NMR (101 MHz, CDCl<sub>3</sub>) δ 143.6, 139.4, 136.9, 134.4, 132.6, 129.7, 129.4, 129.3, 129.2, 127.7, 127.1, 126.2, 65.4, 61.8, 34.1, 33.0, 30.0, 21.6, 21.2; <sup>77</sup>Se NMR (76 MHz, CDCl<sub>3</sub>) δ 275.03 (d, *J* 24.4); IR: 2941, 2918, 2851, 1731, 1596, 1578, 1510,

1492, 1477, 1439  $\text{cm}^{-1}$ ; MS: ( $\text{ES}^+$ ) 486.10  $[\text{M} + \text{H}]^+$ ; HRMS: Calc'd for  $\text{C}_{25}\text{H}_{28}\text{NO}_2\text{S}^{76}\text{Se}^+$ : 482.1033; found: 482.1024;  $R_f$  = 0.44 (20% EtOAc in hexane); M.P.: 113 - 115  $^{\circ}\text{C}$ .



***trans*-2-(4-Methoxyphenyl)-5-((phenylselanyl)methyl)-1-tosylpyrrolidine (126-*trans*)**

Following general procedure E, a mixture of *N*-(1-(4-methoxyphenyl)pent-4-en-1-yl)-4-methylbenzenesulfonamide (104 mg, 0.3 mmol), diphenyl diselenide (47 mg, 0.15 mmol), sodium methoxide (16 mg, 0.3 mmol) and tetrabutylammonium bromide (10 mg, 0.03 mmol) were dissolved in HFIP (3 mL) and subjected to constant current electrolysis until 5 F/mol had passed. The compound was purified with a 0  $\rightarrow$  10% EtOAc in hexane gradient to afford the title compound as a white solid in 55% yield (83 mg).  $^1\text{H}$  NMR (400 MHz,  $\text{CDCl}_3$ )  $\delta$  7.67 – 7.62 (m, 2H), 7.38 – 7.27 (m, 3H), 7.04 (d, *J* 8.3, 2H), 6.93 (d, *J* 8.0, 2H), 6.80 (d, *J* 8.7, 2H), 6.58 (d, *J* 8.7, 2H), 5.00 (dd, *J* 8.6 & 1.1, 1H), 4.16 (ddd, *J* 10.4, 7.4 & 2.8, 1H), 3.96 (ddd, *J* 12.5, 2.8 & 1.6, 1H), 3.74 (s, 3H), 2.86 (dd, *J* 12.5 & 11.3, 1H), 2.49 – 2.35 (m, 1H), 2.31 (s, 3H), 2.30 – 2.19 (m, 1H), 2.13 (dd, *J* 12.9 & 7.1, 1H), 1.71 (dd, *J* 12.7 & 7.0, 1H);  $^{13}\text{C}$  NMR (101 MHz,  $\text{CDCl}_3$ )  $\delta$  158.8, 142.4, 138.2, 133.7, 132.5, 129.6, 129.4, 128.9, 128.2, 127.0, 127.0, 113.5, 64.2, 61.0, 55.4, 32.8, 31.8, 29.2, 21.5;  $^{77}\text{Se}$  NMR (76 MHz,  $\text{CDCl}_3$ )  $\delta$  276.49 (d, *J* 24.3); IR: 3057, 3003, 2953, 2929, 2835, 1612, 1579, 1514, 1483  $\text{cm}^{-1}$ ; MS: ( $\text{ES}^+$ ) 502.10  $[\text{M} + \text{H}]^+$ ; HRMS: Calc'd for  $\text{C}_{25}\text{H}_{28}\text{NO}_3\text{S}^{76}\text{Se}^+$ : 498.0982; found: 498.0979;  $R_f$ : 0.35 (20% EtOAc in hexane); M.P.: 111 – 113  $^{\circ}\text{C}$ .

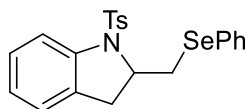


***cis*-2-(4-Methoxyphenyl)-5-((phenylselanyl)methyl)-1-tosylpyrrolidine (126-*cis*)**

Following general procedure F, a mixture of *N*-(1-(4-methoxyphenyl)pent-4-en-1-yl)-4-methylbenzenesulfonamide (173 mg, 0.5 mmol), diphenyl diselenide (80 mg, 0.5 mmol) and tetrabutylammonium bromide (16 mg, 0.05 mmol) were dissolved in HFIP (5 mL) and subjected to constant current electrolysis until 7 F/mol had passed. The compound was purified with a 0  $\rightarrow$  10% EtOAc in hexane gradient to afford the title compound as a white solid in 79% yield (197 mg).  $^1\text{H}$  NMR (400 MHz,  $\text{CDCl}_3$ )  $\delta$  7.64 – 7.58 (m, 2H), 7.48 (d, *J* 8.3, 2H), 7.38 – 7.28 (m, 5H), 7.21 (d, *J* 7.9, 2H), 6.86 (d, *J* 8.8, 2H), 4.67 (t, *J* 5.7, 1H), 3.80 (s, 3H), 3.89 – 3.75 (m, 2H), 2.90 (dd, *J* 12.2 & 11.6, 1H), 2.40 (s, 3H), 1.88 – 1.68 (m, 4H);  $^{13}\text{C}$  NMR (101 MHz,  $\text{CDCl}_3$ )  $\delta$  158.9, 143.6, 134.5, 134.4, 132.7, 129.7, 129.4, 129.3, 127.7, 127.4, 127.2, 113.9, 65.1, 61.8, 55.4, 34.0, 33.0, 30.0, 21.7;  $^{77}\text{Se}$  NMR (76 MHz,  $\text{CDCl}_3$ )  $\delta$

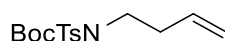


274.61 (d, *J* 24.3); IR: 3069, 2963, 2925, 2837, 1612, 1596, 1577, 1512, 1493, 1479, 1463 cm<sup>-1</sup>; MS: (ES<sup>+</sup>) 502.10 [M + H]<sup>+</sup>; HRMS: Calc'd for C<sub>25</sub>H<sub>28</sub>NO<sub>3</sub>S<sup>76</sup>Se<sup>+</sup>: 498.0982; found: 498.0988; R<sub>f</sub> = 0.26 (20% EtOAc in hexane); M.P.: 124 - 126 °C.



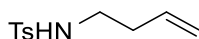
## 2-((Phenylselanyl)methyl)-1-tosylindoline (128)

Following general procedure E, a mixture of *N*-(2-allylphenyl)-4-methylbenzenesulfonamide (86 mg, 0.3 mmol), diphenyl diselenide (47 mg, 0.15 mmol), sodium methoxide (16 mg, 0.3 mmol) and tetrabutylammonium bromide (10 mg, 0.03 mmol) were dissolved in HFIP (3 mL) and subjected to constant current electrolysis until 5 F/mol had passed. The title compound was afforded as a white solid in 55% yield (73 mg). <sup>1</sup>H NMR (400 MHz, CDCl<sub>3</sub>) δ 7.65 (d, *J* 8.2, 1H), 7.61 – 7.55 (m, 2H), 7.39 – 7.28 (m, 5H), 7.23 – 7.18 (m, 1H), 7.11 – 7.07 (m, 2H), 7.04 – 6.99 (m, 2H), 4.24 (dddd, *J* 10.7, 8.1, 4.6 & 3.5, 1H), 3.65 (dd, *J* 12.5 & 3.5, 1H), 2.93 (dd, *J* 12.5 & 10.8, 1H), 2.89 – 2.82 (m, 2H), 2.32 (s, 3H); <sup>13</sup>C NMR (101 MHz, CDCl<sub>3</sub>) δ 144.0, 141.4, 134.7, 132.6, 131.1, 129.7, 129.4, 128.9, 128.0, 127.2, 127.1, 125.3, 124.8, 117.2, 61.7, 34.2, 33.2, 21.7; <sup>77</sup>Se NMR (76 MHz, CDCl<sub>3</sub>) δ 258.13 (d, *J* 24.6); IR: 3048, 2923, 2855, 1598, 1579, 1493, 1478, 1460, 1438 cm<sup>-1</sup>; MS: (ES<sup>+</sup>) 444.06 [M + H]<sup>+</sup>; HRMS: Calc'd for C<sub>22</sub>H<sub>22</sub>NO<sub>2</sub>S<sup>76</sup>Se<sup>+</sup>: 440.0563; found: 440.0566. Data is consistent with that reported for the title compound by Amri *et al.*<sup>138</sup>



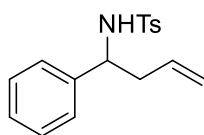
## tert-Butyl but-3-en-1-yl(tosyl)carbamate

Following general procedure C, a mixture of 4-butene-1-ol (510 μL, 506 mg, 6.93 mmol), *tert*-butyl carbamate, (2.83 g, 10.40 mmol), DIAD (3.40 mL, 3.49 g, 17.3 mmol) and triphenylphosphine (5.50 g, 20.74 mmol) were stirred in THF (35 mL) for 16 hours. The title compound was afforded as a colourless oil in 99% yield (2.27 g). <sup>1</sup>H NMR (300 MHz, CDCl<sub>3</sub>) δ 7.78 (d, *J* 8.4, 2H), 7.29 (d, *J* 8.0, 2H), 5.80 (ddt, *J* 17.1, 10.2 & 7.0, 1H), 5.17 – 5.03 (m, 2H), 3.93 – 3.83 (m, 2H), 2.50 (qt, *J* 7.2 & 1.3, 2H), 2.43 (s, 3H), 1.33 (s, 9H); <sup>13</sup>C NMR (101 MHz, CDCl<sub>3</sub>) δ 151.0, 144.2, 137.6, 134.5, 129.3, 128.0, 117.6, 84.3, 46.5, 34.7, 28.0, 21.7; HRMS: Calc'd for C<sub>16</sub>H<sub>23</sub>NO<sub>4</sub>SN<sup>+</sup>: 348.1245; found 348.1255. Data is consistent with that reported for the title compound by Qi *et al.*<sup>139</sup>



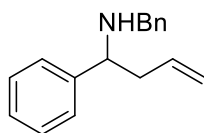
## *N*-(But-3-en-1-yl)-4-methylbenzenesulfonamide (136)

Following general procedure D, a mixture of *tert*-butyl but-3-en-1-yl(tosyl)carbamate (2.04g, 6.25 mmol) and trifluoroacetic acid (9.6 mL, 14.3 g) were dissolved in CH<sub>2</sub>Cl<sub>2</sub> (40 mL) and stirred for four hours. The title compound was afforded as a colourless oil in 87% yield (1.23 g). <sup>1</sup>H NMR (400 MHz, CDCl<sub>3</sub>) δ 7.74 (d, *J* 8.3, 2H), 7.30 (d, *J* 7.9, 2H), 5.62 (ddt, *J* 17.1, 10.4 & 6.8, 1H), 5.08 – 4.97 (m, 2H), 4.66 (s, 1H), 3.00 (t, *J* 6.8, 2H), 2.42 (s, 3H), 2.19 (qt, *J* 6.8 & 1.3, 2H). <sup>13</sup>C NMR (101 MHz, CDCl<sub>3</sub>) δ 143.6, 137.0, 134.3, 129.8, 127.2, 118.2, 42.2, 33.7, 21.6. MS: (ES<sup>+</sup>) 248.07 [M + Na]<sup>+</sup>; HRMS: Calc'd for C<sub>11</sub>H<sub>15</sub>NO<sub>2</sub>Na<sup>+</sup>: 248.0721; found: 248.0728. Data is consistent with that reported for the title compound by Cui *et al.*<sup>140</sup>



#### 4-Methyl-*N*-(1-phenylbut-3-en-1-yl)benzenesulfonamide (140)

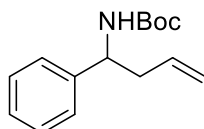
*N*-Benzyldiene-4-methylbenzenesulfonamide (800 mg, 3.08 mmol) was added to an oven-dried flask under argon and dissolved in dry THF (15 mL) followed by the dropwise addition of allylmagnesium bromide (1 M in THF, 4.00 mL, 4 mmol, 1.3 equiv.). The reaction was stirred for a further 16 hours and quenched with saturated aqueous sodium bicarbonate. The aqueous layer was extracted with EtOAc three times and then the organic layers were washed with brine. The organic layer was dried (MgSO<sub>4</sub>), filtered and the solvent removed *in vacuo*. The crude mixture was subjected to column chromatography (0 → 20% EtOAc gradient) which afforded the title compound as a white solid in 63% yield (582 mg). <sup>1</sup>H NMR (400 MHz, CDCl<sub>3</sub>) δ 7.55 (d, *J* 8.3, 2H), 7.21 – 7.12 (m, 5H), 7.10 – 7.04 (m, 2H), 5.51 (ddt, *J* 18.4, 9.2 & 7.1, 1H), 5.08 (s, 1H), 5.06 – 5.02 (m, 1H), 4.84 (d, *J* 6.1, 1H), 4.38 (q, *J* 6.6, 1H), 2.50 – 2.40 (m, 2H), 2.37 (s, 3H); <sup>13</sup>C NMR (101 MHz, CDCl<sub>3</sub>) δ 143.2, 140.5, 137.6, 133.2, 129.4, 128.5, 127.5, 127.3, 126.7, 119.4, 57.3, 42.0, 21.6; IR: 3250, 2897, 1643, 1601, 1498, 1458 cm<sup>-1</sup>. Data is consistent with that reported for the title compound by Fang *et al.*<sup>141</sup>



#### *N*-Benzyl-1-phenylbut-3-en-1-amine (138)

*N*-Benzyl-1-phenylmethanimine (394 mg, 2.02 mmol) was added to an oven-dried flask under argon and dissolved in dry THF (5 mL) followed by the dropwise addition of allylmagnesium bromide (1 M in THF, 3.00 mL, 3 mmol, 1.5 equiv.). The reaction was stirred for a further 16 hours and quenched with saturated aqueous sodium bicarbonate. The aqueous layer was extracted with EtOAc three times and then the organic layer was washed with brine. The organic layer was dried (MgSO<sub>4</sub>), filtered and

the solvent removed *in vacuo*. The crude mixture was subjected to column chromatography (0 -> 20% EtOAc gradient) which afforded the title compound as an orange oil in 72% yield (347 mg). <sup>1</sup>H NMR (400 MHz, CDCl<sub>3</sub>) δ 7.42 – 7.13 (m, 10H), 5.81 – 5.58 (m, 1H), 5.12 – 4.93 (m, 2H), 3.67 (dd, *J* 13.6 & 6.2, 2H), 3.51 (d, *J* 13.3, 1H), 2.48 – 2.31 (m, 2H), 1.78 (s, 1H); <sup>13</sup>C NMR (101 MHz, CDCl<sub>3</sub>) δ 143.9, 140.7, 135.6, 128.5, 128.5, 128.3, 127.4, 127.2, 127.0, 117.7, 61.7, 51.6, 43.2; IR: 3063, 3026, 2909, 2834, 1639, 1603, 1453 cm<sup>-1</sup>. Data is consistent with that reported for the title compound by Peterson *et al.*<sup>142</sup>



***tert*-Butyl (1-phenylbut-3-en-1-yl)carbamate (141)**

Procedure described from Veenstra and Schmid.<sup>114</sup> Benzaldehyde (531 mg, 5 mmol), *tert*-butyl carbamate (756 mg, 5 mmol) and allyltrimethylsilane (800 μL, 575 mg, 5 mmol) were dissolved in MeCN (8 mL) and cooled to 0 °C. Boron trifluoride etherate was added in one portion (370 μL, 426 mg, 3 mmol, 0.6 equiv.) and the solution was warmed to room temperature and stirred for 16 hours. Upon completion of the reaction, the mixture was diluted with toluene (10 mL) and saturated aqueous sodium bicarbonate (10 mL) and stirred for a further 15 minutes. The mixture is transferred to a separating funnel and the aqueous layer is removed, and the organic layer is washed with brine twice, dried (MgSO<sub>4</sub>), filtered and the solvent removed *in vacuo*. The crude mixture was subjected to column chromatography (0 -> 20% EtOAc in hexane gradient) to afford the title compound as a white solid in 39% yield, (483 mg). <sup>1</sup>H NMR (400 MHz, CDCl<sub>3</sub>) δ 7.37 – 7.30 (m, 2H), 7.29 – 7.20 (m, 3H), 5.68 (ddt, *J* 17.2, 10.2 & 7.1, 1H), 5.15 – 5.03 (m, 2H), 4.86 (s, 1H), 4.74 (s, 1H), 2.52 (s, 2H), 1.41 (s, 9H); <sup>13</sup>C NMR (101 MHz, CDCl<sub>3</sub>) δ 155.3, 140.1, 134.1, 128.6, 127.3, 126.4, 118.3, 79.6, 54.2, 41.4, 28.5; HRMS: Calc'd for C<sub>15</sub>H<sub>22</sub>NO<sub>2</sub><sup>+</sup>: 248.1651; found: 248.1647. Data is consistent with that reported for the title compound by Caputo *et al.*<sup>143</sup>

### 4.3. X-Ray Crystallographic Information (All data provided by Dr Louise Male, UoB)

#### 4.3.1. X-Ray Crystallography General Information

The datasets of **JPM\_237A** and **JPM\_355B** were measured on an Agilent SuperNova diffractometer using an Atlas detector. The data collections were driven and processed and an absorption correction was applied using CrysAlisPro.<sup>144</sup> The structures were solved using ShelXT<sup>145</sup> and refined by a full-matrix least-squares procedure on  $F^2$  in ShelXL.<sup>146</sup> All non-hydrogen atoms were refined with anisotropic displacement parameters. All hydrogen atoms were fixed as riding models and the isotropic thermal parameters ( $U_{iso}$ ) of all hydrogen atoms were based on the  $U_{eq}$  of the parent atom. Figures and reports were produced using OLEX2.<sup>147</sup>

##### **JPM\_237A:**

Crystal Data for  $C_{24}H_{24}BrNO_2SSe$  ( $M = 549.37$  g/mol): orthorhombic, space group  $Pbca$  (no. 61),  $a = 12.7139(6)$  Å,  $b = 11.0611(5)$  Å,  $c = 30.7055(14)$  Å,  $V = 4318.1(3)$  Å<sup>3</sup>,  $Z = 8$ ,  $T = 100.0(3)$  K,  $\mu(CuK\alpha) = 5.600$  mm<sup>-1</sup>,  $D_{calc} = 1.690$  g/cm<sup>3</sup>, 8268 reflections measured ( $9.03^\circ \leq 2\theta \leq 140.092^\circ$ ), 4056 unique ( $R_{int} = 0.0502$ ,  $R_{sigma} = 0.0580$ ) which were used in all calculations. The final  $R_1$  was 0.0768 ( $I > 2\sigma(I)$ ) and  $wR_2$  was 0.2130 (all data).

The structure occupies a centrosymmetric space group such that in half of cases C(1) and C(4) are *S*, while in the other half C(1) and C(4) are *R*. In all molecules the relative stereochemistry of the chiral centres is the same.

The crystal was the best quality that could be grown, but despite this the diffraction peaks were somewhat elongated, which has resulted in somewhat high residual electron density peaks.

##### **JPM\_355B:**

Crystal Data for  $C_{26.5}H_{24}ClF_6NO_2SSe$  ( $M = 648.94$  g/mol): triclinic, space group  $P-1$  (no. 2),  $a = 8.1424(3)$  Å,  $b = 18.2419(6)$  Å,  $c = 18.7517(6)$  Å,  $\alpha = 96.646(3)^\circ$ ,  $\beta = 101.128(3)^\circ$ ,  $\gamma = 97.979(3)^\circ$ ,  $V = 2677.15(16)$  Å<sup>3</sup>,  $Z = 4$ ,  $T = 99.9(3)$  K,  $\mu(CuK\alpha) = 4.165$  mm<sup>-1</sup>,  $D_{calc} = 1.610$  g/cm<sup>3</sup>, 19495 reflections measured ( $7.424^\circ \leq 2\theta \leq 146.21^\circ$ ), 10372 unique ( $R_{int} = 0.0314$ ,  $R_{sigma} = 0.0373$ ) which were used in all calculations. The final  $R_1$  was 0.0483 ( $I > 2\sigma(I)$ ) and  $wR_2$  was 0.1365 (all data).

The structure contains two crystallographically-independent molecules and a molecule of dichloromethane.

The structure occupies a centrosymmetric space group such that in half of cases C(1) is *S*, C(4) is *R*, C(101) is *R* and C(104) is *S* while in the other half C(1) is *R*, C(4) is *S*, C(101) is *S* and C(104) is *R*. In all molecules, the relative stereochemistry of the chiral centres is the same.

#### 4.3.2. X-Ray Crystallographic Information for *trans*-Pyrrolidine JPM\_237A

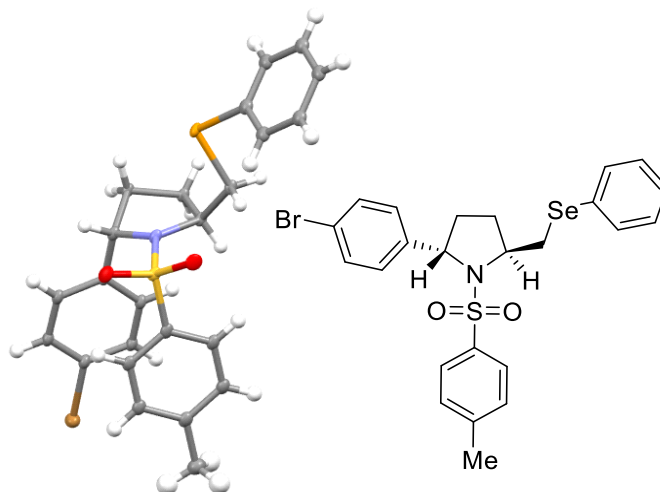


**Table 7:** Crystal data and structure refinement of JPM\_237A

Identification code	JPM_237A
Empirical formula	C <sub>24</sub> H <sub>24</sub> BrNO <sub>2</sub> SSe
Formula weight	549.37
Temperature/K	100.0(3)
Crystal system	orthorhombic
Space group	Pbca
a/Å	12.7139(6)
b/Å	11.0611(5)
c/Å	30.7055(14)
α/°	90
β/°	90
γ/°	90
Volume/Å <sup>3</sup>	4318.1(3)
Z	8
ρ <sub>calc</sub> /g/cm <sup>3</sup>	1.690
μ/mm <sup>-1</sup>	5.600
F(000)	2208.0
Crystal size/mm <sup>3</sup>	0.35 × 0.053 × 0.044
Radiation	CuKα (λ = 1.54184)
2θ range for data collection/°	9.03 to 140.092
Index ranges	-10 ≤ h ≤ 15, -9 ≤ k ≤ 13, -26 ≤ l ≤ 37
Reflections collected	8268
Independent reflections	4056 [R <sub>int</sub> = 0.0502, R <sub>sigma</sub> = 0.0580]
Data/restraints/parameters	4056/174/272
Goodness-of-fit on F <sup>2</sup>	1.100

Final R indexes [ $I \geq 2\sigma(I)$ ]  $R_1 = 0.0768$ ,  $wR_2 = 0.2072$

Final R indexes [all data]  $R_1 = 0.0876$ ,  $wR_2 = 0.2130$

Largest diff. peak/hole /  $e \text{ \AA}^{-3}$  1.96/-1.22

**Table 8:** Fractional Atomic Coordinates ( $\times 10^4$ ) and Equivalent Isotropic Displacement Parameters ( $\text{\AA}^2 \times 10^3$ ) for JPM\_237A.  $U_{eq}$  is defined as 1/3 of the trace of the orthogonalised  $U_{ij}$  tensor

Atom	x	y	z	U(eq)
Br1	5238.4 (8)	3175.9 (9)	4855.0 (3)	21.0 (3)
C1	6484 (7)	5201 (8)	2589 (3)	13.0 (9)
C2	5665 (6)	4208 (8)	2494 (3)	12.7 (10)
C3	4608 (7)	4752 (8)	2650 (3)	13.1 (10)
C4	4903 (7)	5559 (8)	3035 (3)	13.3 (8)
C5	6942 (7)	5798 (8)	2182 (3)	13.3 (12)
C6	6829 (7)	7175 (9)	1393 (3)	18.1 (11)
C7	7621 (7)	7967 (8)	1527 (3)	18.3 (11)
C8	8325 (7)	8433 (9)	1229 (3)	18.8 (11)
C9	8244 (8)	8146 (9)	791 (3)	19.0 (11)
C10	7454 (8)	7342 (9)	657 (3)	19.0 (11)
C11	6751 (8)	6863 (9)	954 (3)	18.7 (11)
C12	4980 (7)	4915 (8)	3470 (3)	13.8 (9)
C13	5751 (7)	4067 (8)	3562 (3)	14.2 (10)
C14	5825 (7)	3518 (8)	3970 (3)	14.8 (10)
C15	5108 (7)	3890 (8)	4288 (3)	15.2 (10)
C16	4324 (7)	4693 (8)	4208 (3)	15.3 (10)
C17	4265 (7)	5222 (8)	3798 (3)	14.6 (10)
C18	7116 (7)	6477 (8)	3608 (3)	15.3 (10)
C19	8031 (7)	5839 (8)	3548 (3)	16.1 (11)
C20	8507 (7)	5252 (8)	3903 (3)	17.6 (11)
C21	8074 (7)	5366 (9)	4320 (3)	18.0 (10)
C22	7157 (7)	6053 (8)	4373 (3)	16.8 (11)
C23	6671 (7)	6593 (8)	4021 (3)	15.9 (11)
C24	8582 (8)	4724 (10)	4699 (3)	25.2 (18)
N1	5916 (6)	6080 (7)	2876 (2)	13.0 (8)
O1	7304 (5)	7637 (6)	2880 (2)	17.8 (12)
O2	5669 (5)	7908 (5)	3313 (2)	17.1 (12)
S1	6487.8 (16)	7135.8 (18)	3153.3 (7)	13.2 (4)
Se1	5855.9 (7)	6534.9 (9)	1810.7 (3)	14.3 (3)

**Table 9:** Anisotropic Displacement Parameters ( $\text{\AA}^2 \times 10^3$ ) for JPM\_237A. The Anisotropic displacement factor exponent takes the form:  $-2\pi^2[h^2a^2U_{11}+2hka*b*U_{12}+...]$

Atom	U <sub>11</sub>	U <sub>22</sub>	U <sub>33</sub>	U <sub>23</sub>	U <sub>13</sub>	U <sub>12</sub>
Br1	21.4 (5)	22.7 (5)	19.0 (5)	3.9 (4)	0.8 (4)	3.5 (4)
C1	10.3 (17)	7.8 (17)	20.9 (18)	0.4 (16)	-0.7 (16)	-1.8 (16)
C2	10.2 (19)	7.6 (19)	20 (2)	0.4 (18)	-0.9 (18)	-1.7 (18)
C3	10.4 (19)	8.9 (19)	20 (2)	0.1 (17)	-0.9 (17)	-2.4 (17)
C4	10.3 (16)	9.4 (16)	20.4 (17)	-0.5 (15)	-0.8 (15)	-1.6 (15)
C5	11 (2)	7 (2)	22 (2)	0 (2)	0 (2)	-3 (2)
C6	17 (2)	14 (2)	23 (2)	0.8 (19)	0 (2)	3 (2)
C7	18 (2)	14 (2)	23 (2)	1 (2)	0 (2)	3 (2)
C8	18 (2)	14 (2)	24 (2)	1 (2)	0 (2)	3 (2)
C9	19 (2)	14 (2)	24 (2)	2 (2)	1 (2)	4 (2)
C10	19 (2)	15 (2)	23 (2)	1 (2)	0 (2)	4 (2)
C11	18 (2)	15 (2)	23 (2)	1 (2)	0 (2)	4 (2)
C12	10.2 (16)	10.8 (17)	20.5 (18)	-0.9 (16)	-0.3 (16)	-0.8 (16)
C13	10.8 (19)	11 (2)	20 (2)	-0.8 (18)	0.4 (18)	0.1 (18)
C14	10.9 (19)	14 (2)	20 (2)	-0.5 (19)	0.1 (18)	0.2 (19)
C15	11 (2)	15 (2)	20 (2)	0.2 (19)	0.0 (19)	0.3 (19)
C16	11 (2)	14 (2)	21 (2)	-1.1 (19)	0.8 (18)	0.0 (19)
C17	10.5 (19)	12 (2)	21 (2)	-1.3 (18)	0.0 (18)	0.0 (18)
C18	11 (2)	12 (2)	23 (2)	-2.2 (19)	-0.9 (19)	-3.7 (19)
C19	12 (2)	13 (2)	23 (2)	-2.7 (19)	-0.8 (19)	-2 (2)
C20	13 (2)	15 (2)	24 (2)	-2.7 (19)	-1.5 (19)	-1.9 (19)
C21	14 (2)	15 (2)	24 (2)	-2.2 (19)	-2.0 (19)	-3.2 (19)
C22	13 (2)	14 (2)	24 (2)	-2.1 (19)	-0.9 (19)	-3.7 (19)
C23	12 (2)	13 (2)	23 (2)	-2.3 (19)	-1.0 (19)	-3.6 (19)
C24	24 (4)	24 (4)	28 (4)	1 (3)	-5 (3)	0 (3)
N1	10.3 (14)	8.3 (15)	20.4 (15)	-0.4 (13)	-1.2 (13)	-1.8 (13)
O1	17 (3)	10 (3)	26 (3)	2 (2)	-1 (2)	-10 (2)
O2	18 (3)	4 (2)	29 (3)	-3 (2)	-3 (2)	2 (2)
S1	11.7 (9)	7.4 (9)	20.5 (10)	-0.1 (7)	-2.0 (8)	-2.4 (7)
Se1	8.6 (4)	13.4 (5)	21.0 (5)	3.1 (4)	0.0 (3)	0.9 (4)

**Table 10:** Bond Lengths for JPM\_237A

Atom	Atom	Length/Å	Atom	Atom	Length/Å
Br1	C15	1.920 (9)	C12	C17	1.400 (12)
C1	C2	1.540 (11)	C13	C14	1.397 (13)
C1	C5	1.528 (12)	C14	C15	1.397 (12)
C1	N1	1.498 (11)	C15	C16	1.356 (13)
C2	C3	1.549 (12)	C16	C17	1.390 (13)
C3	C4	1.528 (12)	C18	C19	1.373 (13)
C4	C12	1.515 (12)	C18	C23	1.393 (13)
C4	N1	1.494 (11)	C18	S1	1.767 (9)
C5	Se1	1.968 (9)	C19	C20	1.404 (13)
C6	C7	1.396 (13)	C20	C21	1.400 (13)
C6	C11	1.397 (13)	C21	C22	1.400 (13)
C6	Se1	1.917 (10)	C21	C24	1.508 (13)
C7	C8	1.380 (13)	C22	C23	1.382 (13)
C8	C9	1.385 (13)	N1	S1	1.618 (7)
C9	C10	1.403 (14)	O1	S1	1.444 (6)
C10	C11	1.383 (13)	O2	S1	1.433 (7)
C12	C13	1.386 (12)			



**Table 11:** Bond Angles for JPM\_237A

Atom	Atom	Atom	Angle/°	Atom	Atom	Atom	Angle/°
C5	C1	C2	114.3 (7)	C16	C15	C14	123.1 (9)
N1	C1	C2	104.3 (7)	C15	C16	C17	118.6 (8)
N1	C1	C5	112.6 (7)	C16	C17	C12	121.0 (8)
C1	C2	C3	104.6 (7)	C19	C18	C23	120.9 (9)
C4	C3	C2	104.7 (7)	C19	C18	S1	119.3 (7)
C12	C4	C3	115.0 (8)	C23	C18	S1	119.8 (7)
N1	C4	C3	100.6 (7)	C18	C19	C20	119.9 (9)
N1	C4	C12	114.5 (7)	C21	C20	C19	119.9 (9)
C1	C5	Se1	112.7 (6)	C20	C21	C22	118.8 (9)
C7	C6	C11	119.3 (9)	C20	C21	C24	119.7 (9)
C7	C6	Se1	120.1 (7)	C22	C21	C24	121.5 (9)
C11	C6	Se1	120.6 (7)	C23	C22	C21	121.2 (9)
C8	C7	C6	120.5 (9)	C22	C23	C18	119.3 (9)
C7	C8	C9	120.6 (9)	C1	N1	S1	124.2 (6)
C8	C9	C10	119.0 (9)	C4	N1	C1	111.0 (7)
C11	C10	C9	120.7 (9)	C4	N1	S1	119.6 (6)
C10	C11	C6	119.8 (9)	N1	S1	C18	108.8 (4)
C13	C12	C4	122.9 (8)	O1	S1	C18	107.0 (4)
C13	C12	C17	118.5 (8)	O1	S1	N1	107.2 (4)
C17	C12	C4	118.6 (8)	O2	S1	C18	107.7 (4)
C12	C13	C14	121.7 (8)	O2	S1	N1	106.5 (4)
C13	C14	C15	117.0 (8)	O2	S1	O1	119.4 (4)
C14	C15	Br1	117.1 (7)	C6	Se1	C5	95.1 (4)
C16	C15	Br1	119.8 (7)				

**Table 12:** Torsion Angles for JPM\_237A

A	B	C	D	Angle/°	A	B	C	D	Angle/°
Br1	C15	C16	C17	178.3 (7)	C12	C13	C14	C15	-2.1 (13)
C1	C2	C3	C4	-32.3 (9)	C13	C12	C17	C16	0.2 (13)
C1	N1	S1	C18	-75.1 (8)	C13	C14	C15	Br1	-178.0 (7)
C1	N1	S1	O1	40.2 (8)	C13	C14	C15	C16	3.9 (14)
C1	N1	S1	O2	169.0 (7)	C14	C15	C16	C17	-3.6 (14)
C2	C1	C5	Se1	57.9 (9)	C15	C16	C17	C12	1.5 (14)
C2	C1	N1	C4	12.1 (9)	C17	C12	C13	C14	0.2 (13)
C2	C1	N1	S1	166.1 (6)	C18	C19	C20	C21	-3.1 (13)
C2	C3	C4	C12	-85.2 (9)	C19	C18	C23	C22	-0.3 (13)
C2	C3	C4	N1	38.3 (8)	C19	C18	S1	N1	74.7 (8)
C3	C4	C12	C13	67.3 (11)	C19	C18	S1	O1	-40.8 (8)
C3	C4	C12	C17	-115.0 (9)	C19	C18	S1	O2	-170.3 (7)
C3	C4	N1	C1	-31.6 (8)	C19	C20	C21	C22	1.2 (13)
C3	C4	N1	S1	173.0 (6)	C19	C20	C21	C24	179.4 (9)
C4	C12	C13	C14	177.8 (8)	C20	C21	C22	C23	1.1 (14)
C4	C12	C17	C16	-177.6 (8)	C21	C22	C23	C18	-1.6 (13)
C4	N1	S1	C18	76.9 (7)	C23	C18	C19	C20	2.6 (13)
C4	N1	S1	O1	-167.8 (6)	C23	C18	S1	N1	-104.2 (8)
C4	N1	S1	O2	-39.0 (7)	C23	C18	S1	O1	140.3 (7)
C5	C1	C2	C3	-110.7 (8)	C23	C18	S1	O2	10.8 (8)
C5	C1	N1	C4	136.6 (7)	C24	C21	C22	C23	-177.0 (9)
C5	C1	N1	S1	-69.4 (9)	N1	C1	C2	C3	12.7 (9)
C6	C7	C8	C9	1.4 (14)	N1	C1	C5	Se1	-61.0 (8)
C7	C6	C11	C10	-0.2 (14)	N1	C4	C12	C13	-48.4 (12)
C7	C8	C9	C10	-2.0 (14)	N1	C4	C12	C17	129.2 (8)
C8	C9	C10	C11	1.4 (14)	S1	C18	C19	C20	-176.3 (7)
C9	C10	C11	C6	-0.4 (14)	S1	C18	C23	C22	178.6 (7)
C11	C6	C7	C8	-0.3 (14)	Se1	C6	C7	C8	-180.0 (7)
C12	C4	N1	C1	92.3 (9)	Se1	C6	C11	C10	179.4 (7)
C12	C4	N1	S1	-63.1 (9)					

**Table 13:** Hydrogen Atom Coordinates ( $\text{\AA}\times 104$ ) and Isotropic Displacement Parameters ( $\text{\AA}^2\times 103$ ) for JPM\_237A

Atom	<i>x</i>	<i>y</i>	<i>z</i>	U(eq)
H1	7062.1	4842.04	2755.9	16
H2A	5829.57	3474.68	2653.64	15
H2B	5640.71	4024.01	2185.73	15
H3A	4280.51	5221.61	2420.66	16
H3B	4126.74	4119.05	2740.61	16
H4	4383.38	6209.72	3059.63	16
H5A	7322.53	5197.27	2015.04	16
H5B	7438.96	6417.33	2270.32	16
H7	7675.42	8180.93	1818.9	22
H8	8859.33	8945.52	1322.73	23
H9	8705.3	8480.28	589.54	23
H10	7403.31	7129.84	364.24	23
H11	6227.69	6334.4	860.95	22
H13	6232.03	3858.91	3346.31	17
H14	6329.89	2931.14	4028.52	18
H16	3837.23	4884.8	4423.29	18
H17	3741.41	5787.56	3741.24	18
H19	8335.95	5796.21	3273.44	19
H20	9107.53	4786.82	3860.4	21
H22	6871.33	6146.29	4649.41	20
H23	6052.13	7029.86	4058.67	19
H24A	8607.8	3871.46	4640.59	38
H24B	8178.16	4865.28	4958.16	38
H24C	9283.48	5024.9	4739.31	38

### 4.3.3. X-Ray Crystallographic Information for *cis*-Pyrrolidine JPM\_355B

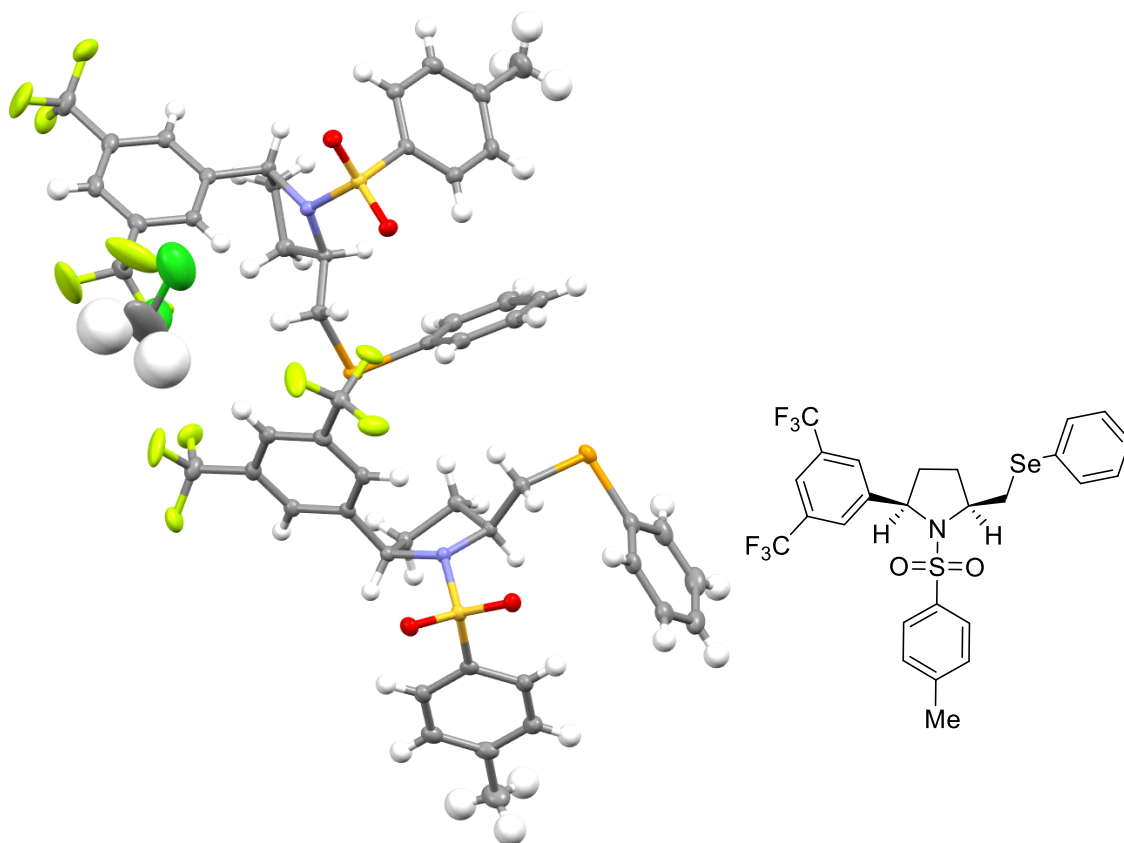


**Table 14:** Crystal data and structure refinement for JPM\_355B

Identification code	JPM_355B
Empirical formula	C <sub>26.5</sub> H <sub>24</sub> ClF <sub>6</sub> NO <sub>2</sub> SSe
Formula weight	648.94
Temperature/K	99.9(3)
Crystal system	triclinic
Space group	P-1
a/Å	8.1424(3)
b/Å	18.2419(6)
c/Å	18.7517(6)
α/°	96.646(3)
β/°	101.128(3)
γ/°	97.979(3)
Volume/Å <sup>3</sup>	2677.15(16)
Z	4
ρ <sub>calc</sub> /cm <sup>3</sup>	1.610
μ/mm <sup>-1</sup>	4.165
F(000)	1308.0
Crystal size/mm <sup>3</sup>	0.309 × 0.149 × 0.098
Radiation	CuKα (λ = 1.54184)
2Θ range for data collection/°	7.424 to 146.21
Index ranges	-9 ≤ h ≤ 7, -22 ≤ k ≤ 22, -22 ≤ l ≤ 23

Reflections collected	19495
Independent reflections	10372 [ $R_{\text{int}} = 0.0314$ , $R_{\text{sigma}} = 0.0373$ ]
Data/restraints/parameters	10372/0/696
Goodness-of-fit on $F^2$	1.038
Final R indexes [ $I \geq 2\sigma(I)$ ]	$R_1 = 0.0483$ , $wR_2 = 0.1315$
Final R indexes [all data]	$R_1 = 0.0532$ , $wR_2 = 0.1365$
Largest diff. peak/hole / $e \text{ \AA}^{-3}$	1.59/-2.02

**Table 15:** Fractional Atomic Coordinates ( $\times 104$ ) and Equivalent Isotropic Displacement Parameters ( $\text{\AA}^2 \times 10^3$ ) for JPM\_355B.  $U_{\text{eq}}$  is defined as 1/3 of the trace of the orthogonalised  $U_{ij}$  tensor.

Atom	<i>x</i>	<i>y</i>	<i>z</i>	U(eq)
C1	669 (4)	4722.5 (17)	2365.3 (16)	16.2 (6)
C2	2579 (4)	4677.6 (18)	2521.0 (17)	18.6 (6)
C3	2975 (4)	4524.6 (18)	1762.6 (17)	18.8 (6)
C4	1895 (4)	5004.9 (17)	1306.9 (17)	16.3 (6)
C5	155 (4)	5267.3 (18)	2929.3 (17)	18.5 (6)
C6	-1448 (4)	4038.8 (19)	3573.7 (18)	22.7 (7)
C7	-2929 (4)	4035 (2)	3053.9 (18)	23.4 (7)
C8	-4129 (5)	3384 (2)	2839 (2)	27.2 (7)
C9	-3872 (5)	2745 (2)	3158 (2)	32.2 (8)
C10	-2433 (5)	2757 (2)	3686 (2)	35.1 (9)
C11	-1208 (5)	3397 (2)	3890 (2)	30.2 (8)
C12	2776 (4)	5799.2 (17)	1324.7 (16)	16.2 (6)
C13	2232 (4)	6424.0 (18)	1637.1 (17)	18.2 (6)
C14	3084 (4)	7139.7 (18)	1616.1 (17)	18.9 (6)
C15	4450 (4)	7239.6 (18)	1280.0 (18)	20.0 (6)
C16	4964 (4)	6611.9 (18)	960.7 (18)	19.7 (6)
C17	4155 (4)	5899.7 (18)	982.9 (17)	17.6 (6)
C18	2491 (4)	7810.3 (18)	1970.0 (19)	22.7 (7)
C19	6445 (4)	6707 (2)	588 (2)	27.9 (7)
C20	-1582 (4)	3729.5 (17)	793.9 (17)	17.7 (6)
C21	-2477 (4)	3209.9 (19)	1124.9 (18)	22.9 (7)
C22	-2507 (5)	2451 (2)	918.3 (19)	26.5 (7)
C23	-1632 (5)	2201.8 (19)	392.9 (19)	26.6 (7)
C24	-761 (4)	2734 (2)	65.4 (19)	24.7 (7)
C25	-735 (4)	3491.8 (19)	253.5 (18)	21.0 (6)
C26	-1675 (6)	1375 (2)	167 (2)	40.7 (10)
F1	801 (3)	7732.2 (13)	1855.9 (13)	36.9 (5)
F2	3022 (4)	8434.8 (13)	1718.3 (16)	52.3 (7)
F3	3038 (3)	7934.2 (13)	2696.7 (11)	33.5 (5)
F4	6246 (3)	6209.6 (13)	-12.8 (12)	33.7 (5)
F5	6698 (3)	7388.8 (14)	379.3 (17)	51.5 (7)
F6	7892 (3)	6634.7 (14)	1027.1 (14)	39.0 (5)
N1	366 (3)	4988.1 (14)	1633.6 (14)	15.8 (5)

O1	-2742 (3)	4776.6 (13)	1509.4 (12)	20.7 (5)
O2	-1473 (3)	5070.5 (13)	449.7 (12)	20.4 (5)
S1	-1481.4 (9)	4692.2 (4)	1077.7 (4)	16.08 (15)
Se1	273.8 (4)	4909.2 (2)	3878.6 (2)	22.30 (10)
C101	8418 (4)	7679.5 (16)	3828.5 (16)	15.8 (6)
C102	10176 (4)	7509.7 (18)	3757.6 (18)	20.1 (6)
C103	11403 (4)	8128.7 (18)	4297.3 (18)	19.0 (6)
C104	10555 (4)	8820.3 (17)	4190.1 (17)	16.7 (6)
C105	7048 (4)	7428.3 (17)	3137.8 (17)	18.9 (6)
C106	5617 (4)	6265.6 (17)	3862.8 (18)	19.2 (6)
C107	4162 (4)	6556.4 (18)	3967.9 (18)	20.7 (6)
C108	3591 (4)	6493.6 (18)	4611.0 (19)	21.8 (6)
C109	4444 (4)	6136.2 (18)	5149.9 (19)	22.7 (7)
C110	5889 (4)	5851.9 (18)	5046 (2)	23.7 (7)
C111	6474 (4)	5915.2 (18)	4405.5 (19)	22.2 (7)
C112	11039 (4)	9216.1 (17)	3571.6 (17)	17.7 (6)
C113	9892 (4)	9223.7 (17)	2922.3 (17)	19.1 (6)
C114	10405 (4)	9590.9 (19)	2372.4 (18)	23.0 (7)
C115	12059 (4)	9965.3 (18)	2465.8 (19)	24.2 (7)
C116	13191 (4)	9961.7 (18)	3118 (2)	22.5 (7)
C117	12699 (4)	9587.1 (17)	3666.2 (18)	19.6 (6)
C118	9149 (5)	9589 (2)	1673.6 (19)	28.9 (8)
C119	14989 (5)	10353 (2)	3235 (2)	31.0 (8)
C120	8161 (4)	8564.5 (17)	5429.9 (17)	17.2 (6)
C121	7244 (4)	7924.7 (19)	5585.0 (18)	21.5 (6)
C122	7755 (5)	7679 (2)	6257.0 (19)	25.6 (7)
C123	9153 (5)	8071 (2)	6772.4 (18)	25.5 (7)
C124	10054 (4)	8714.3 (19)	6604.8 (18)	23.6 (7)
C125	9575 (4)	8962.5 (18)	5933.5 (18)	19.5 (6)
C126	9708 (6)	7800 (3)	7498 (2)	38.7 (9)
F101	8100 (6)	8972 (2)	1463 (2)	114 (2)
F102	9841 (4)	9718 (3)	1119.0 (16)	89.2 (14)
F103	8205 (5)	10111 (3)	1728.8 (18)	98.8 (16)
F104	16047 (3)	9880.5 (14)	3090.0 (15)	40.6 (6)
F105	15150 (3)	10877.9 (15)	2796.8 (17)	51.1 (7)
F106	15619 (3)	10687.3 (14)	3918.6 (15)	43.9 (6)
N101	8709 (3)	8514.2 (14)	4028.3 (14)	16.1 (5)
O101	5831 (3)	8510.1 (13)	4261.2 (12)	20.5 (5)
O102	8010 (3)	9655.3 (12)	4658.5 (13)	20.9 (5)
S101	7553.2 (9)	8857.0 (4)	4567.3 (4)	16.01 (15)
Se11	6404.2 (4)	6337.2 (2)	2968.6 (2)	20.56 (10)
C201	3272 (10)	11033 (9)	532 (5)	160 (6)
Cl21	2899 (3)	11768.0 (17)	1199.6 (13)	111.5 (8)
Cl22	4513 (3)	10469.7 (12)	910.1 (12)	101.7 (7)

**Table 16:** Anisotropic Displacement Parameters ( $\text{\AA}^2 \times 10^3$ ) for JPM\_355B. The Anisotropic displacement factor exponent takes the form:  $-\pi^2[h^2a^{*2}U_{11}+2hka^*b^*U_{12}+\dots]$

Atom	U <sub>11</sub>	U <sub>22</sub>	U <sub>33</sub>	U <sub>23</sub>	U <sub>13</sub>	U <sub>12</sub>
C1	16.6 (14)	19.0 (14)	13.3 (14)	3.2 (11)	3.3 (11)	3.3 (11)
C2	16.0 (14)	21.5 (15)	18.1 (15)	2.5 (12)	2.2 (12)	5.0 (12)
C3	16.8 (14)	19.7 (15)	21.8 (16)	4.0 (12)	7.1 (12)	4.7 (12)
C4	13.6 (13)	18.5 (14)	16.7 (14)	0.2 (11)	4.8 (11)	2.3 (11)
C5	18.7 (15)	20.4 (15)	16.6 (15)	1.2 (12)	4.9 (12)	3.5 (12)
C6	24.6 (16)	28.0 (17)	19.4 (16)	4.7 (13)	10.5 (13)	8.3 (13)
C7	23.0 (16)	28.9 (17)	21.4 (16)	7.4 (13)	8.4 (13)	6.2 (13)
C8	25.9 (17)	32.1 (19)	26.8 (18)	4.4 (14)	11.8 (14)	7.1 (14)
C9	35 (2)	26.6 (18)	39 (2)	3.7 (16)	20.5 (17)	4.5 (15)
C10	47 (2)	27.2 (19)	42 (2)	14.2 (16)	22.8 (19)	16.9 (17)
C11	32.9 (19)	39 (2)	26.5 (18)	12.2 (16)	12.9 (15)	18.1 (16)
C12	15.0 (14)	20.4 (15)	12.9 (14)	2.1 (11)	1.4 (11)	3.7 (11)
C13	17.3 (14)	23.0 (16)	15.2 (14)	3.2 (12)	4.9 (11)	4.2 (12)
C14	20.1 (15)	19.4 (15)	16.9 (15)	0.4 (12)	2.5 (12)	6.2 (12)
C15	20.3 (15)	19.6 (15)	19.1 (15)	4.8 (12)	2.3 (12)	1.2 (12)
C16	15.3 (14)	25.1 (16)	19.4 (15)	5.7 (12)	3.9 (12)	3.7 (12)
C17	15.1 (14)	21.0 (15)	17.0 (15)	3.5 (12)	2.8 (11)	4.7 (12)
C18	24.7 (16)	20.2 (16)	23.0 (16)	0.3 (13)	6.2 (13)	4.2 (13)
C19	24.0 (17)	24.8 (17)	39 (2)	8.9 (15)	13.8 (15)	4.3 (14)
C20	16.2 (14)	19.6 (15)	14.7 (14)	1.0 (11)	-2.2 (11)	3.1 (12)
C21	22.1 (16)	26.6 (17)	17.8 (15)	1.6 (13)	3.4 (12)	-0.5 (13)
C22	31.3 (18)	24.2 (17)	21.5 (17)	4.2 (13)	4.0 (14)	-1.9 (14)
C23	31.7 (18)	21.8 (17)	22.5 (17)	0.5 (13)	-2.9 (14)	6.2 (14)
C24	23.1 (16)	28.3 (17)	20.6 (16)	-1.5 (13)	1.1 (13)	6.2 (13)
C25	17.4 (15)	26.9 (17)	17.9 (15)	2.6 (12)	3.3 (12)	2.8 (12)
C26	58 (3)	25.9 (19)	39 (2)	1.5 (16)	10 (2)	11.7 (18)
F1	25.7 (11)	39.0 (12)	41.1 (13)	-13.0 (10)	-1.4 (9)	16.2 (9)
F2	87 (2)	20.8 (11)	67.9 (18)	12.8 (11)	53.6 (16)	17.6 (12)
F3	33.5 (11)	40.5 (12)	23.7 (11)	-10.1 (9)	2.3 (9)	14.2 (9)
F4	32.5 (11)	43.7 (13)	29.8 (11)	4.3 (9)	18.5 (9)	7.7 (10)
F5	56.0 (16)	32.0 (12)	89 (2)	28.1 (13)	54.1 (16)	14.3 (11)
F6	16.0 (10)	48.7 (14)	49.4 (14)	-1.3 (11)	7.1 (9)	1.7 (9)
N1	12.9 (12)	20.2 (13)	14.0 (12)	2.1 (10)	3.5 (9)	1.4 (10)
O1	14.5 (10)	27.2 (12)	20.7 (11)	2.4 (9)	4.7 (9)	4.2 (9)
O2	21.1 (11)	23.8 (11)	17.0 (11)	5.3 (9)	2.9 (9)	5.6 (9)
S1	13.5 (3)	20.1 (4)	14.5 (3)	2.3 (3)	2.3 (3)	3.4 (3)
Se1	20.29 (18)	33.2 (2)	14.54 (17)	3.50 (14)	3.98 (13)	7.67 (14)
C101	15.3 (14)	15.7 (14)	15.1 (14)	0.7 (11)	2.1 (11)	1.3 (11)
C102	17.1 (15)	19.8 (15)	23.0 (16)	2.4 (12)	3.2 (12)	4.0 (12)
C103	13.6 (14)	22.5 (16)	19.9 (15)	4.9 (12)	1.2 (12)	1.4 (12)
C104	11.9 (14)	19.5 (15)	16.8 (14)	1.4 (11)	1.6 (11)	0.0 (11)
C105	18.1 (15)	20.1 (15)	17.0 (15)	1.7 (12)	0.9 (12)	2.8 (12)

C106	17.0 (14)	15.9 (14)	21.5 (16)	-1.9 (12)	1.7 (12)	-1.5 (11)
C107	17.0 (15)	21.8 (15)	20.8 (16)	1.1 (12)	-0.8 (12)	3.0 (12)
C108	16.1 (15)	22.6 (16)	25.6 (17)	0.9 (13)	3.5 (12)	2.7 (12)
C109	21.9 (16)	19.5 (15)	24.9 (17)	3.8 (13)	4.1 (13)	-1.6 (12)
C110	22.9 (16)	19.5 (16)	27.9 (17)	7.0 (13)	0.8 (13)	4.4 (13)
C111	17.4 (15)	18.4 (15)	29.5 (18)	0.4 (13)	3.4 (13)	3.8 (12)
C112	19.1 (15)	14.4 (14)	20.3 (15)	-0.2 (11)	6.8 (12)	3.9 (11)
C113	19.0 (15)	18.6 (15)	18.5 (15)	0.2 (12)	4.3 (12)	1.1 (12)
C114	28.9 (17)	21.3 (16)	20.1 (16)	0.8 (12)	7.4 (13)	6.9 (13)
C115	29.2 (17)	19.9 (16)	28.0 (18)	6.4 (13)	13.7 (14)	6.3 (13)
C116	22.7 (16)	17.2 (15)	30.3 (18)	2.9 (13)	11.8 (14)	4.0 (12)
C117	18.4 (15)	17.9 (15)	22.9 (16)	2.3 (12)	4.7 (12)	4.1 (12)
C118	34.8 (19)	31.4 (19)	19.9 (17)	4.1 (14)	5.1 (14)	4.4 (15)
C119	26.1 (18)	27.2 (18)	43 (2)	12.7 (16)	13.6 (16)	2.5 (15)
C120	19.3 (15)	18.2 (14)	14.8 (14)	-0.1 (11)	5.2 (12)	4.8 (12)
C121	19.1 (15)	24.0 (16)	20.0 (16)	0.7 (13)	4.7 (12)	-0.2 (12)
C122	28.4 (17)	26.8 (17)	23.4 (17)	7.1 (13)	11.0 (14)	0.3 (14)
C123	28.9 (17)	32.0 (18)	17.7 (16)	4.0 (13)	8.1 (13)	7.2 (14)
C124	21.7 (16)	27.3 (17)	19.9 (16)	-1.6 (13)	1.8 (13)	5.8 (13)
C125	17.5 (15)	19.6 (15)	20.6 (16)	-1.2 (12)	4.9 (12)	2.1 (12)
C126	44 (2)	47 (2)	25.5 (19)	13.1 (17)	6.6 (17)	6.7 (19)
F101	136 (4)	82 (3)	72 (2)	46 (2)	-70 (2)	-59 (3)
F102	62 (2)	183 (4)	27.3 (15)	35 (2)	11.1 (14)	19 (2)
F103	111 (3)	138 (4)	42.0 (18)	-20 (2)	-26.6 (18)	92 (3)
F104	24.8 (11)	42.6 (13)	61.7 (16)	12.6 (12)	20.9 (11)	9.5 (10)
F105	32.3 (12)	47.4 (15)	79 (2)	42.6 (14)	11.4 (12)	-3.0 (11)
F106	28.0 (11)	44.2 (14)	52.7 (15)	-2.1 (11)	9.0 (11)	-10.5 (10)
N101	13.7 (12)	16.6 (12)	17.0 (12)	0.3 (10)	3.1 (10)	0.9 (10)
O101	13.9 (10)	23.9 (11)	22.1 (11)	0.2 (9)	2.3 (9)	1.9 (9)
O102	21.8 (11)	17.5 (11)	22.9 (11)	2.0 (9)	4.2 (9)	3.1 (9)
S101	13.8 (3)	16.8 (3)	16.7 (3)	0.7 (3)	2.8 (3)	2.2 (3)
Se11	19.38 (18)	20.32 (18)	19.15 (18)	-4.57 (13)	3.05 (13)	1.25 (13)
C201	45 (4)	354 (19)	63 (5)	-2 (8)	-4 (3)	18 (7)
Cl21	86.1 (13)	170 (2)	92.8 (14)	30.3 (15)	30.0 (11)	45.3 (14)
Cl22	121.0 (16)	86.5 (12)	99.8 (14)	-7.4 (11)	62.1 (13)	-12.3 (11)



**Table 17:** Bond Lengths for JPM\_355B

Atom	Atom	Length/Å	Atom	Atom	Length/Å
C1	C2	1.542 (4)	C101	C105	1.515 (4)
C1	C5	1.525 (4)	C101	N101	1.500 (4)
C1	N1	1.495 (4)	C102	C103	1.526 (4)
C2	C3	1.521 (4)	C103	C104	1.535 (4)
C3	C4	1.539 (4)	C104	C112	1.521 (4)
C4	C12	1.519 (4)	C104	N101	1.488 (4)
C4	N1	1.488 (4)	C105	Se11	1.959 (3)
C5	Se1	1.956 (3)	C106	C107	1.402 (5)
C6	C7	1.395 (5)	C106	C111	1.389 (5)
C6	C11	1.393 (5)	C106	Se11	1.919 (3)
C6	Se1	1.917 (4)	C107	C108	1.384 (5)
C7	C8	1.394 (5)	C108	C109	1.391 (5)
C8	C9	1.393 (5)	C109	C110	1.388 (5)
C9	C10	1.376 (6)	C110	C111	1.386 (5)
C10	C11	1.388 (6)	C112	C113	1.387 (5)
C12	C13	1.387 (4)	C112	C117	1.393 (4)
C12	C17	1.398 (4)	C113	C114	1.391 (5)
C13	C14	1.400 (4)	C114	C115	1.392 (5)
C14	C15	1.381 (5)	C114	C118	1.498 (5)
C14	C18	1.507 (4)	C115	C116	1.384 (5)
C15	C16	1.384 (5)	C116	C117	1.388 (5)
C16	C17	1.382 (4)	C116	C119	1.501 (5)
C16	C19	1.506 (4)	C118	F101	1.285 (5)
C18	F1	1.336 (4)	C118	F102	1.304 (5)
C18	F2	1.332 (4)	C118	F103	1.310 (5)
C18	F3	1.331 (4)	C119	F104	1.342 (4)
C19	F4	1.332 (4)	C119	F105	1.341 (4)
C19	F5	1.347 (4)	C119	F106	1.325 (5)
C19	F6	1.333 (4)	C120	C121	1.387 (4)
C20	C21	1.391 (5)	C120	C125	1.390 (4)
C20	C25	1.393 (4)	C120	S101	1.764 (3)
C20	S1	1.761 (3)	C121	C122	1.393 (5)
C21	C22	1.390 (5)	C122	C123	1.389 (5)
C22	C23	1.393 (5)	C123	C124	1.397 (5)
C23	C24	1.392 (5)	C123	C126	1.510 (5)
C23	C26	1.512 (5)	C124	C125	1.391 (5)
C24	C25	1.383 (5)	N101	S101	1.638 (3)
N1	S1	1.637 (3)	O101	S101	1.434 (2)
O1	S1	1.438 (2)	O102	S101	1.434 (2)
O2	S1	1.433 (2)	C201	Cl21	1.825 (12)
C101	C102	1.533 (4)	C201	Cl22	1.662 (13)

**Table 18:** Bond Angles for JPM\_355B

Atom	Atom	Atom	Angle/°	Atom	Atom	Atom	Angle/°
C5	C1	C2	114.1 (3)	N101	C101	C102	103.5 (2)
N1	C1	C2	103.4 (2)	N101	C101	C105	110.8 (2)
N1	C1	C5	109.6 (2)	C103	C102	C101	103.9 (2)
C3	C2	C1	104.2 (2)	C102	C103	C104	102.7 (2)
C2	C3	C4	103.4 (2)	C112	C104	C103	113.2 (3)
C12	C4	C3	114.4 (2)	N101	C104	C103	103.6 (2)
N1	C4	C3	103.3 (2)	N101	C104	C112	111.4 (2)
N1	C4	C12	111.9 (2)	C101	C105	Se11	110.7 (2)
C1	C5	Se1	112.5 (2)	C107	C106	Se11	120.2 (2)
C7	C6	Se1	122.0 (3)	C111	C106	C107	119.6 (3)
C11	C6	C7	119.5 (3)	C111	C106	Se11	120.1 (2)
C11	C6	Se1	118.5 (3)	C108	C107	C106	119.8 (3)
C8	C7	C6	119.9 (3)	C107	C108	C109	120.3 (3)
C9	C8	C7	120.0 (4)	C110	C109	C108	119.7 (3)
C10	C9	C8	119.9 (4)	C111	C110	C109	120.3 (3)
C9	C10	C11	120.5 (3)	C110	C111	C106	120.2 (3)
C10	C11	C6	120.1 (4)	C113	C112	C104	122.5 (3)
C13	C12	C4	123.0 (3)	C113	C112	C117	119.1 (3)
C13	C12	C17	119.0 (3)	C117	C112	C104	118.4 (3)
C17	C12	C4	117.9 (3)	C112	C113	C114	120.1 (3)
C12	C13	C14	119.7 (3)	C113	C114	C115	121.0 (3)
C13	C14	C18	118.9 (3)	C113	C114	C118	119.3 (3)
C15	C14	C13	121.3 (3)	C115	C114	C118	119.7 (3)
C15	C14	C18	119.8 (3)	C116	C115	C114	118.5 (3)
C14	C15	C16	118.4 (3)	C115	C116	C117	121.0 (3)
C15	C16	C19	119.3 (3)	C115	C116	C119	120.0 (3)
C17	C16	C15	121.3 (3)	C117	C116	C119	119.0 (3)
C17	C16	C19	119.4 (3)	C116	C117	C112	120.3 (3)
C16	C17	C12	120.2 (3)	F101	C118	C114	113.6 (3)
F1	C18	C14	112.5 (3)	F101	C118	F102	106.3 (4)
F2	C18	C14	112.1 (3)	F101	C118	F103	105.4 (4)
F2	C18	F1	106.9 (3)	F102	C118	C114	113.9 (3)
F3	C18	C14	112.4 (3)	F102	C118	F103	104.3 (4)
F3	C18	F1	105.6 (3)	F103	C118	C114	112.6 (3)
F3	C18	F2	107.0 (3)	F104	C119	C116	112.2 (3)
F4	C19	C16	112.8 (3)	F105	C119	C116	112.1 (3)
F4	C19	F5	106.6 (3)	F105	C119	F104	106.0 (3)
F4	C19	F6	106.4 (3)	F106	C119	C116	113.3 (3)
F5	C19	C16	111.8 (3)	F106	C119	F104	105.8 (3)
F6	C19	C16	112.1 (3)	F106	C119	F105	106.9 (3)
F6	C19	F5	106.6 (3)	C121	C120	C125	121.1 (3)
C21	C20	C25	120.3 (3)	C121	C120	S101	119.1 (2)
C21	C20	S1	119.6 (2)	C125	C120	S101	119.8 (2)

C25	C20	S1	120.1 (2)	C120 C121 C122	119.2 (3)
C22	C21	C20	119.5 (3)	C123 C122 C121	120.9 (3)
C21	C22	C23	121.0 (3)	C122 C123 C124	118.9 (3)
C22	C23	C26	120.9 (3)	C122 C123 C126	120.7 (3)
C24	C23	C22	118.2 (3)	C124 C123 C126	120.4 (3)
C24	C23	C26	120.9 (3)	C125 C124 C123	121.0 (3)
C25	C24	C23	121.8 (3)	C120 C125 C124	118.9 (3)
C24	C25	C20	119.1 (3)	C101 N101 S101	116.7 (2)
C1	N1	S1	117.9 (2)	C104 N101 C101	110.6 (2)
C4	N1	C1	111.2 (2)	C104 N101 S101	117.9 (2)
C4	N1	S1	117.2 (2)	N101 S101 C120	107.43 (14)
N1	S1	C20	106.88 (14)	O101 S101 C120	107.73 (14)
O1	S1	C20	108.05 (15)	O101 S101 N101	106.53 (13)
O1	S1	N1	106.53 (13)	O102 S101 C120	108.04 (14)
O2	S1	C20	108.26 (14)	O102 S101 N101	106.50 (13)
O2	S1	N1	106.32 (13)	O102 S101 O101	120.02 (14)
O2	S1	O1	120.11 (13)	C106 Se11 C105	95.94 (13)
C6	Se1	C5	98.50 (14)	C122 C201 C121	113.1 (5)
C105	C101	C102	114.5 (3)		

**Table 19:** Torsion Angles for JPM\_355B

A	B	C	D	Angle/°	A	B	C	D	Angle/°
C1	C2	C3	C4	38.3 (3)	C101	C102	C103	C104	-39.9 (3)
C1	N1	S1	C20	-68.7 (2)	C101	N101	S101	C120	66.4 (2)
C1	N1	S1	O1	46.6 (2)	C101	N101	S101	O101	-48.9 (2)
C1	N1	S1	O2	175.8 (2)	C101	N101	S101	O102	-178.1 (2)
C2	C1	C5	Se1	-70.8 (3)	C102	C101	C105	Se11	72.8 (3)
C2	C1	N1	C4	7.5 (3)	C102	C101	N101	C104	-8.8 (3)
C2	C1	N1	S1	147.1 (2)	C102	C101	N101	S101	-147.3 (2)
C2	C3	C4	C12	88.7 (3)	C102	C103	C104	C112	-86.8 (3)
C2	C3	C4	N1	-33.1 (3)	C102	C103	C104	N101	33.9 (3)
C3	C4	C12	C13	-114.6 (3)	C103	C104	C112	C113	111.4 (3)
C3	C4	C12	C17	68.0 (4)	C103	C104	C112	C117	-68.9 (4)
C3	C4	N1	C1	15.9 (3)	C103	C104	N101	C101	-15.7 (3)
C3	C4	N1	S1	-124.0 (2)	C103	C104	N101	S101	122.1 (2)
C4	C12	C13	C14	-178.4 (3)	C104	C112	C113	C114	-179.6 (3)
C4	C12	C17	C16	177.7 (3)	C104	C112	C117	C116	-179.4 (3)
C4	N1	S1	C20	68.5 (2)	C104	N101	S101	C120	-69.0 (2)
C4	N1	S1	O1	-176.2 (2)	C104	N101	S101	O101	175.8 (2)
C4	N1	S1	O2	-47.0 (2)	C104	N101	S101	O102	46.6 (2)
C5	C1	C2	C3	-147.3 (3)	C105	C101	C102	C103	150.8 (3)
C5	C1	N1	C4	129.6 (3)	C105	C101	N101	C104	-132.1 (3)
C5	C1	N1	S1	-90.9 (3)	C105	C101	N101	S101	89.5 (3)
C6	C7	C8	C9	1.8 (5)	C106	C107	C108	C109	-0.7 (5)
C7	C6	C11	C10	0.2 (5)	C107	C106	C111	C110	0.2 (5)
C7	C8	C9	C10	0.0 (5)	C107	C108	C109	C110	1.0 (5)
C8	C9	C10	C11	-1.8 (6)	C108	C109	C110	C111	-0.7 (5)
C9	C10	C11	C6	1.6 (6)	C109	C110	C111	C106	0.1 (5)
C11	C6	C7	C8	-2.0 (5)	C111	C106	C107	C108	0.1 (5)
C12	C4	N1	C1	-107.6 (3)	C112	C104	N101	C101	106.3 (3)
C12	C4	N1	S1	112.5 (2)	C112	C104	N101	S101	-115.9 (2)
C12	C13	C14	C15	0.9 (5)	C112	C113	C114	C115	-1.0 (5)
C12	C13	C14	C18	-179.0 (3)	C112	C113	C114	C118	179.7 (3)
C13	C12	C17	C16	0.2 (5)	C113	C112	C117	C116	0.3 (5)
C13	C14	C15	C16	0.0 (5)	C113	C114	C115	C116	0.3 (5)
C13	C14	C18	F1	-39.6 (4)	C113	C114	C118	F101	-36.4 (5)
C13	C14	C18	F2	-160.1 (3)	C113	C114	C118	F102	-158.3 (4)
C13	C14	C18	F3	79.4 (4)	C113	C114	C118	F103	83.2 (5)
C14	C15	C16	C17	-0.9 (5)	C114	C115	C116	C117	0.7 (5)
C14	C15	C16	C19	179.7 (3)	C114	C115	C116	C119	179.4 (3)
C15	C14	C18	F1	140.5 (3)	C115	C114	C118	F101	144.3 (4)
C15	C14	C18	F2	19.9 (4)	C115	C114	C118	F102	22.4 (5)
C15	C14	C18	F3	-100.5 (4)	C115	C114	C118	F103	-96.1 (5)
C15	C16	C17	C12	0.8 (5)	C115	C116	C117	C112	-1.0 (5)
C15	C16	C19	F4	-143.0 (3)	C115	C116	C119	F104	-97.4 (4)

C15C16C19F5	-22.8 (5)	C115 C116C119F105	21.7 (5)
C15C16C19F6	96.8 (4)	C115 C116C119F106	142.8 (3)
C17C12C13C14	-1.0 (4)	C117 C112C113C114	0.7 (5)
C17C16C19F4	37.6 (4)	C117 C116C119F104	81.3 (4)
C17C16C19F5	157.8 (3)	C117 C116C119F105	-159.6 (3)
C17C16C19F6	-82.6 (4)	C117 C116C119F106	-38.5 (4)
C18C14C15C16	179.9 (3)	C118 C114C115C116	179.6 (3)
C19C16C17C12	-179.9 (3)	C119 C116C117C112	-179.7 (3)
C20C21C22C23	1.0 (5)	C120 C121 C122C123	0.6 (5)
C21C20C25C24	-1.7 (5)	C121 C120C125C124	-0.7 (5)
C21C20S1 N1	100.3 (3)	C121 C120S101 N101	-94.9 (3)
C21C20S1 O1	-14.0 (3)	C121 C120S101 O101	19.5 (3)
C21C20S1 O2	-145.5 (2)	C121 C120S101 O102	150.5 (2)
C21C22C23C24	-1.7 (5)	C121 C122C123C124	-0.5 (5)
C21C22C23C26	-179.7 (3)	C121 C122C123C126	-179.6 (3)
C22C23C24C25	0.6 (5)	C122 C123C124C125	-0.3 (5)
C23C24C25C20	1.0 (5)	C123 C124C125C120	0.9 (5)
C25C20C21C22	0.6 (5)	C125 C120C121C122	0.0 (5)
C25C20S1 N1	-78.1 (3)	C125 C120S101 N101	83.2 (3)
C25C20S1 O1	167.6 (2)	C125 C120S101 O101	-162.4 (2)
C25C20S1 O2	36.0 (3)	C125 C120S101 O102	-31.4 (3)
C26C23C24C25	178.7 (3)	C126 C123C124C125	178.9 (3)
N1 C1 C2 C3	-28.3 (3)	N101C101C102C103	30.1 (3)
N1 C1 C5 Se1	173.77 (19)	N101C101C105Se11	-170.61 (19)
N1 C4 C12C13	2.3 (4)	N101C104C112C113	-4.9 (4)
N1 C4 C12C17	-175.1 (3)	N101C104C112C117	174.8 (3)
S1 C20C21C22	-177.8 (3)	S101 C120C121C122	178.0 (3)
S1 C20C25C24	176.8 (2)	S101 C120C125C124	-178.7 (2)
Se1 C6 C7 C8	178.7 (2)	Se11 C106C107C108	179.2 (2)
Se1 C6 C11C10	179.6 (3)	Se11 C106C111C110	-178.9 (2)

**Table 20:** Hydrogen Atom Coordinates ( $\text{\AA}\times 10^4$ ) and Isotropic Displacement Parameters ( $\text{\AA}^2\times 10^3$ ) for JPM\_355B.

Atom	<i>x</i>	<i>y</i>	<i>z</i>	U(eq)
H1	6.63	4223.06	2328.94	19
H2A	3242.53	5144.94	2790.46	22
H2B	2815.13	4275.91	2802	22
H3A	2649.6	3998.2	1562.15	23
H3B	4172.95	4676.01	1779.17	23
H4	1554.38	4758.25	795.89	20
H5A	-995.52	5344.28	2742.3	22
H5B	895.64	5746.01	2997.68	22
H7	-3115.16	4465.73	2851.35	28
H8	-5101.84	3375.98	2482.32	33
H9	-4672.57	2310.42	3014.11	39
H10	-2278.86	2334.33	3907.33	42
H11	-225.39	3396.38	4237.78	36
H13	1304.09	6367.55	1859.55	22
H15	5010.43	7716.95	1268.45	24
H17	4530.33	5485.56	769.8	21
H21	-3050.76	3369.35	1481.96	27
H22	-3121.34	2103.31	1134.08	32
H24	-180.25	2575.62	-289.51	30
H25	-160.3	3837.95	22.48	25
H26A	-856.91	1308.3	-130.9	61
H26B	-2787.54	1152.64	-108.7	61
H26C	-1407.59	1140.28	597.83	61
H101	8073.65	7446.76	4233.79	19
H10A	10327.12	7020.78	3888.98	24
H10B	10338.95	7526.35	3260.37	24
H10C	12516.6	8193.52	4178.14	23
H10D	11510.91	8023.44	4798.09	23
H104	10850.79	9171.91	4649.43	20
H10E	7457.48	7591.72	2720.19	23
H10F	6059.96	7657.14	3185.05	23
H107	3581.25	6790.92	3606.65	25
H108	2633.05	6691.32	4683.2	26
H109	4047.63	6088.07	5578.03	27
H110	6468.27	5617.79	5408.06	28
H111	7441.42	5722.78	4338.55	27
H113	8776.79	8982.78	2854.39	23
H115	12395.83	10212.39	2097.92	29
H117	13480.92	9583.8	4098.29	24
H121	6300.19	7662.7	5244.49	26
H122	7151.17	7248.21	6362.02	31
H124	10988.69	8980.9	6947.55	28
H125	10189.57	9387.9	5823.13	23

H12A	9997.91	8217.82	7885.74	58
H12B	10679.94	7558.88	7484.15	58
H12C	8799.1	7449.95	7585.52	58
H20A	2190.58	10737.7	276.75	192
H20B	3791.91	11262.78	170.08	192

## 5. References

1. M. Yan, Y. Kawamata and P. S. Baran, *Chem. Rev.*, 2017, **117**, 13230-13319.
2. E. J. Horn, B. R. Rosen and P. S. Baran, *ACS Cent. Sci.*, 2016, **2**, 302-308.
3. C. Kingston, M. D. Palkowitz, Y. Takahira, J. C. Vantourout, B. K. Peters, Y. Kawamata and P. S. Baran, *Acc. Chem. Res.*, 2020, **53**, 72-83.
4. G. Hilt, *ChemElectroChem*, 2019, **7**, 395-405.
5. C. Sandford, M. A. Edwards, K. J. Klunder, D. P. Hickey, M. Li, K. Barman, M. S. Sigman, H. S. White and S. D. Minter, *Chem. Sci.*, 2019, **10**, 6404-6422.
6. H. C. Xu and K. D. Moeller, *J. Am. Chem. Soc.*, 2008, **130**, 13542-13543.
7. H. C. Xu and K. D. Moeller, *J. Am. Chem. Soc.*, 2010, **132**, 2839-2844.
8. H. C. Xu and K. D. Moeller, *Org. Lett.*, 2010, **12**, 1720-1723.
9. Y. Ashikari, A. Shimizu, T. Nokami and J. Yoshida, *J. Am. Chem. Soc.*, 2013, **135**, 16070-16073.
10. Y. Ashikari, T. Nokami and J. I. Yoshida, *Org. Biomol. Chem.*, 2013, **11**, 3322-3331.
11. A. Feula, L. Male and J. S. Fossey, *Org. Lett.*, 2010, **12**, 5044-5047.
12. A. Feula, S. S. Dhillon, R. Byravan, M. Sangha, R. Ebanks, M. A. Hama Salih, N. Spencer, L. Male, I. Magyary, W. P. Deng, F. Müller and J. S. Fossey, *Org. Biomol. Chem.*, 2013, **11**, 5083-5093.
13. B. Elsler, D. Schollmeyer, K. M. Dyballa, R. Franke and S. R. Waldvogel, *Angew. Chem. Int. Ed.*, 2014, **53**, 5210-5213.
14. B. R. Rosen, E. W. Werner, A. G. O'Brien and P. S. Baran, *J. Am. Chem. Soc.*, 2014, **136**, 5571-5574.
15. M. Faraday, *Philos. Trans.*, 1834, 77-122.
16. H. Lund, *J. Electrochem. Soc.*, 2002, **149**.
17. H. Kolbe, *Ann. Chem. Pharm.*, 1849, **69**, 257-294.
18. Z. Wang, in *Comprehensive Organic Name Reactions and Reagents*, John Wiley & Sons, Inc., 2010, pp. 1656-1660.
19. A. Wurtz, *Ann. Chim. Phys.*, 1855, **44**, 291-291.
20. H. Hofer and M. Moest, *Ann. Chem.*, 1902, **323**, 284-284.
21. N. Elgrishi, K. J. Rountree, B. D. McCarthy, E. S. Rountree, T. T. Eisenhart and J. L. Dempsey, *J. Chem. Educ.*, 2018, **95**, 197-206.
22. P. Xiong and H. C. Xu, *Acc. Chem. Res.*, 2019, **52**, 3339-3350.
23. J. B. Sperry and D. L. Wright, *Chem. Soc. Rev.*, 2006, **35**, 605-621.
24. D. Pletcher, R. A. Green and R. C. D. Brown, *Chem. Rev.*, 2018, **118**, 4573-4591.
25. G. Laudadio, E. Barmopoulos, C. Schotten, L. Struik, S. Govaerts, D. L. Browne and T. Noël, *J. Am. Chem. Soc.*, 2019, **141**, 5664-5668.
26. M. Selt, R. Franke and S. R. Waldvogel, *Org. Process Res. Dev.*, 2020, **24**, 2347-2355.
27. *ChemViews Magazine*, 24 August 2017, DOI: 10.1002/chemv.201700062.
28. M. Yan, Y. Kawamata and P. S. Baran, *Angew. Chem. Int. Ed.*, 2018, **57**, 4149-4155.
29. C. Schotten, T. P. Nicholls, R. A. Bourne, N. Kapur, B. N. Nguyen and C. E. Willans, *Green Chemistry*, 2020, **22**, 3358-3375.
30. IKA ElectraSyn 2.0. Package, <https://www.ika.com/en/Products-Lab-Eq/Electrochemistry-Kit-csp-516/ElectraSyn-20-Package-cpdt-20008980/>, (accessed 18th January 2021).
31. IKA Carousel complete, <https://www.ika.com/en/Products-Lab-Eq/Electrochemistry-Kit-csp-516/IKA-Carousel-complete-cpdt-40005427/>, (accessed 18th January 2021).
32. IKA e-Hive, <https://www.ika.com/en/Products-Lab-Eq/Electrochemistry-Kit-csp-516/IKA-e-Hive-cpdt-40004945/>, (accessed 18th January 2021).
33. IKA Pro-Divide, <https://www.ika.com/en/Products-Lab-Eq/Electrochemistry-Kit-csp-516/IKA-Pro-Divide-cpdt-40006482/>, (accessed 29th January 2021).
34. C. G. W. van Melis, M. R. Penny, A. D. Garcia, A. Petti, A. P. Dobbs, S. T. Hilton and K. Lam, *ChemElectroChem*, 2019, **6**, 4144-4148.
35. Vial 20ml, Complete, <https://www.ika.com/en/Products-Lab-Eq/Electrochemistry-Kit-csp-516/Vial-20ml-complete-cpdt-40003168/>, (accessed 22nd April 2021).
36. D. M. Heard and A. J. J. Lennox, *Angew. Chem. Int. Ed.*, 2020, **59**, 18866-18884.



37. IKA CV Package, <https://www.ika.com/en/Products-Lab-Eq/Electrochemistry-Kit-csp-516/CV-Package-cpdt-40002864/>, (accessed 25th January 2021).
38. G. Kreysa, K.-i. Ota and R. F. Savinell, *Encyclopedia of Applied Electrochemistry*, 2014.
39. A. J. Bard and L. R. Faulkner, *Electrochemical Methods: Fundamentals and Applications*, Wiley, 2000.
40. IKA Overpotentials, <https://www.ika.com/electrasyn/Practical-tips.html#Overpotentials>, (accessed 23 April, 2020).
41. T. Shono, in *Comprehensive Organic Synthesis*, Pergamon Press, 1991, DOI: 10.1016/b978-0-08-052349-1.00213-4, pp. 789-813.
42. M. Hayyan, F. S. Mjalli, M. A. Hashim, I. M. AlNashef and T. X. Mei, *Journal of Industrial and Engineering Chemistry*, 2013, **19**, 106-112.
43. S. Bornemann and S. T. Handy, *Molecules*, 2011, **16**, 5963-5974.
44. X.-J. Meng, Y.-Z. Pan, S.-K. Mo, H.-S. Wang, H.-T. Tang and Y.-M. Pan, *Org. Chem. Front.*, 2020, **7**, 2399-2404.
45. A. M. Jones and C. E. Banks, *Beilstein J. Org. Chem.*, 2014, **10**, 3056-3072.
46. T. Shono, Y. Matsumura and K. Tsubata, *Org. Synth.*, 1990, **7**, 206-206.
47. N. Tanbouza, T. Ollevier and K. Lam, *iScience*, 2020, **23**, 101720.
48. R. J. Palmer, in *Encyclopedia of Polymer Science and Technology*, John Wiley & Sons, DOI: <https://doi.org/10.1002/0471440264.pst251>, pp. 618 - 643.
49. D. E. Blanco, B. Lee and M. A. Modestino, *Proc. Natl. Acad. Sci. U.S.A.*, 2019, **116**, 17683-17689.
50. D. E. Blanco, A. Z. Dookhith and M. A. Modestino, *React. Chem. Eng.*, 2019, **4**, 8-16.
51. D. S. P. Cardoso, B. Šljukić, D. M. F. Santos and C. A. C. Sequeira, *Org. Process Res. Dev.*, 2017, **21**, 1213-1226.
52. C. A. C. Sequeira and D. M. F. Santos, *J. Braz. Chem. Soc.*, 2009, **20**, 387-406.
53. H. J. Schäfer, *C. R. Chim.*, 2011, **14**, 745-765.
54. The Nobel Prize in Chemistry 1906, <https://www.nobelprize.org/prizes/chemistry/1906/summary/>, (accessed 20th September 2020).
55. A. Tressaud, *Angew. Chem. Int. Ed.*, 2006, **45**, 6792-6796.
56. S. Schneider and K. Christe, Fluorine, <https://www.britannica.com/science/fluorine>.
57. N. V. Ignat'ev, U. Welz-Biermann, U. Heider, A. Kucheryna, S. von Ahsen, W. Habel, P. Sartori and H. Willner, *J. Fluorine Chem.*, 2003, **124**, 21-37.
58. G. W. Gribble, *Organofluorines*, 2006, **3**, 121-136.
59. B. E. Smart, *J. Fluorine Chem.*, 2001, **109**, 3-11.
60. N. V. Ignat'ev, in *Modern Synthesis Processes and Reactivity of Fluorinated Compounds*, 2017, DOI: doi.org/10.1016/b978-0-12-803740-9.00004-4, pp. 71-123.
61. J. H. Simons, *J. Electrochem. Soc.*, 1949, **95**, 47-52.
62. L. Conte and G. P. Gambaretto, *J. Fluorine Chem.*, 2004, **125**, 139-144.
63. M. Tokuda, Y. Yamada, T. Takagi and H. Suginome, *Tetrahedron Lett.*, 1985, **26**, 6085-6088.
64. M. Tokuda, H. Fujita, T. Miyamoto and H. Suginome, *Tetrahedron*, 1993, **49**, 2413-2426.
65. T. Shono, Y. Matsumura, S. Katoh, K. Inoue and Y. Matsumoto, *Tetrahedron Lett.*, 1986, **27**, 6083-6086.
66. H. C. Xu, J. D. Brandt and K. D. Moeller, *Tetrahedron Lett.*, 2008, **49**, 3868-3871.
67. Y. Sun, B. Liu, J. Kao, D. Andre' D'Avignon and K. D. Moeller, *Org. Lett.*, 2001, **3**, 1729-1732.
68. J. D. Brandt and K. D. Moeller, *Org. Lett.*, 2005, **7**, 3553-3556.
69. L. Becking and H. J. Schäfer, *Tetrahedron Lett.*, 1988, **29**, 2797-2800.
70. M. Huhtasaari, H. J. Schäfer and L. Becking, *Angew. Chem. Int. Ed.*, 1984, **23**, 980-981.
71. J. Weiguny and H. J. Schäfer, *J. Liebigs Ann. Chem.*, 1994, **1994**, 235-242.
72. T. Shono, Y. Matsumura, S. Katoh and J. Ohshita, *Chem. Lett.*, 1988, **17**, 1065-1068.
73. N. Kise, H. Ozaki, N. Moriyama, Y. Kitagishi and N. Ueda, *J. Am. Chem. Soc.*, 2003, **125**, 11591-11596.
74. A. Feula and J. S. Fossey, *RSC Adv.*, 2013, **3**, 5370-5373.
75. A. Leung and L. Braverman, *Nat. Rev. Endocrinol.*, 2014, **10**, 136-142.

76. L. G. Abood, X. Lu and S. Banerjee, *Biochem. Pharmacol.*, 1987, **36**, 2337-2341.
77. J. F. Schneider, C. L. Ladd and S. Bräse, *Chapter 5. Proline as an Asymmetric Organocatalyst*, 2015.
78. L. Fowden, *Nature*, 1955, **176**, 347-348.
79. T. Takemoto, K. Nomoto, S. Fushiya, R. Ouchi, G. Kusano, H. Hiking, S.-i. Takagi, Y. Matsuura and M. Kakud, *Proc. Jpn. Acad., Ser. B, Phys. Biol. Sci.*, 1978, **54**, 469-473.
80. J. Kobayashi, J.-F. Cheng, M. Ishibashi, M. R. Wälschli, S. Yamamura and Y. Ohizumi, *J. Chem. Soc., Perkin Trans. 1*, 1991, 1135-1137.
81. B. Drouillat, I. V. Dorogan, M. Kletschii, O. N. Burov and F. Couty, *J. Org. Chem.*, 2016, **81**, 6677-6685.
82. L. Reisman, E. A. Rowe, J. A. Jefcoat and P. A. Rupar, *ACS Macro Lett.*, 2020, **9**, 334-338.
83. J. P. Milton and J. S. Fossey, *Tetrahedron*, 2021, **77**, 131767.
84. X. J. Meng, P. F. Zhong, Y. M. Wang, H. S. Wang, H. T. Tang and Y. M. Pan, *Adv. Synth. Catal.*, 2020, **362**, 506-511.
85. P. Röse, S. Emge, J. I. Yoshida and G. Hilt, *Beilstein J. Org. Chem.*, 2015, **11**, 174-183.
86. K. Uneyama, S. Fujibayashi and S. Torii, *Tetrahedron Lett.*, 1985, **26**, 4637-4638.
87. S. Konstantinović, R. Vukićević and M. L. Mihailović, *Tetrahedron Lett.*, 1987, **28**, 6511-6512.
88. R. Vukićević, S. Konstantinović and M. L. Mihailović, *Tetrahedron Lett.*, 1991, **47**, 859-865.
89. Platinum plated, Set of 2, <https://www.ika.com/en/Products-Lab-Eq/Electrochemistry-Kit-csp-516/Platinum-plated,-Set-of-2-cpdt-40002852/>, (accessed 6th January 2021).
90. J. B. Feltenberger, R. Hayashi, Y. Tang, E. S. C. Babiash and R. P. Hsung, *Org. Lett.*, 2009, **11**, 3666-3669.
91. X. Xiao, W. Zhang, X. Lu, Y. Deng, H. Jiang and W. Zeng, *Adv. Synth. Catal.*, 2016, **358**, 2497-2509.
92. K. Thai, L. Wang, T. Dudding, F. Bilodeau and M. Gravel, *Org. Lett.*, 2010, **12**, 5708-5711.
93. J. F. Teichert, S. Zhang, A. W. v. Zijl, J. W. Slaa, A. J. Minnaard and B. L. Feringa, *Org. Lett.*, 2010, **12**, 4658-4660.
94. I. Cheng-Sánchez, P. Carrillo, A. Sánchez-Ruiz, B. Martínez-Poveda, A. R. Quesada, M. A. Medina, J. M. López-Romero and F. Sarabia, *J. Org. Chem.*, 2018, **83**, 5365-5383.
95. H. Yamamoto, E. Ho, K. Namba, H. Imagawa and M. Nishizawa, *Chem. Eur. J.*, 2010, **16**, 11271-11274.
96. J. E. Baldwin, *J.C.S. Chem. Comm.*, 1976, 734-736.
97. Y. Zhao, J. Li, H. Gu, D. Wei, Y.-c. Xu, W. Fu and Z. Yu, *Interdiscip. Sci.*, 2015, **7**, 211-220.
98. F. A. Cotton and P. F. Stokely, *J. Am. Chem. Soc.*, 1970, **92**, 294 - 302.
99. H. P. Klug, *Acta Crystallogr., Sect. B: Struct. Sci., Cryst. Eng. Mater.*, 1968, **B24**, 792-802.
100. T. Jordan, H. W. Smith, L. L. Lohr and W. N. Lipscomb, *J. Am. Chem. Soc.*, 1963, **85**, 846-851.
101. R. G. Laughlin and W. Yellin, *J. Am. Chem. Soc.*, 1967, **89**, 2435-2443.
102. R. G. Laughlin, *J. Am. Chem. Soc.*, 1968, **90**, 2651-2656.
103. K. Hatada and T. Kitayama, in *NMR Spectroscopy of Polymers*, Springer, 2004, DOI: [https://doi.org/10.1007/978-3-662-08982-8\\_1](https://doi.org/10.1007/978-3-662-08982-8_1), pp. 1 - 42.
104. I. Colomer, A. E. R. Chamberlain, M. B. Haughey and T. J. Donohoe, *Nat. Rev. Chem.*, 2017, **1**, 0088.
105. E. Duñach, A. P. Esteves, M. J. Medeiros, C. S. dos Santos Neves and S. Olivero, *C. R. Chim*, 2009, **12**, 889-894.
106. L. P. Hammett, *J. Am. Chem. Soc.*, 1937, **59**, 96-103.
107. S. Torii, K. Uneyama, M. Ono and T. Bannou, *J. Am. Chem. Soc.*, 1981, **103**, 4606-4608.
108. D. L. J. Clive and C. G. Russell, *Tetrahedron*, 1980, **36**, 1399-1408.
109. B. Berthe, F. Outurquin and C. Paulmier, *Tetrahedron Lett.*, 1997, **38**, 1393-1396.
110. M. A. Cooper and A. D. Ward, *Aust. J. Chem.*, 1997, **50**, 181-187.
111. F. Outurquin, X. Pannecoucke, B. Berthe and C. Paulmier, *Eur. J. Org. Chem.*, 2002, 1007-1014.
112. K. J. Fraunhofer and M. C. White, *J. Am. Chem. Soc.*, 2007, **129**, 7274-7276.
113. B. Nyasse, L. Grehn and U. Ragnarsson, *Chem. Commun.*, 1997, 1017-1018.
114. S. J. Veenstra and P. Schmid, *Tetrahedron Lett.*, 1997, **38**, 997-1000.

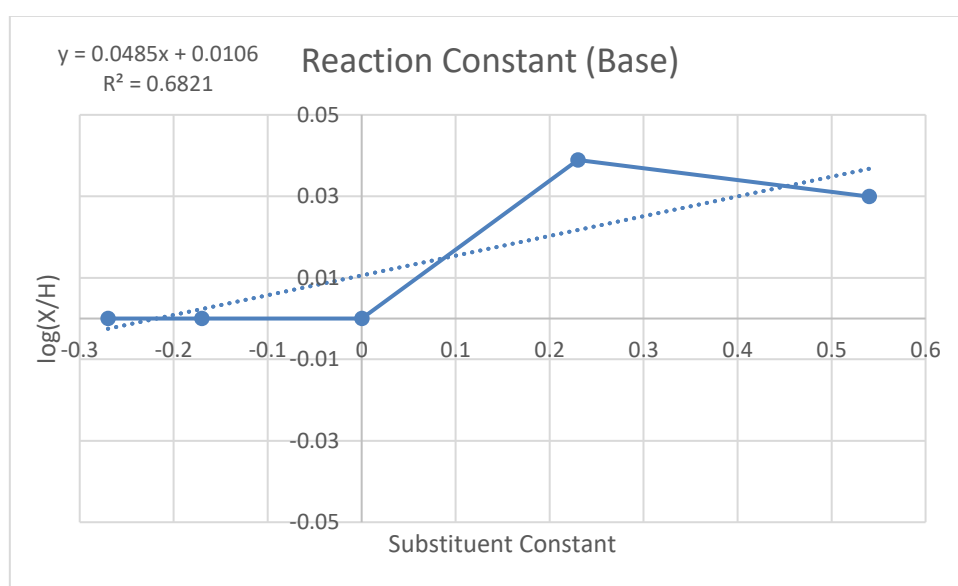
115. L. A. Wessjohann and U. Sinks, *Journal für Praktische Chemie/Chemiker-Zeitung*, 1998, **340**, 189-203.
116. J. E. Spallholz, *Free Radic. Biol. Med.*, 1994, **17**, 45-64.
117. J. A. Wiles, A. S. Phadke, B. J. Bradbury, M. J. Pucci, J. A. Thanassi and M. Deshpande, *J. Med. Chem.*, 2011, **54**, 3418-3425.
118. B. E. Haskell and S. B. Bowlus, *J. Org. Chem.*, 1976, **41**, 159-160.
119. E. Vedejs and S. Lin, *J. Org. Chem.*, 1994, **59**, 1602-1603.
120. R. C. Roemmele and H. Rapoport, *J. Org. Chem.*, 1988, **53**, 2367-2371.
121. O. Scialdone, C. Belfiore, G. Filardo, A. Galia, M. A. Sabatino and G. Silvestri, *Electrochim. Acta*, 2005, **51**, 598-604.
122. H. Senboku, K. Nakahara, T. Fukuhara and S. Hara, *Tetrahedron Lett.*, 2010, **51**, 435-438.
123. X. Pannecoucke, F. Outurquin and C. Paulmier, *Eur. J. Org. Chem.*, 2002, 995-1006.
124. W. E. Brenzovich, Jr., D. Benitez, A. D. Lackner, H. P. Shunatona, E. Tkatchouk, W. A. Goddard, 3rd and F. D. Toste, *Angew. Chem. Int. Ed.*, 2010, **49**, 5519-5522.
125. L. J. Peterson and J. P. Wolfe, *Adv. Synth. Catal.*, 2015, **357**, 2339-2344.
126. B. M. Trost, C. I. Hung and G. Mata, *Angew. Chem. Int. Ed.*, 2020, **59**, 4240-4261.
127. M.-C. Wang, Q.-J. Zhang, W.-X. Zhao, X.-D. Wang, X. Ding, T.-T. Jing and M.-P. Song, *J. Org. Chem.*, 2008, **73**, 168-176.
128. A. Yoshizawa, A. Feula, L. Male, A. G. Leach and J. S. Fossey, *Sci. Rep.*, 2018, **8**, 1-16.
129. D. Li, K. Wang, L. Wang, Y. Wang, P. Wang, X. Liu, D. Yang and R. Wang, *Org. Lett.*, 2017, **19**, 3211-3214.
130. A. Russo and A. Lattanzi, *Eur. J. Org. Chem.*, 2008, **2008**, 2767-2773.
131. D. G. Stark, T. J. C. O'Riordan and A. D. Smith, *Org. Lett.*, 2014, **16**, 6496-6499.
132. S. Barrett, P. O'Brien, H. C. Steffens, T. D. Towers and M. Voith, *Tetrahedron*, 2000, **56**, 9633-9640.
133. J. R. Henry, L. R. Marcin and M. C. McIntosh, *Tetrahedron Lett.*, 1989, **30**, 5709-5712.
134. D. Stead, *Tetrahedron Lett.*, 2020, **61**, 152325.
135. B. G. Reed-Berendt and L. C. Morrill, *J. Org. Chem.*, 2019, **84**, 3715-3724.
136. D. Huang, X. Wang, X. Wang, W. Chen, X. Wang and Y. Hu, *Org. Lett.*, 2016, **18**, 604-607.
137. G. Zhang, L. Cui, Y. Wang and L. Zhang, *J. Am. Chem. Soc.*, 2010, **132**, 1474-1475.
138. T. Wirth and N. Amri, *Synthesis*, 2020, **52**, 1751-1761.
139. X. Qi, F. Yu, P. Chen and G. Liu, *Angew. Chem. Int. Ed.*, 2017, **56**, 12692-12696.
140. J. Cui, Q. Jia, R.-Z. Feng, S.-S. Liu, T. He and C. Zhang, *Org. Lett.*, 2014, **16**, 1442-1445.
141. G. Fang, Z. Liu, S. Cao, H. Yuan, J. Zhang and L. Pan, *Org. Lett.*, 2018, **20**, 7113-7116.
142. L. J. Peterson, J. Luo and J. P. Wolfe, *Org. Lett.*, 2017, **19**, 2817-2820.
143. J. Caputo, M. Naodovic and D. Weix, *Synlett*, 2015, **26**, 323-326.
144. CrysAlisPro, Agilent Technologies, Version 1.171.36.28, 2013).
145. G. M. Sheldrick, *Acta Crystallogr., Sect. A: Found. Crystallogr.*, 2015, **71**, 3-8.
146. G. M. Sheldrick, *Acta Crystallogr., Sect. C: Cryst. Struct. Commun.*, 2015, **71**, 3-8.
147. O. V. Dolomanov, L. J. Bourhis, R. J. Gildea, J. A. K. Howard and H. Puschmann, *J. Appl. Crystallogr.*, 2009, **42**, 339-341.

## 6. Appendices

### 6.1. Appendix 1 – Hammett Plots

#### Hammett Plot for the electrochemical cyclisation under basic conditions

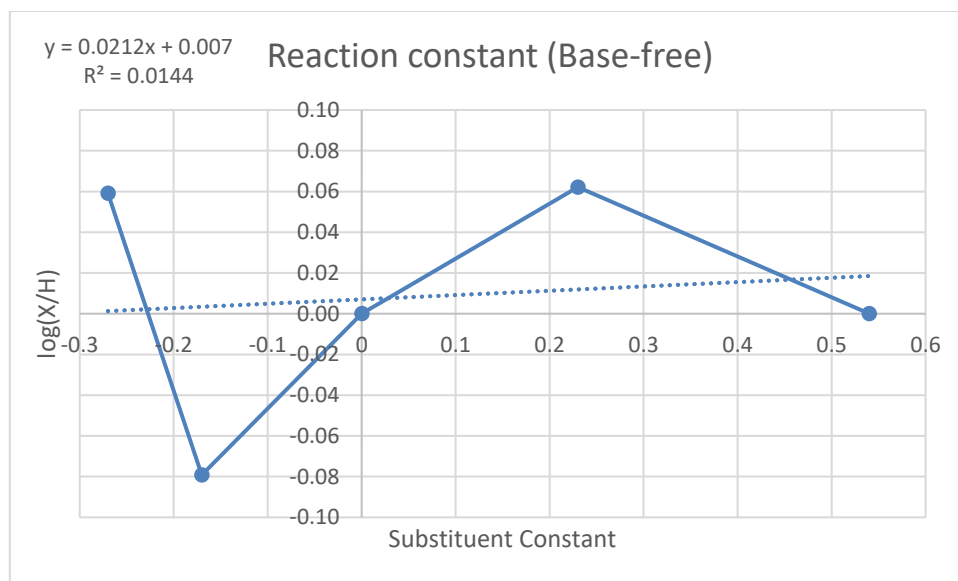
Substituent	<i>p</i> -OMe	<i>p</i> -Me	<i>p</i> -H	<i>p</i> -Br	<i>p</i> -CF <sub>3</sub>
% of <i>trans</i>	80.00	80.00	80.00	87.50	85.71
log(X/H)	0.00	0.00	0.00	0.04	0.03
Sub. Constant	-0.27	-0.17	0	0.23	0.54



$$\rho = 0.05$$

#### Hammett Plot for the electrochemical cyclisation under base-free conditions

Substituent	<i>p</i> -OMe	<i>p</i> -Me	<i>p</i> -H	<i>p</i> -Br	<i>p</i> -CF <sub>3</sub>
% of <i>cis</i>	91.67	66.67	80.00	92.31	80.00
log(X/H)	0.06	-0.08	0.00	0.06	0.00
Sub. Constant	-0.27	-0.17	0	0.23	0.54



$$\rho = 0.02$$

## 6.2. Appendix 2 – Green Copy of Review Article

Pre-peer review version (“green copy”) of “Azetidines and their applications in asymmetric catalysis”. Compound numbers, schemes, figures and references are to be treated separate from the thesis. The published article is available at [doi.org/10.1016/j.tet.2020.131767](https://doi.org/10.1016/j.tet.2020.131767) in the journal *Tetrahedron*.

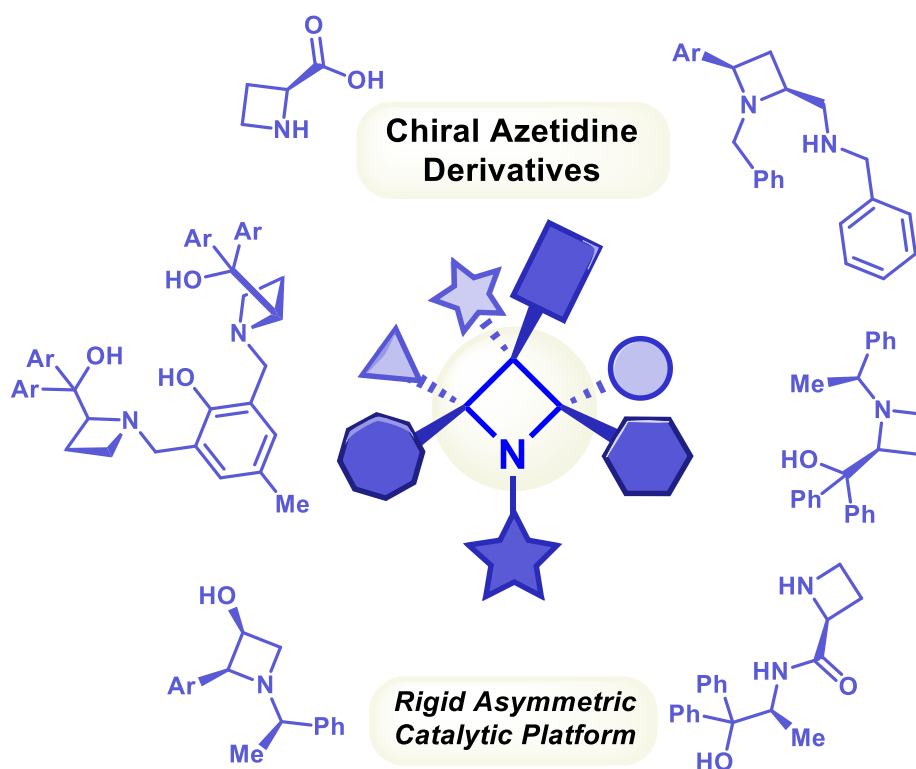
# Azetidines and their applications in asymmetric catalysis

Joseph P. Milton <sup>(a)\*</sup> and John S. Fossey <sup>(a)</sup>

<sup>(a)</sup> School of Chemistry, University of Birmingham, Edgbaston,  
Birmingham, West Midlands, B15 2TT, UK

**Keywords:** azetidines; asymmetric catalysis; pyrrolidines; aziridines; AzePhenol; ProPhenol.

## Abstract:



Since the early 1990s asymmetric catalytic applications of chiral, azetidine-derived, ligands and organocatalysts have been developed and utilised to engender asymmetry in reactions including Friedel-Crafts alkylations, Henry reactions and Michael-type reactions. This review surveys the effective synthetic opportunities presented by chiral azetidines in asymmetric catalysis. In order to benchmark, contrast and evaluate these asymmetric azetidine-containing catalysts, comparisons with aziridine- and pyrrolidine-containing analogues are drawn.

## Author Profiles:



**Figure 1:** Co-authors Joseph P. Milton (left) and John S. Fossey (right)

**Joseph P. Milton** was born in Somerset, England in 1998. After receiving a BSc in Chemistry from the University of Birmingham, he is currently undertaking an MSc by Research at the same university in the group of Prof. John S. Fossey. His current research focuses on the synthesis of azetidines and pyrrolidines *via* electrochemical methodology.

**John S. Fossey** obtained an MChem degree from Cardiff University and a PhD from Queen Mary University of London. After stints at the University of Tokyo and the University of Bath he joined the University of Birmingham in 2008 for his first permanent academic position as a Lecturer and where he is now Professor of Synthetic Chemistry. His research interests lie at the interface of catalysis and sensing and has recently begun to develop medicinal chemistry aspects of research.

## 1. Introduction

The ability to control the stereochemistry of a chemical reaction is crucial for the successful and efficient synthesis of many useful molecular products.<sup>1</sup> This is imperative in drug design where different stereoisomers can exhibit significantly different pharmacokinetic properties<sup>2</sup> hence, a large portion of drugs are synthesised as single stereoisomers.<sup>3</sup> The continuous development of new asymmetric methods is vital, among them asymmetric catalysis represents the fulcrum of the synthetic approaches for exquisite facilitation and control of chiral reaction outcomes.<sup>4</sup>

Five-membered heterocyclic structures are a mainstay in asymmetric catalyst design and have been incorporated in a wide range of chiral ligands. Oxazolines are among the most widely known nitrogen-containing heterocyclic ligand motifs for coordination to a catalytically active metal centre.<sup>5</sup> Evans'<sup>6-8</sup> and Corey's<sup>9</sup> BOX ligands (**1** and **2**)<sup>10</sup> in conjunction with a diverse collection of ligands including PHOX (**3**)<sup>11-13</sup> and TRISOX (**4**)<sup>14</sup> have contributed to setting benchmarks in the field of metal-mediated catalysis (Figure 2, upper). Metal-free asymmetric catalysts comprised of five-membered nitrogen-containing heterocyclic core components have been crucial in the development of organocatalysis.<sup>15</sup>

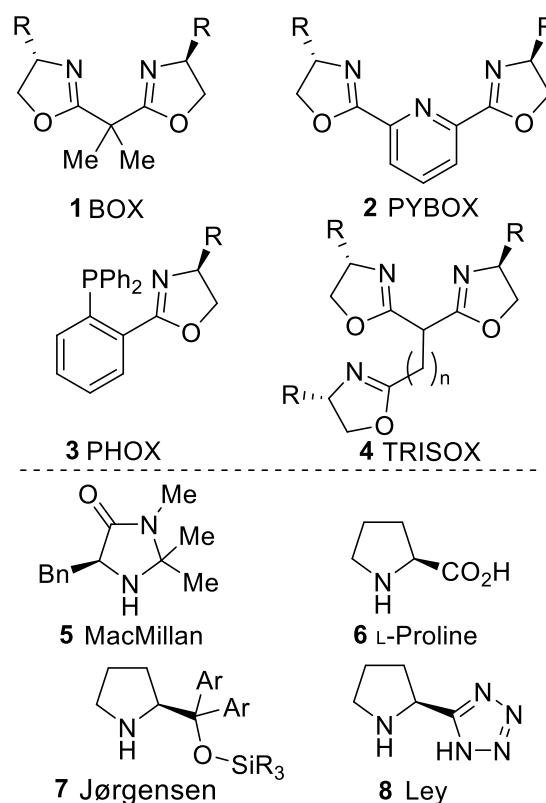


**Figure 2:** Prominent five-membered chiral heterocyclic ligands [Upper: BOX (1), PYBOX (2), PHOX (3) and TRISOX (4)] and organocatalysts [Lower: MacMillan's catalyst (5), L-proline (6) and derivatives from Jørgensen (7) and Ley (8)]

Imidazolidinone derivatives of MacMillan and co-workers (5)<sup>16</sup> along with proline derivatives (6)<sup>17,18</sup> and analogues, such as those of Jørgensen (7),<sup>19</sup> Ley (8)<sup>20</sup> and their respective co-workers have played an important role in developing organocatalysis to the relatively mature discipline it is today (Figure 2, lower).

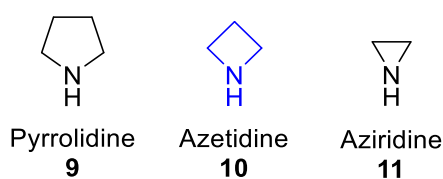


**Figure 3.** Saturated nitrogen-containing heterocycles: Pyrrolidine (9), Azetidine (10) and aziridine (11)

Whilst five-membered nitrogen-containing heterocycles, such as those based on pyrrolidine (9) cores are extensively studied, derivatives of azetidine (10), saturated four-membered nitrogen-containing heterocycles, are under reported in comparison, as well as its three-membered congener, aziridine (11), Figure 3. This is often attributed to the difficulty of synthesising such four-membered rings,<sup>21,22</sup> despite this obstacle though, derivatives of 10 hold their own place as potent pharmaceutical motifs<sup>23-25</sup> and are present in alkaloids and pharmaceuticals, Figure 4. Calblock (12) and Exanta (13) are commercially available drugs that exhibit an azetidine moiety within their structure and behave as a calcium channel blocker<sup>26</sup> and a thrombin inhibitor respectively.<sup>27</sup> Azetidine-containing alkaloids penaresidin A and B (14) have been shown to increase the ATPase activity of myofibrils in rabbit



skeletal muscle<sup>28</sup> and mugineic acid (**15**) is a highly relevant species within plants that facilitates iron uptake.<sup>29</sup>

Alongside this, azetidines are versatile building blocks<sup>30,31</sup> and occupy an advantageous position where they may share applications, due to their similarity to derivatives of pyrrolidine and aziridine (**9** and **11** respectively), which allows a range of uses to be compared, contrasted and developed such as ring-opening polymerisation<sup>32</sup> and organocatalysis.<sup>33</sup> Appropriate substitution about the azetidine scaffold grants derivatives of **10** the opportunity to act as efficient chelating ligands and in turn, provide a viable coordination platform for asymmetric metal-complex-catalysed reaction development.<sup>34</sup> This review assesses the application of chiral azetidine derivatives in asymmetric metal-mediated- and organo- catalysis, since its first reported use in 1992 from Behnen *et al.*, whilst comparing derivatives of **9** and **11** where appropriate.

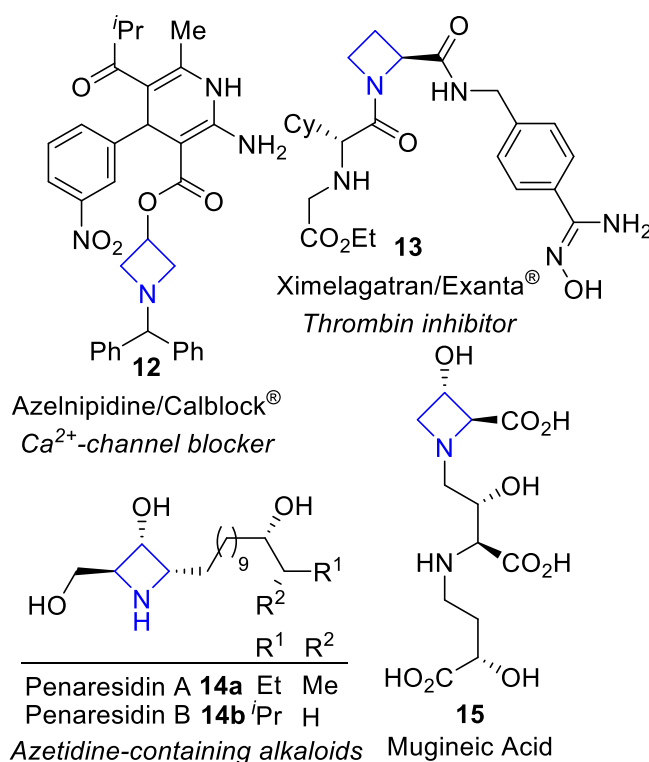


**Figure 4:** Azetidine-containing drugs [Calblock (**12**) and Exanta (**13**)] and alkaloids [Penaresidin family (**14a** and **14b**) and Mugineic Acid (**15**)]

## 2. Asymmetric catalysis utilising chiral azetidines

Catalysis is a core concept of chemistry that underpins many organic processes by allowing a reaction to proceed at an accelerated rate with the use of an additional additive in a substoichiometric amount.<sup>35,36</sup> Asymmetric catalysis builds on this base idea and confers chirality within the catalytic manifold to selectively or preferentially generate a single stereoisomer as the major product of a reaction.<sup>37</sup> Generating asymmetry *via* catalysis provides a flexible approach to designing asymmetric

synthetic routes, allowing one to engender asymmetry wherever necessary at ideally any step. This can be far more beneficial than the traditional chiral pool approach, where one is restricted to a selection of asymmetric starting materials from nature and must build upon this scaffold which may prove inconvenient.<sup>38</sup> Asymmetric catalysis should also be more straightforward to afford the desired enantiomer in comparison to chiral resolution, where separating stereoisomers can prove to be heavily time-consuming and yields are capped to 50% maximum.<sup>39</sup>

The field of applied asymmetric metal-mediated catalysis is dominated by so-called *privileged* ligand structures,<sup>40</sup> which tend to use multiple donor atoms, such as oxygen, nitrogen and phosphorus as coordination sites to create a rigid structure about the catalytic core.<sup>41</sup> With this line of thinking in mind, a myriad of structures are potentially viable as alternatives to the *privileged* ligands with saturated nitrogen-containing heterocycles, such as **9**, **10** and **11**, having great potential. Azetidines are an ideal candidate as a catalytic platform, in that they provide a rigid core due to the restrictive nature of the four-membered ring<sup>34</sup> and natively include a nitrogen atom. Henceforth, the discussion will first address metal-catalysed reactions utilising azetidine-containing ligands followed by an interrogation of their asymmetric organocatalytic capabilities.

## 2.1. Dinuclear zinc AzePhenol complexes as catalysts

In 2000, Trost and Ito reported a novel semi-crown ligand,<sup>42</sup> now coined *ProPhenol*, which comprises of two functionalised pyrrolidine rings attached to a phenolic core, **16**, Figure 5. Addition of diethylzinc followed by concomitant loss of ethane gas affords the complex, **17**; **17** displays two distinct zinc sites, one (upon the loss of ethane) becoming Brønsted basic and the other Lewis acidic, Scheme 1. As such, dinuclear zinc complexes of **16** serve as dual activation mode catalysts<sup>43,44</sup> bringing a nucleophile and an electrophile of a reaction within the chiral coordination sphere of the complex. Dinuclear zinc complexes of the **16** family have been successfully deployed as asymmetric catalysts across a wide variety of reactions such as aldol,<sup>45,46</sup> alkynylation,<sup>47</sup> aza-Henry,<sup>48</sup> Friedel-Crafts<sup>49</sup> and they have been comprehensively reviewed elsewhere.<sup>50</sup>

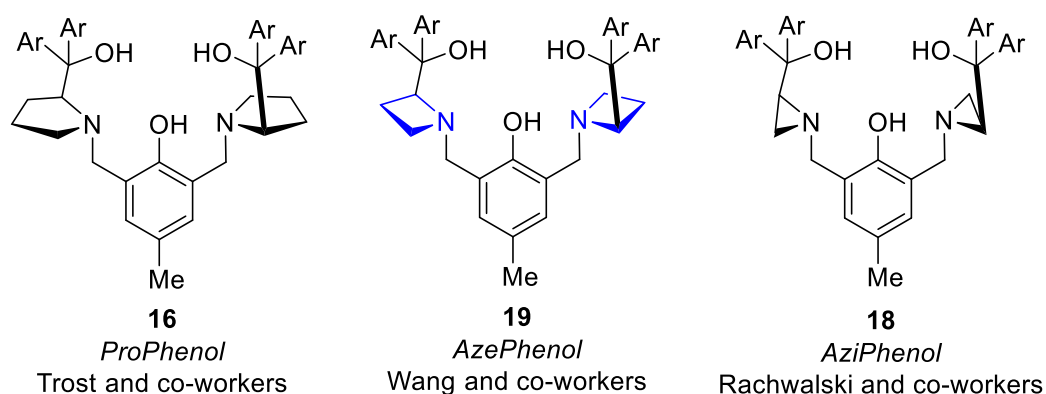
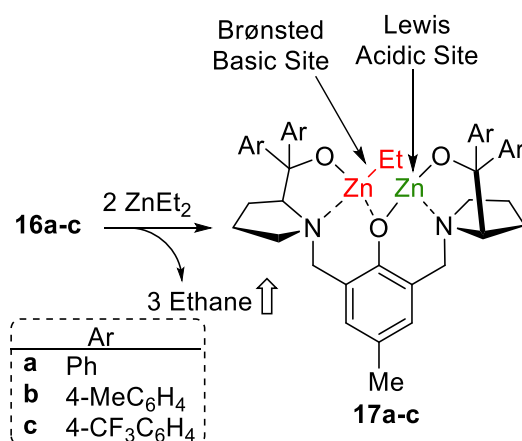
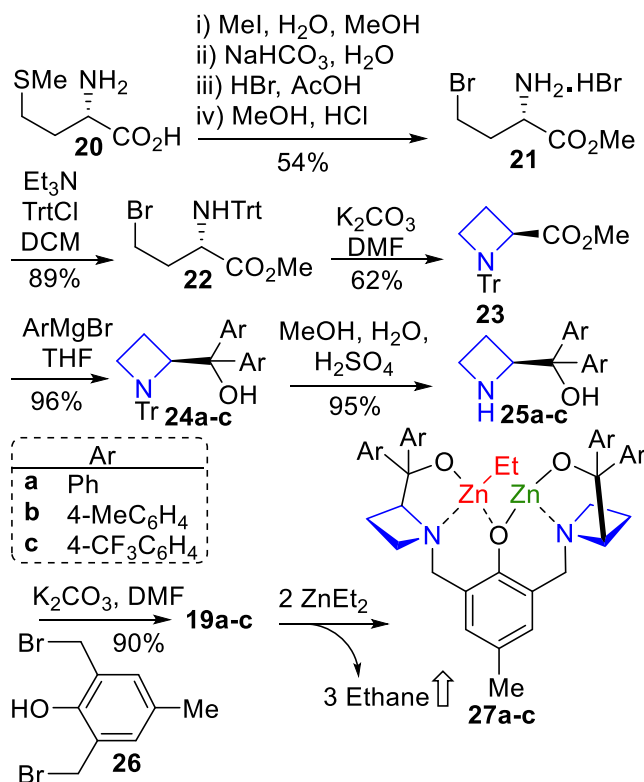


**Figure 5:** Series of bis-*N*-heterocyclic ligands on a phenolic core: *ProPhenol* (**16**), *AzePhenol* (**19**), *AziPhenol* (**18**)



**Scheme 1:** Complexation of *ProPhenol* ligands **16a-c** using diethylzinc to afford dinuclear zinc complex, **17a-c**

From the successful demonstration of dinuclear zinc complexes utilising semi-crown *N*-heterocyclic ligands working effectively and efficiently by Trost and co-workers, analogues of the **16** family have been investigated. Rachwalski and co-workers have developed an aziridine analogue of **16** where the *N*-heterocyclic rings are aziridines (**18**, *AziPhenol*)<sup>51</sup> and more pertinent to this review, the Wang group have developed the azetidine analogue, referred by the term *AzePhenol* (**19**). The Wang group proposed that the *AzePhenol* family of ligands (**19**) should be more effective than the pyrrolidine-derived ligand *ProPhenol* ligands (**16**) because of the smaller ring size, which in turn has a lower flexibility and therefore creates a more sterically hindered microenvironment for the reaction.<sup>52,53</sup>

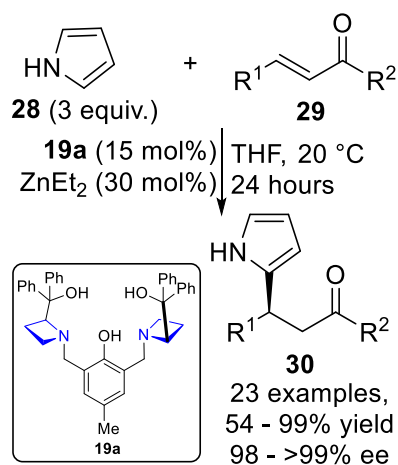


**Scheme 2:** Synthesis of **19a-c** and subsequent complexation *via* the addition of diethylzinc to form **27a-c**

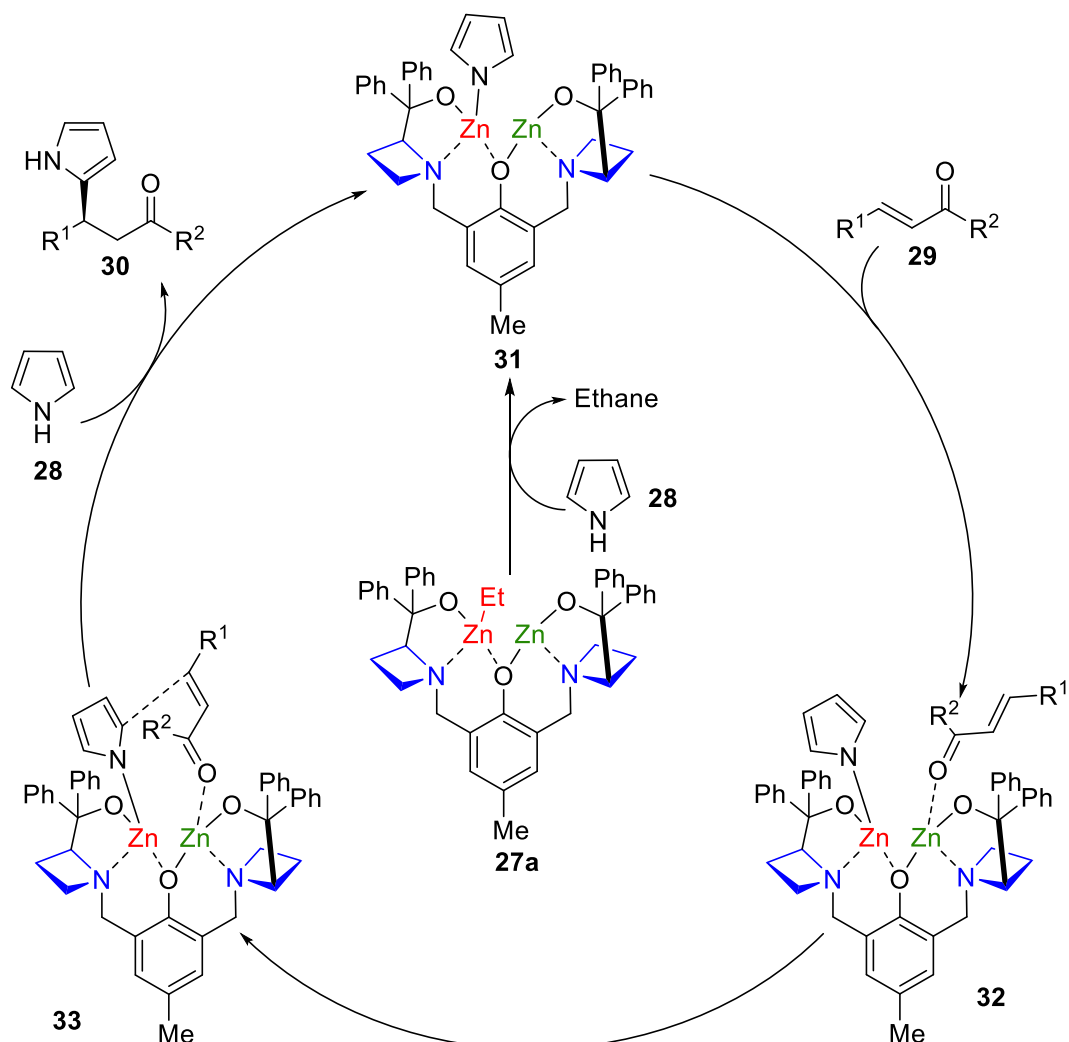
Ligands **19a-c** were synthesised in nine linear steps from L-(+)-methionine (**20**), Scheme 2. Transformation of **20** over 4 steps generated the ammonium salt **21** in 54% yield followed by subsequent trityl protection and benzoylation of methyl (S)-1-tritylazetidine-2-carboxylic acid (**22**) in 89% yield. The key ring-forming step was introduced *via* an intramolecular nucleophilic substitution of **22** generating the trityl protected azetidine (**23**) in 62% yield. Conversion of the methyl ester upon **23** to bisaryl tertiary alcohol units is easily achieved with the addition of aryl Grignard reagents with phenylmagnesium bromide, *p*-tolylmagnesium bromide and (4-(trifluoromethyl)phenyl)magnesium bromide generating **24a**, **24b**, and **24c** respectively in 96% yield. Removal of the trityl protecting group with a methanolic aqueous solution of sulfuric acid afforded N-H functionalized azetidines (**25a-c**) in 95% yield. Two equivalents of an azetidine (**25a-c**) are then attached to the *para*-cresol derivative (**26**) in combination with potassium carbonate in dimethylformamide to afford the corresponding ligand **19a-c**. Complexation with diethylzinc is then achieved in an analogous manner as already demonstrated in Scheme 1.<sup>52</sup>

Comparatively, the bispyrrolidinyl family (**16**) requires only two steps to synthesise compared to the nine steps for the formation of the bisazetidine-derived (**19**) family therefore the azetidine ligand synthesis is inherently more time-consuming. The family of pyrrolidine-containing compounds (**16**) are synthesised from L-proline methyl ester reacting with the *para*-cresol derivative (**26**) followed by subsequent addition of a desired Grignard reagent to afford the tertiary alcohol units.<sup>42</sup> In fact, the bispyrrolidine ligand **16a** (substituted with phenyl groups) is commercially available, allowing ready access for a trial reaction; upon successful deployment of **16a**, further exploration could be undertaken comparing the ProPhenol (**16**) and AzePhenol (**19**) families for the same reaction.

Wang and co-workers have used the AzePhenol family of ligands for zinc-catalysed reactions in many situations, pre-dominantly using the phenyl-containing derivative, **19a**. The following text discusses the reported uses of the AzePhenol ligands in synthesis whilst offering comparisons with Trost and co-worker's pyrrolidine-containing ProPhenol (**16**) ligands where appropriate.



**Scheme 3:** Enantioselective dinuclear zinc-catalysed Friedel-Crafts alkylation of pyrroles and chalcones affording 2-substituted pyrroles

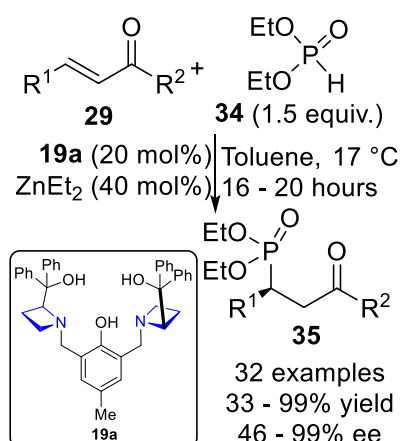


**Scheme 4:** Representative catalytic cycle demonstrating the proposed mechanism of the reaction shown in Scheme 3

A well-exemplified case for the use of dinuclear zinc complexes with bis-azetidyl ligands (**19a**) is the highly stereoselective Friedel-Crafts alkylation of pyrrole (**28**) and chalcones (**29**) affording 2-substituted pyrroles (**30**), Scheme 3. The catalytic cycle, displayed in Scheme 4, demonstrates the use

of the **27a** complex appropriately, where pyrrole (**28**) binds to the Brønsted basic site (**31**) (affording ethane gas) and the chalcone (**29**) binds to the Lewis acidic site (**32**); all other reactions with these catalytic systems react in a homologous manner. After optimisation of the reaction conditions, a wide range of aromatically substituted chalcones (**29**) were shown to react with pyrrole (**28**) in quantitative yields and at least 98% ee; one alkyl substituted chalcone (**29**) was tested and no reaction proceeded.<sup>52</sup> *N*-substituted pyrroles (**28**) produced no reaction indicating that the N-H bond is crucial to activate the reaction, leading to the proposed mechanism with pyrrole (**28**) adding to the Brønsted basic site (**31**), Scheme 4. With  $R^1 = R^2 = \text{Ph}$  (upon **29**), both enantiomers of **30** could be isolated with 99% yield and 99% ee by making use of the ligand **19a** and its enantiomer respectively. Chalcones (**29**) substituted with aromatic rings containing electron-donating groups demonstrated outlying results, such as when 4-methoxyphenyl was used in the 1- or 4-position, no reaction was observed and the use of *ortho*- and *para*-tolyl as substituents achieved noticeably lower yields in comparison to other derivatives of **29**, although they still managed equally as good enantioselectivity (99% ee).<sup>52</sup>

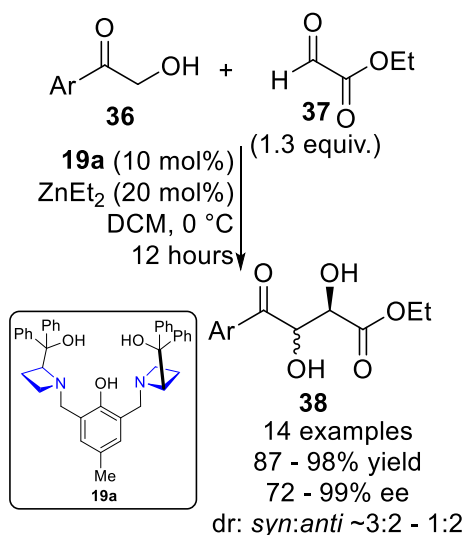
A similar reaction using the bis-pyrrolidine ligand, **16a**, has been demonstrated by Trost and Müller, for the Friedel-Crafts alkylation of pyrroles to nitroalkenes which generated high ee of at least 85% for the majority of substrates.<sup>49</sup> Utilisation of ligand **19a** for the Friedel-Crafts alkylation of indoles has been attempted but the azetidine moiety produces very poor enantioselectivity, as low as 4% ee, in comparison to the ligand **19a** and therefore was not investigated further.<sup>54,55</sup>



**Scheme 5:** Enantioselective dinuclear zinc-catalysed Michael addition of diethylphosphite to aromatically substituted chalcones to afford phosphonate-containing products

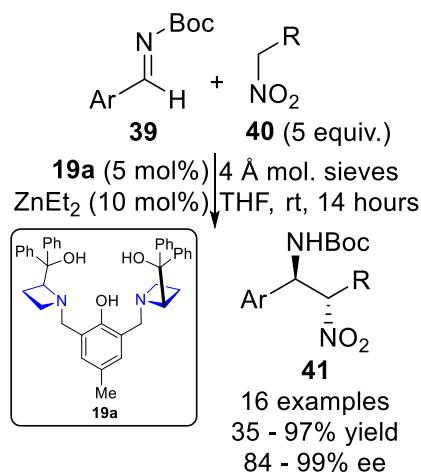
Chalcones (**29**) in combination with the dinuclear zinc complex of **19a** have been utilised for the Michael addition of diethyl phosphite (**34**), Scheme 5. A variety of aromatically substituted chalcones (**29**) were tested for the reaction and generated the phosphonate-containing product (**35**) in both high yields and ee of at least 90% for the majority of substrates; one notable exception was observed where  $R^1 = 3\text{-pyridine}$  (**29**), which saw a large decrease in yield to 48%. The reduced performance was theorised to be from the nitrogen in the heterocycle which poisoned the catalyst and therefore

lowered its efficiency. A related series of  $\alpha,\beta$ -unsaturated *N*-acylpyrroles (i.e. **29** with  $R^2 = N$ -pyrrole) were also tested for the reaction, which resulted in equally high enantioselectivity (90% ee and higher) for most substrates but notably worse yields with the best result of only 69%.<sup>56</sup> A similar phosphamichael reaction has been performed with  $\alpha$ -benzylidene-1-tetralones which demonstrated 99% ee for a wide range of substrates.<sup>57</sup>



**Scheme 6:** Enantioselective dinuclear zinc-catalysed aldol reaction of 2-hydroxyacetophenones and ethyl glyoxalate to afford  $\alpha,\beta$ -dihydroxy  $\gamma$ -keto esters

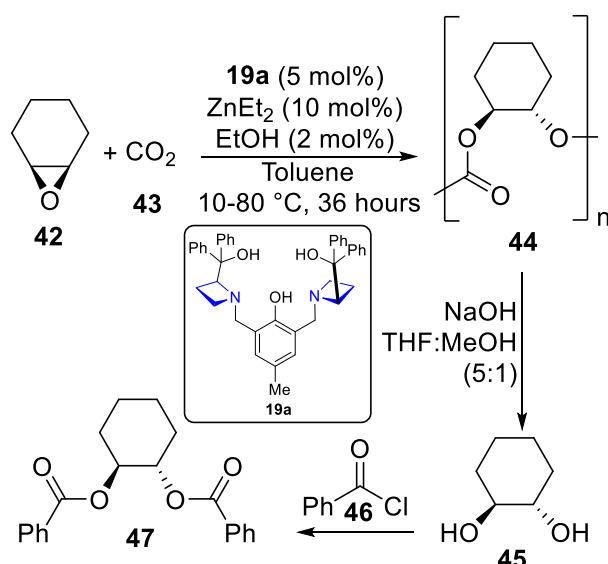
The AzePhenol ligand (**19a**) and diethylzinc have been used for the aldol condensation of 2-hydroxyacetophenones (**36**) and ethyl glyoxalate (**37**) allowing the highly enantioselective formation of  $\alpha,\beta$ -dihydroxy  $\gamma$ -keto esters (**38**), Scheme 6. High enantioselectivity of at least 72% ee was observed for nearly all fifteen 2-hydroxyacetophenones (**36**) investigated with one exception witnessed when 4-nitrophenyl was used as aromatic substituent. In this situation, only 4% yield and 4% ee was observed which was anomalously poor in comparison to the other results, especially when the reaction generated good results when substituted with other electron-withdrawing substituents such as fluorine, bromine and chlorine. One potential drawback of the methodology was the unsatisfactory regioselectivity to generate the *syn* and *anti* products; most substrates favoured the *anti*-product but the ratios are practically 1:1 in most cases.<sup>58</sup>



**Scheme 7:** Enantioselective dinuclear zinc-catalysed aza-Henry reaction of *N*-Boc imines and nitroalkanes to generate nitroamines

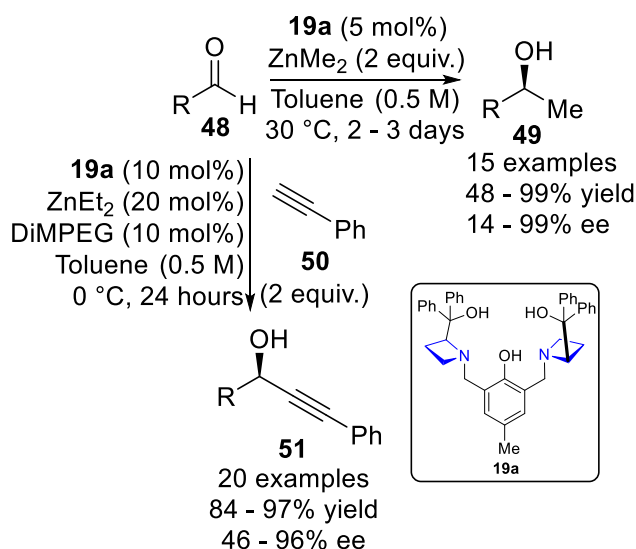
Asymmetric aza-Henry reactions of *N*-Boc imines (**39**) with nitroalkanes (**40**) are viable with the dinuclear zinc complex of the azetidine-containing ligand (**19a**) under mild reaction conditions, producing the desired nitroamine (**41**) with good selectivity of at least 84% ee, Scheme 7. A clear pattern emerged, where electron-donating substituents on the aryl group of **39** increased the yield whereas electron-withdrawing substituents reduced the yield in comparison to when examining the reaction with benzaldehyde (**39**) and nitromethane (**40**). Using the phenyl *N*-Boc imine of **39** with nitroethane (**40**) formed the product with 94% ee, 94% yield and a diastereomeric ratio of 14:1; similar results were also produced when using nitropropane (**48**).<sup>59</sup> Trost *et al.* reported the same reaction of **39** (Ar = Ph) using nitromethane (**40**) with the ProPhenol ligand (**16a**) in conjunction with dimethylzinc, which required higher catalytic loading of 30 mol% and generated a yield of 67% and 91% ee,<sup>48</sup> in comparison, the AzePhenol (**19a**) ligand (with diethylzinc) provided an improved result of 75% yield and 99% ee.<sup>59</sup>





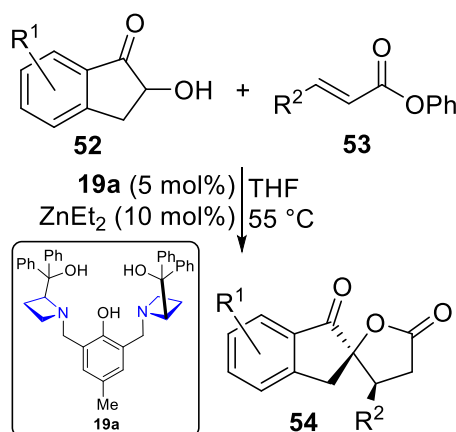
**Scheme 8:** Enantioselective dinuclear zinc-catalysed copolymerisation of cyclohexene oxide and carbon dioxide

The AzePhenol ligand **19a** with diethylzinc has also been used for the copolymerisation of cyclohexene oxide (**42**) and carbon dioxide (**43**), Scheme 8. The enantioselectivity of the desymmetrisation reaction of the epoxide upon **42** was determined by hydrolysis of the resultant polymer (**44**) to afford *trans*-cyclohexane-1,2-diol monomers (**45**) followed by subsequent addition of benzoyl chloride (**46**) to produce diesters (**47**). Temperature played a crucial role of the polymerisation where lowering the temperature from 80 °C to 10 °C, increased the yield, the average molar mass and the ee.<sup>60</sup> Later work, investigated the copolymerisation with cyclopentene oxide and demonstrated a similar pattern of reactivity.<sup>61</sup> Copolymerisation of cyclohexene oxide using the bispyrrolidinyl ligand (**16a**) in conjunction with diethylzinc has been reported but demonstrated a poor enantiomeric excess of the hydrolysed polymer at 22% ee.<sup>62</sup>



**Scheme 9:** Enantioselective dinuclear zinc-catalysed methylation (left to right) and alkynylation (top to bottom) of aldehydes

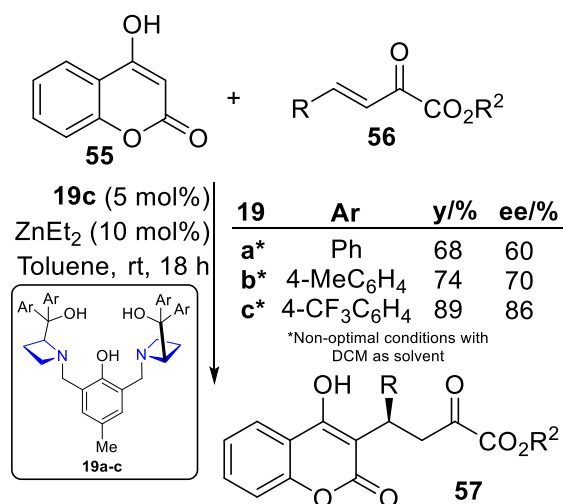
The AzePhenol ligand (**19a**) has been utilised for the enantioselective addition of dimethylzinc to benzaldehydes (**48**) to generate 1-arylethanol derivatives (**49**), Scheme 9 (left to right). A preliminary investigation of the methylation reaction with seven benzaldehydes generated 48–99% yield and 14–79% ee, the only benzaldehydes (**48**) to generate an ee above 50% were those substituted with electron-donating substituents such as methoxy or dimethylamine. Another relatively simple transformation was attempted on aldehydes (**48**) such as alkynylation with phenylacetylene (**50**) to generate propargylic alcohols (**51**), where relatively high ee was again observed with the use of a methoxy group, Scheme 9 (top to bottom). Both reactions shared a common feature where *ortho*-methoxybenzaldehyde (**48**) generated relatively high yield and ee for the respective reaction (99% yield, 73% ee for methylation; 89% yield and 95% ee for alkynylation); these improved results were justified from the authors by postulating that when using *ortho*-methoxybenzaldehyde (**48**) both oxygen atoms coordinate to the Lewis acidic site, generating a six-membered ring intermediate and providing a more stable and rigid transition state. From this observation, a secondary study was investigated that probed di- and tri-substituted benzaldehydes (**48**) with multiple methoxy groups for both the methylation and alkynylation reaction. Methylation of 2,4,6-trimethoxybenzaldehyde generated the best result of 99% yield and 99% ee and 2,3-dimethoxybenzaldehyde was the best substrate for the alkynylation with 97% yield and 96% ee. In addition, furfural, which incorporates an oxygen within the ring system, also appears to benefit from the *ortho*-methoxy effect for the alkynylation reaction with phenylacetylene (**50**) affording 93% yield and 85% ee.<sup>53</sup>



**Scheme 10:** Enantioselective dinuclear zinc-catalysed cascade reaction affording spirocyclic butyrolactones

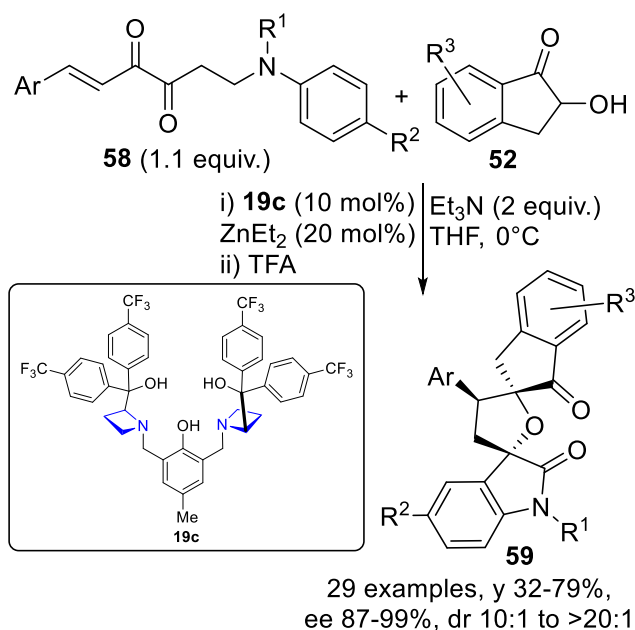
The dinuclear zinc complex containing **19a** has been used for the tandem reaction of 2-hydroxy-1-indanone (**52**) and phenyl acrylates (**53**) to generate spirocyclic butyrolactones (**54**), a frequent pharmaceutical motif,<sup>63</sup> Scheme 10. A variety of substituted indanones (**52**) were tested with phenyl cinnamate (**53**,  $\text{R}^2 = \text{Ph}$ ) and could form **54** with a minimum of 99% ee, >20:1 dr and 77–90% yields with electron-donating and -withdrawing substituents; similar results were also obtained when probing the alkenyl substituent upon **53** with 2-hydroxyindanone (**52**). Two examples were also

presented where **53** was substituted with non-aryl groups, H and methyl, which achieved results in line with the aryl substituted substrates although the  $R^2 = \text{H}$  did have the “poorest” enantioselectivity with 95% ee.<sup>64</sup> Another complex example with **19a** has been reported that produces multi-substituted tetrahydrofurans *via* a cascade reaction granting ee of over 90% for 18 substrates.<sup>65</sup>



**Scheme 11:** Enantioselective dinuclear zinc-catalysed Michael addition of 4-hydroxycoumarins to  $\beta,\gamma$ -unsaturated  $\alpha$ -keto esters

Derivatives of the phenyl appended AzePhenol **19a** paired with diethylzinc have also been used for Michael additions, such as the reaction of 4-hydroxycoumarins (**55**) and 2-oxobut-3-enoates (**56**) to afford  $\beta,\gamma$ -unsaturated  $\alpha$ -keto esters (**57**), Scheme 11. Optimisation of the reaction of **55** and **56** ( $R = \text{Ph}$ ,  $R^2 = \text{Me}$ ) facilitated comparison of the behaviour of bisazetidynyl ligands by altering the aromatic substituent upon the ligand core. Ligand **19a** ( $\text{Ar} = \text{Ph}$ ) produced a moderate result of 68% yield and 60% ee whilst using the bulkier **19b** ( $\text{Ar} = \text{Tolyl}$ ) provided a mild improvement to 74% yield and 70% ee. Ligand **19c** equipped with electron-withdrawing *para*-trifluoromethyl groups on the aromatic ring provided the most desirable results with 89% yield and 86% ee and was able to outperform Trost's **16a** ligand which achieved 82% yield and 80% ee. Sixteen derivatives of **56** were reacted appropriately with the coumarin (**55**) generating the  $\alpha$ -keto esters (**57**) with at least 70% yield and 83% ee.<sup>66</sup> The reaction was also feasible when using the closely related 4-hydroxypyrones instead of 4-hydroxycoumarins (albeit with slightly modified conditions), which on average produced a minor improvement in yield but all reactions observed a reduction in ee.<sup>66</sup>



**Scheme 12:** Enantioselective dinuclear zinc-catalysed cascade reaction affording bispirotetrahydrofuran oxindoles

The bis-azetidinylligand **19c** was the optimal ligand for the reaction of 1-aminopent-4-ene-2,3-diones (**58**) and 2-hydroxyindanone (**52**) to afford bispirotetrahydrofuran oxindoles (**59**), Scheme 12. A wide range of substituents were tolerated upon **58** for the reaction with 2-hydroxyindanone (**52**) where  $\text{R}^1$  could facilitate a methyl, ethyl and benzyl group whilst  $\text{R}^2$  was accepting of electron-withdrawing and -donating substituents with all combinations tested achieving at least 96% ee. The alkenyl substituent (Ar upon **58**) was tolerant of many aromatics even accommodating 2-thienyl, 2-furan and naphthyl groups; one notable outlier was when Ar = 4-nitrophenyl, which had the lowest yield and ee of all substrates (32% yield, 87% ee) despite other electron-withdrawing groups not observing any notable diminished results. Even when **58** was substituted with multiple bromo groups (Ar = 4- $\text{BrC}_6\text{H}_4$ ,  $\text{R}^1$  = (4- $\text{BrC}_6\text{H}_4$ ) $\text{CH}_2$ ,  $\text{R}^2$  = Br) an impressive 99% ee was achieved with a dr of 12:1 and a relatively good yield of 73%. A brief investigation into the substrate scope of the indanone (**52**) was probed which all produced **59** in moderate yields of 68–77%, high dr of >20:1, and at least 89% ee.<sup>67</sup>

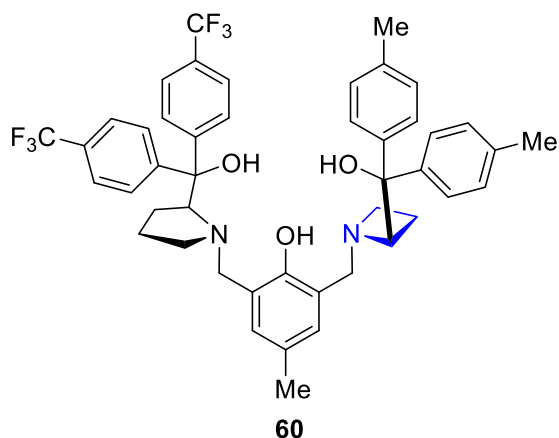
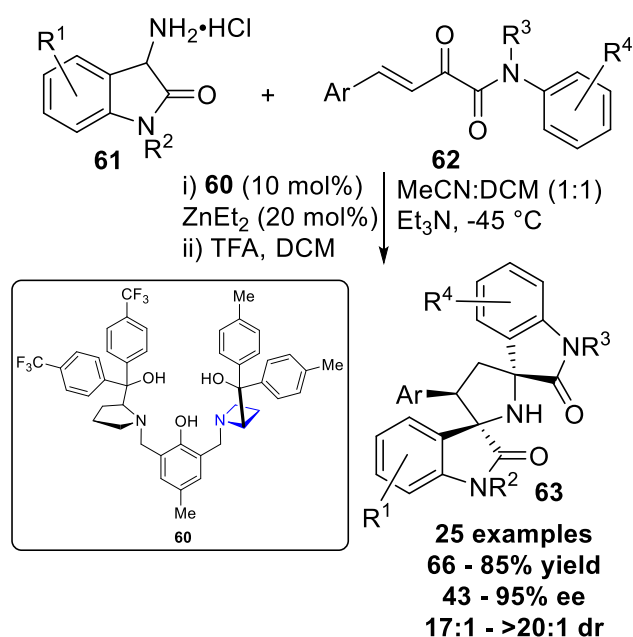


**Figure 6:** A  $C_1$ -symmetric ligand that contains an azetidine and a pyrrolidine ring upon a phenolic core



**Scheme 13:** Use of the  $C_1$ -ligand, **60**, facilitating a cascade reaction with diethylzinc

A hybrid between the AzePhenol and ProPhenol ligands, **60**, has also been developed from the Wang group where one arm contains a pyrrolidine ring and the other, an azetidine ring, with both rings containing a different *para*-substituted aromatic, Figure 6. Initial testing of the tandem reaction with 3-amino-1-methylindolin-2-one hydrochloride (**61**,  $\text{R}^1 = \text{H}$ ,  $\text{R}^2 = \text{Me}$ ) and *N*-methyl-2-oxo-*N*-phenylbut-3-enamide derivatives (**62**,  $\text{R}^3 = \text{H}$ ,  $\text{R}^4 = \text{Me}$ ,  $\text{Ar} = \text{Ph}$ ) using **16a** or **19a** (in conjunction with diethylzinc) generated the product (**63**) with moderate yields around 60% but 24% ee in the best case, Scheme 13. Using the new  $C_1$  symmetric ligand (**60**), under the same conditions generated mildly improved results with 67% yield and 49% ee; after optimisation the test reaction allowed an 85% yield and 89% ee. With many sites to incorporate modularity, 25 derivatives of **63** were synthesised with >20:1 diastereomeric ratios and a maximum 95% ee.<sup>68</sup>

## 2.2. Chiral $\beta$ -aminohydroxy azetidinyl ligands for asymmetric diethylzinc additions

Single enantiomer  $\beta$ -aminohydroxy azetidines such as (*S*)-(1-benzylazetidin-2-yl)diphenylmethanol (**64**), the closely related *N*- $\alpha$ -(*S*)-methylbenzyl diastereomers (**65** and **66**) and the  $C_2$ -symmetric *N*-diphenylethan-1-ol derivative (**67**) are viable ligands for asymmetric zinc-catalysed reactions, Figure 7. These ligands all exhibit the same  $\beta$ -aminoalcohol moiety that was previously demonstrated by Oguni and Omi with species such as (*S*)-valinol, (*S*)-prolinol and (*S*)-phenylalaninol that can be used to engender asymmetry for the reaction of diethylzinc and benzaldehyde.<sup>69</sup>

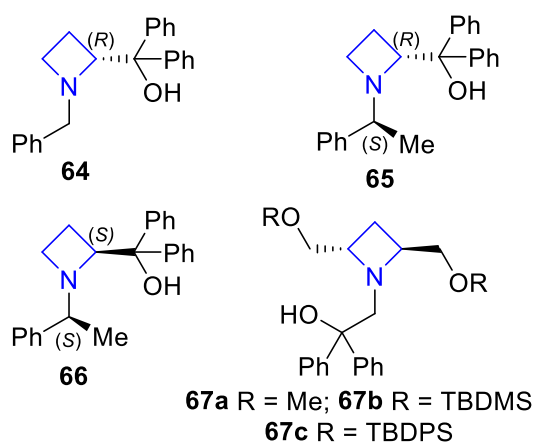


**Figure 7:**  $\beta$ -Aminohydroxy azetidinyl ligands

**Table 1:** Comparison of the  $\beta$ -aminohydroxy azetidinyl ligands for the reaction of diethylzinc with benzaldehyde

$  \begin{array}{c}  \text{O} \\  \parallel \\  \text{Ph}-\text{C}-\text{H} \\  \textbf{48}  \end{array}  \xrightarrow[\text{ZnEt}_2]{\text{Ligand (X mol\%)}}  \begin{array}{c}  \text{OH} \\    \\  \text{Ph}-\text{CH}-\text{Et} \\  \textbf{68-(R)}  \end{array}  +  \begin{array}{c}  \text{OH} \\    \\  \text{Ph}-\text{CH}-\text{Et} \\  \textbf{68-(S)}  \end{array}  $				
Entry	Ligand	Loading (X %)	Yield (%)	ee (%)
1	<b>64</b>	20	62	88 ( <i>R</i> )
2	<b>65</b>	20	85	95 ( <i>R</i> )
3	<b>66</b>	20	75	35 ( <i>S</i> )
4	<b>67a</b>	5	99	92 ( <i>S</i> )
5	<b>67b</b>	5	96	20 ( <i>S</i> )
6	<b>69</b>	3	97	98 ( <i>S</i> )
7	<b>70</b>	3	95	91 ( <i>S</i> )
8	<b>71</b>	5	97	93 ( <i>S</i> )
9	<b>72</b>	5	68	93 ( <i>S</i> )

Hermesen *et al.* developed three 2-azetindyl diphenylmethanol ligands, (**64–66**, Figure 7) and tested their ability to induce stereoselectivity *via* the classic addition of diethylzinc to benzaldehyde (**35**). The substoichiometric use of **64** and **65**, both containing the 2-diphenylmethanol moiety with (*R*)-stereochemistry, in the reaction facilitated the synthesis of (*R*)-1-phenylethan-1-ol (**68-(R)**) with good yields (62% and 85% respectively) and high ee (88% and 95% respectively), Table 1, entry 1 and 2. Analogous use of the ligand **66** for the reaction also achieved a good yield of 75% to form the (*S*)-isomer (**68-(S)**), but had a relatively poor 35% ee in comparison, which the author's contributed this due to the match/mismatch of the stereogenic centres of the ligand,<sup>70</sup> Table 1, entry 3. The ability of **64** was further probed with *para*-substituted benzaldehydes (**48**) producing improved results compared to benzaldehyde with electron-withdrawing and electron-donating groups. Ligand **65**, as the best ligand for inducing asymmetry with benzaldehyde, was tested with alkyl aldehydes and furnished the (*R*)-isomer with great ee, even for long chain aldehydes such as undecanal (77% ee).<sup>70</sup>

Shi and Jiang developed a set of *C*<sub>2</sub>-symmetric 2,4-*trans* azetidine ligands, **67a–67c**, Figure 7, that was also feasible for the addition of diethylzinc to benzaldehydes enabling good enantioselectivity. Good enantioselectivity was observed when using **67a** equipped with methoxy groups and allowed 99% yield and 92% ee (Table 1, entry 4); when using **67b** and **67c**, which uses bulkier TBDMS and TBDPS groups respectively upon the ether oxygen, a steep decline to 20% ee was reported (Table 1, entry 5). The authors of the paper suggested that zinc was binding to the flexible methoxy group when using **67a** and adjusting the substituent on the ether oxygen (as seen with **67b** and **67c**) to a larger group obstructs this desirable coordination and could potentially alter the approach of the aldehyde in the transition state and therefore impeding optimum reactivity and reducing enantioselectivity.<sup>71</sup>

Wang *et al.* developed a (*S*)-azetidin-2-yl-diphenylmethanol ligand substituted with an *N*-methyleneferrocenyl group (**69**), Figure 8. The structure of the ligand closely resembles Hermesen and co-worker's **64** ligand which had a benzyl group attached to nitrogen; the increased steric bulk of the ferrocene group upon **69** provided an improved platform for inducing asymmetry and produced a better selectivity over **64** with 98% ee for the diethylzinc addition to benzaldehyde. Ferrocene-containing ligand (**69**) also provided a higher yield of 97% with only 3 mol% loading in comparison to the reaction when using **64** (Table 1, entry 6).<sup>72</sup> The ligand **69** has been further probed for the arylation,<sup>72</sup> methylation and alkynylation of aldehydes.<sup>73</sup>

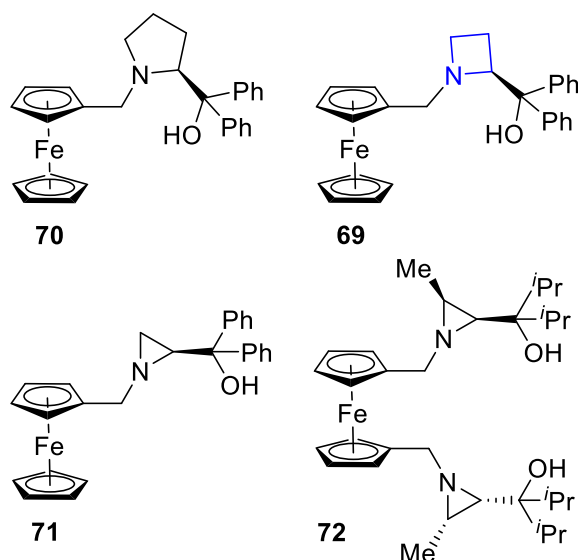
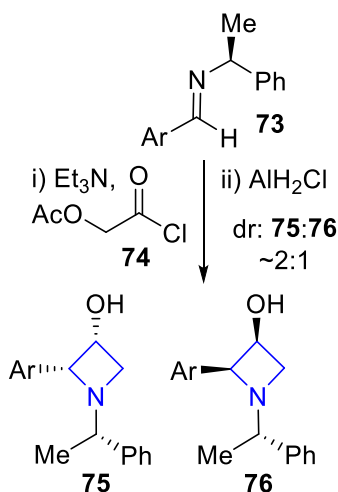


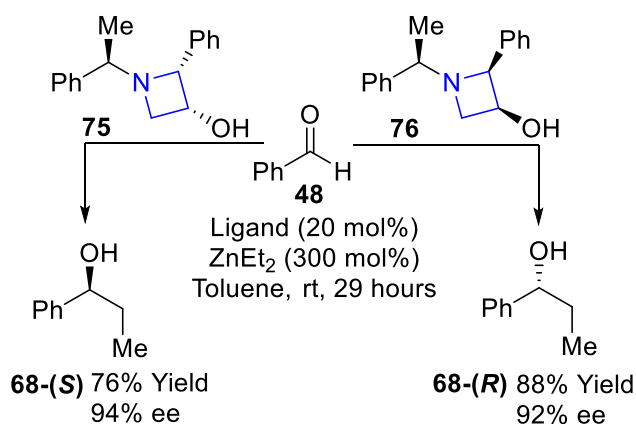
**Figure 8:** Single enantiomer *N*-Ferrocenyl heterocyclic ligands

The azetidine-containing ferrocene derivative **69** proved to be a more effective ligand than Wang's prior ligands which were direct analogues containing a pyrrolidine or aziridine ring (Figure 8, **70** and **71** respectively). Substoichiometric use of the pyrrolidine-containing ligand (**70**) for the reaction of benzaldehyde and diethylzinc could achieve an ee of 91%<sup>74</sup> and the aziridine congener (**71**) used in a similar manner achieved an ee of 93%<sup>75</sup> (Table 1, entry 7 and 8) and both outperformed their *N*-benzyl-containing analogues.<sup>73</sup> As stated prior, neither could outperform the azetidine-containing ligand (**69**) which achieved an ee of 98%; this difference was explained from the authors by comparing the two transition states of the reaction with **69** and **71** where the increased steric congestion around the smaller ring of **71** caused some hindrance which reduced the effectiveness of the reaction, although no justification for **70**'s performance was given.<sup>73</sup> Bis-aziridine ligand (**72**), Figure 8, is an interesting ligand that has no azetidine-analogue, where aziridines are attached to both cyclopentadienyl rings, although, it did achieve the same ee to the mono-aziridine ligand (**71**) for the reaction of benzaldehyde and diethylzinc (Table 1, entry 9).<sup>76</sup>





**Scheme 14:** Formation of two 3-hydroxyazetidine ligands, derived from both regioisomers of the Staudinger reaction

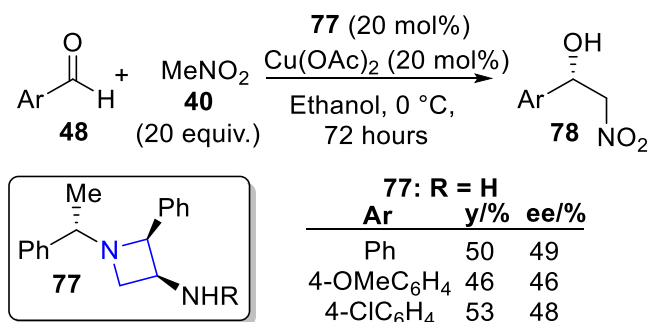


**Scheme 15:** Substoichiometric use of 3-hydroxyazetidines for enantioselective diethylzinc additions to benzaldehyde

Zhang *et al.* developed two series of 2-aryl-3-hydroxyazetidines (**75** and **76**) derived from the two regioisomers of the Staudinger reaction using aryl (*S*)-*N*- $\alpha$ -methylbenzyl imines **73** with acetoxyacetyl chloride (**74**) followed by a reduction step to generate **75** as the major product, Scheme 14. Using the phenyl appended **75** and **76** ligands for the reaction of diethylzinc and benzaldehyde allowed over 90% ee with both diastereoisomers whilst also demonstrating that the chirality on the ring is most influential to the scaffold, Scheme 15. Addition of substituents upon the aromatic ring of the ligands on the azetidine core garnered interesting results; **76** showed a clear pattern when investigating chlorine substituents where moving the position from *para* to *meta* to *ortho* gradually increased the yield and ee where *o*-chlorophenyl delivered the best result of the study with 98% yield and 95% ee. On the other hand, its diastereoisomers (**75**) could not display any clear trend and *ortho*-chlorophenyl was the best performing in its subset; similar observations were observed when investigating methoxy substituents also.<sup>77</sup> The group produced another set of similar ligands, changing the benzylic phenyl ring to a 4-methoxyphenyl which demonstrated similar results.<sup>78</sup>

## 2.3. Miscellaneous Metal Catalysed Reactions with Azetidine Ligands

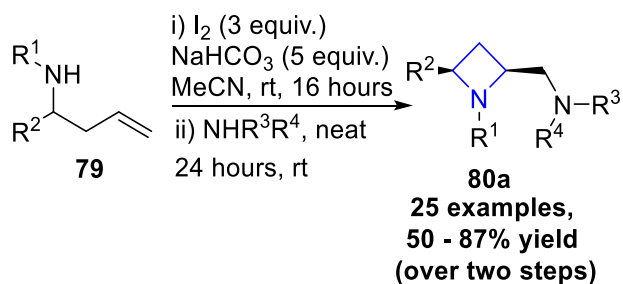
As already demonstrated, azetidines can be used as highly effective ligands for zinc-catalysed reactions and are widely reported. They are equally as viable as ligands with other metals, although there are fewer reports in the literature.



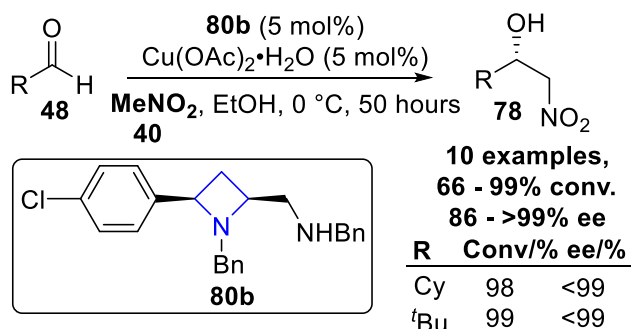
**Scheme 16:** Copper-catalysed Henry reaction with the use of a 2-aryl-3-aminoazetidine ligand

The Zhang group extended their work on the 3-hydroxyazetidines (**75** and **76**) which led to the synthesis of 2-aryl-3-aminoazetidines (**77**). These ligands were notably inferior compared to the 3-hydroxyazetidines (**75** and **76**) for the reaction of diethylzinc and benzaldehyde (**48**); using identical conditions to Scheme 15 the best result generated only 53% ee with a tosyl amino group on **77**.<sup>79</sup>

The ligands (**77**) were also investigated for the copper-catalysed Henry reaction of benzaldehyde (**48**) to generate 2-nitro-ethanol derivatives (**78**), Scheme 16. These ligands could only demonstrate a moderate yield of 50% and 49% ee with an amino group appended to **77**; all other substituents failed to achieve any noteworthy results with the exception of a pyrrolidine group, which had the best yield of 67% but still had a poor ee of 36%. Using an amino group upon **77** (R = H) with *para*-substituted benzaldehydes (4-OMe and 4-Cl) produced almost identical results to using benzaldehyde, with around 50% yield and ee.<sup>79</sup>

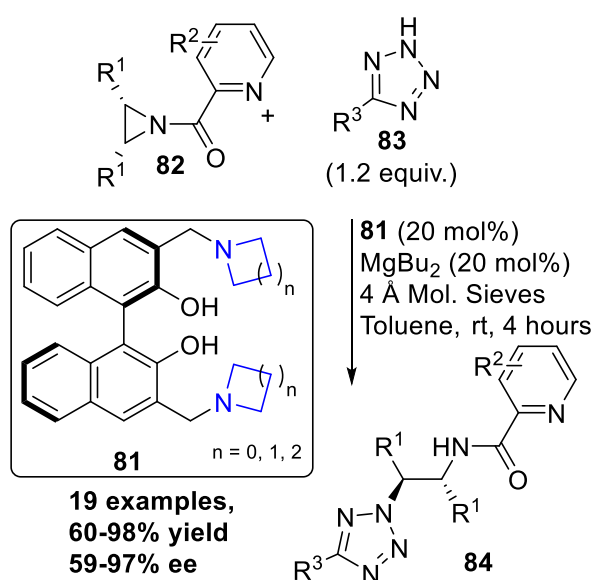


**Scheme 17:** Iodocyclisation for the formation of 2,4-*cis* azetidines



**Scheme 18:** Copper-catalysed Henry reaction with the use of a 2,4-*cis* substituted azetidine ligand

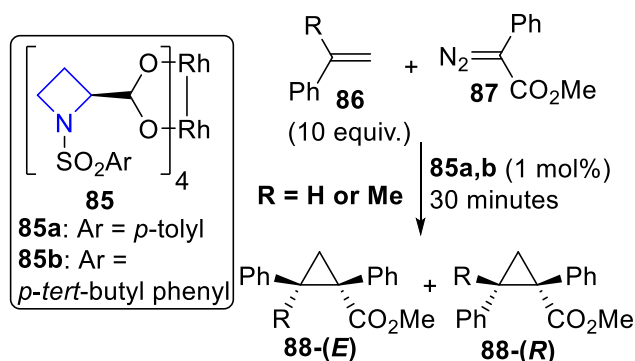
Research from our own group by Feula *et al.* developed the iodocyclisation of homoallylamines (**79**) to synthesise a collection of 2,4-*cis* substituted azetidines (**80a**), Scheme 17.<sup>80,81</sup> These azetidine products (**80a**) have been documented for a wide variety of palladium and platinum complexes<sup>82</sup> and are also able to complex with copper.<sup>34</sup> Copper complexes (generated *in-situ*) were probed for the Henry reaction using a wide scope of 15 different azetidines, where the ligand **80b** provided the optimum catalytic platform allowing the highest conversion and best enantiomeric excess of all azetidines tested, Scheme 18. A sample size of ten aldehydes were tested with the optimum conditions and were able to generate 90% ee or higher for virtually all aldehydes. Of note, the alkyl substituted aldehydes (R = Cy and <sup>t</sup>Bu) demonstrated the most impressive results with near complete conversion and enantiospecific formation of the desired 2-nitro-ethanol derivatives (**78**).<sup>34</sup> Our azetidine (**80b**) performed considerably better than the 3-amino azetidines (**77**) and comes with many advantages such as higher ee for the reaction, lower loading for the ligand and copper source and shorter reaction times.



**Scheme 19:** Magnesium-catalysed desymmetrisation reaction of aziridines with the use of an azetidine-BINOL derivative

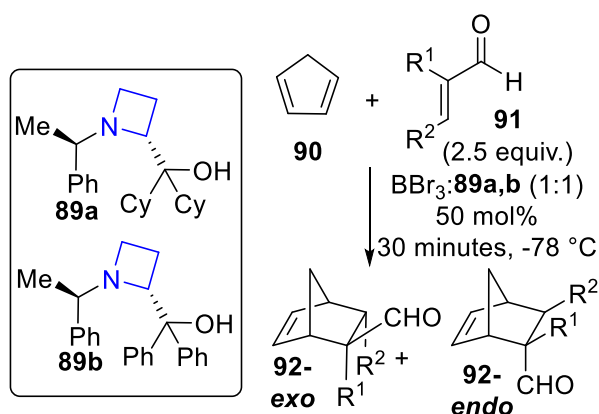
A BINOL derivative (**81**) was developed from Li *et al.* which incorporates two azetidine arms and was utilised for the magnesium-catalysed desymmetrisation reaction of aziridines (**82**) with tetrazoles (**83**), Scheme 19. For the test reaction of (7-azabicyclo[4.1.0]heptan-7-yl)(pyridin-2-yl)methanone (**82**, R<sup>1</sup> = -(CH<sub>2</sub>)<sub>4</sub>-, R<sup>2</sup> = H) and phenyltetrazole (**83**, R<sup>3</sup> = Ph), several N-containing heterocycles such as pyrrolidine, piperidine and morpholine were investigated as the appendage of **81**, which all generated approximately 30% ee. Using an azetidine moiety upon the arms, exhibited enhanced results with an 80% ee and after optimisation, the reaction achieved 95% ee; the authors attributed the improved behaviour of the azetidine ring compared to other heterocycles simply due to its smaller size. A series of cyclic, acyclic and aromatic substituted aziridines (**82**) were tested with phenyltetrazole (**83**),

generating at least 90% yield and over 90% ee to afford **84** for the majority of substrates. Scaling up to a gram scale was possible and could facilitate a reduction in catalytic loading, dropping from 20 mol% to 10 mol%, with quantitative yields and 99% ee.<sup>83</sup>



**Scheme 20:** Cyclopropanation reactions facilitated by an azetidine-rhodium catalyst

Starmans *et al.* formed a novel dirhodium catalyst (**85**) derived from a L-azetidine-2-carboxylic acid starting material and was subsequently utilised for cyclopropanation reactions, Scheme 20. Using either of dirhodium **85** catalysts for the reaction of styrene (**86**) and methyl phenyldiazoacetate (**87**) using dichloromethane as solvent, generated high regioselectivity for **88-(E)** with an *E*:*Z* ratio of least 98:2 but had poor enantioselectivity for the majority product at 36% ee. This was improved with the use of **85b** (appended with a *para-tert*-butyl phenyl group) with only 0.1 mol% loading and changing the solvent to cyclohexane which provided a 57% ee, although the lowest yield was presented with this combination.<sup>84</sup> Doyle *et al.* provided a pyrrolidine equivalent to **85b** which provided an improved 85% ee in comparison to the azetidinyll catalysts, but it did have a slight decrease in *E*:*Z* selectivity.<sup>85</sup>



**Scheme 21:** Boron-catalysed Diels-Alder reaction with the use of chiral azetidine-derived ligands

Starmans *et al.* also investigated  $\beta$ -aminohydroxy azetidines (**89**) for a boron-catalysed Diels-Alder reaction of cyclopentadiene (**90**) with acrolein and closely related compounds (**91**), Scheme 21. All reactions proceeded with over 95% yield but less than 10% ee for most reactions. When the  $\alpha$ -position of **91** ( $\text{R}^1$ ) is substituted with hydrogen, formation of **92-endo** is the major product with around 90%

selectivity whereas larger groups in the  $\alpha$ -position such as methyl generate **92-*exo*** with around the same selectivity. Reactions with acrolein (**91**,  $R^1 = R^2 = H$ ) demonstrated essentially no enantioselectivity with the best result generating only 5% ee when azetidiny ligand **89a** was used as ligand source attached with cyclohexyl rings. Substitution of methyl groups to either position on **91** still rendered the reaction with relatively poor enantioselectivity, where the best result enabled 33% ee **89b** that was substituted with phenyl group instead of cyclohexyl rings. A pyrrolidine derivative of **89b** was also synthesised, which achieved the optimum ee of 65% when  $R^1 = H$  and  $R^2 = Me$ , but when  $R^1 = Me$  and  $R^2 = H$  or when using acrolein (**91**) interestingly no enantioselectivity was observed.<sup>86</sup>

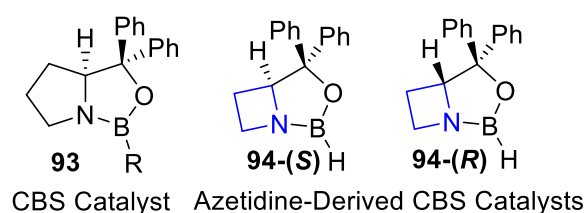
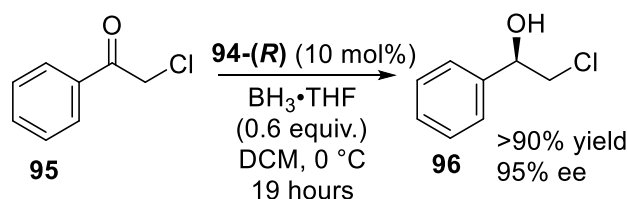
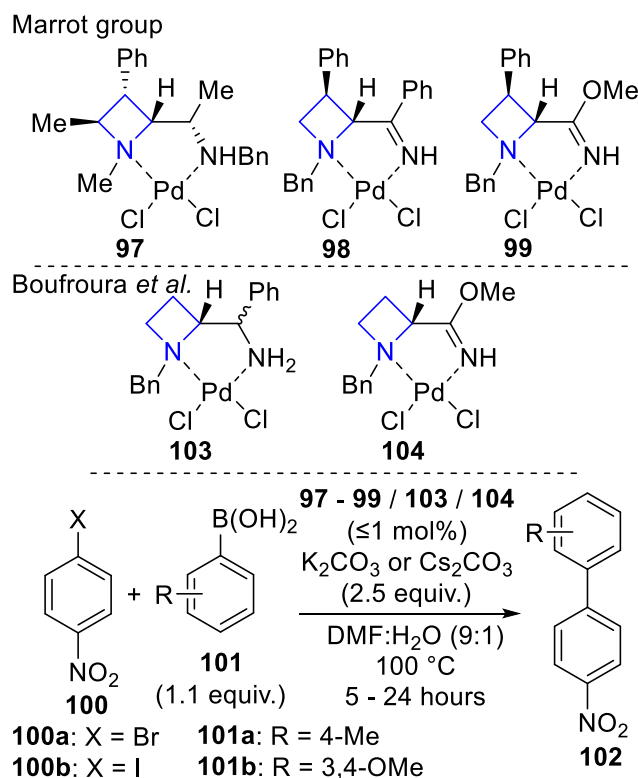


**Figure 9:** Corey, Bakshi and Shibata's oxazaborolidine catalyst, **93**, and azetidine-derived analogues: **94-S** and **94-R**



**Scheme 22:** CBS reduction of acetophenones with an azetidine analogue of Corey's oxazaborolidine catalyst

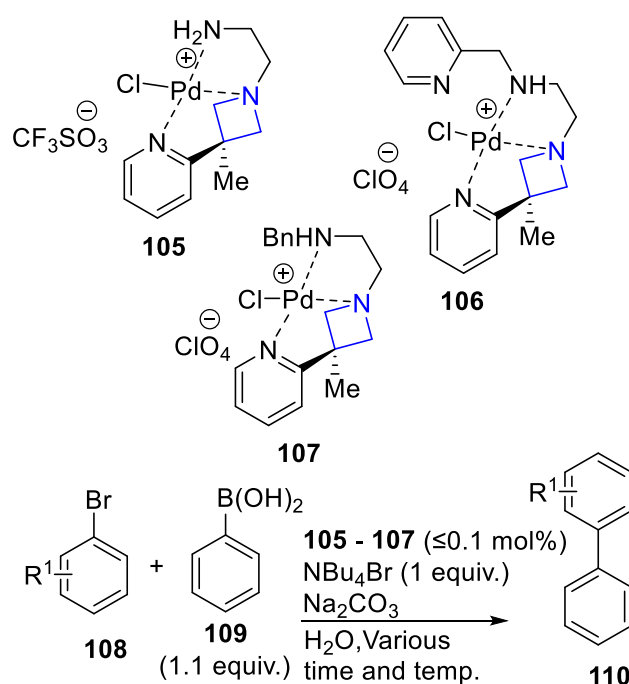
Corey, Bakshi and Shibata developed a catalytic reduction of prochiral ketones utilising a pyrrolidine skeleton oxazaborolidine (**93**), Figure 9.<sup>87</sup> Behnen *et al.* utilised an azetidine-derived analogue of Corey's catalyst, **94-(S)**, for the reduction of acetophenone and propiophenone with optical yields of 98%.<sup>88</sup> Rao *et al.* developed the opposite enantiomer **94-(R)** and subsequently utilised both enantiomers to reduce a small collection of five ketones with yields above 90% and ee ranging from 95–97%. This reduction was used for the first step in the total synthesis of tetramisole, by reducing 2-chloro-1-phenylethan-1-one, (**95**) to the desired (*R*)-2-chloro-1-phenylethan-1-ol (**96**) with a catalytic amount of **94-(R)**, Scheme 22.<sup>89</sup> Corey's catalyst (**93**) did have some benefits compared to the azetidine-containing **94** catalysts such as reactions only taking 1 minute whilst generating similar ee with 5 mol% loading but, the **94** catalysts did generated slightly better enantioselectivity, although it is hard to draw solid comparisons between the two reports with both exhibiting the reaction with a small substrate set of five ketones.



**Scheme 23:** Suzuki cross-coupling reactions utilising palladium-azetidine complexes

As already discussed, chiral azetidines are effective ligands for many metal-catalysed reactions to deliver high enantioselectivity; *N,N*-azetidines (or 1,2-diaminoazetidines) are also viable ligands for non-asymmetric reactions such as Suzuki cross-coupling reactions. The Marrot group were the first to utilise *N,N*-azetidines for the Suzuki reaction, using palladium catalysts **97–99**, where all three catalysts were able to couple 1-bromo-4-nitrobenzene (**100a**) and *p*-tolylboronic acid (**101a**) with 1 mol% loading producing a maximum yield of 85% with catalyst **98**, Scheme 23. The complex **99** was also notable for coupling **100a** with (3,4-dimethoxyphenyl)boronic acid (**101b**) with only 0.1 mol% catalytic loading and producing the Suzuki product (**102**) with a yield of 87%.<sup>90</sup>

Boufroura *et al.* developed similar palladium azetidine-containing complexes (**103** and **104**), alongside aziridine congeners, and investigated their capabilities as ligands for Suzuki cross-couplings. The reaction of 1-iodo-4-nitrobenzene (**100b**) and *p*-tolylboronic acid (**101a**) with Boufroura's complexes achieved 93% yield with the diamino complex (**103**) and quantitative yields with the imidate azetidinyll complex (**104**) with 1 mol% loading of the catalyst; the same reaction with 1-bromo-4-nitrobenzene observed a dramatic drop in reactivity with the diamino complex (**103**) only managing 29% yield and the imidate complex (**104**) produced 70% yield. Ultimately, the imidate azetidine (**104**) performed better than the diamino azetidine (**103**) in all cases but neither could outperform the imidate aziridine analogue of **104** which had the highest yield for every reaction tested.<sup>91</sup>



**Scheme 24:** Suzuki cross-coupling reaction utilising tridentate azetidine ligands

Lee *et al.* investigated the use of tridentate palladium complexes containing azetidines (**105–107**), for Suzuki couplings and showed very promising results with the bispyridinyl complex **106**. Screening of the reaction with bromobenzene (**108**) and phenylboronic acid (**109**) demonstrated highly auspicious results with only 0.01 mol% catalytic loading allowing a minimum of 90% yield for all 3 catalysts, Scheme 24. The complex **106** performed as the optimum catalyst and was largely unaffected by changes in reaction conditions; for example, the reaction of bromobenzene (**108**) and phenylboronic acid (**109**) at 70 °C with **106** using 0.01 mol% catalytic loading produced a yield of 98% over 1 hour, reducing the loading to  $1 \times 10^{-3}$  mol% formed the product with a yield of 90% over 5 hours, and even at  $5 \times 10^{-4}$  mol% loading, a yield of 71% was achieved, although the reaction time was significantly increased to 24 hours. The cross-coupling is feasible at room temperature within 10 hours with a relatively “high” catalytic loading of 0.1 mol% (although it is still highly efficient). Azetidine-containing complex **106** remained an effective catalyst for various substituted aryl halides (**108**), coupling to phenylboronic acid (**109**) and achieved yields above 90% for many pairings. It is also worth noting that all of these reactions were performed with only water as solvent, although tetrabutylammonium bromide was required to enhance solubility for the hydrophobic species **108**.<sup>92</sup>

## 2.4. Asymmetric organocatalysis

L-Proline (**111**) is a frequently used organocatalyst and a multitude of reviews and book chapters have been published reflecting its widespread use in the field, Figure 10.<sup>93–97</sup> Hence, it is only natural to test similar structures to investigate their organocatalytic ability with other ring sizes. Below outlines

examples of azetidines behaving analogously to L-proline (**6**) primarily focussing on L-azetidine-2-carboxylic acid (**111**) often abbreviated to simply L-aze.

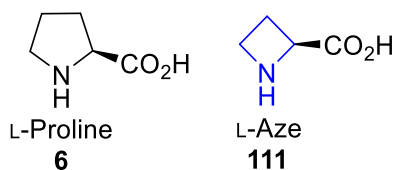
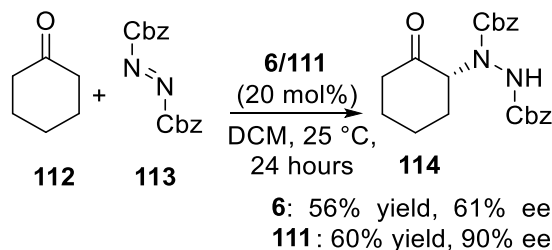
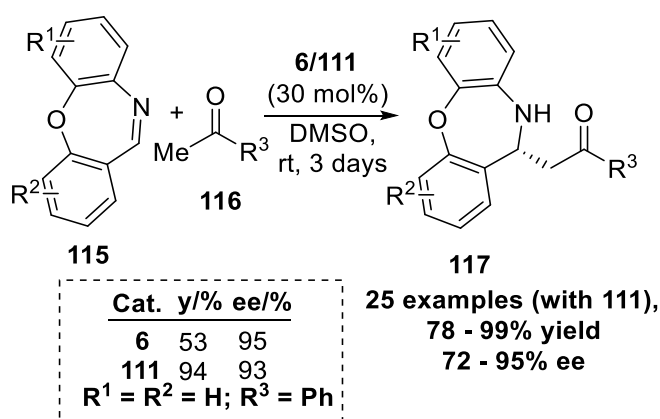


**Figure 10:** L-Aze and L-proline, cyclic amino acids



**Scheme 25:**  $\alpha$ -amination of cyclohexanone *via* organocatalysis with L-aze and L-proline

Thomassigny *et al.* demonstrated L-azetidine-2-carboxylic acid (**111**) as a superior organocatalysis for the  $\alpha$ -amination of cyclohexanone (**112**) with dibenzyl azodicarboxylate (**113**) in comparison to L-proline (**6**), Scheme 25. Amination with L-aze (**111**) produced the desired product (**114**) with a 60% yield and 90% ee; L-proline (**6**) also generated **114** with approximately the same yield but lower ee of 61% was observed for the reaction. Similar results were observed for the amination of propanal where the azetidine organocatalyst (**111**) achieved a superior ee of 74% in comparison to **6**'s 54% ee, although L-aze required a longer reaction time for completion of the reaction.<sup>98</sup>

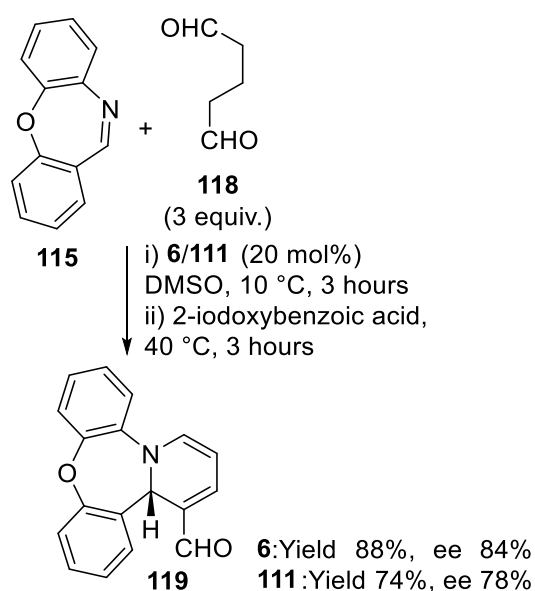


**Scheme 26:** Mannich reaction of dibenzo[*b,f*][1,4]oxazepines with acetophenones *via* organocatalysis with L-aze and L-proline

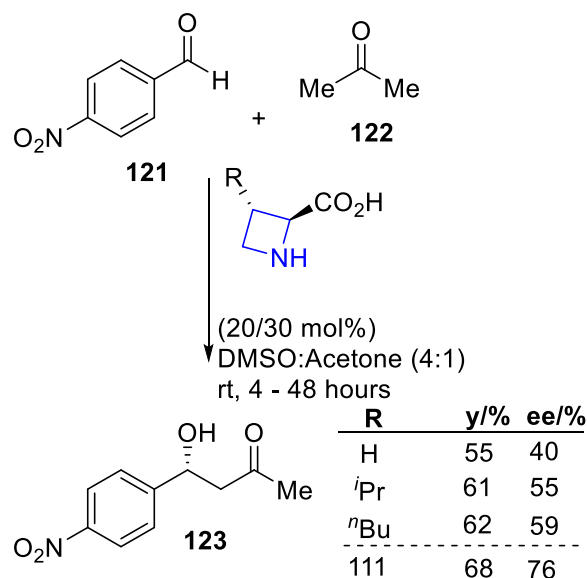
Dibenzo[*b,f*][1,4]oxazepines (**115**) (often abbreviated as DBO) can also take advantage of the organocatalytic capabilities of the cyclic amino acids (**6** and **111**) as reported from Ren *et al.*. Whilst preliminary investigations into the reaction of DBO (**115**) and acetophenone (**116**, R<sup>3</sup> = Ph) with L-proline (**6**) yielded the highest ee of 95%, yields could not surpass 60%, whereas L-aze (**111**) was able



to achieve a fair compromise producing 93% ee with 94% yield, Scheme 26. Twelve acetophenones (**116**) were tested with DBO (**115**) to furnish the ketone products (**117**) with over 90% yield and ee for most substrates. 2'-Methylacetophenone (**116**) produced only a trace amount of product, where the authors theorised steric hindrance impeded the reaction, and an  $\alpha,\beta$ -unsaturated ketone was feasible with the reaction, albeit with a reduction in performance producing the lowest results of 78% yield and 72% ee. The reaction of acetophenone (**116**) with derivatives of **115** were explored similarly by altering different substituents on the aromatic rings of **115** with all reactions producing over 90% yield and ee with no notable changes observed when changing the position or the nature of the substituents. To demonstrate the feasibility of the reaction, a gram scale reaction was performed with DBO (**115**) and acetophenone (**116**) with reduced catalytic loading of L-aze (**111**) to 20 mol% (from 30 mol%), producing the target product (**117**) with 96% yield and 92% ee.<sup>99</sup>

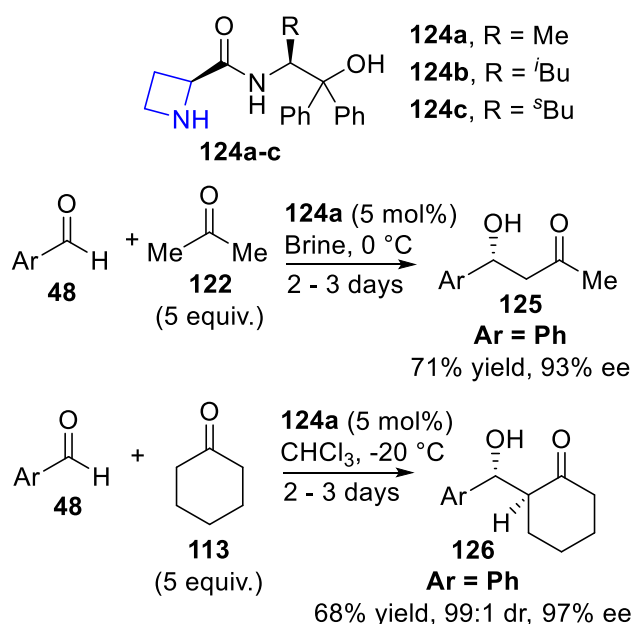


**Scheme 27:** Mannich reaction for the formation of fused 1,2-dihydropyridines *via* organocatalysis with L-aze and L-proline Choudhary *et al.* demonstrated the use of L-aze (**111**) as an effective organocatalyst for a another Mannich reaction using dibenzo[*b,f*][1,4]oxazepines (**115**) with glutaraldehyde (**118**) to form a tricyclic product (**119**), Scheme 27. Azetidine-derived organocatalyst (**111**) completes the reaction with a good yield of 74% and a 78% ee; using the pyrrolidine counterpart (**6**) slightly improves the reaction though, producing an 84% ee and boosting the yield to 88%. From this, L-proline (**6**) was determined as the optimum catalyst and was able to facilitate the transformation to **119** with a wide range of DBO derivatives (**115**) with high yield and 84 – <99% ee.<sup>100</sup> L-aze (**111**) has also been used for other Mannich reactions of acetone with 1-piperidine<sup>101</sup> and benzothiazines<sup>102</sup> where it achieves very similar results to L-proline.



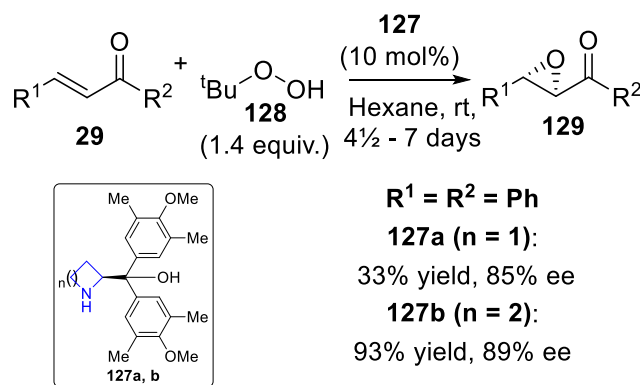
**Scheme 28:** Aldol condensation of 4-nitrobenzaldehyde and acetone *via* organocatalysis with L-azetidine, L-azetidine derivatives and L-proline

List *et al.* investigated a series of L-proline analogues for the aldol reaction of 4-nitrobenzaldehyde (**121**) with acetone (**122**), Scheme 28. This reaction worked well with L-proline (**111**) producing yields of 68% with an ee of 76%; swapping to the smaller L-azetidine **112** produced a sizeable reduction in ee to 40% and a slight decrease in yield to 55% but still performed better than the acyclic organocatalysts such as L-histidine, L-valine and L-tyrosine.<sup>33</sup> The following year, the reaction was looked into further by the same group and the catalytic loading could be lowered from 30 mol% to 20 mol% with no effect on yields and ee.<sup>103</sup> The same reaction was investigated by Enders and Gries, where they explored how a bulky substituent in the 3-position (*i*Pr and *n*Bu) of the azetidine (**111**) would affect the reactivity. Both catalysts performed better than L-azetidine with a boost in ee to 55% and 59% for *i*Pr and *n*Bu respectively but, L-proline still outperformed all of the 4-membered catalysts with its 76% ee for the reaction.<sup>104</sup>



**Scheme 29:** Aldol condensation of benzaldehydes and ketones facilitated by azetidine-2-carboxamide organocatalysts

A small family of organocatalysts were developed by Wang *et al.* and were investigated for their utility in enantioselective aldol reactions, Scheme 29. Methyl-substituted catalyst **124a** delivered the highest ee for the test reaction of benzaldehyde (**48**) and acetone (**122**), despite **124b** and **124c** having an identical skeleton containing a bulkier group, where it would be expected for them to deliver higher enantioselectivity. Reactions with acetone (**122**) and a variety of benzaldehydes (**48**) generated at least 67% ee with a wide range of yields from 38–88%. Interestingly, 4-nitrobenzaldehyde (**48**) could not produce a 1,3-hydroxyketone product (**125**) with sufficient yield as it rapidly dehydrates to the  $\alpha,\beta$ -unsaturated ketone. The aldol reaction was also possible with cyclohexanone (**113**) and was performed under modified conditions, which generated a similar range of yields as seen when using acetone (**122**) but most products had significantly higher ee where most substrates achieved over 90% ee. Cyclohexanone (**113**) and benzaldehyde (**48**) produced a diastereomeric ratio of 99:1 with an ee of 97% and using *p*-tolylaldehyde generated the best ee with only the *S*-isomer being detectable by HPLC. Cyclopentanone and benzaldehyde (**48**) were also tested as a one-off reaction which generated a high ee of 99% but a disappointing yield of only 30%.<sup>105</sup>



**Scheme 30:** Stereoselective epoxidation of chalcones with sterically bulky azetidine- and pyrrolidine-derived organocatalysts

Russo and Lattanzi demonstrated the highly enantioselective epoxidation of aromatically-substituted chalcones (**29**) with the use of heterocyclic organocatalysts (**127**) with *tert*-butyl hydroperoxide (**128**), Scheme 30. A study was developed that focused on comparing the azetidinyl **127a** and pyrrolidinyl organocatalysts **127b** for the reaction where a clear trend was presented. The azetidine catalyst **127a** always provided a minor reduction in ee, in comparison to when the reaction was performed with **127b**, alongside a large reduction of at least 40% yield for all six chalcones tested. As an example, when substituting  $\text{R}^1 = \text{R}^2 = \text{Ph}$  upon **29**, the epoxide product (**129**) was formed with an ee of 85% and 89% respectively for **127a** and **127b** respectively but the yields were vastly different at 33 and 93%, a dramatic difference.<sup>106</sup>

### 3. Conclusion

Azetidines are a useful class of nitrogen-containing heterocycle for asymmetric catalysis and can be used for a wide array of transformations. Azetidines can act as effective organocatalysts and are able to perform similarly to the commonly encountered L-proline catalyst, as seen with the reaction of acetophenones and DBO derivatives (section 2.4.). They are also highly effective ligands for metal-catalysis where they can engender asymmetry with many metals such as magnesium, copper and palladium permitting ring-opening, Henry and Suzuki reactions respectively (section 2.3.). A large focus of azetidine-derived ligands so far has been on zinc-mediated catalysis, with the AzePhenol ligand proving to be a worthy companion to the more established ProPhenol ligand (section 2.1.). Alongside this, many chiral azetidine-derived ligands have been synthesised that allow highly enantioselective addition of diethylzinc to benzaldehydes (section 2.2.).

Changing the ring size of a nitrogen-containing heterocyclic catalyst clearly plays a role in any observed behaviour. In certain applications, the use of an azetidine ring provides the optimum result, such as in the case of diethylzinc addition to benzaldehyde under control of ferrocene-containing azetidine ligands (compound **69**). Conversely, it can also be detrimental to make a similar change in catalyst

structure and severely impact a given reaction, as seen when using L-aze as an organocatalyst instead of L-proline for aldol reactions. It is difficult to distinguish a clear trend where one of these catalytic systems should triumph over another and optimisation largely remains in the realms of systematic alteration of variables (including ring size). This should be encouraging though, where experimentation of three-, four- and five-membered nitrogen-containing heterocyclic systems are all on a level playing field. Pyrrolidine-derived systems do have an advantage due to their economical commercial availability and smoother synthesis in comparison to the smaller rings but its larger size can prove as a downfall providing a less rigid coordination sphere within the reaction limiting its potential. Azetidines are constricted into a butterfly orientation with restricted movement administering a far tighter microenvironment about a reaction that may be influenced by it. Azetidine-containing asymmetric catalysis is a relatively small field but with the onset of superior and selective synthetic methods to access them, it has significant potential to grow. It is with hope that the area continues to grow using the references included within the article for inspiration, and to take advantage of the many reviews on the synthesis of these cyclic moities<sup>107-109</sup> as a starting point.

### **Acknowledgements**

JPM and JSF would like to thank the University of Birmingham for support. JPM and JSF thank members of our research group for assistance in the latter stages of manuscript preparation.

### **Declaration of competing interest**

The authors declare no conflict of interest.

### **References**

1. Singh, K.; Shakya, P.; Kumar, A.; Alok, S.; Kamal, M.; Singh, S. P. *Int. J. Pharm. Sci. Res.* **2014**, *5*, 4644-4659.
2. Chhabra, N.; Aseri, M. L.; Padmanabhan, D. *Int. J. Appl. Basic Med. Res.* **2013**, *3*, 16-18.
3. Carey, J. S.; Laffan, D.; Thomson, C.; Williams, M. T. *Org. Biomol. Chem.* **2006**, *4*, 2337-47.
4. Busacca, C. A.; Fandrick, D. R.; Song, J. J.; Senanayake, C. H. *Adv. Synth. Catal.* **2011**, *353*, 1825-1864.
5. Hargaden, G. C.; Guiry, P. J. *Chem. Rev.* **2009**, *109*, 2505-2550.
6. Evans, D. A.; Woerpel, K. A.; Hinman, M. M.; Faul, M. M. *J. Am. Chem. Soc.* **1991**, *113*, 726-728.
7. Evans, D. A.; Willis, M. C.; Johnston, J. N. *Org. Lett.* **1999**, *1*, 865-868.
8. Johnson, J. S.; Evans, D. A. *Acc. Chem. Res.* **2000**, *33*, 325-335.
9. Corey, E. J.; Imai, N.; Zhang, H. Y. *J. Am. Chem. Soc.* **1991**, *113*, 728-729.
10. Desimoni, G.; Faita, G.; Jørgensen, K. A. *Chem. Rev.* **2006**, *106*, 3561-3651.
11. Dawson, G. J.; Frost, C. G.; Williams, J. M. J. *Tetrahedron Lett.* **1993**, *34*, 3149-3150.
12. Sprinz, J.; Helmchen, G. *Tetrahedron Lett.* **1993**, *34*, 1769-1772.
13. Pfaltz, A. *Acc. Chem. Res.* **1993**, *26*, 339-345.
14. Zhou, J.; Tang, Y. *Chem. Soc. Rev.* **2005**, *34*, 664-76.
15. Dalko, P. I.; Moisan, L. *Angew. Chem. Int. Ed.* **2004**, *43*, 5138-5175.

16. Ahrendt, K. A.; Borths, C. J.; MacMillan, D. W. C. *J. Am. Chem. Soc.* **2000**, *122*, 4243-4244.
17. Hajos, Z. G.; Parrish, D. R. *J. Org. Chem.* **1974**, *39*, 1615-1621.
18. Eder, U.; Sauer, G.; Wiechert, R. *Angew. Chem. Int. Ed.* **1971**, *10*, 496-497.
19. Reyes-Rodriguez, G. J.; Rezayee, N. M.; Vidal-Albalat, A.; Jørgensen, K. A. *Chem. Rev.* **2019**, *119*, 4221-4260.
20. Longbottom, D. A.; Franckevičius, V.; Ley, S. V. *CHIMIA* **2007**, *61*, 247-256.
21. Becker, M. R.; Richardson, A. D.; Schindler, C. S. *Nat. Commun.* **2019**, *10*, 1-8.
22. Parthasarathy, K.; Cheng, C. H., 2014; pp. 222-272.
23. Antermite, D.; Degennaro, L.; Luisi, R. *Org. Biomol. Chem.* **2017**, *15*, 34-50.
24. Kato, N.; Comer, E.; Sakata-Kato, T.; Sharma, A.; Sharma, M.; Maetani, M.; Bastien, J.; Brancucci, N. M.; Bittker, J. A.; Corey, V.; Clarke, D.; Derbyshire, E. R.; Dornan, G. L.; Duffy, S.; Eckley, S.; Itoe, M. A.; Koolen, K. M.; Lewis, T. A.; Lui, P. S.; Lukens, A. K.; Lund, E.; March, S.; Meibalan, E.; Meier, B. C.; McPhail, J. A.; Mitasev, B.; Moss, E. L.; Sayes, M.; Van Gessel, Y.; Wawer, M. J.; Yoshinaga, T.; Zeeman, A. M.; Avery, V. M.; Bhatia, S. N.; Burke, J. E.; Catteruccia, F.; Clardy, J. C.; Clemons, P. A.; Dechering, K. J.; Duvall, J. R.; Foley, M. A.; Gusovsky, F.; Kocken, C. H.; Marti, M.; Morningstar, M. L.; Munoz, B.; Neafsey, D. E.; Sharma, A.; Winzeler, E. A.; Wirth, D. F.; Scherer, C. A.; Schreiber, S. L. *Nature* **2016**, *538*, 344-349.
25. Han, M.; Song, C.; Jeong, N.; Hahn, H. G. *ACS Med. Chem. Lett.* **2014**, *5*, 999-1004.
26. Zhang, W.; Chen, B.; Zhang, Y.; Luo, J. *Ther. Clin. Risk Manag.* **2015**.
27. Christy, V. *Proc (Bayl Univ Med Cent)* **2005**, *18*, 76-80.
28. Kobayashi, J.; Cheng, J.-F.; Ishibashi, M.; Wälchli, M. R.; Yamamura, S.; Ohizumi, Y. *J. Chem. Soc., Perkin Trans. 1* **1991**, 1135-1137.
29. Takemoto, T.; Nomoto, K.; Fushiya, S.; Ouchi, R.; Kusano, G.; Hiking, H.; Takagi, S.-i.; Matsuura, Y.; Kakud, M. *Proc. Japan Acad.* **1978**, *54*, 469-473.
30. Wright, K.; Drouillat, B.; Menguy, L.; Marrot, J.; Couty, F. *Eur. J. Org. Chem.* **2018**, *2019*, 112-117.
31. Kern, N.; Felten, A. S.; Weibel, J. M.; Pale, P.; Blanc, A. *Org. Lett.* **2014**, *16*, 6104-6107.
32. Gleede, T.; Reisman, L.; Rieger, E.; Mbarushimana, P. C.; Rupar, P. A.; Wurm, F. R. *Polym Chem-Uk* **2019**, *10*, 3257-3283.
33. List, B.; Lerner, R. A.; Barbas III, C. F. *J. Am. Chem. Soc.* **2000**, *122*, 2395-2396.
34. Yoshizawa, A.; Feula, A.; Male, L.; Leach, A. G.; Fossey, J. S. *Sci. Rep.* **2018**, *8*, 1-16.
35. Sunoj, R. B. *Acc. Chem. Res.* **2016**, *49*, 1019-28.
36. Roduner, E. *Chem. Soc. Rev.* **2014**, *43*, 8226-8239.
37. Li, Y.; Bouteiller, L.; Raynal, M. *ChemCatChem* **2019**, *11*, 5212-5226.
38. Brill, Z. G.; Condakes, M. L.; Ting, C. P.; Maimone, T. J. *Chem. Rev.* **2017**, *117*, 11753-11795.
39. Andrushko, V.; Andrushko, N. *Stereoselective Synthesis of Drugs and Natural Products* **2013**, 1-42.
40. Pfaltz, A.; Drury, W. J. *Proc. Natl. Acad. Sci. U. S. A.* **2004**, *101*, 5723.
41. Yoon, T. P.; Jacobsen, E. N. *Science* **2003**, *299*, 1691.
42. Trost, B. M.; Ito, H. *J. Am. Chem. Soc.* **2000**, *122*, 12003-12004.
43. Shibasaki, M.; Kanai, M.; Matsunaga, S.; Kumagai, N. *Acc. Chem. Res.* **2009**, *42*, 1117-1127.
44. Kumagai, N.; Kanai, M.; Sasai, H. *ACS Catal.* **2016**, *6*, 4699-4709.
45. Trost, B. M.; Michaelis, D. J.; Truica, M. I. *Org. Lett.* **2013**, *15*, 4516-4519.
46. Trost, B. M.; Shin, S.; Sclafani, J. A. *J. Am. Chem. Soc.* **2005**, *127*, 8602-8603.
47. Trost, B. M.; Fettes, A.; Shireman, B. T. *J. Am. Chem. Soc.* **2004**, *126*, 2660-2661.
48. Trost, B. M.; Lupton, D. W. *Org. Lett.* **2007**, *9*, 2023-2026.
49. Trost, B. M.; Müller, C. *J. Am. Chem. Soc.* **2008**, *130*, 2438-2439.
50. Trost, B. M.; Hung, C. I.; Mata, G. *Angew. Chem. Int. Ed.* **2020**, *59*, 4240-4261.
51. Jarzyński, S.; Utecht, G.; Leśniak, S.; Rachwalski, M. *Tetrahedron: Asymmetry* **2017**, *28*, 1774-1779.
52. Hua, Y.-Z.; Han, X.-W.; Yang, X.-C.; Song, X.; Wang, M.-C.; Chang, J.-B. *J. Org. Chem.* **2014**, *79*, 11690-11699.

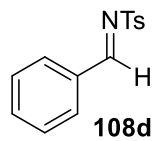
53. Liu, S.; Li, G.-W.; Yang, X.-C.; Zhang, D.-Y.; Wang, M.-C. *Org. Biomol. Chem.* **2017**, *15*, 7147-7156.
54. Wang, X.-W.; Hua, Y.-Z.; Wang, M.-C. *J. Org. Chem.* **2016**, *81*, 9227-9234.
55. Hua, Y.-Z.; Chen, J.-W.; Yang, H.; Wang, M.-C. *J. Org. Chem.* **2018**, *83*, 1160-1166.
56. Liu, S.; Shao, N.; Li, F.-Z.; Yang, X.-C.; Wang, M.-C. *Org. Biomol. Chem.* **2017**, *15*, 9465-9474.
57. Shao, N.; Luo, Y.-Y.; Lu, H.-J.; Hua, Y.-Z.; Wang, M.-C. *Tetrahedron* **2018**, *74*, 2130-2142.
58. Zhang, Z.-F.; Yang, X.-C.; Lu, H.-J.; Wang, M.-C. *Eur. J. Org. Chem.* **2018**, *2018*, 785-793.
59. Liu, S.; Gao, W.-C.; Miao, Y.-H.; Wang, M.-C. *J. Org. Chem.* **2019**, *84*, 2652-2659.
60. Hua, Y.-Z.; Lu, L.-J.; Huang, P.-J.; Wei, D.-H.; Tang, M.-S.; Wang, M.-C.; Chang, J.-B. *Chem. Eur. J.* **2014**, *20*, 12394-12398.
61. Hua, Y.-Z.; Yang, X.-C.; Liu, M.-M.; Song, X.; Wang, M.-C.; Chang, J.-B. *Macromolecules* **2015**, *48*, 1651-1657.
62. Xiao, Y.; Wang, Z.; Ding, K. *Chem. Eur. J.* **2005**, *11*, 3668-78.
63. Quintavalla, A. *Curr. Med. Chem* **2018**, *25*, 917-962.
64. Liu, M.-M.; Yang, X.-C.; Hua, Y.-Z.; Chang, J.-B.; Wang, M.-C. *Org. Lett.* **2019**, *21*, 7089-7093.
65. Hua, Y.-Z.; Liu, M.-M.; Huang, P.-J.; Song, X.; Wang, M.-C.; Chang, J.-B. *Chem. Eur. J.* **2015**, *21*, 11994-11998.
66. Liu, S.; Xu, Z.-H.; Wang, X.; Zhu, H.-R.; Wang, M.-C. *J. Org. Chem.* **2019**, *84*, 13881-13889.
67. Liu, M.-M.; Yang, X.-C.; Hua, Y.-Z.; Chang, J.-B.; Wang, M.-C. *Org. Lett.* **2019**, *21*, 2111-2115.
68. Yang, X.-C.; Liu, M.-M.; Mathey, F.; Yang, H.; Hua, Y.-Z.; Wang, M.-C. *J. Org. Chem.* **2019**, *84*, 7762-7775.
69. Oguni, N.; Omi, T. *Tetrahedron Lett.* **1984**, *25*, 2823-2824.
70. Hermesen, P. J.; Cremers, J. G. O.; Thijs, L.; Zwanenburg, B. *Tetrahedron Lett.* **2001**, *42*, 4243-4245.
71. Shi, M.; Jiang, J. K. *Tetrahedron Asymmetry* **1999**, *10*, 1673-1679.
72. Wang, M.-C.; Zhao, W.-X.; Wang, X.-D.; Song, M.-P. *Synlett* **2006**, *2006*, 3443-3446.
73. Wang, M.-C.; Zhang, Q.-J.; Zhao, W.-X.; Wang, X.-D.; Ding, X.; Jing, T.-T.; Song, M.-P. *J. Org. Chem.* **2008**, *73*, 168-176.
74. Xu, C.-L.; Wang, M.-C.; Hou, X.-H.; Liu, H.-M.; Wang, D.-K. *Chin. J. Chem.* **2005**, *23*, 1443-1448.
75. Wang, M.-C.; Wang, D.-K.; Zhu, Y.; Liu, L.-T.; Guo, Y.-F. *Tetrahedron Asymmetry* **2004**, *15*, 1289-1294.
76. Wang, M.-C.; Hou, X.-H.; Xu, C.-L.; Liu, L.-T.; Li, G.-L.; Wang, D.-K. *Synthesis* **2005**, *2005*, 3620-3626.
77. Zhang, Z.; Li, M.; Zi, G. *Chirality* **2007**, *19*, 802-808.
78. Liu, R.; Bai, X.; Zhang, Z.; Zi, G. *Appl. Organomet. Chem.* **2008**, *22*, 671-675.
79. Zhang, Z.; Bai, X.; Liu, R.; Zi, G. *Inorg. Chim. Acta* **2009**, *362*, 1687-1691.
80. Feula, A.; Male, L.; Fossey, J. S. *Org. Lett.* **2010**, *12*, 5044-5047.
81. Feula, A.; Dhillon, S. S.; Byravan, R.; Sangha, M.; Ebanks, R.; Hama Salih, M. A.; Spencer, N.; Male, L.; Magyary, I.; Deng, W. P.; Müller, F.; Fossey, J. S. *Org. Biomol. Chem.* **2013**, *11*, 5083-5093.
82. Yoshizawa, A.; Feula, A.; Leach, A. G.; Male, L.; Fossey, J. S. *Front. Chem.* **2018**, *6*, 1-9.
83. Li, D.; Wang, K.; Wang, L.; Wang, Y.; Wang, P.; Liu, X.; Yang, D.; Wang, R. *Org. Lett.* **2017**, *19*, 3211-3214.
84. Starmans, W. A. J.; Thijs, L.; Zwanenburg, B. *Tetrahedron* **1998**, *54*, 629-636.
85. Doyle, M. P.; Zhou, Q. L.; Charnsangavej, C.; Longoria, M. A.; McKerver, M. A.; García, C. F. *Tetrahedron Lett.* **1996**, *37*, 4129-4132.
86. Starmans, W. A. J.; Walgers, R.; Thijs, L.; Gelder, R. d.; Smits, J. M. M.; Zwanenburg, B. *Tetrahedron* **1998**, *54*, 4991-5004.
87. Corey, E. J.; Bakshi, R. K.; Shibata, S. *J. Am. Chem. Soc.* **1987**, *109*, 5551-5553.
88. Behnen, W.; Dauelsberg, C.; Wallbaum, S.; Martens, J. *Synth. Commun.* **1992**, *22*, 2143-2153.
89. Rao, A. V. R.; Gurjar, M. K.; Kaiwar, V. *Tetrahedron: Asymmetry* **1992**, *3*, 859-862.
90. Keller, L.; Sanchez, M. V.; Prim, D.; Couty, F.; Evano, G.; Marrot, J. *J. Organomet. Chem.* **2005**, *690*, 2306-2311.

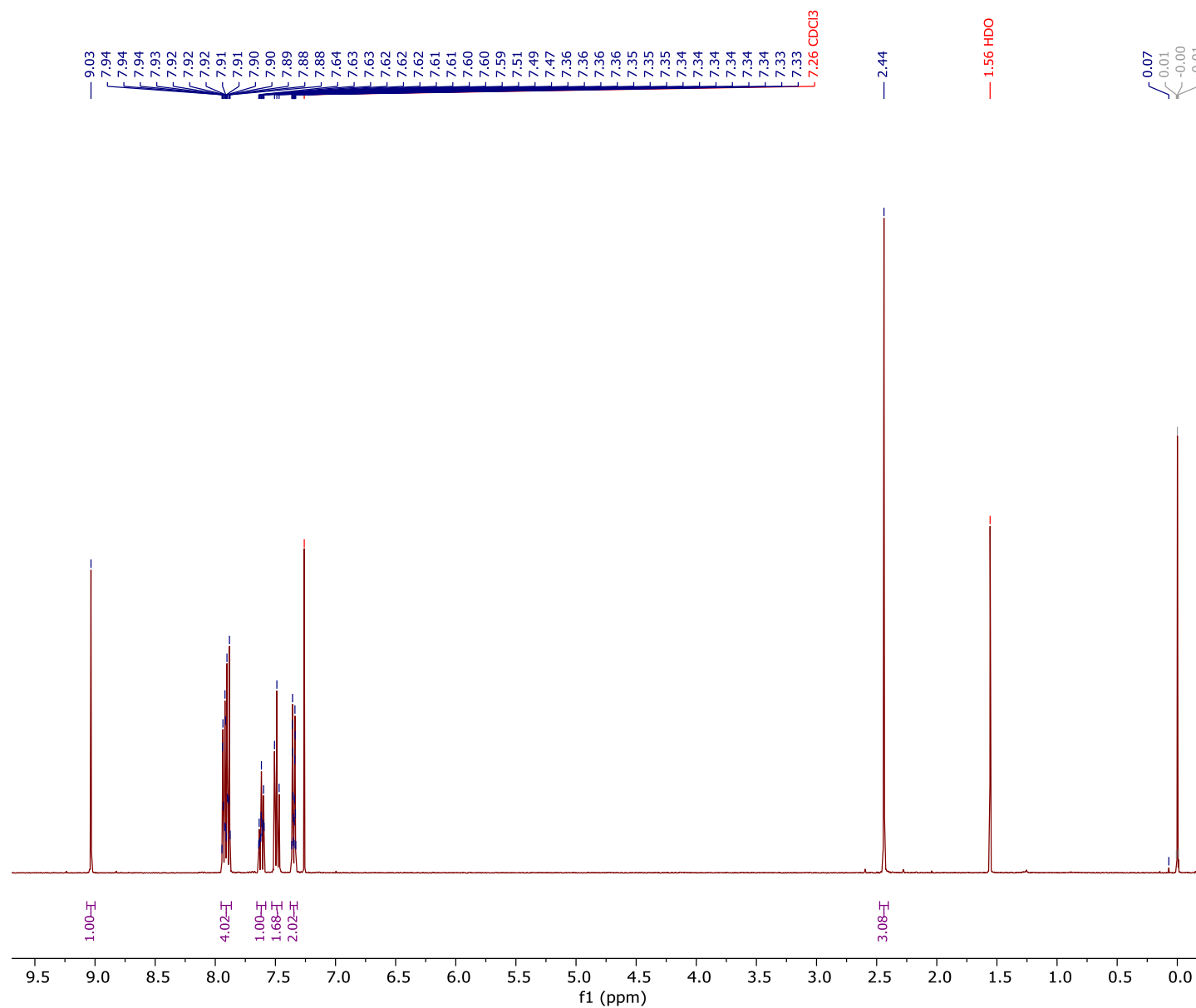
91. Boufroura, H.; Large, B.; Bsaibess, T.; Perato, S.; Terrasson, V.; Gaucher, A.; Prim, D. *Catalysts* **2017**, *7*, 27.
92. Lee, D.-H.; Lee, Y. H.; Kim, D. I.; Kim, Y.; Lim, W. T.; Harrowfield, J. M.; Thuéry, P.; Jin, M.-J.; Park, Y. C.; Lee, I.-M. *Tetrahedron* **2008**, *64*, 7178-7182.
93. Mukherjee, S.; Yang, J. W.; Hoffmann, S.; List, B. *Chem. Rev.* **2007**, *107*, 5471-5569.
94. Kotsuki, H.; Ikishima, H.; Okuyama, A. *Heterocycles* **2008**, *75*, 493-529.
95. Kotsuki, H.; Ikishima, H.; Okuyama, A. *Heterocycles* **2008**, *75*, 757-797.
96. Vachan, B. S.; Karuppasamy, M.; Vinoth, P.; Vivek Kumar, S.; Perumal, S.; Sridharan, V.; Menéndez, J. C. *Adv. Synth. Catal.* **2020**, *362*, 87-110.
97. Schneider, J. F.; Ladd, C. L.; Bräse, S. *Chapter 5. Proline as an Asymmetric Organocatalyst*, 2015.
98. Thomassigny, C.; Prim, D.; Greck, C. *Tetrahedron Lett.* **2006**, *47*, 1117-1119.
99. Ren, Y.-Y.; Wang, Y.-Q.; Liu, S.; Pan, K. *ChemCatChem* **2014**, *6*, 2985-2992.
100. Choudhary, S.; Pawar, A. P.; Yadav, J.; Sharma, D. K.; Kant, R.; Kumar, I. *J. Org. Chem.* **2018**, *83*, 9231-9239.
101. Monaco, M. R.; Renzi, P.; Scarpino Schietroma, D. M.; Bella, M. *Org. Lett.* **2011**, *13*, 4546-4549.
102. Schulz, K.; Ratjen, L.; Martens, J. *Tetrahedron* **2011**, *67*, 546-553.
103. Sakthivel, K.; Notz, W.; Bui, T.; Barbas III, C. F. *J. Am. Chem. Soc.* **2001**, *123*, 5260-5267.
104. Enders, D.; Gries, J. *Synthesis* **2005**, *2005*, 3508-3516.
105. Song, X.; Liu, A.-X.; Liu, S.-S.; Gao, W.-C.; Wang, M.-C.; Chang, J. *Tetrahedron* **2014**, *70*, 1464-1470.
106. Russo, A.; Lattanzi, A. *Eur. J. Org. Chem.* **2008**, *2008*, 2767-2773.
107. Mehra, V.; Lumb, I.; Anand, A.; Kumar, V. *RSC Adv.* **2017**, *7*, 45763-45783.
108. Reidl, T. W.; Anderson, L. L. *Asian J. Org. Chem.* **2019**, *8*, 931-945.
109. Brandi, A.; Cicchi, S.; Cordero, F. M. *Chem. Rev.* **2008**, *108*, 3988-4035.

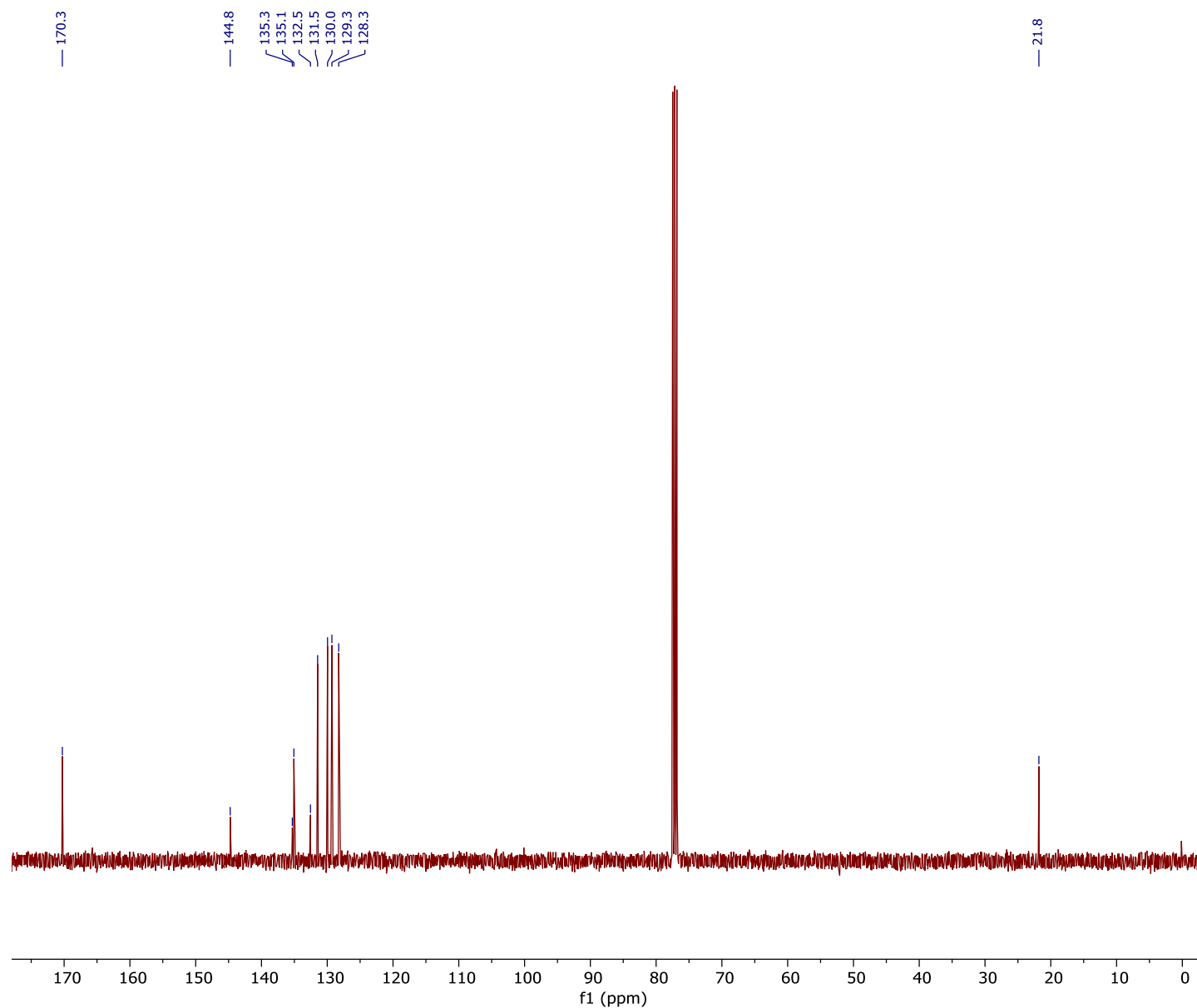


### 6.3. Appendix 3 - Representative NMR spectra for *N*-tosyl imines

Representative NMR spectra of *N*-tosyl imines using **108d**. NMR data for all other imines are stored on an RDS drive available from myself or Prof. John S. Fossey.







# <sup>13</sup>C NMR spectrum (108d)

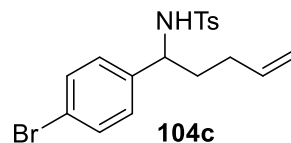
Current Data Parameters  
NAME JPM\_302\_FINAL\_NMR  
EXPNO 11  
PROCNO 1

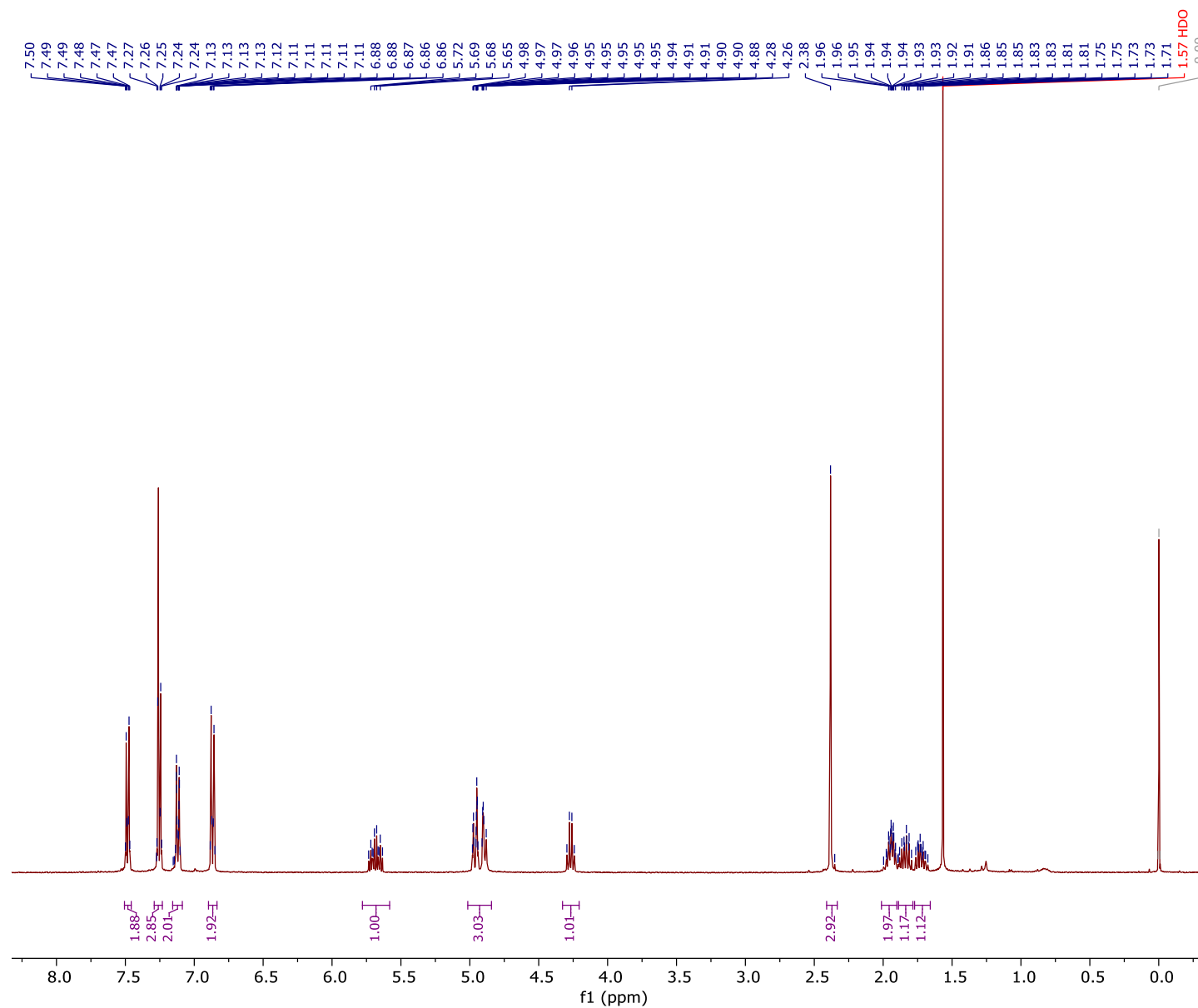
F2 - Acquisition Parameters  
Date\_ 20201019  
Time 19.30 h  
INSTRUM AvanceNeo  
PROBHD Z116098\_0793 (  
PULPROG zgpg30  
TD 119044  
SOLVENT CDCl3  
NS 512  
DS 0  
SWH 25000.000 Hz  
FIDRES 0.420013 Hz  
AQ 2.3808801 sec  
RG 14.6484  
DW 20.000 usec  
DE 7.12 usec  
TE 298.0 K  
D1 1.00000000 sec  
D11 0.03000000 sec  
TD0 1  
SFO1 100.6243390 MHz  
NUC1 13C  
P0 3.33 usec  
P1 10.00 usec  
PLW1 83.92700195 W  
SFO2 400.1318006 MHz  
NUC2 1H  
CPDPRG[2 waltz64  
PCPD2 90.00 usec  
PLW2 18.69700050 W  
PLW12 0.20396000 W  
PLW13 0.10259000 W

F2 - Processing parameters  
SI 131072  
SF 100.6127685 MHz  
WDW EM  
SSB 0  
LB 1.00 Hz  
GB 0  
PC 1.40

#### 6.4. Appendix 4 - Representative NMR spectra for 2-substituted 4-methyl-*N*-(pent-4-en-1-yl)benzenesulfonamides

Representative NMR spectra of 2-substitued 4-methyl-*N*-(pent-4-en-1-yl)benzenesulfonamides using **104c**. Complete NMR data for all other imines are stored on an RDS drive available from myself or Prof. John S. Fossey.



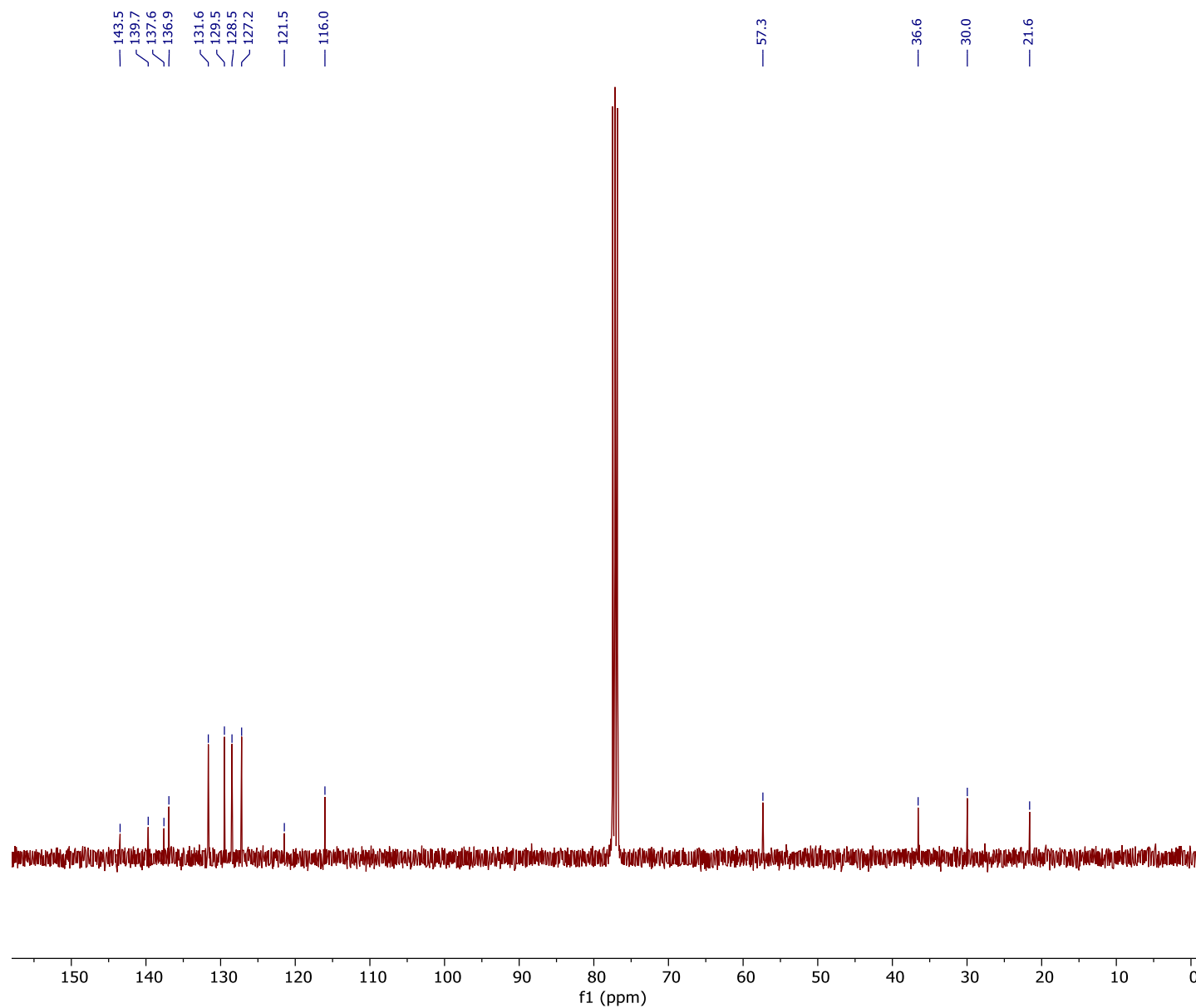


# <sup>1</sup>H NMR spectrum (104c)

Current Data Parameters  
NAME JPM\_193  
EXPNO 12  
PROCNO 1

F2 - Acquisition Parameters  
Date\_ 20200824  
Time 8.23 h  
INSTRUM AvanceNeo  
PROBHD Z116098\_0793 (  
PULPROG zg30  
TD 65536  
SOLVENT CDCl<sub>3</sub>  
NS 4  
DS 0  
SWH 7142.857 Hz  
FIDRES 0.217983 Hz  
AQ 4.5875201 sec  
RG 101  
DW 70.000 usec  
DE 14.80 usec  
TE 298.0 K  
D1 2.00000000 sec  
TD0 1  
SFO1 400.1324008 MHz  
NUC1 1H  
P0 3.13 usec  
P1 9.40 usec  
PLW1 18.69700050 W

F2 - Processing parameters  
SI 131072  
SF 400.1300090 MHz  
WDW EM  
SSB 0  
LB 0.10 Hz  
GB 0  
PC 1.00



**<sup>13</sup>C NMR spectrum (104c)**

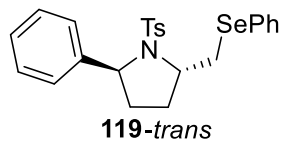
Current Data Parameters  
NAME JPM\_193  
EXPNO 13  
PROCNO 1

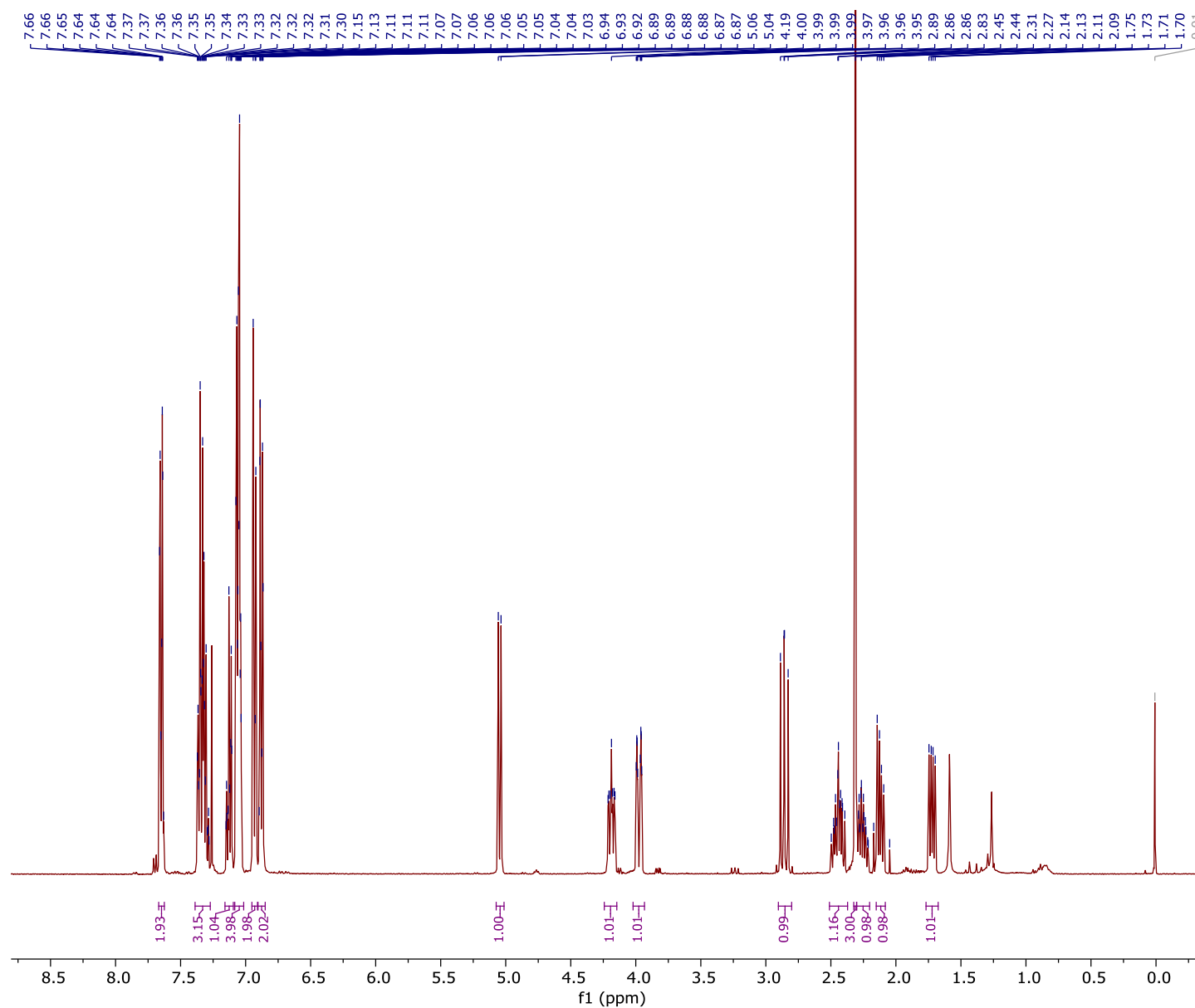
F2 - Acquisition Parameters  
Date\_ 20200824  
Time 8.53 h  
INSTRUM AvanceNeo  
PROBHD Z116098\_0793 (  
PULPROG zgpg30  
TD 119044  
SOLVENT CDCl3  
NS 512  
DS 0  
SWH 25000.000 Hz  
FIDRES 0.420013 Hz  
AQ 2.3808801 sec  
RG 15.9801  
DW 20.000 usec  
DE 7.12 usec  
TE 298.0 K  
D1 1.00000000 sec  
D11 0.03000000 sec  
TD0 1  
SFO1 100.6243390 MHz  
NUC1 13C  
P0 3.33 usec  
P1 10.00 usec  
PLW1 83.92700195 W  
SFO2 400.1318006 MHz  
NUC2 1H  
CPDPRG[2 waltz64  
PCPD2 90.00 usec  
PLW2 18.69700050 W  
PLW12 0.20396000 W  
PLW13 0.10259000 W

F2 - Processing parameters  
SI 131072  
SF 100.6127685 MHz  
WDW EM  
SSB 0  
LB 1.00 Hz  
GB 0  
PC 1.40

## 6.5. Appendix 5 – Representative NMR spectra of *trans*-pyrrolidines

Representative NMR spectra of *cis*-pyrrolidines using **119-*trans***. Complete NMR data for all other *cis*-pyrrolidines are stored on an RDS drive available from myself or Prof. John S. Fossey.



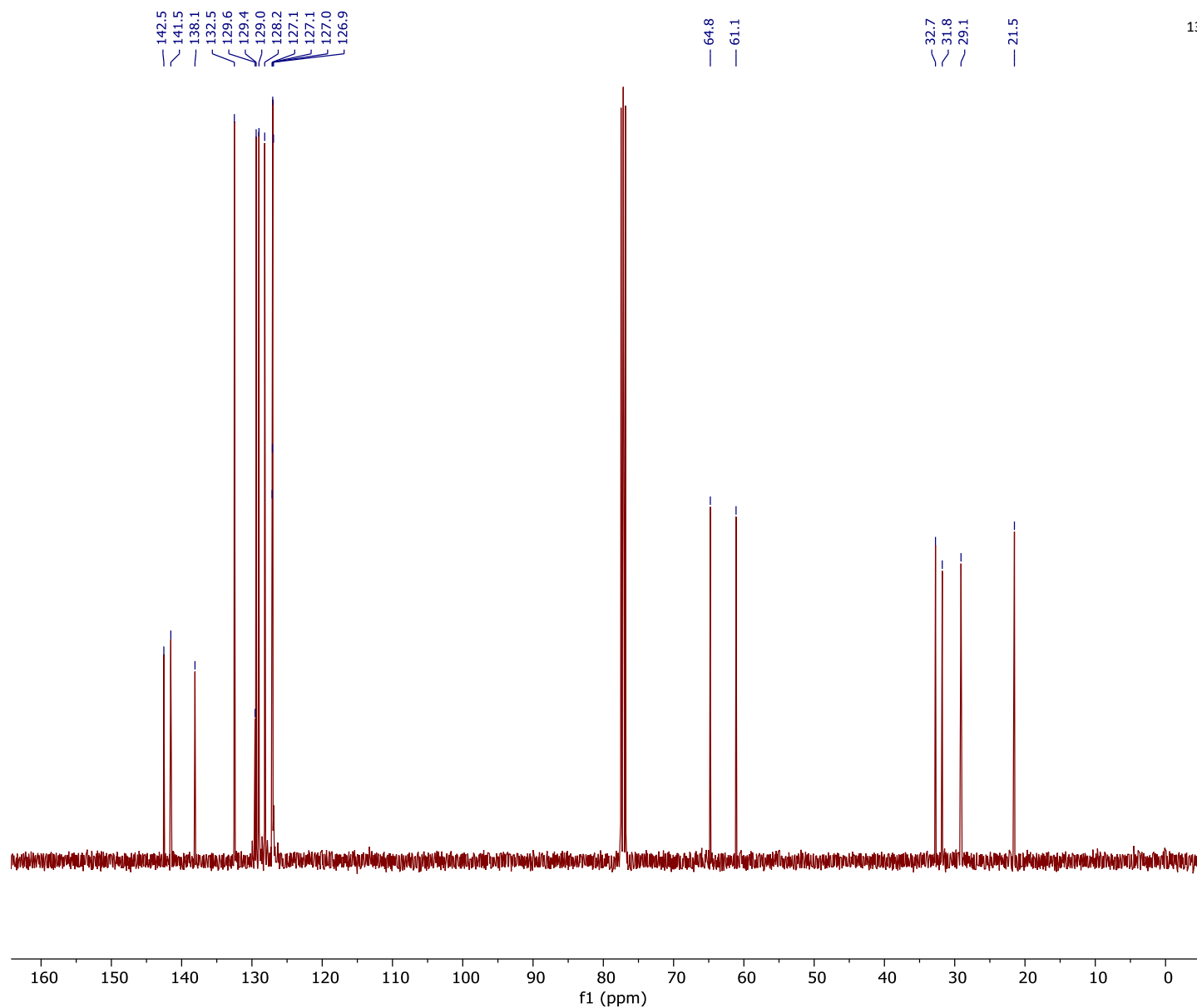


Current Data Parameters  
 NAME JPM\_194\_F3-4  
 EXPNO 10  
 PROCNO 1

F2 - Acquisition Parameters  
 Date\_ 20200825  
 Time 22.56 h  
 INSTRUM AvanceNeo  
 PROBHD Z116098\_0793 (  
 PULPROG zg30  
 TD 65536  
 SOLVENT CDCl3  
 NS 4  
 DS 0  
 SWH 7142.857 Hz  
 FIDRES 0.217983 Hz  
 AQ 4.5875201 sec  
 RG 75  
 DW 70.000 usec  
 DE 14.80 usec  
 TE 298.0 K  
 D1 2.00000000 sec  
 TD0 1  
 SFO1 400.1324008 MHz  
 NUC1 1H  
 P0 3.13 usec  
 P1 9.40 usec  
 PLW1 18.69700050 W

F2 - Processing parameters  
 SI 131072  
 SF 400.1300132 MHz  
 WDW EM  
 SSB 0  
 LB 0.10 Hz  
 GB 0  
 PC 1.00





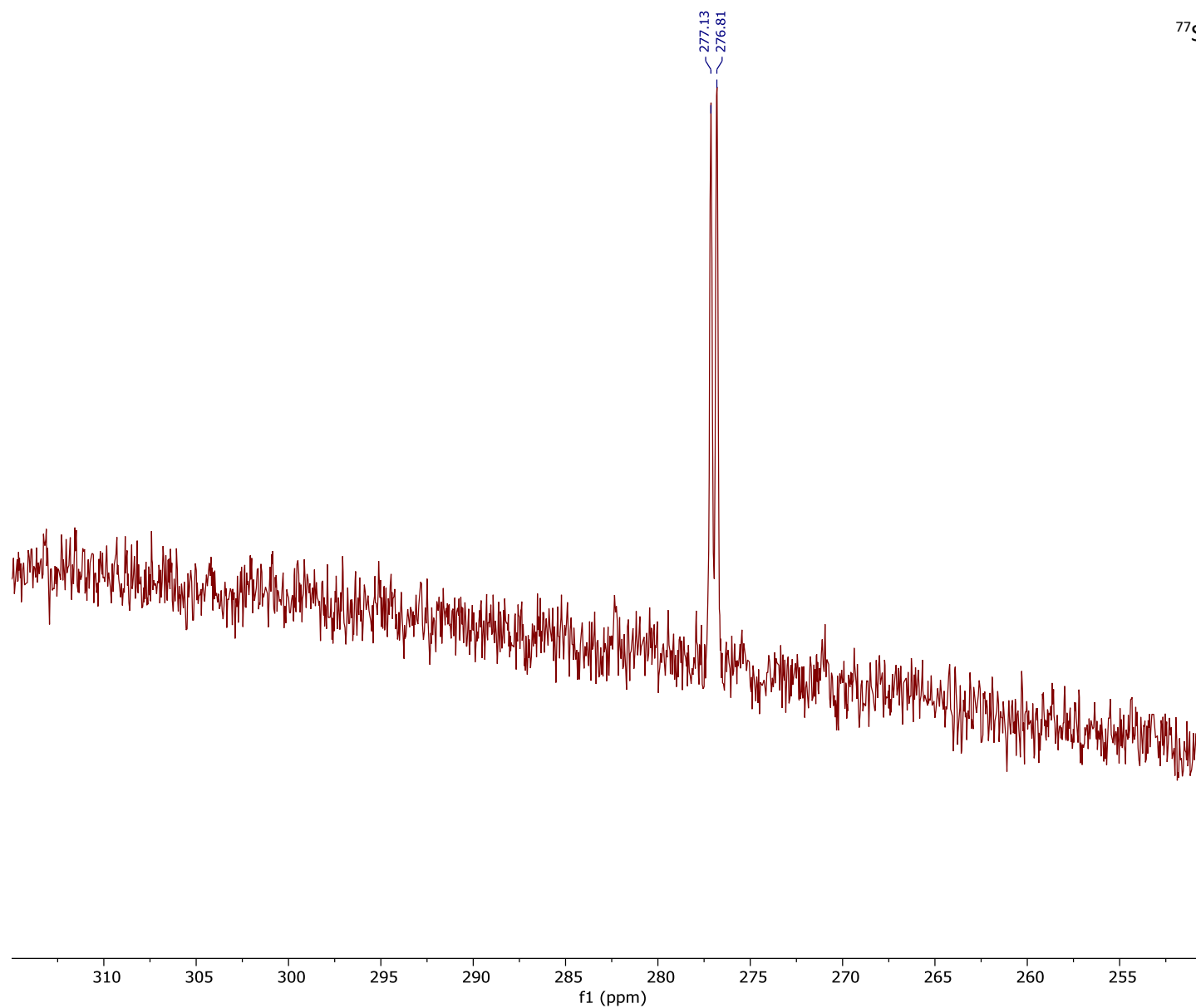
**<sup>13</sup>C NMR spectrum (119-*trans*)**

Current Data Parameters  
NAME JPM\_194\_F3-4  
EXPNO 11  
PROCNO 1

F2 - Acquisition Parameters  
Date\_ 20200825  
Time 23.26 h  
INSTRUM AvanceNeo  
PROBHD Z116098\_0793 (  
PULPROG zgpg30  
TD 119044  
SOLVENT CDCl3  
NS 512  
DS 0  
SWH 25000.000 Hz  
FIDRES 0.420013 Hz  
AQ 2.3808801 sec  
RG 15.2853  
DW 20.000 usec  
DE 7.12 usec  
TE 298.0 K  
D1 1.00000000 sec  
D11 0.03000000 sec  
TD0 1  
SFO1 100.6243390 MHz  
NUC1 13C  
P0 3.33 usec  
P1 10.00 usec  
PLW1 83.92700195 W  
SFO2 400.1318006 MHz  
NUC2 1H  
CPDPRG[2 waltz64  
PCPD2 90.00 usec  
PLW2 18.69700050 W  
PLW12 0.20396000 W  
PLW13 0.10259000 W

F2 - Processing parameters  
SI 131072  
SF 100.6127685 MHz  
WDW EM  
SSB 0  
LB 1.00 Hz  
GB 0  
PC 1.40

<sup>77</sup>Se NMR spectrum (**119-trans**)

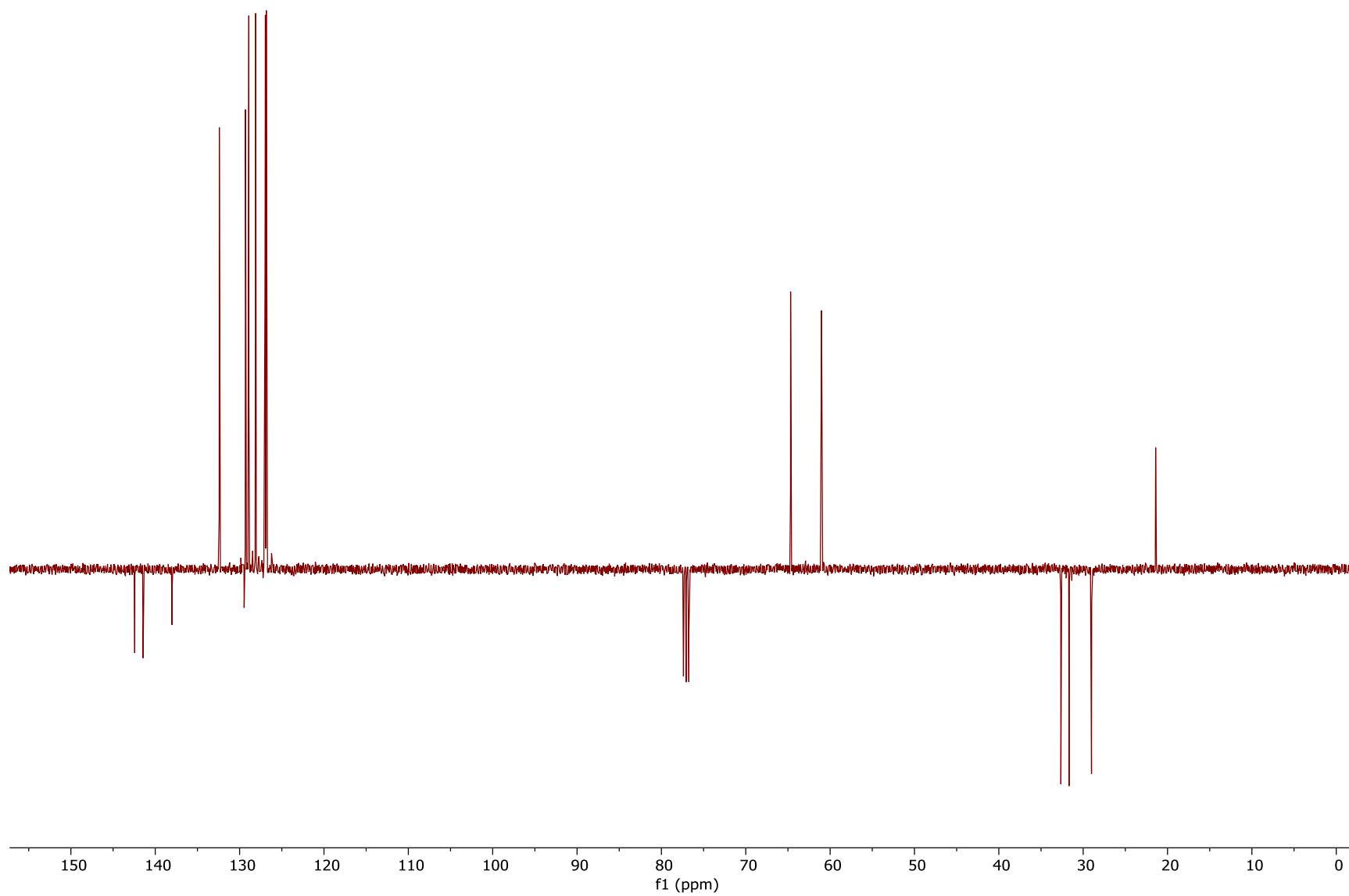


Current Data Parameters  
NAME JPM\_194\_F3-4  
EXPNO 12  
PROCNO 1

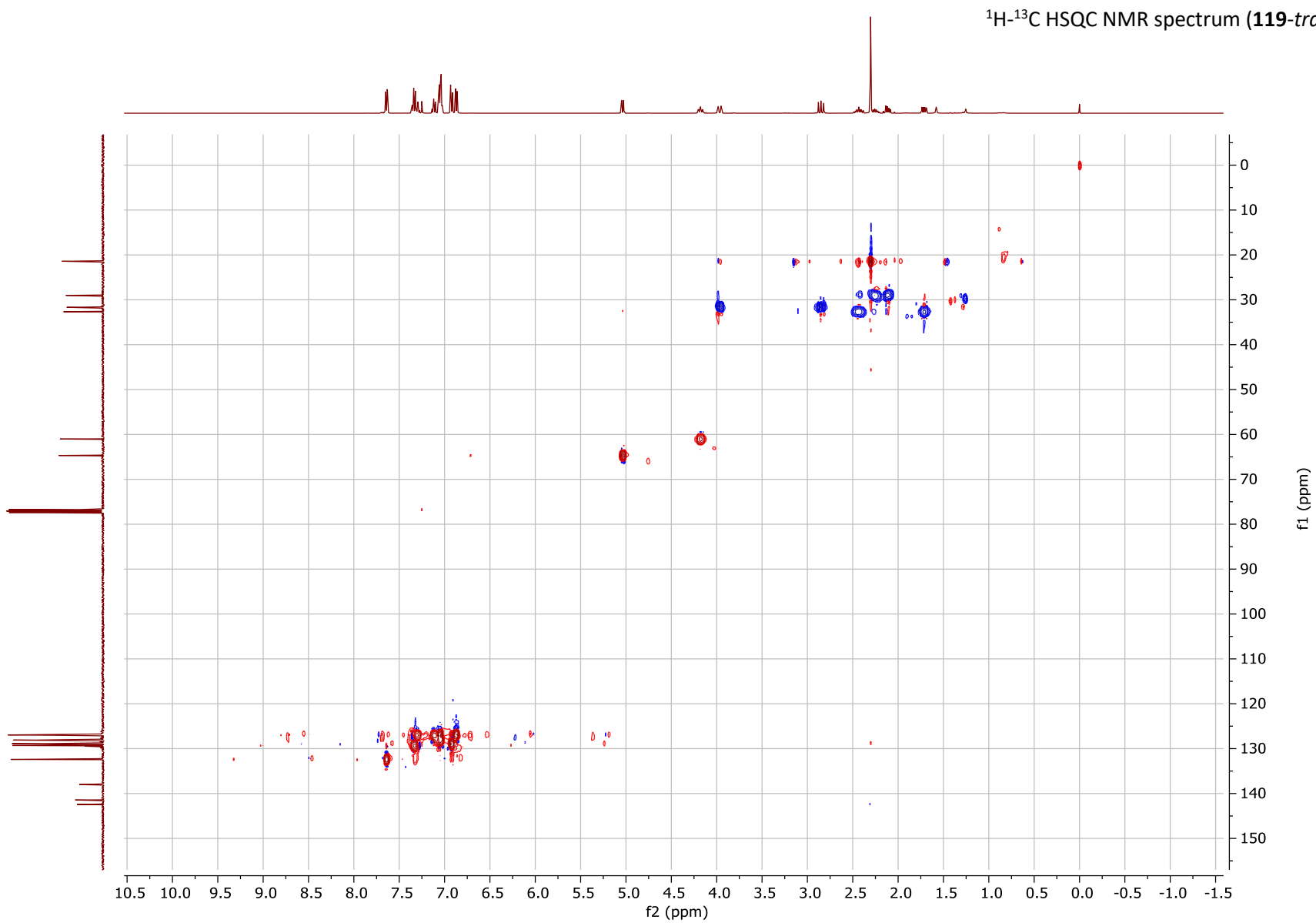
F2 - Acquisition Parameters  
Date\_ 20200825  
Time 23.46 h  
INSTRUM AvanceNeo  
PROBHD Z116098\_0793 (  
PULPROG zg  
TD 32768  
SOLVENT CDCl3  
NS 1500  
DS 0  
SWH 62500.000 Hz  
FIDRES 3.814697 Hz  
AQ 0.2621440 sec  
RG 4.6875  
DW 8.000 usec  
DE 6.50 usec  
TE 298.0 K  
D1 0.50000000 sec  
TD0 1  
SFO1 76.3490004 MHz  
NUC1 77Se  
P1 11.00 usec  
PLW1 90.00000000 W

F2 - Processing parameters  
SI 65536  
SF 76.3108450 MHz  
WDW EM  
SSB 0  
LB 2.00 Hz  
GB 0  
PC 1.40

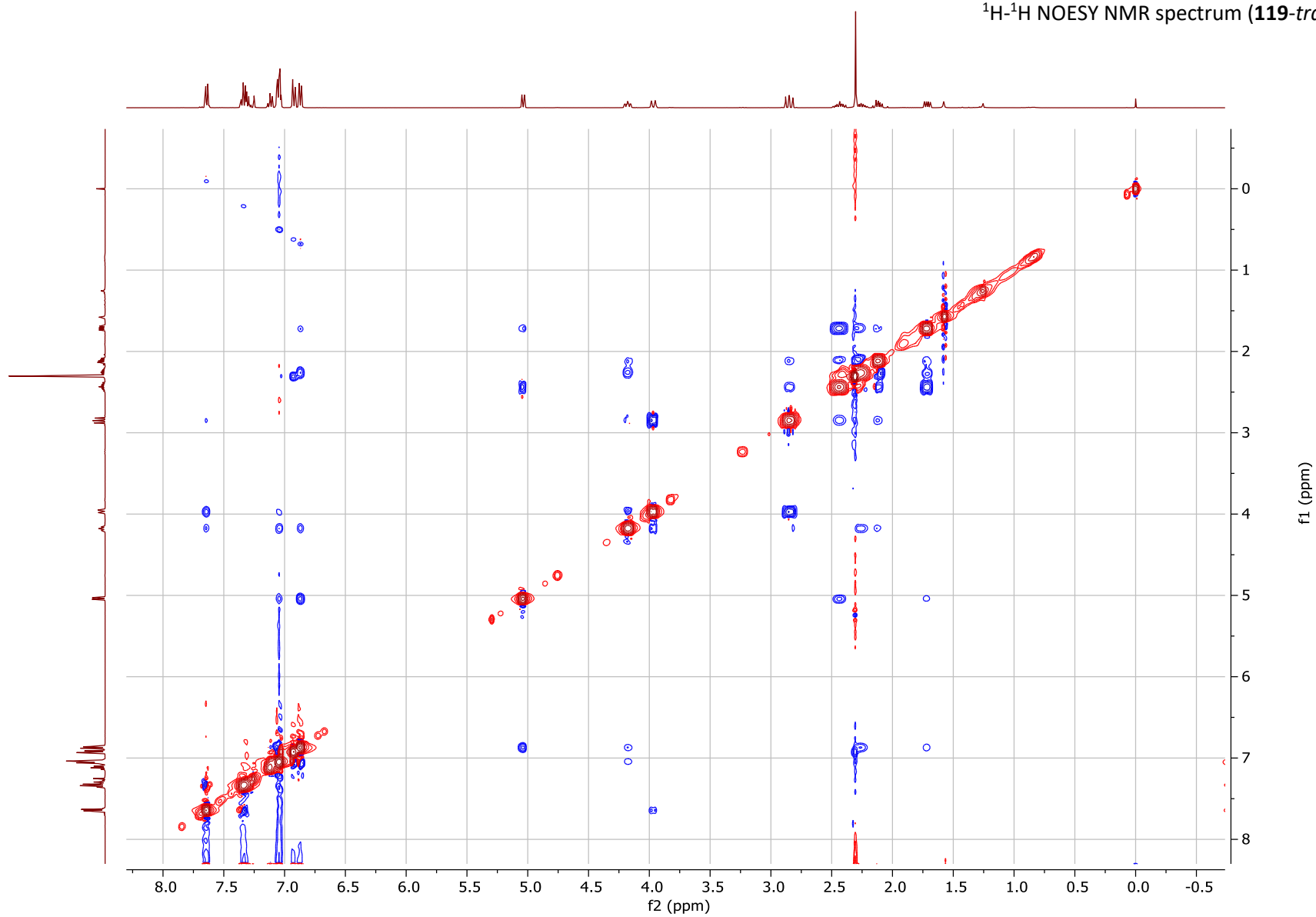
$^{13}\text{C}$  JMOD NMR spectrum (**119-trans**)





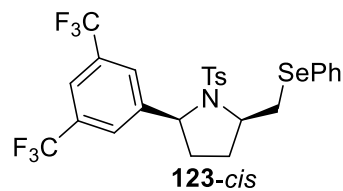


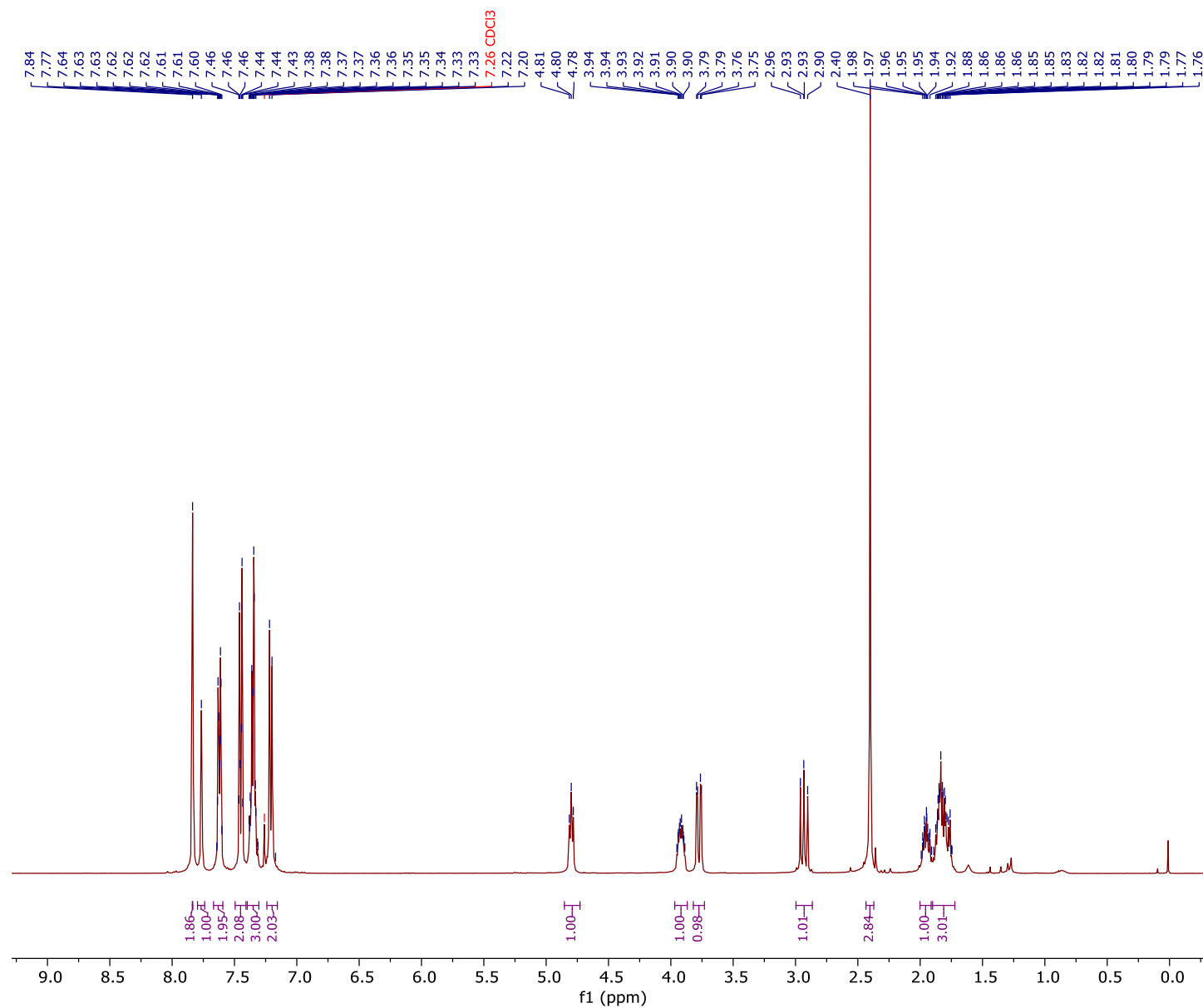
$^1\text{H}$ - $^1\text{H}$  NOESY NMR spectrum (**119-trans**)



## 6.6. Appendix 6 – Representative NMR spectra for *cis*-pyrrolidines

Representative NMR spectra of *cis*-pyrrolidines using **123-*cis***. Complete NMR data for all other *cis*-pyrrolidines are stored on an RDS drive available from myself or Prof. John S. Fossey.



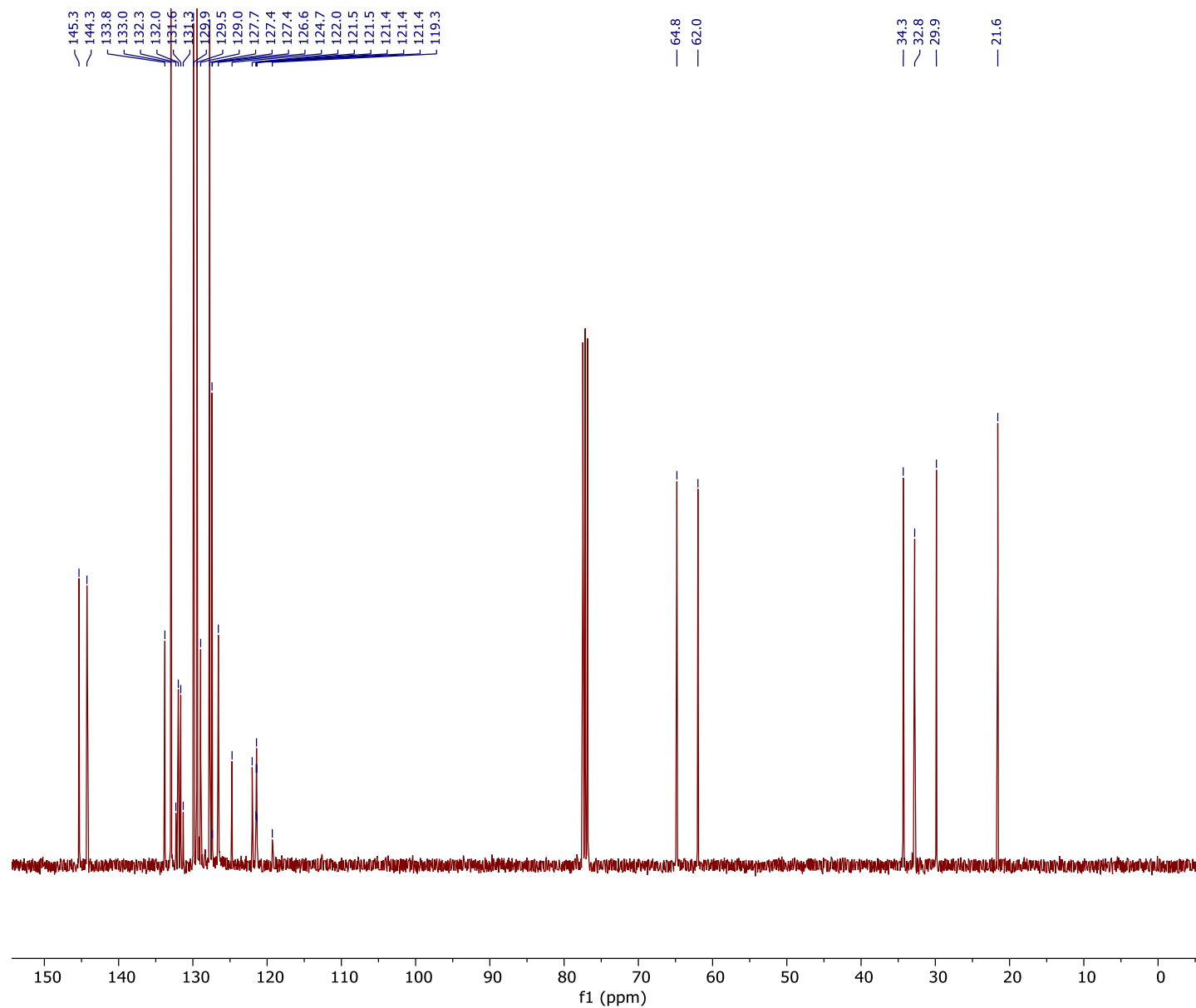


Current Data Parameters  
NAME JPM\_383  
EXPNO 10  
PROCNO 1

F2 - Acquisition Parameters  
Date\_ 20201119  
Time 16.22 h  
INSTRUM AvanceNeo  
PROBHD Z116098\_0793 (PULPROG zg30  
TD 65536  
SOLVENT CDCl<sub>3</sub>  
NS 4  
DS 0  
SWH 7142.857 Hz  
FIDRES 0.217983 Hz  
AQ 4.5875201 sec  
RG 32  
DW 70.000 usec  
DE 14.80 usec  
TE 294.5 K  
D1 2.00000000 sec  
TD0 1  
SFO1 400.1324008 MHz  
NUC1 1H  
P0 3.13 usec  
P1 9.40 usec  
PLW1 18.69700050 W

F2 - Processing parameters  
SI 131072  
SF 400.1300142 MHz  
WDW EM  
SSB 0  
LB 0.10 Hz  
GB 0  
PC 1.00



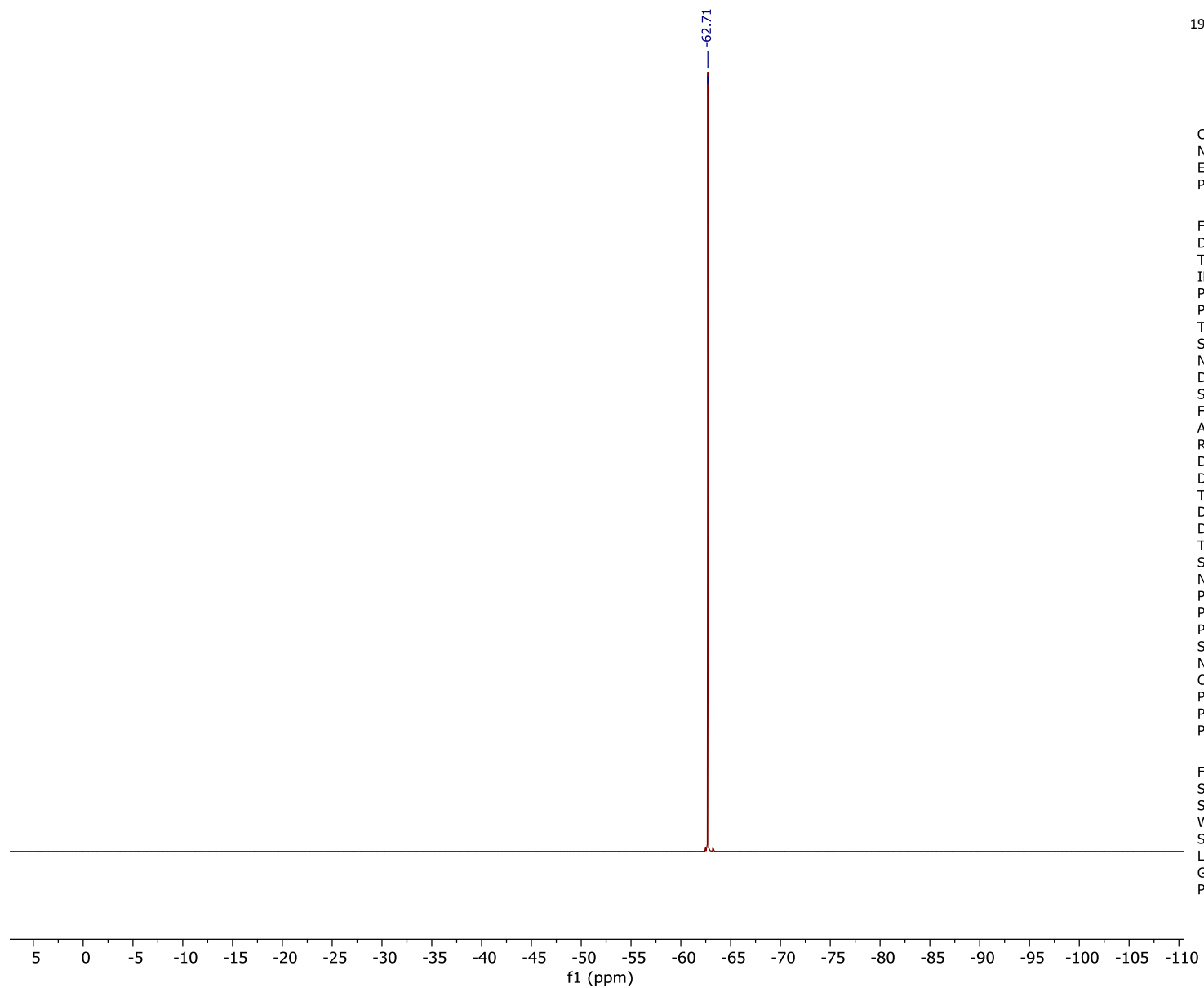


<sup>13</sup>C NMR spectrum (**123-cis**)

Current Data Parameters  
NAME JPM\_383  
EXPNO 14  
PROCNO 1

F2 - Acquisition Parameters  
Date\_ 20201119  
Time 21.09 h  
INSTRUM AvanceNeo  
PROBHD Z116098\_0793 (  
PULPROG zgpg30  
TD 119044  
SOLVENT CDCl3  
NS 512  
DS 0  
SWH 25000.000 Hz  
FIDRES 0.420013 Hz  
AQ 2.3808801 sec  
RG 14.6484  
DW 20.000 usec  
DE 7.12 usec  
TE 295.3 K  
D1 1.00000000 sec  
D11 0.03000000 sec  
TD0 1  
SFO1 100.6243390 MHz  
NUC1 13C  
P0 3.33 usec  
P1 10.00 usec  
PLW1 83.92700195 W  
SFO2 400.1318006 MHz  
NUC2 1H  
CPDPRG[2] waltz64  
PCPD2 90.00 usec  
PLW2 18.69700050 W  
PLW12 0.20396000 W  
PLW13 0.10259000 W

F2 - Processing parameters  
SI 131072  
SF 100.6127685 MHz  
WDW EM  
SSB 0  
LB 1.00 Hz  
GB 0  
PC 1.40

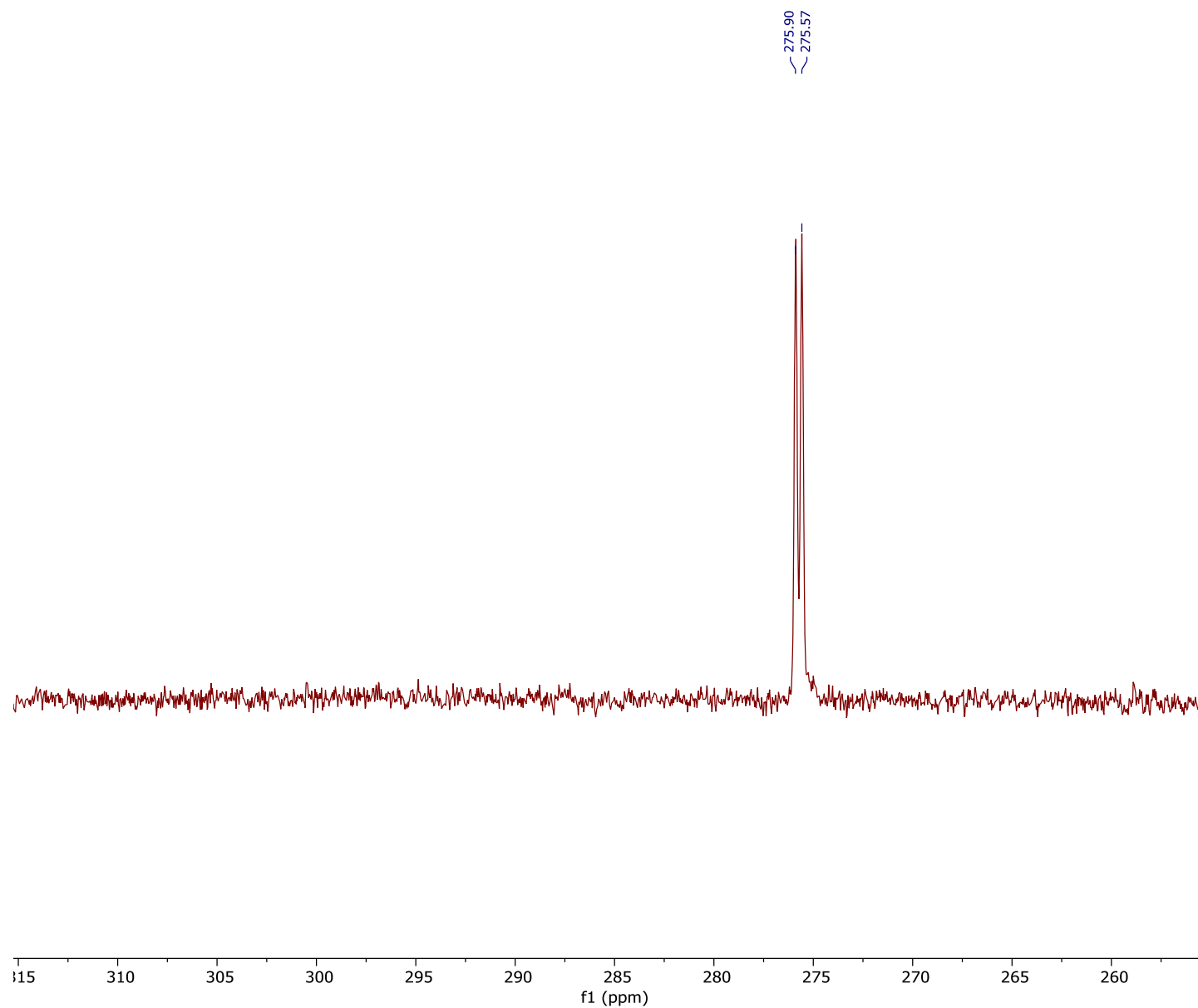


$^{19}\text{F}$  NMR spectrum (123-cis)

Current Data Parameters  
NAME JPM\_383  
EXPNO 11  
PROCNO 1

F2 - Acquisition Parameters  
Date\_ 20201119  
Time 16.23 h  
INSTRUM AvanceNeo  
PROBHD Z116098\_0793 (  
PULPROG zgig30  
TD 261948  
SOLVENT CDCl3  
NS 16  
DS 0  
SWH 156250.000 Hz  
FIDRES 1.192985 Hz  
AQ 0.8382336 sec  
RG 101  
DW 3.200 usec  
DE 6.82 usec  
TE 294.7 K  
D1 2.00000000 sec  
D11 0.03000000 sec  
TD0 1  
SFO1 376.5021312 MHz  
NUC1 19F  
P0 6.00 usec  
P1 18.00 usec  
PLW1 18.94099998 W  
SFO2 400.1318006 MHz  
NUC2 1H  
CPDPRG[2 waltz16  
PCPD2 90.00 usec  
PLW2 18.69700050 W  
PLW12 0.20396000 W

F2 - Processing parameters  
SI 262144  
SF 376.4983662 MHz  
WDW EM  
SSB 0  
LB 1.00 Hz  
GB 0  
PC 2.00



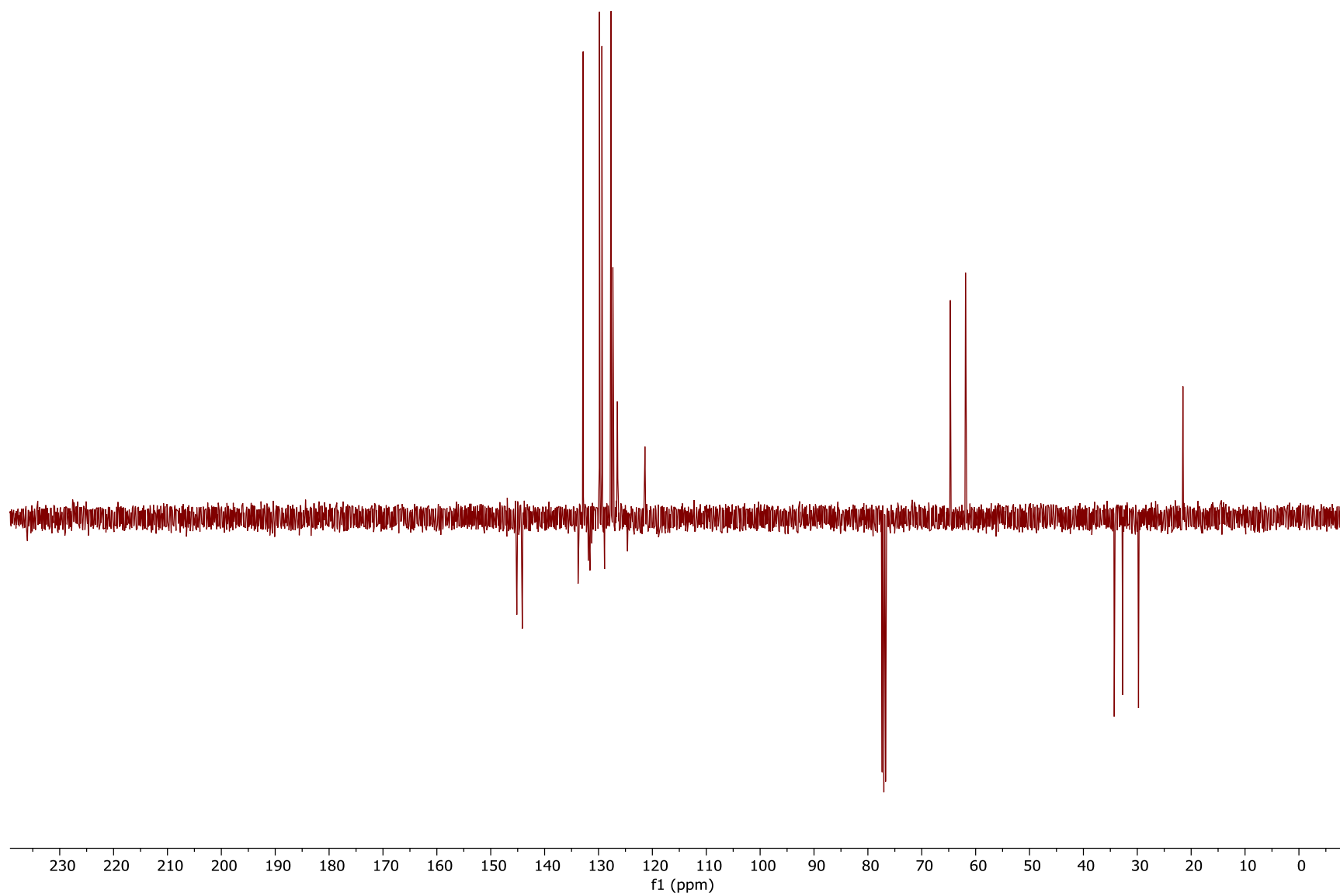
<sup>77</sup>Se NMR spectrum (**123-cis**)

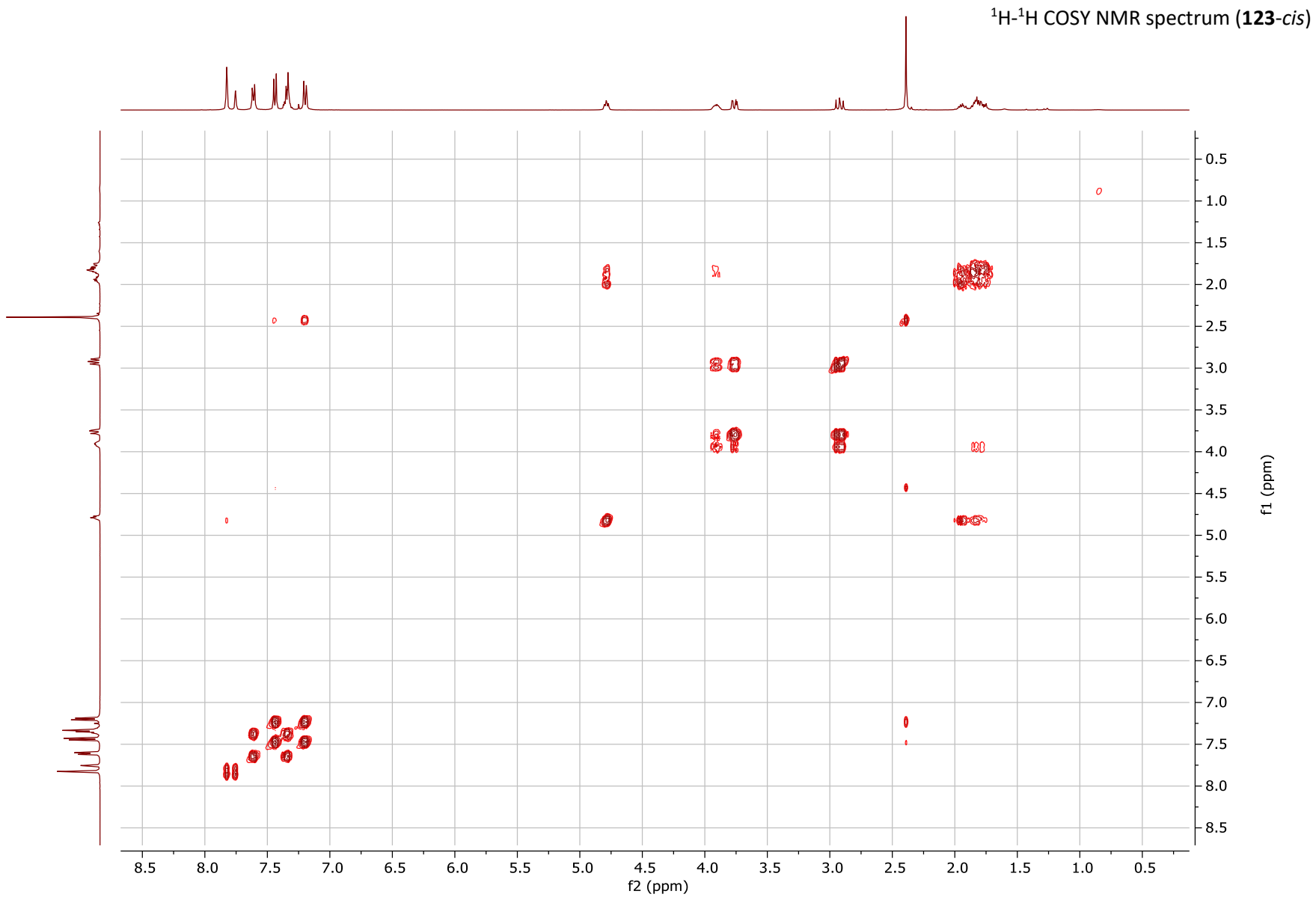
Current Data Parameters  
NAME JPM\_383  
EXPNO 12  
PROCNO 1

F2 - Acquisition Parameters  
Date\_ 20201119  
Time 16.44 h  
INSTRUM AvanceNeo  
PROBHD Z116098\_0793 (  
PULPROG zg  
TD 32768  
SOLVENT CDCl3  
NS 1500  
DS 0  
SWH 62500.000 Hz  
FIDRES 3.814697 Hz  
AQ 0.2621440 sec  
RG 3.125  
DW 8.000 usec  
DE 6.50 usec  
TE 294.5 K  
D1 0.50000000 sec  
TD0 1  
SFO1 76.3490004 MHz  
NUC1 77Se  
P1 11.00 usec  
PLW1 90.00000000 W

F2 - Processing parameters  
SI 65536  
SF 76.3108450 MHz  
WDW EM  
SSB 0  
LB 2.00 Hz  
GB 0  
PC 1.40

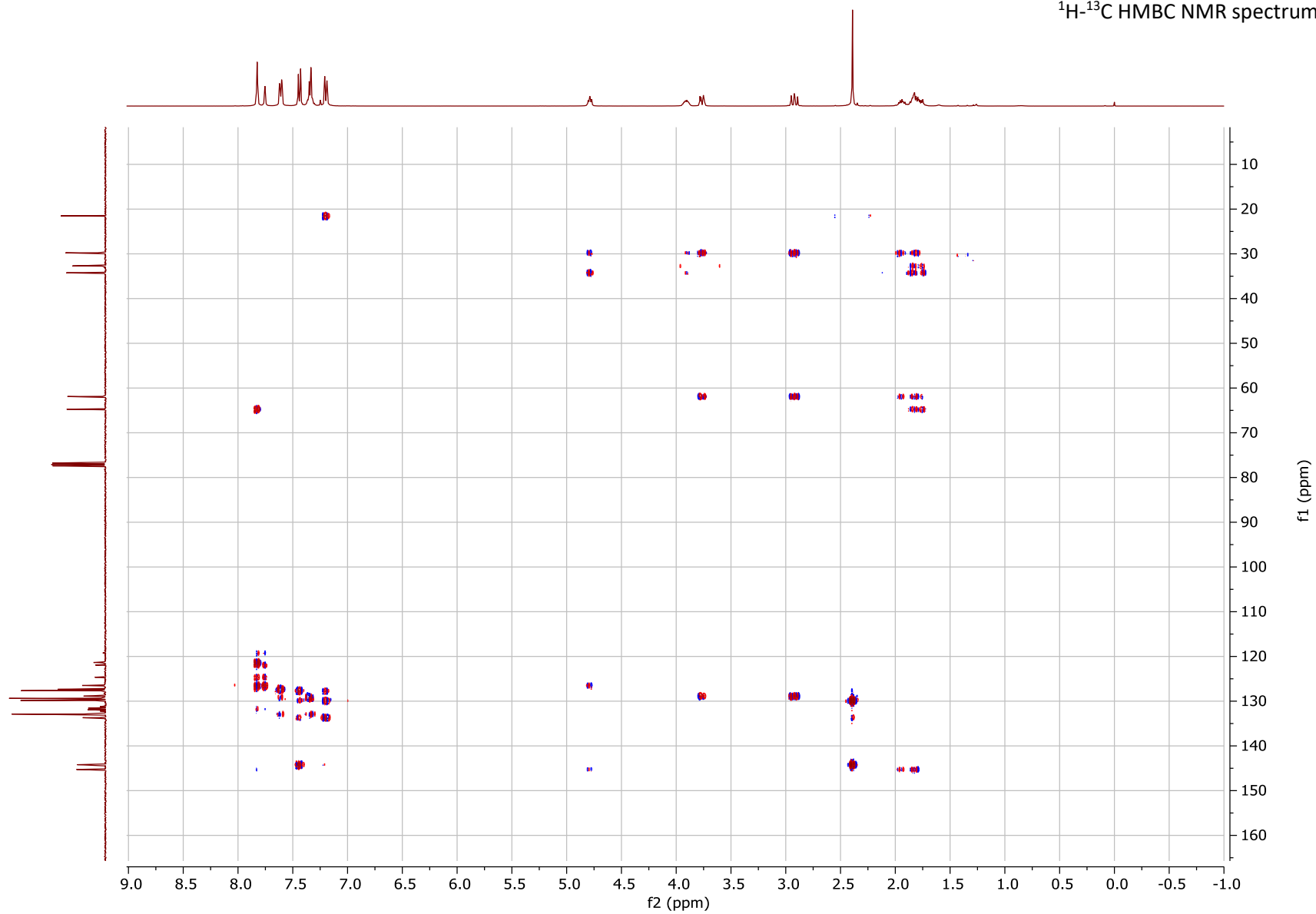
<sup>13</sup>C JMOD NMR spectrum (**123-cis**)

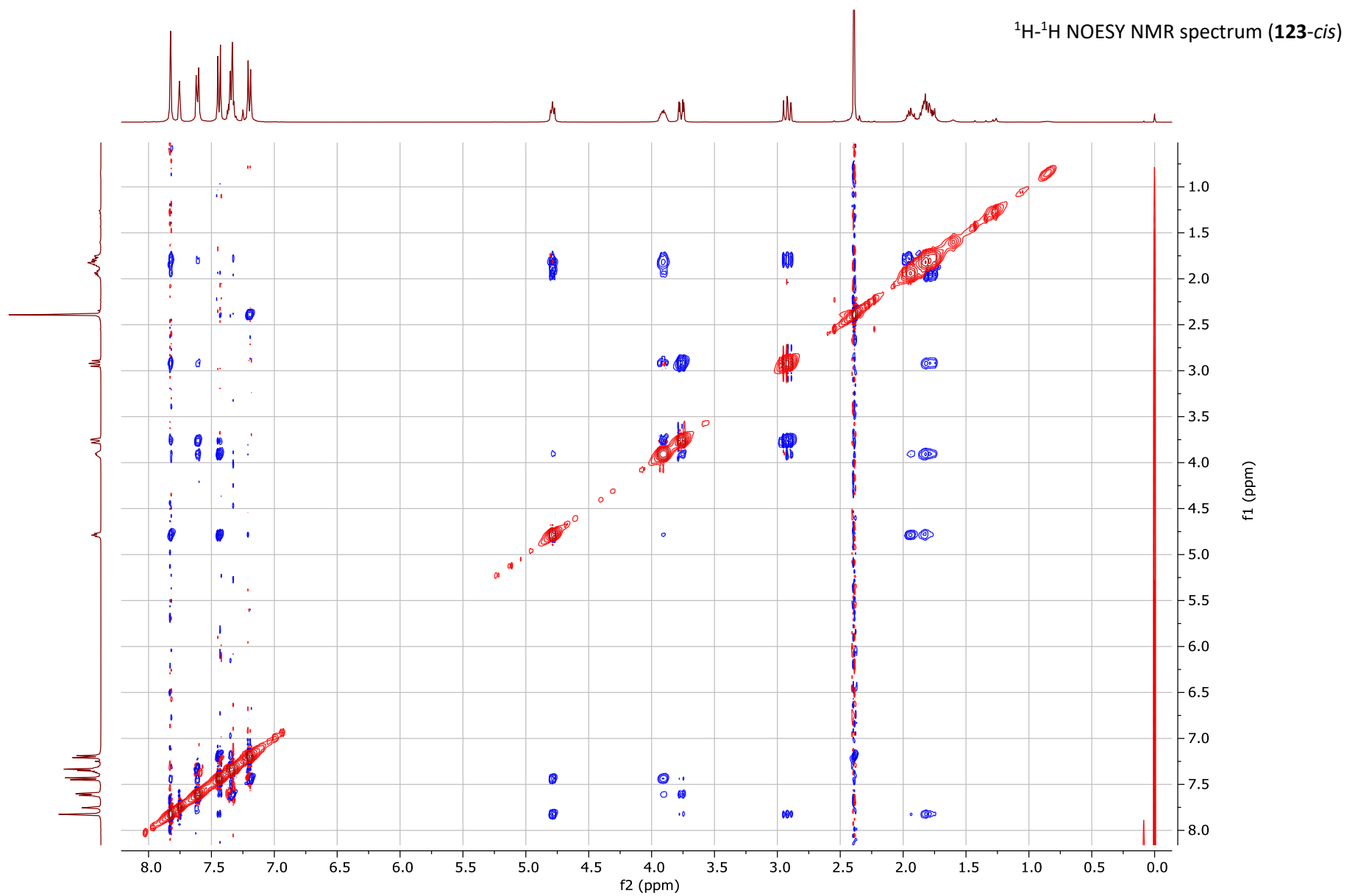






$^1\text{H}$ - $^{13}\text{C}$  HMBC NMR spectrum (**123-cis**)





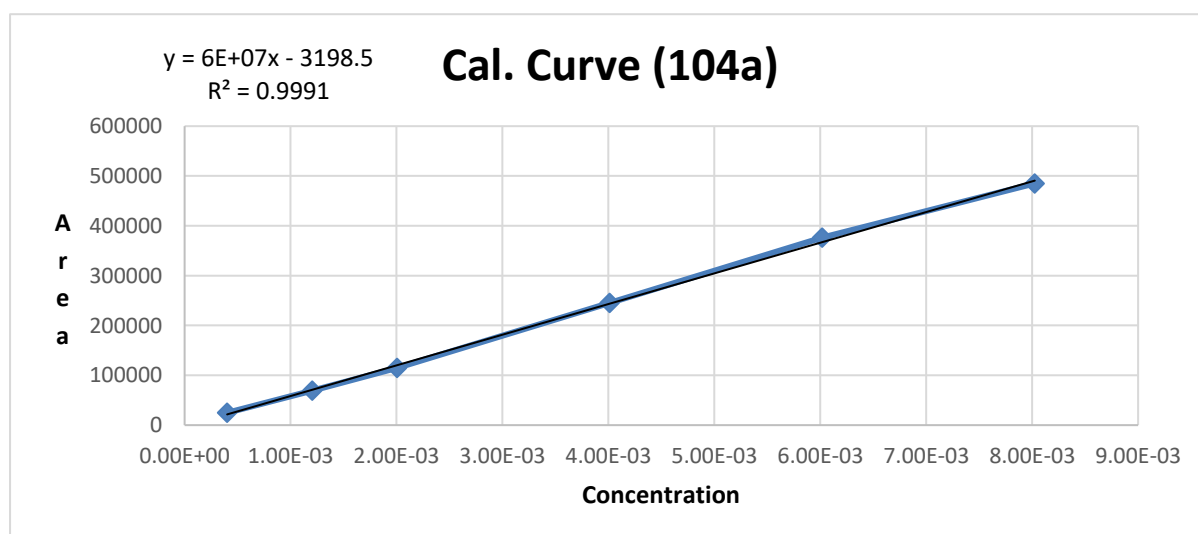


## 6.7. Appendix 7 – Representative gas chromatography data

Gas chromatography data for the reaction optimisation discussed in Section 2.1.5. Samples were injected at the inlet at 260 °C with the column at 50 °C. The column remained at 50 °C for two further minutes, followed by a 50 °C to 300 °C gradient over 18 minutes and maintained at 300 °C for a further 15 minutes. Gas chromatography data was obtained with a Shimadzu GC-2010 with FID using a Phenomenex ZB-5 column (95% dimethylpolysiloxane/5% diphenylpolysiloxane) of dimensions 30m x 0.25 mm (ID) x 0.25 µm (film thickness). All other GC data is stored on an RDS drive available from myself or Prof. John S Fossey.

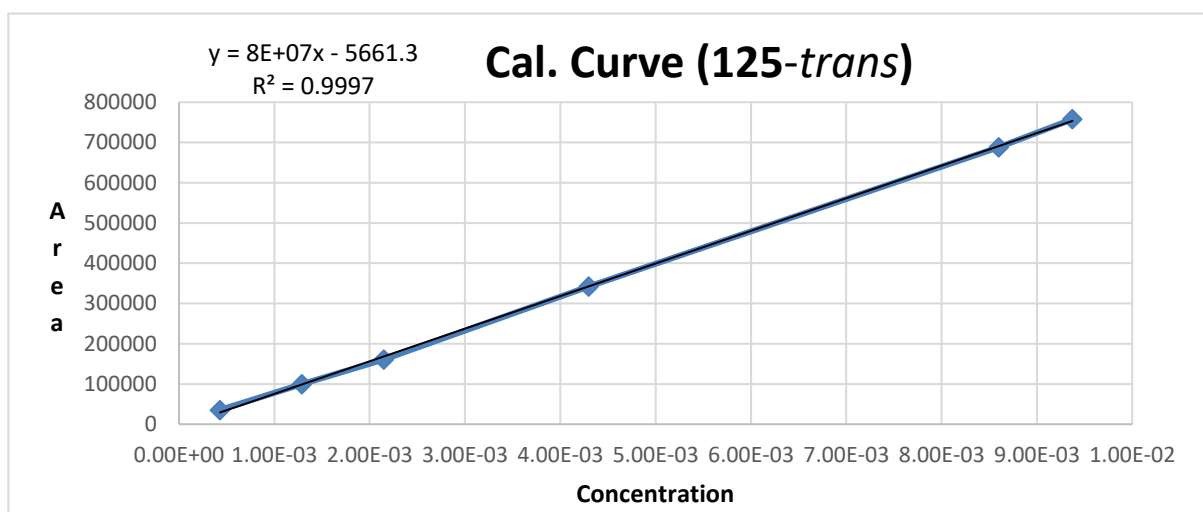
### Calibration curve of starting material (**104a**)

	MW	mg	Vol. of Stock	Conc. (M)		
<b>100a</b>	383.43	10	650	0.040		
Entry	Vol. of stock (µl)	Vol. of standard (µl)	Vol. of MeCN (µl)	Total	Conc. (M)	Area
1	10	10	980	1ml	4.01E-04	24758.5
2	30	10	960	1ml	1.20E-03	68955.2
3	50	10	940	1ml	2.01E-03	114592.4
4	100	10	890	1ml	4.01E-03	245005.7
5	150	10	840	1ml	6.02E-03	376036.5
6	200	10	790	1ml	8.02E-03	485070.9



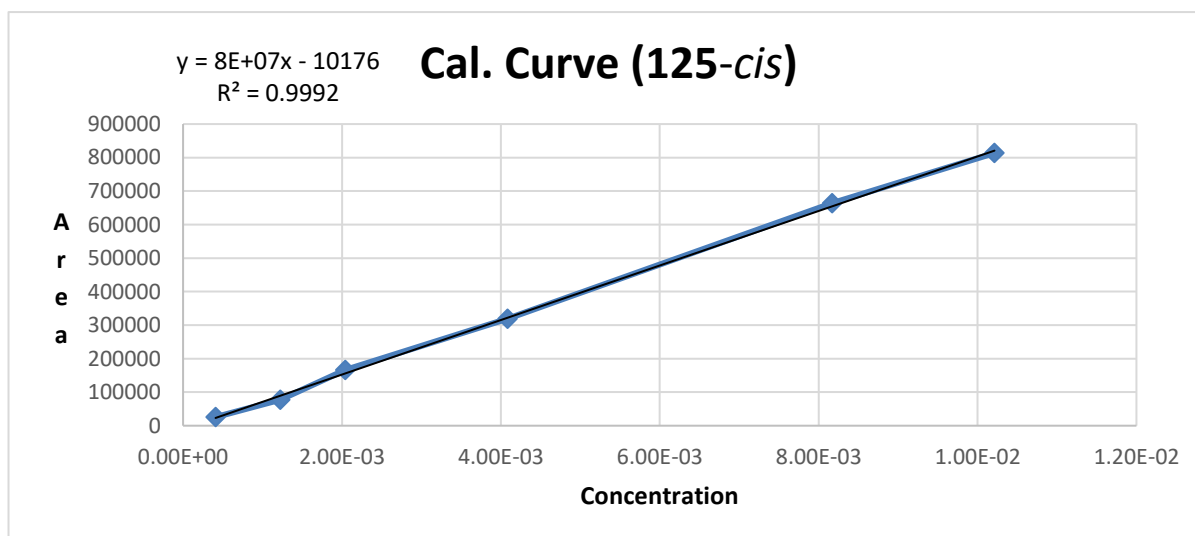
Calibration curve of *trans*-pyrrolidine (**125-trans**)

	MW	mg	Vol. of Stock	Conc. (M)		
<b>121-trans</b>	538.50	14.2	650	0.041		
Entry	Vol. of stock (μl)	Vol. of standard (μl)	Vol. of MeCN (μl)	Total	Conc. (M)	Area
1	10	10	980	1ml	4.30E-04	35474.9
2	30	10	960	1ml	1.29E-03	99558.9
3	50	10	940	1ml	2.15E-03	160642.9
4	100	10	890	1ml	4.30E-03	341977.9
5	200	10	840	1ml	8.60E-03	688250.4
6	218	10	782	1ml	9.37E-03	757878.2



Calibration curve of *cis*-pyrrolidine (**125-*cis***)

	MW	mg	Vol. of Stock	Conc. (M)		
<b>121-<i>cis</i></b>	538.50	14.3	650	0.041		
Entry	Vol. of stock (μl)	Vol. of standard (μl)	Vol. of MeCN (μl)	Total	Conc. (M)	Area
1	10	10	980	1ml	4.09E-04	25570.7
2	30	10	960	1ml	1.23E-03	77737.1
3	50	10	940	1ml	2.04E-03	166097.5
4	100	10	890	1ml	4.09E-03	318697.5
5	200	10	790	1ml	8.17E-03	664408.8
6	250	10	740	1ml	1.02E-02	813486.4



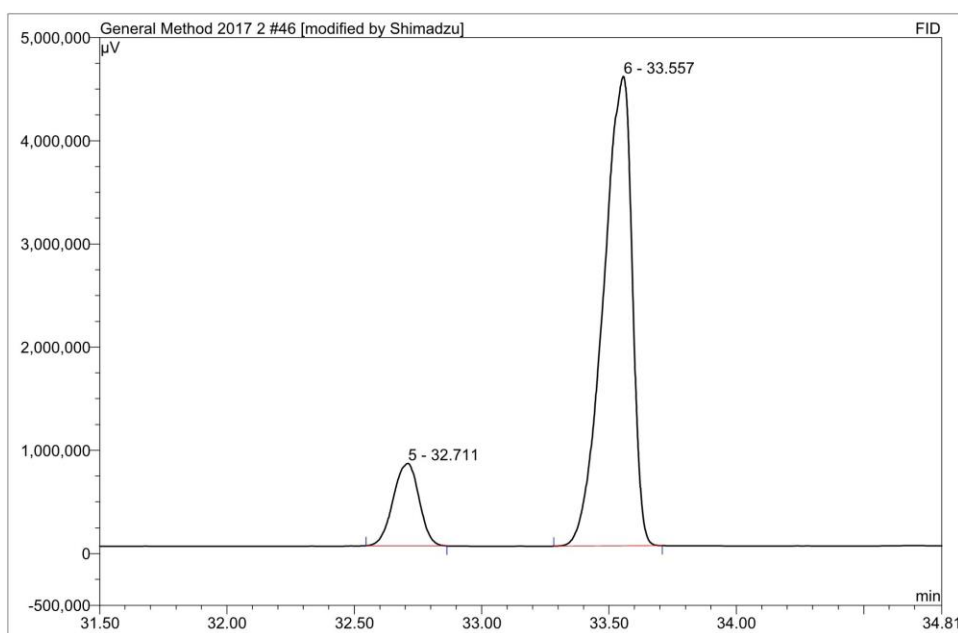
Gas chromatography data for optimum basic conditions, favouring *trans*-pyrrolidines.

Operator:Shimadzu Timebase:GC2010\_SYSTEM2 Sequence:General Method 2017 2

Page 1-1  
20/10/2020 9:59 AM

**46 JPM NBu4Br HFIP NaOMe**

Sample Name:	JPM NBu4Br HFIP NaOMe	Injection Volume:	1.0
Vial Number:	2	Channel:	FID
Sample Type:	unknown	Wavelength:	n.a.
Control Program:	JPM Method 35mins sys2	Bandwidth:	n.a.
Quantif. Method:	General Method	Dilution Factor:	1.0000
Recording Time:	19/10/2020 16:34	Sample Weight:	1.0000
Run Time (min):	35.00	Sample Amount:	1.0000



No.	Ret.Time min	Peak Name	Height μV	Area μV*min	Rel.Area %	Amount
1	9.47	n.a.	2104811.00	84381.1	9.88	n.a.
2	17.33	n.a.	678983.00	23734.3	2.78	n.a.
3	20.18	n.a.	256663.00	31408.3	3.68	n.a.
4	20.49	n.a.	577639.00	24711.4	2.89	n.a.
5	32.71	n.a.	798137.00	94239.5	11.04	n.a.
6	33.56	n.a.	4546870.00	595289.8	69.73	n.a.
<b>Total:</b>			8963103.00	853764.41	100.00	0.000

Default Test/Integration

Chromeleon (c) Dionex 1996-2006  
Version 6.80 SR8 Build 2623 (156243)

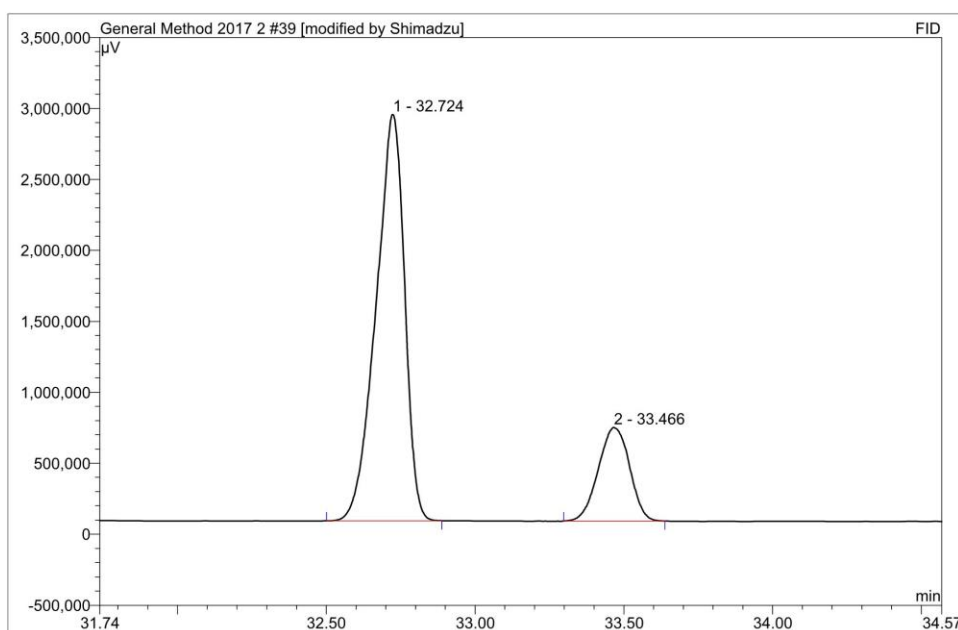
# Gas chromatography data for optimum base-free conditions favouring *cis*-pyrrolidines.

Operator: Shimadzu Timebase: GC2010\_SYSTEM2 Sequence: General Method 2017 2

Page 1-1  
20/10/2020 10:00 AM

## 39 JPM NBu4Br HFIP

Sample Name:	JPM NBu4Br HFIP	Injection Volume:	1.0
Vial Number:	4	Channel:	FID
Sample Type:	unknown	Wavelength:	n.a.
Control Program:	JPM Method 35mins sys2	Bandwidth:	n.a.
Quantif. Method:	General Method	Dilution Factor:	1.0000
Recording Time:	16/10/2020 15:07	Sample Weight:	1.0000
Run Time (min):	35.00	Sample Amount:	1.0000



No.	Ret.Time min	Peak Name	Height μV	Area μV*min	Rel.Area %	Amount
1	32.72	n.a.	2862780.00	318623.1	79.93	n.a.
2	33.47	n.a.	658553.00	79987.5	20.07	n.a.
Total:			3521333.00	398610.59	100.00	0.000

Default Test/Integration

Chromeleon (c) Dionex 1996-2006  
Version 6.80 SR8 Build 2623 (156243)